THESIS

SUBMITTED TO THE FACULTY BOARD IN THE UNIVERSITY OF OXFORD, IN PART FULFILLMENT OF THE REQUIREMENTS FOR THE DEGREE OF DOCTOR OF PHILOSOPHY.

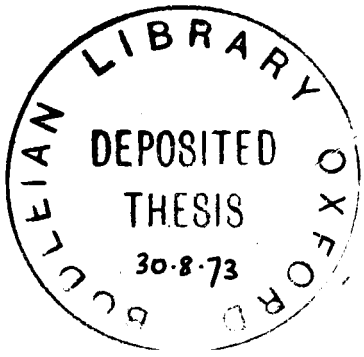

A. HAMNETT
THE QUEEN'S COLLEGE
OXFORD

PHOTOELECTRON SPECTROSCOPY IN INORGANIC CHEMISTRY

A STUDY OF TRANSITION METAL COMPLEXES USING ULTRAVIOLET AND X-RAY PHOTOELECTRON SPECTROSCOPY

ACKNOWLEDGEMENTS

I would like to express my gratitude to my supervisor Mr. A.F. Orchard for the immense help he has given me, especially when I seemed to be making very little progress. I would also like to thank Mr. P.A. Cox for numerous illuminating exegetical conversations and Dr. S. Evans who ran many of the UV-PE spectra for me.
I especially wish to thank Mr. P. Burroughs, not only for his assistance in running many of the ESCA spectra, but also for the considerable help he has given me in preparing the figures for this thesis.
Finally, I would like to thank all those members of my college and of the group who have so patiently striven to improve the grammar of the thesis. The solecisms which remain are of course mine and mine alone.

A. Hamnett

CONTENTS

Chapter one
INTRODUCTION

And so I turn to the abyss
Of necromancy, try if art
Can voice or power of spirits start,
To do me service and reveal
The things of nature's secret seal,
And save me from the weary dance
Of holding forth in ignorance.
Then shall I see, with vision clear,
How secret elements cohere,
And what the universe engirds,
And give up huckstering with words.

Goethe
Faust/part I
Trans: P. Wayne

INTRODUCTION

This thesis is concerned with the application of photoelectron spectroscopy (PES) to the study of transition metal compounds in an attempt to clarify the details of their molecular electronic structures. Photoelectron spectroscopy is a new technique[1] (the first ultra-violet PE spectra were obtained in the early sixties) which has already proved to be of immense value in understanding the nature of the chemical bond, and is based upon the energy analysis of photoelectrons ejected using ultra-violet or X-radiation of fixed frequency. The kinetic energy of such emitted electrons is directly related to the binding energy I_i by the Einstein equation[2]

$$h\nu = I_i + (K.E.)_i$$

where ν is the frequency of the incident photoionising radiation and h is Planck's constant. For gases the binding energy I_i may be equated with the ionisation potential of the electron, but for solids, correcting factors are needed to take account of the work function and other cooperative phenomena[3], and it is for this reason that no absolute binding energies will be quoted for solids.

Although there is no fundamental dichotomy between UV-PES and X-PES(ESCA), owing to instrumental difficulties, it has normally been the case until very recently that samples studied by UV-PES have been examined in the vapour phase,

whereas ESCA samples have been studied as solids, as is the case for all the spectra reproduced in this thesis. As a corollary to this, a series of transition-metal complexes had to be synthesised which were sufficiently volatile at room temperature for their vapours to be analysed in the UV-PE spectrometer employed in this work, which required a static vapour pressure of ca. 10^{-2} mm Hg. After some consideration, a series of complexes of the ligand hexafluoroacetylacetone (hfa) were selected. These had been found to be volatile enough for gas-chromatographic separation[4] at only slightly elevated temperatures and gave excellent UV-PE spectra. Their ESCA spectra were examined at low temperatures for reasons discussed in chapter two. In addition a second series of compounds, the transition-metal metallocenes $M(C_5H_5)_2$, were also examined by ESCA though their UV-PE spectra have been reported by previous workers.[5] A substantial quantity of new information will thus be presented in this thesis and subsequent chapters will contain a detailed account of how this information can be used to supplement and clarify that obtained by earlier studies.

In the early development of PES, attention was confined mainly to either small inorganic molecules, where the problems are mainly spectroscopic, or to organic molecules, where fairly well defined electronic theories can be employed. Metal

complexes differ in several respects from these two types of system, and, in order to interpret the spectra, new theories and approaches have proved necessary.

The most important difference between metal and non-metal compounds is that the potential field generated by charge separation in metal complexes is much larger. In simple terms, if we invoke Koopmans' theorem[6], the ionisation energy is given by an equation of the general form

$$I_i = - T_i + V_i - R_i = - \varepsilon_i \qquad (1)$$

where, V_i is the potential acting on an electron in orbital i, R_i the electron repulsion between it and the electrons in the remaining orbitals, T_i the kinetic energy, and ε_i the orbital energy. Thus, if we compare an aluminium complex with one of scandium, the bond contraction between Sc^{III} and Al^{III} will lead to an increase in positive potential V_i for all the ligand orbitals, and, if there is little change in real charge on the central metal ion, we would expect the observed ionisation energies (IE's) for the ligand orbitals in the Al^{III} complex to be higher than those in the corresponding Sc^{III} complex.

In addition, of course, the ligands will exert a potential on the central metal in a complex, lowering the observed IE of the metal very substantially from the value observed for the corresponding orbital in the free ion, even in the absence

of any covalence. We can quantify this by noting that, if the charge is written in units of e(1.6×10^{-19} coulombs) and r expressed in Angstroms, the potential V is given by[7]

$$V = \frac{qe}{4\pi\varepsilon_0 r} \equiv \frac{q}{r(\text{Å})} \times 14.45 \text{ volts}$$

Thus, for a neutral complex of the tris-chelate form, in which $-\frac{1}{2}e$ charge is present on each oxygen, the potential <u>at</u> each oxygen due to the central metal is 22.5 volts, and <u>at</u> the central metal due to <u>all</u> the oxygen atoms -22.5 volts. If we were to include the destabilising potential from the remaining oxygen atoms, the net potential is +11 volts at each oxygen. These are substantial figures in any considerations.

For ESCA spectroscopy, a slightly different formula from (1) is used, since Koopmans' theorem applied directly to core ionisations is found to give rather poor results. The ionisation energy for a core orbital localised on atom A is given by[8]

$$I = kq_a + V_a + l \qquad (2)$$

where, q_a is the charge on atom A, and V_a the potential <u>at</u> atom A arising from all the other atoms in the unit considered. For molecular solids, we will assume throughout that only the individual molecules need to be considered, but, for ionic solids, it would of course be necessary to consider the

complete Madelung potential at the given site, in a manner analogous to the evaluation of lattice energies.[9] The relationship between the equations (1) and (2) is difficult to derive in the most general case; perhaps the simplest explanation is to divide V_i into two parts, that potential derived from the nucleus concerned (since a core orbital may be regarded as being effectively localised about one particular nucleus) and the potential from the remaining nuclei. From each nuclear potential, we subtract the repulsion of those electrons located at or near that nucleus to generate the intra-molecular Madelung term V_a. The kinetic energy T_i may be assumed proportional to the net potential derived from atom A, by a sort of virial theorem, and, subtracting the repulsion of all electrons located about atom A gives an effective potential due to atom A which will be related to the effective charge on that atom.

Thus, the formula (2) is only approximate and is used in an empirical manner. The constant 1 is meant to correct for the reference level used and, as we shall see, can be assumed constant throughout a series of closely related chemicals. The importance of the equation is that it re-emphasises the essential feature of polar molecules, namely that the trends observed in the ionisation energies of metal complexes may not reflect in any simple way the charge on the

metal atom itself.

In addition to the position of a PE band which gives, by inference, a molecular orbital energy, two other properties of the band may be investigated, namely the intensity and the width. The latter will be a function of both the more familiar spectroscopic broadening effects (pressure broadening, Doppler broadening, etc.) and of effects peculiar to PES. In UV-PES the main line broadening is still an instrumental effect in systems such as the inert gas atoms, and the limit here is probably the line width of the Helium resonance radiation (ca. 0.002 eV). However, for larger molecules, the plethora of vibrational modes excited usually leads to broad unresolved bands from which information may be deduced only if the band has a rather unusual shape as is the case when Jahn-Teller interactions are important. Hence we will not be concerned for the most part with the shape exhibited by UV-PE bands. In ESCA however, the main contributions to the much larger half-widths of the bands observed are the width of the exciting Al $K\alpha_{1,2}$ radiation (0.85 eV), the extremely short lifetimes of the core states (Heisenberg broadening) and, in solid state work especially, the creation of local asymmetric potentials due to inadequate neutralisation in the bulk of the solid. Thus little of chemical import can be deduced at present from ESCA linewidths, but precisely the opposite is true of band

intensities. A detailed account of the relevant theory is given in the supplementum to this thesis, but certain fundamental laws may be conveniently stated in this introduction.

1. The fundamental selection rule in photoionisation is that if an electron is ionised from orbital $|a_j\rangle$, the ion states accessible through the removal of this electron are precisely those summed over in the expansion of the molecular ground state wave function into fractional parents.[10,11]

2. For a closed-shell molecule, only one state is attainable by ionisation from a particular orbital, and this will be a spin doublet having the symmetry of that orbital. If, furthermore, we make the assumption that the ionisation probability from each particular MO is the same, the relative ionisation cross-sections for the various states will be proportional to the total spin and orbital degeneracies of the levels $|a_j\rangle$. Thus, in the photoionisation of the methane molecule, whose ground electronic state is $[\text{core}]\, a_1^2 t_2^6$, two bands, of relative intensities 3:1 are expected in the valence region.

3. If the molecule possesses only one open shell, and if this shell is less than half filled, only one state can be attained by ionisation from this shell, and its relative

cross-section will be proportional simply to the occupancy of the shell.

4. Consider the case of ionisation from a closed shell in an open shell molecule. Then in general several ion states can be realised. The total intensity of all these states together will be proportional to the occupancy of the closed subshell, that is, to the total spin and orbital degeneracy of the closed shell level considered in isolation. To consider how the total intensity might be distributed amongst the various possible bands consider first the simple case of a non-degenerate closed shell. Ionisation can only yield the two states of spin $S + \frac{1}{2}$ and $S - \frac{1}{2}$ (where S is the spin of the ground state species) whose relative intensities are as $(S + 1):S$. In the event that the closed shell ionised is degenerate then the various components of $T(j) \otimes T(G)$ will be realised, where $T(j)$ is the orbital symmetry of the ionised level $|a_j\rangle$ and $T(G)$ the symmetry of the ground state, and whose relative intensities will be given by the spin-orbital degeneracies of the states obtained. However, for the ionisation of core levels, spin-orbit splitting may be significant and a complex intensity pattern may be generated.[11]

Although these rules can account semi-quantitatively for the intensity distribution in photoelectron spectroscopy, they

will break down if:

1. Either ground or excited states, or both, are subject to substantial configuration interaction (CI); that is, if the molecular wave function can no longer be adequately represented as a single determinant whose elements are one-electron orbitals.
2. One or more orbitals have anomalously high or low transition moments, a case in point being the 4f orbitals which seem to have a low cross-section in UV-PE and a high cross-section in ESCA.
3. If the excited state can interact strongly with a molecular Rydberg level.

This latter condition is usually termed autoionisation. If a molecular ionisation potential exists with an energy only slightly greater than 21.2 eV, then there will be molecular Rydberg levels near this energy and, if we are using 21.2 eV He(I) radiation, the transition moment to such Rydberg levels will in general be much larger than the photoionisation cross-section for any of the observed PE bands. Fano[12], and later Mies[13], showed that such states could participate in configuration interaction with a photoionised state, the intensity of such interaction depending on the interaction matrix element $\langle \Psi^- | \mathcal{H}_{el} | \Psi_{Ryd} \rangle$ and on the energy difference between the two states, if a simple perturbation treatment is used. In

diatomic molecules, this effect often manifests itself as an anomalous progression of Franck-Condon factors, but in more complex molecules, such as those considered in this thesis, would normally only be seen as an alteration in the expected intensity pattern. Unfortunately, the hexafluoro-acetylacetonates all have intense ionisation regions just above 21 eV arising from F 2p orbitals, and earlier studies brought to light some very strange phenomena which are discussed in the experimental and instrumental sections following.

Reorganisation and Correlation

The numerical values obtained for ionisation energies are, as we indicated above, compared to the theoretical orbital energies calculated using a self-consistent Hartree-Fock method. Several points need to be made about such a comparison.

(i) It is only valid as a direct comparison in the case of closed-shell molecules. For open-shell systems, using Roothaan's formalism, corrections must be made to avoid counting electron-repulsion terms twice. The analysis for atoms has been given elsewhere.[14]

(ii) At the moment, calculations of Hartree-Fock quality are not available for transition-metal complexes, and much more approximate methods are used. In essence, the problem is side-stepped in this thesis, since a set of

orbital energies is defined such that they are qualitatively related to the "true" orbital energies, and obey Koopmans' theorem. Even this algorithm breaks down for complexes possessing more than one open-shell, and no attempt has been made to derive orbital energies for $Mn(hfa)_3$ and $Fe(hfa)_3$.

(iii) Koopmans' approximation involves the assumption that the remaining orbital wave functions do not alter when an electron is ionised from one given orbital. An exhaustive analysis of the situation in atoms showed that Koopmans' theorem was only successful numerically owing to a fortuitous cancellation of the neglected re-organisation and correlation terms. To understand how this might be so, consider fig. 1.1, where the potential curves for a diatomic molecule and ion XY and XY^+ are plotted. The continuous lines A and A^+ are the potential functions determined experimentally or by exhaustive CI calculation, and the corresponding dotted lines are the Hartree-Fock potential energy curves calculated using respectively the best molecular and (separately optimised) ionic Hartree-Fock orbitals. It is fairly clear that if we use the molecular HF orbitals to calculate the energy of the ion we will obtain curve B, which will always be at an energy higher than the ionic

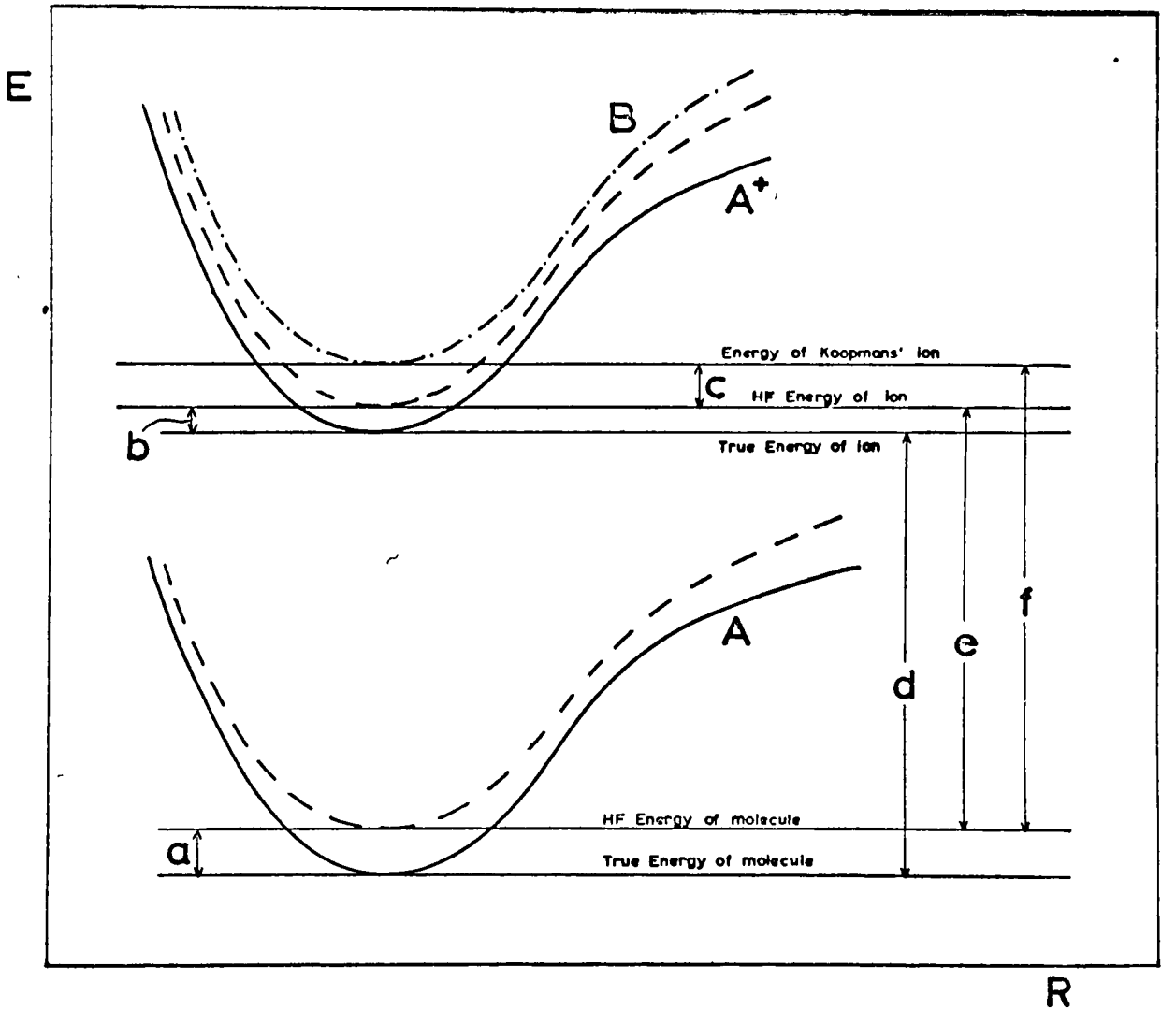
E
B
A+
Energy of Koopmans' ion
c
HF Energy of ion
b
True Energy of ion
A
d
e
f
HF Energy of molecule
a
True Energy of molecule
R

Figure 1.1

Hartree-Fock energy (which is, by definition, the best orbital approximation). It follows that the energy $\langle c \rangle$ on the diagram is always positive. The correlation energies of ground and ionic states can be represented by the values $\langle a \rangle$ and $\langle b \rangle$ respectively as shown on the diagram, and, since we have removed an electron from the molecule, we would expect that, in general $\langle a \rangle$ will be greater than $\langle b \rangle$. The experimental ionisation energy $\langle d \rangle$ is shown in the figure, as are the Hartree-Fock IE $\langle e \rangle$ and the Koopmans' IE $\langle f \rangle$, and the following relationships exist

$$\langle e \rangle = \langle d \rangle + \langle b \rangle - \langle a \rangle$$

$$\langle f \rangle = \langle d \rangle + \langle b \rangle + \langle c \rangle - \langle a \rangle$$

and it can be seen that the Koopmans' IE $\langle f \rangle$ may be a better approximation to $\langle d \rangle$ than is at first sight apparent if there is a fortuitous cancellation between $\langle a \rangle - \langle b \rangle$ and $\langle c \rangle$; that is, if the reorganisation energy $\langle c \rangle$ and the change in correlation energy $\langle a \rangle - \langle b \rangle$ are approximately equal. Save where there is a disproportionately large change in one of these, the approximation does lead to excellent results, at least for atoms. Significant deviations in the early periods only occur for Be and Mg, where there is a large ground-state CI term derived from the ^1S (core) $2p^2$ state which

is lost in the ion, and for the later elements of the first short period, where reorganisation energies are particularly large; that is, for F and Ne, the ground-state orbitals approximate very poorly to those of F^+ and Ne^+ respectively.

Chapter two

INSTRUMENTAL SECTION

Exegi monumentum aere perennius

Horace

Odes III xxx 1

INSTRUMENTAL SECTION

The great majority of the UV-PE spectra reported in this thesis were obtained using a compactly designed spectrometer constructed in this laboratory.[15] The basic design of the spectrometer has been adequately described elsewhere, but certain points are worth emphasising. The plates of the 127° analyser were coated with aquadag (colloidal graphite in water) and then covered with benzene soot to absorb the scattered electrons. Owing, however, to the very large number of near-zero kinetic energy electrons produced by multiple scattering effects in the target chamber, a sharp peak (the zero-energy peak) is always seen at an apparent binding energy of 21.2 eV which provides an additional calibration line and a check on the scale expansion.

The detector used for the electrons is a Mullard "channeltron" type consisting of an efficient secondary emitter baked into lead-glass which is fashioned into a spiral. These multipliers offer a number of advantages over the more common plate multipliers; being smaller in size, having an enhanced resistance to corrosion, and, from the point of view of the involatility of some of the samples investigated, most importantly, they do not tend to develop large background count rates swamping the photoelectron signal.

The sensitivity characteristics of retarding analysers, such as that used here have been the subject of some controversy.[16] It is now clear that such analysers do not, in general, give constant sensitivity over the entire spectrum, due to dispersive effects within the electron optical arrangements. Furthermore, the count rates obtained from simple deflection analysers such as those in the commercially available Perkin-Elmer series, cannot be simply corrected to the count rates of the retarding type by dividing by the electron kinetic energy. Thus the situation at the moment is rather confused and only for closely spaced bands should the relative intensities be taken as a measure of the relative ionisation cross-sections for the orbitals involved.

Samples were introduced into the spectrometer using the vacuum lock assembly described by Evans. They were prepared in specially designed tubes which each incorporated a greaseless "rotaflo" tap. When opened, the sample vapour was pumped into the target chamber, and photoionisation occurred in this region.

To extend the range of compounds which could be studied, a second spectrometer was also constructed in this laboratory which had built into it a heatable probe and target chamber. The analyser design was altered to incorporate a parallel-

plate deflection system used in conjunction with a pre-accelerating slit, and scanned in a retarding mode as the instrument above. Unfortunately, the second instrument did not function well, since fringing effects caused a serious loss in resolution and counts. On replacing the analyser by a more conventional 90^{o} sector, sufficient improvement in performance was realised to warrant the study of a few acetylacetonato complexes using temperatures of ca. $100^{o}C$. Spectra were also obtained using the heated probe arrangement available on the commercial Perkin-Elmer PS-16.

A number of instrumental problems have arisen in running the UV-PE spectra of these complexes which have been dealt with in various ways. An early and apparently unique phenomenon, as discussed in the introduction, was induced oscillation of the helium discharge lamp, first observed in the spectrum of $Co(hfa)_3$. The figure shows a clear oscillation in the count rate with a period of about five minutes. Experimentally, it was observed that increasing the helium flow rate in the lamp caused the oscillations to disappear, and all subsequent spectra were recorded at a much higher helium pressure than that normally employed. Presumably, as the flow rate is increased, the differential pumping on the helium lamp can no longer cope adequately and much more gas

Figure 2.1

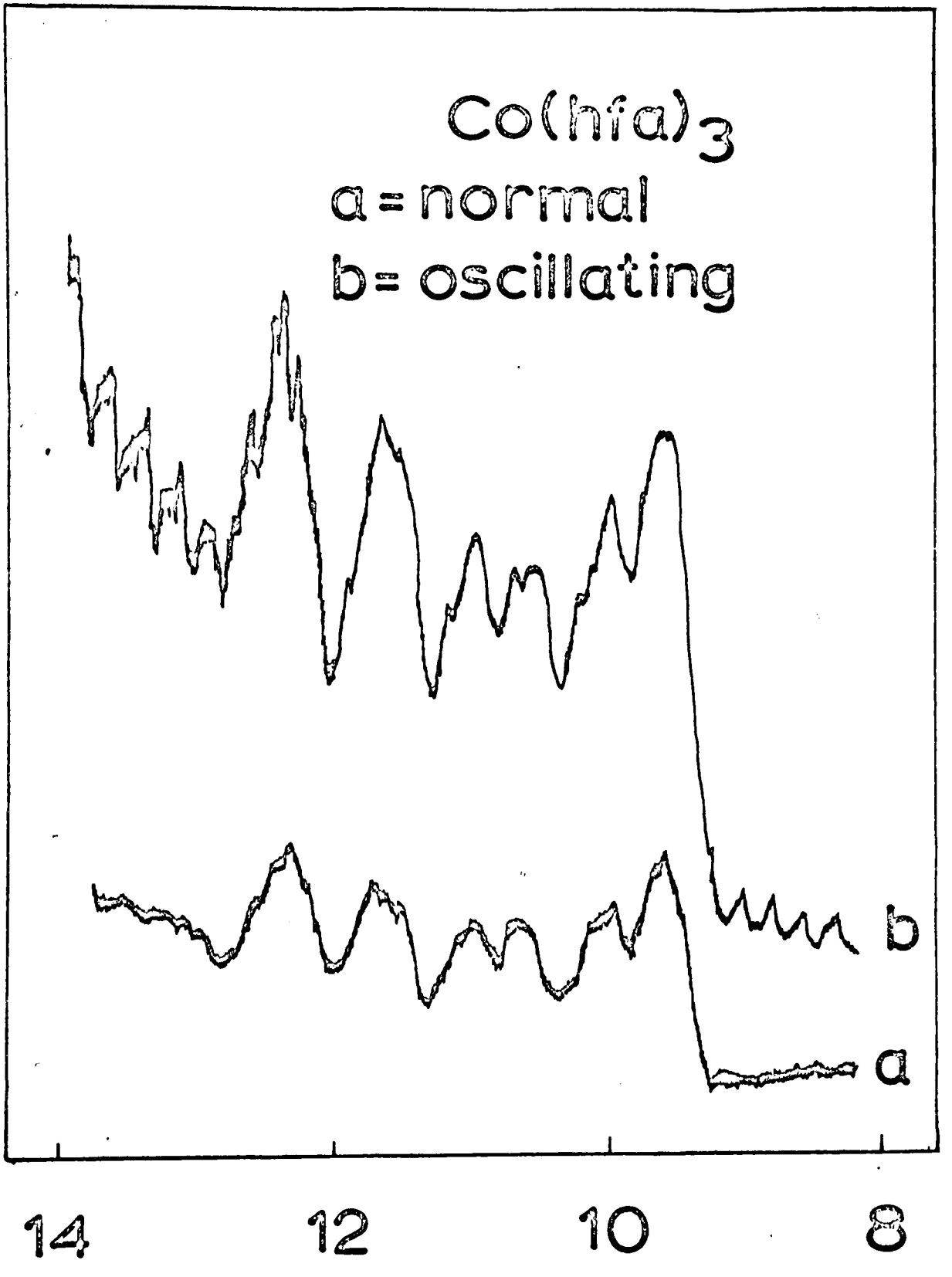

diffuses down the collimating capillary of the lamp, thus preventing back diffusion of the metal chelate into the discharge area. However, the periodic nature of the effect remains unexplained. It may be that an autoionisation resonance can occur. Rydberg levels are sensitive to pressure (as is the He(I) line itself, very slightly) and it is possible, as Smith[17] has pointed out, that at low helium pressures, and hence low target chamber pressures, there is an autoionising level at precisely the frequency of the He(I) line. The oscillation may then be the result of a slow cycling effect in the rotary pumping system. The fact that such oscillations in the spectrum have only been observed clearly for $Co(hfa)_3$ is then understandable. Russian workers[18] who have also noted this effect, attributed it to secondary transient effects within the lamp, though the origin of these effects was not discussed. A possibly related phenomenon is the very high background sometimes obtained with a variety of compounds. With some of those containing hydrogen, the explanation seems to be that decomposition of the compound occurs in the target chamber, and the hydrogen liberated diffuses into the discharge region giving rise to an intense Lyman-α emission. The effect may, in some cases, be ameliorated by increasing the helium flow rate as above.

A second effect, which has proved rather more troublesome,

arises from adsorption of molecules onto the carbon-soot surfaces. As a result, the surfaces cease to be equipotential, and the resulting fringing effects cause a progressive deterioration in both the sensitivity and resolution. It is curious that only a very few compounds are adsorbed to the extent where such effects can be observed; thus tris(hexafluoroacetylacetonato)manganese(III) gave rise to a rapid and complete loss of signal and indeed, a satisfactory spectrum could not be obtained using the laboratory spectrometer. An attempt was made to obtain the spectrum on a commercial PS-15 spectrometer, which has gold-coated analyser plates, but the compound was found to attack the plate multiplier used in the instrument irreversibly. Thus, two spectra of this compound have been reproduced, but neither is particularly satisfactory. Other compounds which have had this effect include cobaltocene and a number of transition-metal organometallic derivatives containing cyclopentadiene and carbon monoxide as ligands. Some improvement could be obtained by warming the whole spectrometer to 60°C, but no higher a temperature could be used since the channeltron series of multipliers employed developed a large background count rate above this temperature. Unfortunately, 60°C was not high enough to cause the desorption of $Mn(hfa)_3$ though cobaltocene could be run quite easily at 50°C. Characteristically, complete

recovery of the machine occurred after pumping overnight.

A third, and catastrophic effect has been occasionally noted. The main symptom is a steady loss in sensitivity without a concomitant loss in resolution. No recovery occurred, even after prolonged pumping and it seems that irreversible attack of the coatings of the multiplier by certain compounds may take place. Again, no consistent chemical pattern can be distinguished, and it seems that a different set of compounds attack plate multipliers. One substance that was found to cause severe though not permanent damage in this way was VCl_4, but RuO_4 caused a very permanent loss of sensitivity, presumably because it attacked the layer of hydrocarbon on the surface of the multiplier. Very recently, $Os(hfa)_3$ was found to raise the threshold operating potential of the multiplier rapidly on being introduced into the spectrometer, and no explanation of this remarkable effect has been found.

Finally, a minor problem in UV-PE work, though a major one in ESCA, is the question of the calibration of the spectra. In He(I) work, this is achieved by measuring the ionisation energies of the three inert gases, argon, krypton and xenon. Their ionisation potentials may be accurately determined from atomic spectral data and the three together provide a check on the absolute values of the observed ionisation energies

and on the linearity of the scale. However, it was observed that certain compounds caused a substantial shift in the apparent positions of these ionisation potentials, presumably by some kind of reversible adsorption on the carbon coatings, which, whilst large enough to cause a shift, is not sufficiently large to cause the effects discussed above. This means that the calibration of all the spectra had to be made simultaneously, both the inert gas and the sample being fed in at the same time.

The X-ray photoelectron spectra were obtained using the commercially available AEI ES 100 spectrometer, which was modified as described below. The design of the source chamber is shown in fig. 2.2. It is machined out of a stainless steel block which is sealed to the analyser at the top and to the X-ray source at the bottom. All seals are UHV compatible, using compressed gold wire, though the normal operating pressure in daily use has been only ca. 10^{-7} torr. The X-ray gun is fed by a standard Elliott power supply and transformer which delivers 15 - 20 mA at 15 - 20 kV, though the power drawn has never been greater than 300 watts. The filament supplies are also fed from the same power unit through separate leads not shown on the diagram, which give about two amps., and the normal lifetime of the filament appears to be about three months. Experiment has shown that the alignment of the filament is critical but unfortunately there seems at the moment to be no simple method, other than by trial and error, of determining the position of optimum alignment. Electrons released from the filament and accelerated through 15 - 20 kV bombard an aluminium anode; the X-rays produced from the Al KLL transition have an energy of 1486.6 eV with a fwhm* of 0.85 eV. The very large number of scattered

---

* full width at half-maximum height

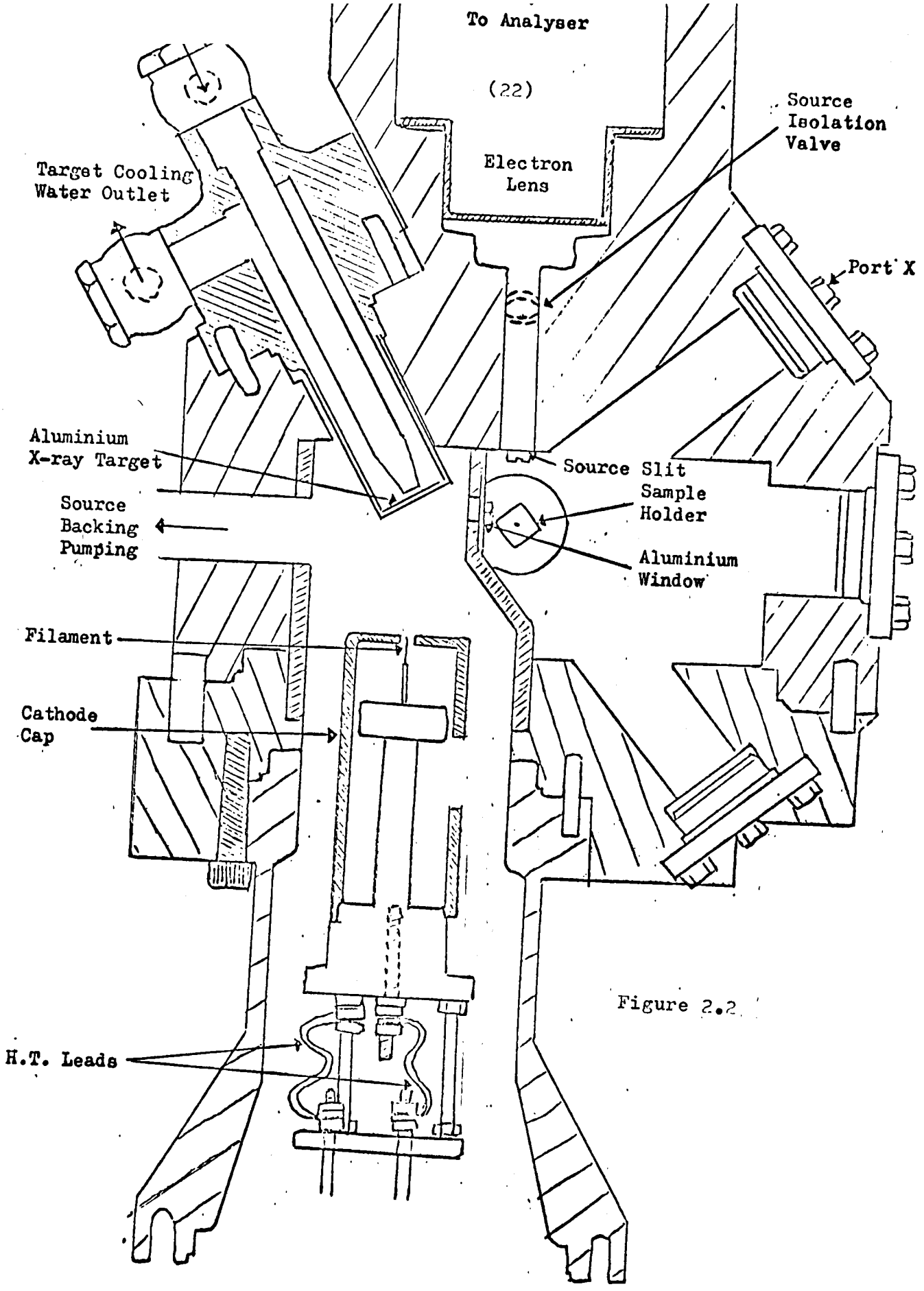
To Analyser
(22)
Source Isolation Valve
Electron Lens
Target Cooling Water Outlet
Port X
Aluminium X-ray Target
Source Slit
Sample Holder
Source Backing Pumping
Aluminium Window
Filament
Cathode Cap
H.T. Leads

Figure 2.2

and secondary electrons are filtered out by an aluminium window 0.0003 inches thick, though this in turn produces a substantial number of secondary electrons which flood the sample. Photoionised electrons pass through a slit at earth potential and then through an isolation valve into a lens system which retards them to one-twentieth of their initial kinetic energy. The scanning mode is a simple deflection type on the analyser plates operating at the necessary reduced voltage, this scan system being fed from a power feed which also supplies the X-axis of the pen-recorder.

Unlike UV-PE spectroscopy, the sample is examined in the solid state. In the simplest possible mode of operation, the sample is introduced by first grinding it into a powder and fixing it to a solid copper probe by double-sided Scotch Tape. The probe arrangement is then introduced slowly into the vacuum lock and subsequently pumped down and driven through a Goddard bellows valve into the main source chamber. Experiments performed with this method have, however, indicated that it is not entirely satisfactory, and for volatile samples a second mode of operation was used, in which the probe was first pushed into position and then cooled by a thermostatted liquid nitrogen bleed. A cylindrical tube was introduced through a second vacuum lock which replaced port X and, attached to the outer end of this tube was a specially

constructed adaptor to which could be fitted a standard sample tube. Continuous bleed of the sample vapour allows the surface of the sample to be clean at all times, and experiments have shown that only micrograms of the sample are normally required.

Photoionised electrons are detected by a Mullard channeltron multiplier of the same type as that used on the UV-PE spectrometers, and the signal from this is fed via a simple pre-amplifying circuit into standard Nuclear Enterprises counting equipment consisting of ratemeter, timer and scalar. A function on the analyser drive supply allows point plotting to be done by stepping the scan voltage. A major instrumental problem is the very low signal/background ratio inherent in the technique. Background arises mainly from the bremstrahlung X-radiation produced classically from the deceleration of the electrons on striking the target, and modern instruments employ a primitive form of X-ray monochromatisation giving much better S/B ratios. Because of the low S/B ratio, very slow scanning is frequently essential, and the spectra of most compounds may take several days to obtain. To preserve the vacuum when the machine is used with a continuous bleed of the sort discussed above, a cryotip is employed to act as a sink, and the machine must be baked out frequently. Since the Goddard valves have nylon seats, these must first be

removed and replaced by blank-flanges before bake-out is commenced. The source and analyser are then warmed to 180°C slowly and uniformly, and the system left pumping for at least 24 hours. Owing to the very large heat capacity, a further 48 hours of pumping are usually necessary to recover the vacuum in the analyser, though the source can be pumped out much more rapidly.

To measure the spectra of less volatile materials, a sample holder is available from AEI which consists of a hollow brass capillary rod into which the sample is driven, the whole then being placed in a cylindrical heating jacket which can be introduced into the source region through a Goddard valve. The maximum temperature attainable is about 400°C. A sample tip was manufactured to provide an eccentric nozzle which could be directed onto the surface of the probe, and this was tested out with $HgCl_2$. However, it was found that the vacuum lock assembly did not have a sufficiently linear drive to accommodate the whole heatable probe assemblage and so, before the initial tests, the Goddard valve was replaced by a UHV-compatible mass-spectrometer inlet valve which consisted of a ball joint separately pumped on either side, the low vacuum side being roughed out and the high vacuum side pumped by a trapped Edward's one inch oil diffusion pump backed by an ED 50 rotary pump. The whole assembly took

several days to pump out, and the vacuum lock facility was lost, so that rapid change-over of compound in the holder was not possible. The rather poor resolution in the mode may be due to the difficulty experienced initially in controlling the temperature, or possibly to the inductive effect of the heater itself, and further experiments are essential before any conclusions concerning the viability of the mode can be drawn.

A number of very serious problems have arisen over the few years in which solid state X-ray photoelectron spectroscopy has been used as a physical technique. Of considerable interest is the actual effective sampling depth.[3,19] Under normal circumstances the maximum depth from which a photoionised electron may escape is considerably less than 100 Å. Non-quantum effects in scattering cause a considerable loss in intensity of the primary electrons even at depths of 20 or 30 Å, especially for the very intense sharp peaks such as those from F 1s or Au 4f, and metals seem to be particularly opaque to the photoelectrons. A corollary of this is that surfaces studied must be scrupulously clean, and, fortunately, for inorganic systems, an immediate check is provided by the C1s peak derived from impurity hydrocarbons on the surface of the sample. The large cross-section of C1s means that this is quite a sensitive test, and almost all powders run

on gauze or tape are found to exhibit strong contaminant lines from carbon and oxygen. Initially, with the machine running at rather poor vacuum, such peaks often dwarfed the remainder of the spectrum, and the surface layer of contaminant usually reduced the count level of the whole sample very substantially. Apart from the inconvenience entailed in running spectra under such poor S/B conditions, little credence can be attached to early valence region studies, since that part of the spectrum is dominated by C 2s and O 2s and 2p. Considerable improvement in the situation was effected after about eight months of operation when the vacuum lines were carefully cleaned and baked and a large cryotip was inserted into the source chamber. This resulted in a much cleaner vacuum and the growth in hydrocarbon contamination on the surface of the sample was reduced to negligible proportions. However, although this has reduced the most serious effects of contamination, there clearly remain some doubts as to the reliability of valence region scans.

A second serious problem is the damaging effect of X-radiation on many samples. Although no general predictions can be made as to which compounds are likely to be sensitive, some types of compound appear to be particularly susceptible. Many metal halides suffer extensive damage due to the induced

formation of free halogen which is rapidly pumped away. In this category of course come the silver halides and, interestingly, those of gold (compare the Edwardian gold tints in early photography). We have, for example, examined the spectrum of $CsAuCl_4$, which shows a strong time dependency; the Au 4f peak, which is initially seen as a clean doublet, splitting slowly into a triplet with an extra band at lower binding energy, which presumably arises from metallic gold or Au^I. A second effect, observed with KCl, is the trapping of photoelectrons in vacant sites giving rise to Farben-centres. The sample, when withdrawn, was bright blue in colour and the count rate had slumped dramatically. After exposure to air for some time, however, the crystals became colourless again, as expected. A similar observation on crystals of the tris(dipivaloylmethanato) complexes of the lanthanides may well have the same explanation, though it may be that induced fluorescence is responsible.

In an attempt to overcome these problems, a method was devised for running volatile solids which is described above. The test compound chosen for the pilot experiments was tris(hexafluoroacetylacetonato)chromium(III), since the carbon 1s signal is very characteristic, and the metal levels extremely weak. The first figure (2.3) shows an attempted run on adhesive tape. No cryotip was used here

Figure 2.3

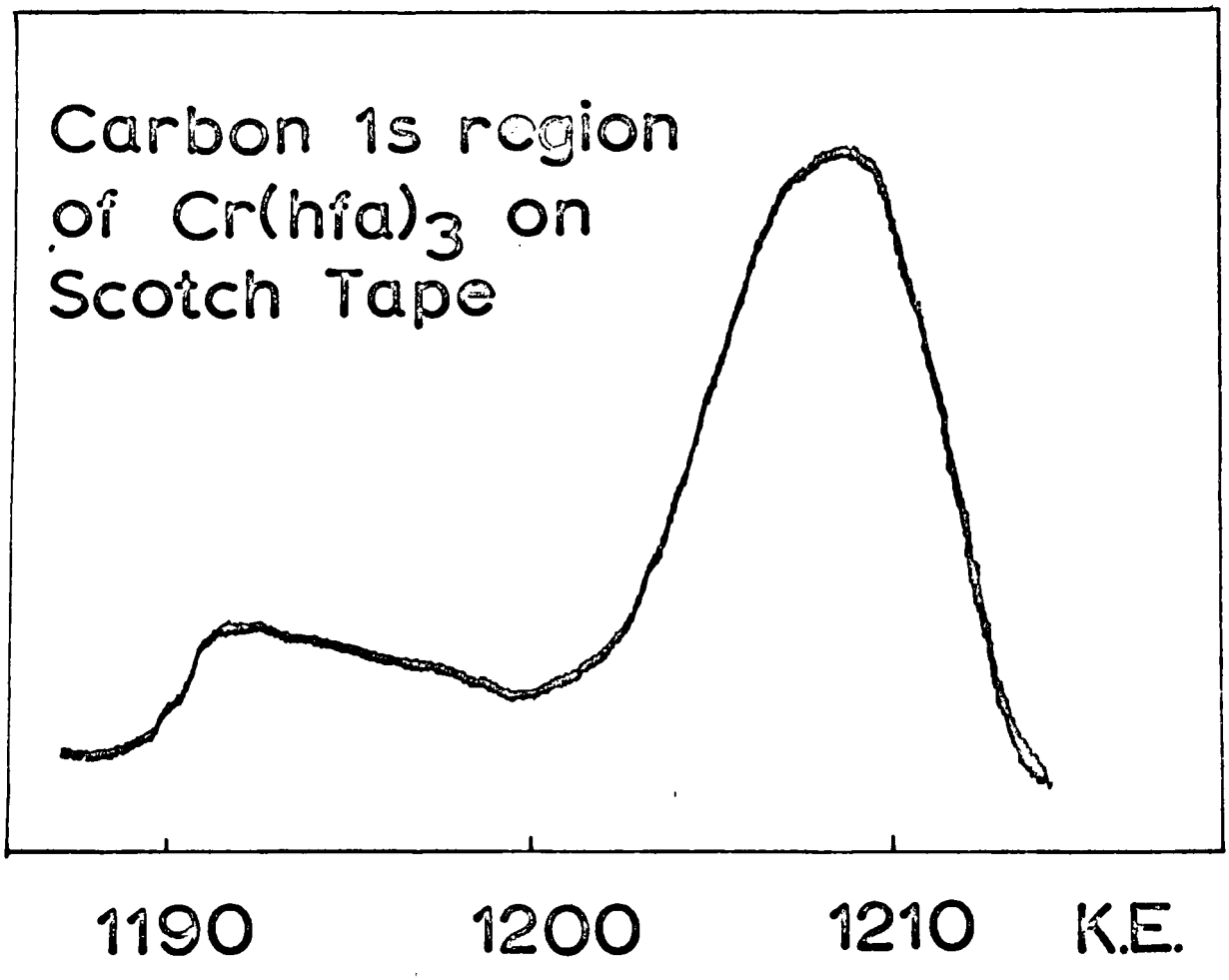

and the carbon signal is seen to be exceedingly ill-resolved. The high volatility of the compound, moreover, was such that it rapidly sublimed off the probe-head and attempts to reduce the rate of sublimation by cooling the probe lead to the complete obliteration of the sample signal, and its replacement by that of hydrocarbon contaminant. In consequence, a bleed experiment was set up in which the cryotip was also installed. This latter was cooled to liquid nitrogen temperature and the bleed was directed onto the probe head which was held at -120°C. Gradually increasing bleed rates were employed and the figures show a slow decline in the intensity of the low binding energy peak. Increasing the bleed rate beyond that for the last spectrum resulted in very little further change in the relative energies and intensities of the three peaks and it was deduced that this represented a situation in which the contribution from hydrocarbon contaminant to the total C 1s signal was negligible. Following this, the contamination from O 1s (almost entirely due to water vapour slowly desorbing from the stainless steel walls of the source region) was examined. It proved very difficult to gauge the extent of this contamination since the O 1s signals from the sample and contaminants were effectively degenerate and the relative intensities of the F 1s and O 1s signals of the pure material

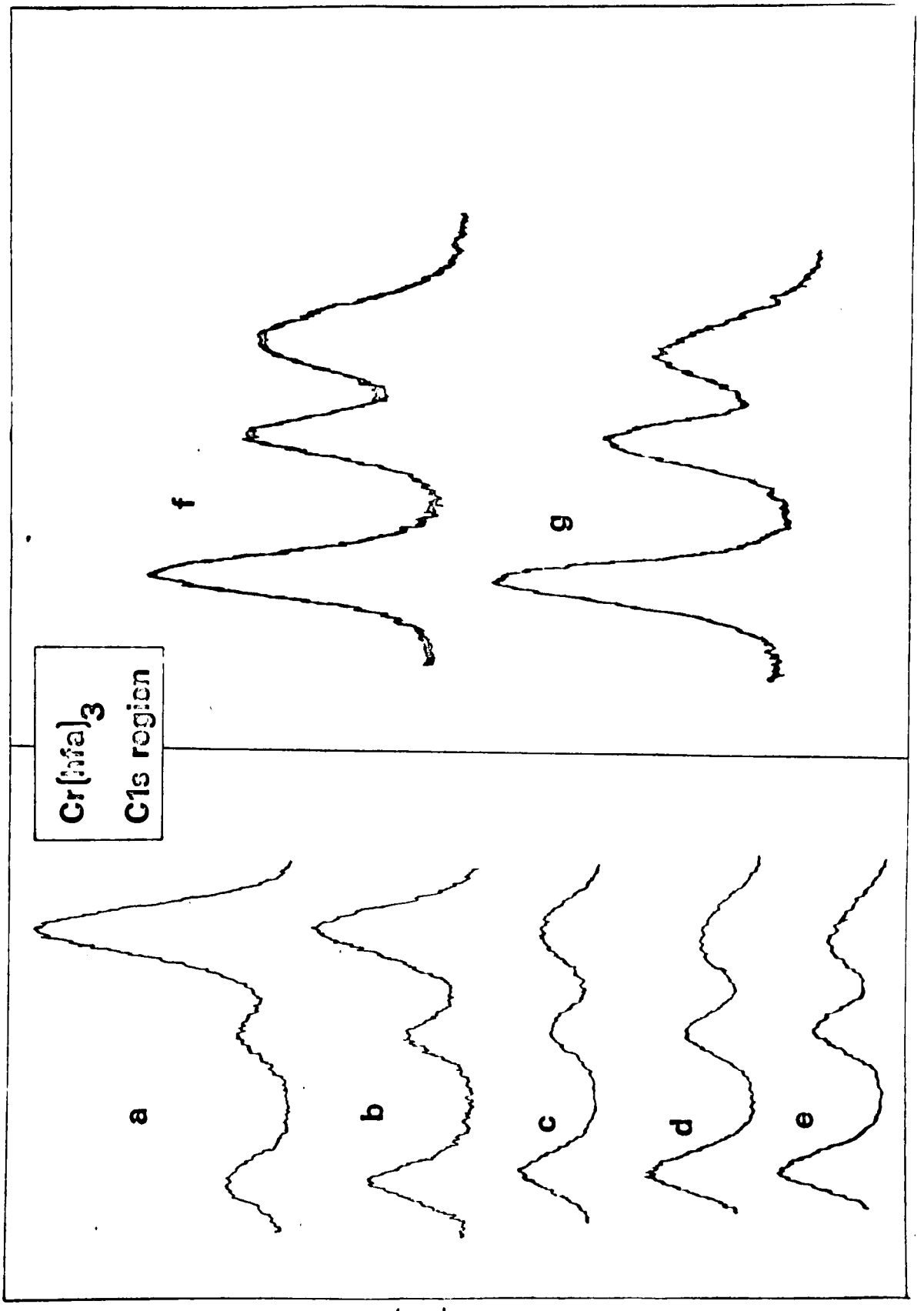

FIGURE / 2.4

were unknown. At length, the following procedure was tried: the whole machine was carefully baked out and the stainless steel inlet pipe rigorously dried in an oven. A pure, dry sample of the most volatile member of the series, $Fe(hfa)_3$, was prepared by multiple sublimation and transferred to a previously flamed-out glass sample tube attached directly to the inlet tube. The spectrum was then run under a very fast bleed rate and the measured F 1s/O 1s ratio taken as standard. For the other compounds, it was found that, provided the inlet tube was pumped overnight before a spectrum was run, little trouble was experienced. Exceptions, however, were $Ti(hfa)_3$, which crystallised in a rather involatile form, and $V(hfa)_3$ which was initially contaminated with traces of $VO(hfa)_2$. Less of a problem was presented by the metallocenes, which were also run in this mode, since for these, the bleed rate was adjusted until the oxygen signal had vanished. The only serious problems were experienced with $Mn(\pi Cp)_2$ which sublimed as the brown, highly involatile form, and all efforts to reduce the O 1s signal to below ca. 10 cps proved unsuccessful. However this represents only about 0.5% of the intensity of the main C 1s peak and this level of contamination is probably tolerable, though by no means satisfactory. To check that both carbon and oxygen peaks could be eliminated, a volatile

tetrahalide was also run in this mode. Figure 2.5 shows the spectrum of $TiBr_4$ run under precisely the same conditions as those chosen for $Cr(hfa)_3$. As can be seen, there is no trace of oxygen and probably none of carbon 1s either, though it is difficult to be certain, since the C 1s signal would occur just where the shadow peak from Br 3s is observed. The very clear Ti ionisations should also be noted. It is in fact very difficult to conceive of any other way of satisfactorily running a compound such as $TiBr_4$, which would certainly attack Scotch Tape, even if the very considerable sample handling problems involved in depositing the powder on tape in the first place could be overcome.

The fact that manganocene was effectively limited by volatility, lead to the introduction of a heated probe system which is also described above. This has a temperature range of up to ca. 400°C and should serve to obtain the spectra of complexes as involatile as the thallous halides by the condensation method. Unfortunately, some teething problems have been experienced with the device but the spectrum of $HgCl_2$ obtained in this fashion was encouraging in that it showed no lines ascribable to oxygen or carbon, figure (2.6).

Finally, though most important in ESCA, is the problem

FIGURE 2.5

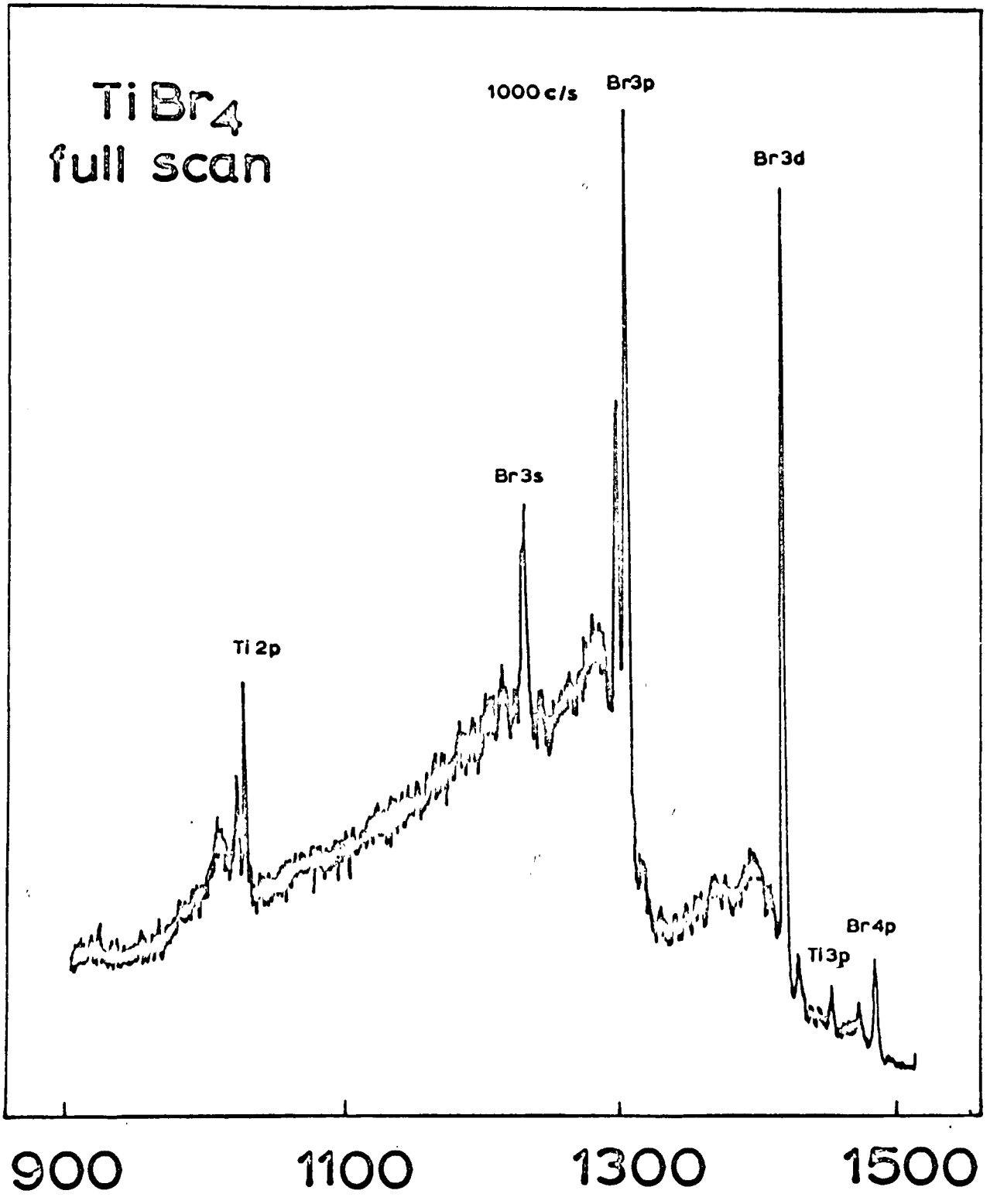
TiBr4
full scan
1000 c/s
Br3p
Br3d
Br3s
Ti2p
Br4p
Ti3p
900
1100
1300
1500

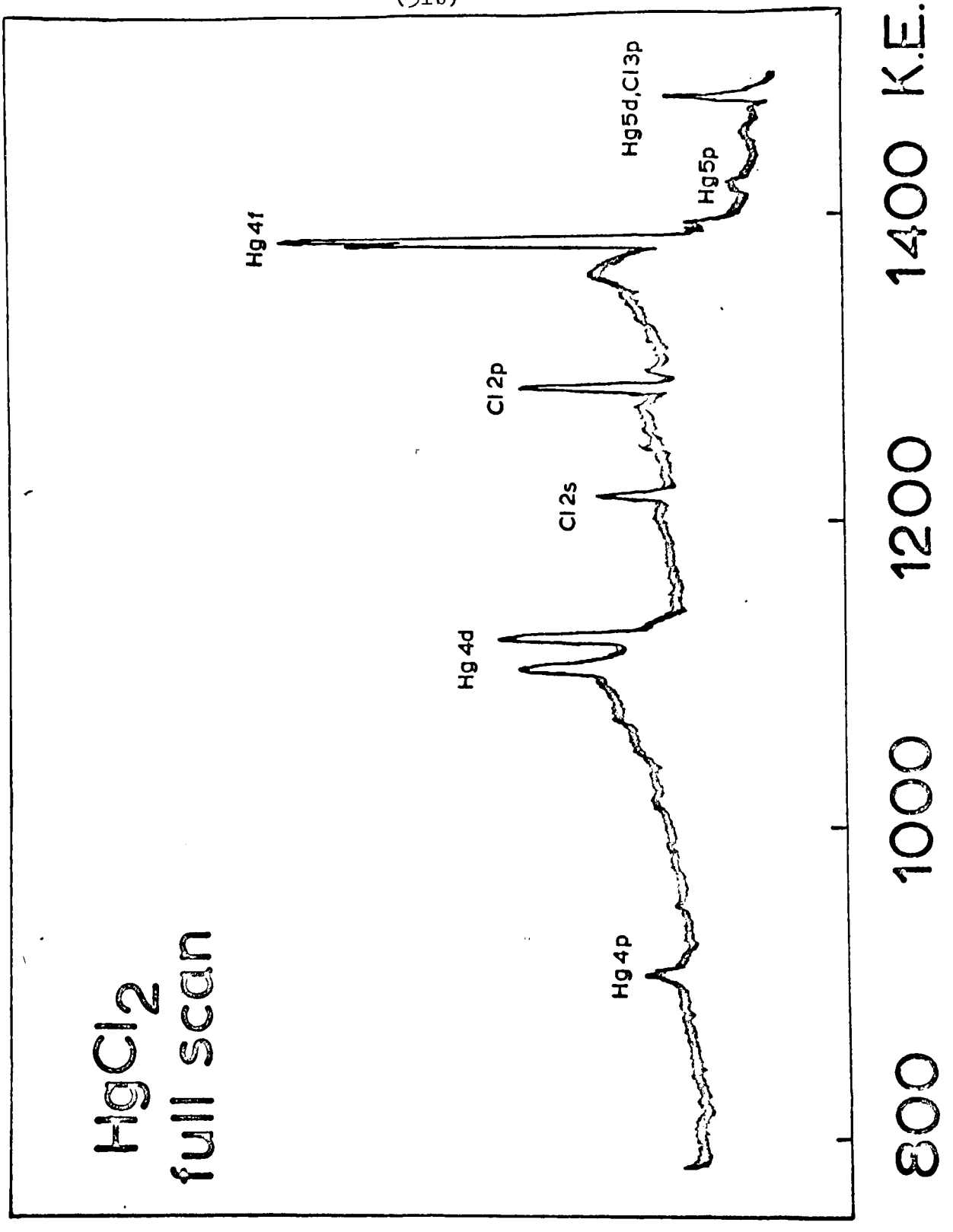
HgCl2
full scan
Hg 4p
Hg 4d
Hg 4f
Cl 2s
Cl 2p
Hg5p
Hg5d,Cl3p
800
1000
1200
1400 K.E.

FIGURE 2.6

of accurate calibration. Unlike UV-PE studies, there are no completely independent sets of data available for comparison which do not suffer from lack of accuracy or from surface effects comparable to ESCA. The original assignments of ESCA spectra were based on X-ray emission work but in many cases the very low cross-sections inherent in ESCA lead to rather doubtful, highly 'optimistic' assignments which subsequent work has shown to be untenable.

The problem is basically to decide to what extent surface charging occurs as a result of electron depletion through the photoionisation effect. In these considerations, the bleed-in method may be ignored, since the extremely thin layers deposited and the continuous replenishment of the surface both imply a negligible charging effect. This is supported by the fact that the line widths in condensed samples are usually no larger than those of the corresponding free metals. The situation is rather different with powders spread on Scotch Tape, since variations in the thickness of the layer may play a significant part in line broadening. However, even for these charging effects may be quite small, since there are two ways in which the sample may be neutralised

(i) Under the influence of X-radiation, the polymeric deposits constituting Scotch Tape become much more

conducting, and so electrons may pass from the earthed probe to the sample. This is not so surprising as it sounds, since the currents involved are very small, and if the resistivity of the tape dropped to 10^{12} ohms only a small p.d. would be necessary to ensure sufficient current flow.

(ii) A second mode of neutralisation is from low energy electrons in the source chamber which arise either from the aluminium window through X-ray irradiation or from the sample as photoionised electrons reflected from the walls of the source.

To test these hypotheses several experiments were performed. A metal sample was first attached to the probe and the whole electrically insulated from the source. A bias voltage was then applied to the probe and, as expected, the apparent binding energy of the electrons varied, being greater for a positive bias and less for a negative bias. The variation was in fact linear with a proportionality constant of unity. A second experiment was then made in which a piece of metal foil was attached to the probe with Scotch Tape. On the application of a positive bias, the apparent binding energy again became larger, but this time, although the variation was linear, the proportionality constant was only 0.7. On applying a negative bias a very

curious effect was observed. Basically, the binding energy became larger, though very much more slowly, following an approximately 5/2 power law until the biasing voltage reached about -60 volts, whereupon the variation became roughly linear with a ratio of 0.2. Now these results are very difficult to understand unless there are at least two neutralising mechanisms as discussed above. In so far as conduction may occur through Scotch Tape, it is unlikely to be ohmic in nature and in fact is likely to show space-charge limited behaviour, as indeed will neutralisation from athermal electrons in the source region. This would imply that a fairly complex dependence on the probe voltage is to be expected. In qualitative terms, we can see that at a positive probe bias, since the potential at the surface of the sample is smaller than that on the probe, electrons will flow through the Scotch Tape from the sample. However, since the probe and sample are becoming more positive, more electrons from the source will be attracted to the sample, offsetting to a certain extent the photoionisation current and the probe current. Thus, as the probe voltage V_p increases, the sample voltage V_s will also increase, though at a slower rate. If the probe voltage becomes negative, electrons will flow from the probe to the sample. However, electrons will now be repelled from

the probe region, and the effective neutralisation of the sample by athermal electrons will no longer take place to the same extent. It appears from the results that this latter is the more important contribution to the sample neutralisation, but a more quantitative assessment of these figures must await more detailed information on the electrical behaviour Scotch Tape when irradiated with X-rays.

The calibration of the ESCA spectra of the hexafluoroacetylacetonato complexes proved rather problematical. If we assume that the condensed sample is at the same potential as the probe, which is very probable since the sample layer is probably less than 1000 Å thick, then two means of calibration are possible:

(i) the co-condensation of a tiny quantity of some chemically inert gas or volatile liquid

(ii) the simultaneous measurement of a sample line and one from a thin underlying strip of metal such as gold.

Method (ii) is quite difficult to achieve in practice, since the gold line is obliterated rapidly as the sample is fed in, but calibration was achieved in this way for $Cr(hfa)_3$ after extensive experimentation with bleed rates. From what has been said above, the layer of sample on the gold surface was probably less than 20 Å thick, so that

perfect electrical contact was obtained. Thus we can refer all the peaks in the $Cr(hfa)_3$ spectrum to a common gold peak. However, the problem remains as to the exact value of the spectrometer work function which will determine the absolute energy scale of the results relative to the vacuum level. Even if we knew this, since the Fermi level of a molecular crystal is a completely undefined quantity, we cannot consider that it in any way equalises with that of the spectrometer. If we could measure the surface BE when completely isolated in the solid state, the binding energies obtained would refer directly to the vacuum level and so, assuming that the only effect of a thin layer of the sample is to ensure that a definite potential is imposed on the surface, then measuring relative to the gold peak gives a definite line from a sample of known binding energy relative to the same potential, namely, the contact potential between the gold sample and the spectrometer. It will readily be perceived that as the layer thickens, the potential on the sample will change from that on the gold probe to that of earth. It appears however that this potential is fortuitously small in the case of gold or copper and stainless steel. Having in this way obtained a binding energy for the F 1s and C 1s of the $Cr(hfa)_3$ $\underline{C}F_3$- group, these were then assumed to be at constant binding energy for the other

tris-hexafluoroacetylacetonates. Although this assumption is open to criticism, it is probably reasonably valid within the general inaccuracies of the technique. The principle of using an invariant chemical label to calibrate ESCA spectra of other groups of compounds has been used before; thus the triphenylphoshine complexes may be calibrated from the phenyl C 1s bands.[20]

Chapter three
EXPERIMENTAL SECTION

Please do not shoot the pianist:
He is doing his best.

Oscar Wilde
Impressions of America

PREPARATION OF THE SAMPLES INVESTIGATED IN THIS THESIS

Although very many TM chelates have been investigated and their volatility characteristics determined, only those compounds whose spectra were actually measured are discussed here.

1. The preparation of the tris-hexafluoroacetylacetonato complexes.

Many of these are either unknown in the literature, or else poorly described, and synthetic methods had to be found to generate the compounds in sufficient yield for measurement.

(i) Synthesis from the anhydrous trihalides.[21,22,23]

The complexes of Al(III)[21], V(III), Ti(III)[22], Fe(III)[23] and Ga(III) were synthesised directly from their respective trihalides. The synthesis of $Ti(hfa)_3$ will serve as an example.

A suspension of dry $TiCl_3$ was dispersed in dry degassed cyclohexane under nitrogen. The suspension was then chilled, the containing vessel evacuated, and free hexafluoroacetylacetone distilled onto the surface from a separate test-tube kept at 0^oC. Roughly 3 moles of hfaH was added per mole of trihalide, a slight excess usually being employed, since the free ligand is a powerful water-scavenger. Instead of cyclohexane, benzene can be used, but, owing to the difficulty of

drying halogenated solvents, chloroform and carbon tetrachloride were not employed, save in early syntheses of $Fe(hfa)_3$, which is much less water sensitive than the others.

The chilled mixture of ligand and trichloride suspension was then allowed to warm up under a slight positive pressure of dry nitrogen, and the reactants thoroughly mixed. The flask was then cautiously warmed with frequent vigorous shaking until effervescence had ceased (usually two to three hours). After the flask had cooled, it was rapidly transferred from the reflux condenser to a sublimation tube and the solvent and excess ligand cautiously removed under vacuum over a period of about two hours. Attempts to remove the solvent at a faster rate always lead to pronounced bumping, possibly because of occluded HCl.

$$MCl_3 + 3CF_3COCH_2COCF_3 \rightleftharpoons M(CF_3COCHCOCF_3)_3 + 3HCl$$

When the reaction mixture had been thoroughly pumped dry, the required compound could be sublimed under high vacuum at ca. 40°C. Usually triple sublimation sufficed to purify the complex adequately, but in some cases, especially with $V(hfa)_3$, further purification steps were needed (see below).

In general, the yield from these reactions, based

on the trihalides, is extremely high and the purity of the chelates was checked by mass-spectrometry and infra-red spectroscopy. It was found impossible to check the purity by elemental analysis, since standard analytical methods give erratic and non-reproducible results for both hydrogen and carbon. This may be due to a failure to break down the C-F bonds completely, and other workers have also commented on this aspect of fluorocarbon chemistry. Fortunately, the cracking patterns of the tris-chelates are highly characteristic, as are their infra-red spectra, and only $Ga(hfa)_3$ gave an anomalous mass-spectrum. To discover whether the sample of $Ga(hfa)_3$, prepared from Ga_2Cl_6, contained any chloro-complexes as impurities, a second sample was synthesised from Ga_2Br_6 which, however, was identical to the first sample in physical properties and UV-PE spectrum. The different cracking presumably reflects the rather different bonding in $Ga(hfa)_3$ though a mass-spectrum of $Al(hfa)_3$ was not measured, since this latter compound is very well known in the literature[21] and its other physical properties exhaustively characterised.

$V(hfa)_3$, and, to a lesser extent $Ti(hfa)_3$, presented rather special problems. In spite of all

attempts to exclude water, a small quantity of $VO(hfa)_2$[14] always formed, presumably from small quantities of hydrate in the commercially supplied VCl_3. $VO(hfa)_2$ has similar volatility characteristics to $V(hfa)_3$ and sublimes as a light green microcrystalline solid. Separation was finally achieved by extremely slow fractional sublimation in a closed system, followed by hand-picking the large lustrous brown crystals of $V(hfa)_3$. Resublimation gave a pure product which was stable indefinitely under vacuum. In the case of $Ti(hfa)_3$, the main impurity was yellow $[TiO(hfa)_2]_x$ which is a comparatively involatile polymer and easily separated by fractional sublimation. The pure product in this case however is extremely sensitive to heat and to air and careful handling was essential.

(ii) Synthesis from the hydrated halides.

This was only attempted for $Sc(hfa)_3$, since $ScCl_3.6H_2O$ was the only scandium compound available and is not easily dehydrated. Furthermore, anhydrous $ScCl_3$ is known to be rather unreactive and the preparation described below would probably not work. The solvent used here was benzene, since experiment had shown that a very efficient azeotrope system could be set up.

Hexafluoroacetylacetone reacts with free water to form the dihydrate as a white, fairly involatile solid, and, when the benzene, hfaH and $ScCl_3.6H_2O$ mixture was refluxed, water was azeotroped into the condenser and there reacted with the concentrated vapour of the free ligand (which is the most volatile component of the mixture) depositing the hydrate on the walls of the condenser. Provided only gentle refluxing conditions were employed, the hydrate was not washed down into the flask so that, in effect, water was continuously removed from the mixture. A large excess of the ligand was necessary in this preparation and the yields were not very high. The product when isolated was very volatile, but rapidly hydrated in air, giving a less volatile form which decomposed on warming in vacuo. A recent paper has suggested an alternative route in which the hydrate, made by standard methods, was dehydrated by P_2O_5 in vacuo.[25] Experience with drying $Cu(hfa)_2.xH_2O$ suggests however that this method is unlikely to be much improvement since the volatile anhydrous chelate tends to sublime onto the drying agent and decompose.

(iii) Synthesis of $Cr(hfa)_3$[4]

Several literature methods exist for synthesising

this well known compound, and the best available appears to be the reduction of K_2CrO_4. Hexafluoroacetylacetone is a powerful reducing agent, a fact which makes the preparation of $Co(hfa)_3$ from a cobaltous salt and hydrogen peroxide extremely hazardous[26], and, on mixing 5 mmoles of hfaH and 1 mmole of dry K_2CrO_4 a vigorous reaction occurred on warming, generating green $Cr(hfa)_3$ and a variety of other products. The product mixture was extracted with boiling CCl_4 and the extract evaporated to dryness in air. The crude complex was recrystallised twice from CCl_4 and resublimed twice onto the sides of a sublimation tube, whence it was removed by scraping. Finally, the complex was slowly sublimed in a closed flamed-out system and sealed off. The melting-point and i.r. spectrum agreed well with previous workers and the compound appears to be stable indefinitely.

(iv) Synthesis of $Mn(hfa)_3$

This compound proved rather difficult to synthesise initially and several different methods were tried. The only literature method appears to be ligand exchange with tris(1,1,1 trifluoro 2,4-pentanedionato)manganese (III), $Mn(tfa)_3$[27]. This compound can be prepared by Cartledge's synthesis[28], in which a mixture of an

aqueous Mn(II) salt and the free ligand at pH 5 is oxidised by $KMnO_4$: $Mn(tfa)_3$ precipitates as a black solid in poor yield. Cartledge's method does not work at all for $Mn(hfa)_3$ and $Mn(hfa)_2.2H_2O$ is thrown down before $KMnO_4$ is added. The ligand exchange was accomplished by dissolving $Mn(tfa)_3$ in pure hexafluoroacetylacetone and throwing out the $Mn(hfa)_3$ with petrol. Unfortunately the yield was extremely poor and the method is too costly to generate $Mn(hfa)_3$ in sufficient quantity.

The anhydrous trichloride $MnCl_3$ is unstable above -40^oC which is too low a temperature for the reaction to occur, but K_2MnCl_5 may be synthesised quite easily by reducing $KMnO_4$ with concentrated HCl and cooling to 0^oC whilst passing HCl through the mixture. The compound is very dark in colour but smelled so strongly of chlorine that further synthetic work was abandoned.

By analogy with the preparation of $Cr(hfa)_3$ described above, it was thought that reduction of $KMnO_4$ with free hexafluoroacetylacetone might generate $Mn(hfa)_3$. For this reaction 6 mmoles of the free ligand which had been dried before use were added to dried $KMnO_4$ with careful safety precautions being

taken. A rather slow reaction occurred when the mixture was gently warmed, and the liquid turned black in colour. Excess ligand was removed under vacuum and an attempt was made to sublime the residual solid material. Small quantities of $Mn(hfa)_3$ could be obtained in this way but the preparation was not sufficiently reliable or repeatable for use as a synthetic method.

Finally it was decided to use the basic properties of Mn_2O_3 (braunite). To a suspension of Mn_2O_3 in petrol was added an excess of free ligand. The mixture was sealed off with a glass-stopper and shaken at frequent intervals for fourteen days. The resulting solution was decanted and the black $Mn(hfa)_3$ recrystallised from petrol at $-80^{o}C$. It was then transferred to a sublimation tube under N_2 and sublimed twice, the second time into a flamed out section of glass tubing which was sealed off under vacuum. The large, jet-black lustrous crystals had the same physical properties as those described in the literature[27]; the yield was about 50% based on Mn_2O_3 and the preparation is quite reproducible. As indicated above, the compound had a rather dramatic effect on the UV-PE spectrometer though its ESCA spectrum was measured

without difficulty.

(v) Synthesis of $Co(hfa)_3$.

As stated above, this compound cannot be safely prepared by oxidation of Co(II) to Co(III) in the presence of the ligand. The only stable trihalide of Co(III) is CoF_3 which is reasonably reactive so that the literature method[29] is based upon the scheme

$$CoF_3 + 3NaF + 3CF_3COCH_2COCF_3 = Co(CF_3COCHCOCF_3)_3 + 3NaHF_2$$

Pure hexafluoroacetylacetone was dried by shaking with conc. H_2SO_4 and then distilled. NaF was dried by baking in an oven for two hours and cooling in vacuo, and CoF_3 was dried by pumping in a flamed-out vessel.

A solution of NaF in hexafluoroacetylacetone was made up under N_2 and added to the CoF_3. The mixture was then gently warmed to 35°C and left for twenty-four hours by which time a dark green colour had developed. After excess ligand had been removed under vacuum, the residue was carefully sublimed to yield dark green crystals of $Co(hfa)_3$, whose physical properties were identical to those described in the literature. The compound is very water sensitive, decomposing rapidly to orange $Co(hfa)_2.2H_2O$, but seems

to be reasonably stable under dry nitrogen.

(vi) Synthesis of $Ru(hfa)_3$.

The literature method[39] involves refluxing $RuCl_3$ in concentrated HCl with hexafluoroacetylacetone, neutralising the resulting solution with $NaHCO_3$ and steam distilling out the $Ru(hfa)_3$. There are several disadvantages to this preparation: the yields are extremely small since the equilibrium

$$RuCl_3 + 3hfaH \rightleftharpoons Ru(hfa)_3 + 3HCl$$

is well to the left in conc. HCl. Secondly, during the neutralisation stage it is essential to warm the solution since $Ru^{3+}aq.$ reacts extremely slowly. Neutralisation is indicated by the development of a maroon colour, but the endpoint proved remarkably difficult to determine with accuracy.

The insolubility of $RuCl_3$ in organic solvents precluded any of the techniques described above and finally a rather complex two phase synthesis was tried. An aqueous solution of $RuCl_3$ and a benzene solution of hexafluoroacetylacetone were mixed and refluxed in air for twenty-four hours. Periodically, the reflux condenser blocked with a white deposit of the ligand dihydrate which was pushed back into the reaction mixture. After the flask had cooled, equal

volumes of benzene and water were added and the whole transferred to a separating funnel where the benzene fraction was removed. The aqueous layer was further extracted with 5 equal volumes of benzene and the benzene extracts were all recombined in a flask connected to a sublimation tube. After removal of the benzene under vacuum, sublimation of the residues gave red microcrystalline $Ru(hfa)_3$ in good yield. The preparation clearly works because the equilibrium described above is disturbed by the extraction of $Ru(hfa)_3$ into the benzene phase as it forms. The complex is air and water stable and has the properties described in the literature.

(vii) Synthesis of $Os(hfa)_3$.

Attempts to prepare this compound by the same method as used for $Ru(hfa)_3$ failed, possibly because the compound is more sensitive to air and water. The $OsCl_3$ supplied by Johnson-Matthey was soluble in THF and so a mixture of $OsCl_3$ and hexafluoroacetylacetone was refluxed for several days in THF. No change was observed however in the colour of the solution and no volatile products could be extracted. Finally, by analogy with the preparation of $Cr(hfa)_3$, it was decided to mix OsO_4 and hexafluoroacetylacetone

together in an inert solvent (petrol) as diluent. A mixture of OsO_4 and petrol was chilled and hexafluoroacetylacetone distilled onto the surface. Then, very cautiously, the mixture was allowed to warm up to room temperature and was left standing under nitrogen for fourteen days, during which time it steadily darkened through maroon to black. After this period the solution was gently warmed to complete the reaction and then recooled to room temperature. On removal of solvent under vacuum a dark red oily residue was left which slowly crystallised on pumping. The compound proved to be very sensitive to air and could only be identified spectroscopically.

3. The preparation of the acetylacetonato complexes. Only four of these were made since the spectra, especially in the low binding-energy region, strongly resembled those of the corresponding hexafluoroacetylacetonato complexes.

(i) Synthesis of $Fe(acac)_3$.

This was prepared by a standard literature method from freshly prepared $Fe(OH)_3$ and acetylacetone.[31] The brick-red crystals recrystallised from benzene had physical properties identical to those described in the literature. In common with other acetylacetone complexes, it showed a tendency to decompose in the vapour phase at temperatures above ca. 150°C and so

sublimation was only used as a last purification step before the spectrum was measured.

(ii) Synthesis of $Cr(acac)_3$.

This complex was also prepared by a standard literature method.[31] An aqueous solution of $CrCl_3$ and urea was boiled with free acetylacetone overnight and the purple crystals were purified by recrystallisation.

(iii) Synthesis of $Mn(acac)_3$.[28]

This was prepared by Cartledge's method described above and the black crystals recrystallised from benzene.

(iv) Synthesis of $Be(acac)_2$.[32]

This was prepared by the literature route from basic beryllium carbonate and its physical properties were in agreement with those found by other workers. The compound is, of course, highly toxic, and special precautions were taken during handling. The laboratory was carefully tested after the synthetic work on this compound to ensure that no beryllium residues were ingrained into the fume-cupboard desk.

4. The preparation of the complexes of trifluoroacetylacetone $CF_3COCH_2COCH_3$.

$Fe(tfa)_3$ was synthesised by the literature method;[33] it is thrown down as a red solid on addition of the free ligand

to a solution of $FeCl_3$ buffered with sodium acetate. Owing to the unsymmetrical nature of the ligand, two geometrical isomers, the cis and trans forms are possible

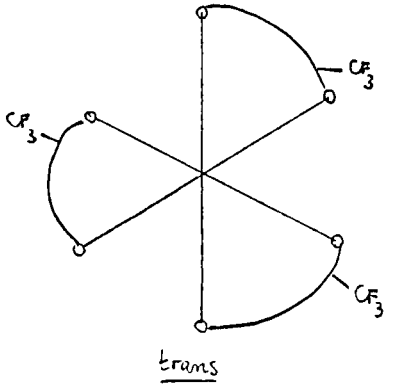

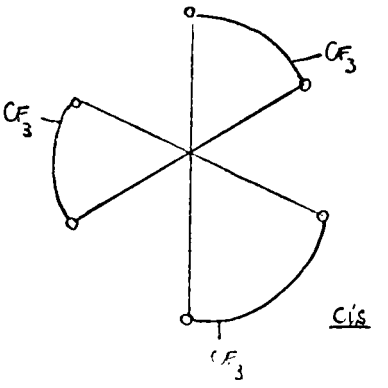

Clearly both can exhibit optical isomerism. In fact, nmr ^1H and ^{19}F evidence strongly suggests that the compound $Fe(tfa)_3$ is highly labile and is synthesised mostly in the trans form. The statistical ratio of trans to cis forms is 3:1 but experimentally it appears that the ratio is very much higher. The other tris-trifluoro-acetylacetonato complexes whose spectra are reproduced are $Al(tfa)_3$ and $Cr(tfa)_3$. The aluminium complex, like that of Fe(III) is labile but $Cr(tfa)_3$ gives two stable isomers, the cis being formed in 17% yield by the method of Piper and Fay. No data is available on the relative volatilities of these two forms, though it is likely that the trans form is the more volatile on the basis of the dipole moment.

5. The preparation of the complexes of dipivaloylmethane $Me_3CCOCH_2COCMe_3$.

(i) Complexes with the transition metals.

These were all made by the methods described by Hammond et al.[34], though in many cases the solvent used, especially the proportions of ethanol and water, had to be varied by trial and error to optimise the yield. The only complex whose UV-PE spectrum was obtained was $Fe(dpm)_3$ prepared by the addition of an ethanolic solution of the free ligand to a buffered aqueous Fe(III) solution. The solvent used to recrystallise the complex was 60-80 petroleum ether, since the original suggestion by Hammond et al. of DMF has the disadvantage that DMF itself is a powerful complexing agent. Indeed the tris-dipivaloyl complexes of the rare earths originally reported by these authors are in fact DMF adducts. The recrystallised $Fe(dpm)_3$ was cautiously sublimed at 120°C before its UV-PE spectrum was examined.

Experimentally, the bis-dipivaloylmethanato complexes of the first transition series have the advantage over the corresponding hexafluoroacetyl-acetonato complexes of having known, well defined structures and being monomeric even in the solid

state. Thus $Ni(dpm)_2$ is a red, square-planar diamagnetic solid and $Co(dpm)_2$ is tetrahedral.

(ii) Complexes with the lanthanide metals.

A number of these were prepared for study by both ESCA and UV-PE and the method of synthesis is a minor modification of the method of Eisentraut and Sievers.[35] An ethanolic solution of Na^+dpm^- was made up and a solution of the lanthanide trinitrate hydrate in 50% ethanol was added rapidly. A pale coloured precipitate usually appeared at once and the solution was rapidly degassed in the usual way to avoid air oxidation of the rather sensitive dipivaloylmethane. At this stage the complex frequently oiled out and rapid stirring for several hours was usually essential to redisperse the oil and obtain a filterable suspension. It was found advisable to have slightly less than the equivalent amount of dipivaloylmethane since this did prevent oiling in a few cases. After the reaction was complete, normally after some twelve hours' stirring, about half the solvent was removed under vacuum and the residue thrown into ten times its own volume of boiled out distilled water. At this stage also oiling out tended to occur, especially with $Nd(dpm)_3$ and

$Yb(dpm)_3$ and, in these cases, instead of filtering, the oil was extracted into chloroform and recrystallised from this solvent under vacuum. The solid filtrate from the other preparations was dried in air and transferred after grinding to a sublimation tube. After pumping at 10^{-3} torr for at least four hours and preferably overnight, the sample was warmed to 120°C at 10^{-3} torr and left for several hours to complete the drying process. When thoroughly dry, the sample was further warmed to ca. 140°C and a slow sublimation over a period of about five hours (of gramme quantities of the chelate) effected. This usually left a fine powder as residue (presumably small quantities of the lanthanide oxide) and sublimations were repeated until all the compound sublimed cleanly. In this pure state the compounds were rather sensitive to surface decomposition by water vapour and were stored under dry nitrogen until required.

The purity of the complexes was checked by elemental analysis and infra-red and mass spectra. The infra-red spectra however bore a remarkable resemblance to one another and were used chiefly as markers for water contamination. One compound,

$Nd(dpm)_3$, gave some trouble since it appeared to exist in two different crystalline forms, one purple and one blue. The analytical results for both forms were the same and agreed with an empirical formula $Nd(dpm)_3$ and no evidence could be found to suggest that one of the forms might be $Na^+Nd(dpm)_4^-$. Of interest perhaps here is the fact that such complexes are known for hexafluoroacetylacetone and appear furthermore to be fairly volatile, presumably subliming as ion-pairs.

Structural studies on the lanthanide dipivaloylmethanato complexes are rather inconclusive. Incomplete X-ray work on $Pr(dpm)_3$ indicates that the substance is a dimer whereas two later lanthanide complexes appear to crystallise as monomers. No gas-phase structural work has been attempted as yet, though there seems to be no reason why these substances should not sublime as monomers. Owing to the low volatility of the complexes, UV-PE spectra had to be determined using a heatable metal-probe arrangement supplied by Perkin-Elmer Ltd., and I am grateful for the assistance of Dr. J. N. A. Ridyard in obtaining the spectra of $La(dpm)_3$, $Pr(dpm)_3$ and $Ho(dpm)_3$.

The ESCA spectra of the metallocenes were obtained for the most part on samples donated by other members of the group to whom I would like to record my thanks. All were resublimed before use and transferred, if necessary, to fresh sample tubes. Cobaltocene was prepared in collaboration with Dr. W. E. Silverthorn by a novel synthesis. Hydrated cobalt chloride was dried by warming to 180°C overnight in vacuo and then taken up into dry THF. Previously purified thallocene was then added in solution and the TlCl thrown down was removed by filtration under nitrogen. The THF filtrate was then transferred, pumped dry, and the residues extracted with petrol in which thallocene is insoluble. The petrol extracts were then, in turn, pumped dry and the residue sublimed as black lustrous crystals. Physical properties were in accord with samples of cobaltocene prepared previously by the normal route (reaction of sodium cyclopentadienide with anhydrous cobalt dichloride) and the ESCA spectrum confirmed the identity of the crystals.

Chapter four
Interpretation of the UV-PE spectra

It is as true as taxes is. And nothing's truer than them.

Charles Dickens
David Copperfield

DISCUSSION OF THE UV-PE SPECTRA OF THE TRIS CHELATE COMPLEXES

Before considering the spectra in detail, it is necessary to develop a suitable theoretical model as an aid to interpretation, since the more usual assignment criteria are not helpful for such large complexes. Having used such a model to gain an initial impression of the orbitals whose ionisations give rise to the often intricately structured low ionisation energy (IE) region, the assignment may be checked by examining trends within the series, and it will be seen that an internally self-consistent picture can be built up which sheds new light on the chemistry and bonding in transition metal complexes.

The model to be used arises naturally out of the group-overlap approach to bonding which has been used to help in the interpretation of the non-metal halides.[36,37] Since we will not in general be concerned with spin-orbit coupling considerations in the early part of this chapter, the model will be developed from a simple MO viewpoint. The essential feature of the method is to build up from the individual MO's or AO's molecular orbitals which transform as irreducible representations of the overall molecular point group. Consider the i^{th} component of an MO transforming as Γ_k ; the wave function is given by

$$|\pi_{ki}\rangle = N^{-\frac{1}{2}} \sum_j c_{ij}^k |j\rangle$$

where $|j\rangle$ are the isolated ligand orbitals used to construct $|\pi_{ki}\rangle$ and c_{ij}^k the symmetry determined expansion coefficients, $N^{-1/2}$ the normalising factor.

The orbital energy of $|\pi_{ki}\rangle$ is given by

$$E_{ki} = \langle \pi_{ki} | \mathcal{H} | \pi_{ki} \rangle = N^{-1} \sum_{j,l} \bar{c}_{ij}^k c_{il}^k \langle j | \mathcal{H} | l \rangle$$

we can immediately find N^{-1} from

$$\langle \pi_{ki} | \pi_{ki} \rangle = 1 = N^{-1} \sum_{j,l} \bar{c}_{ij}^k c_{il}^k \langle j | l \rangle$$

thus finally

$$E_{ki} = \frac{\sum_{j,l} \bar{c}_{ij}^k c_{il}^k \langle j | \mathcal{H} | l \rangle}{\sum_{j,l} \bar{c}_{ij}^k c_{il}^k \langle j | l \rangle}$$

The Hamiltonian $\mathcal{H}$ used is in reality a one-electron Fock operator, and E_{ki} a one-electron orbital energy, which, by Koopmans' theorem, may be subsequently equated with the ionisation energy of orbital $|\pi_k\rangle$ (with, of course, a suitable change of sign).

The expression for E_{ki} can be simplified considerably by introducing the following approximations:

let $\langle j | \mathcal{H} | j \rangle = \varepsilon_m$ where m is an index referring to

the nature of orbital $|j\rangle$, e.g. s, p_σ , p_π etc.

and $\langle j|\hat{\eta}|l\rangle = \eta_{mn}\langle j|l\rangle$, if $|j\rangle, |l\rangle$ are on different atoms

$= 0$ if $|j\rangle, |l\rangle$ are on the same atom.

then immediately we have, from the fact that

$$\sum_j \bar{c}_{ji}^{k} c_{ji}^{k} = -$$

and that

$$\sum_{\substack{j,l \\ j\neq l}} \bar{c}_{ji}^{k} c_{li}^{k} \langle j|l\rangle = \chi'_{ki}$$

a value depending solely on the nature of the MO $|\tau_{ki}\rangle$

then

$$\sum_{j,l} \bar{c}_{ji}^{k} c_{li}^{k} \langle j|\hat{\eta}|l\rangle = \varepsilon_m + \chi'_{ki}\eta_{mn}$$

$$\sum_{j,l} \bar{c}_{ji}^{k} c_{li}^{k} \langle j|l\rangle = 1 + \chi'_{ki}$$

and

$$E_{ki} = \frac{\varepsilon_m + \chi'_{ki}\eta_{mn}}{1+\chi'_{ki}} \approx \varepsilon_m + \chi'_{ki}(\eta_{mn} - \varepsilon_m)$$

provided χ'_{ki} is small.

Empirically, it appears that $\eta_{mn} < \varepsilon_m$, so replacing $(\eta_{mn} - \varepsilon_m)$ by β_{mn} , we obtain

$$E_{ki} = \varepsilon_m + \beta_{mn}\chi'_{ki}$$

$\varepsilon_m, \beta_{mn} < 0$

This equation implies that the extent to which the energy of an isolated ligand orbital is altered on formation of the symmetry determined cluster is dependent on the extent to which this orbital overlaps with similar orbitals on different ligands. The subscript i may be dropped from the equation since all components of $|\sigma_k\rangle$ will have the same energy. Furthermore, clearly the orbital is stabilised for $\gamma_k > 0$ and destabilised for $\gamma_k < 0$. The evaluation of the γ_k for the orbitals required in our analysis will be given below.

In general, there will be more than one orbital transforming as σ_k and it is necessary to consider the interaction between these. In order to do this we may use the technique of matrix perturbation theory.

Consider a matrix M such that

$$M = M^+$$

and let M have eigenvectors c_i such that

$$Mc_i = \lambda_i c_i$$

Since M is Hermitean, the λ_i are real, and

$$c_j^+ M c_i = (c_i^+ M c_j)^+ = \lambda_i \delta_{ij}$$

where δ_{ij} is the Kronecker symbol.

Now, if the matrix may be written as

$$M = M_o + M'$$

where M' has elements small compared to M_o, and the

eigenvectors of M_o are c_i^o a simple perturbation expansion can be developed, giving to second order in λ_i

$$\lambda_i = \lambda_i^o + c_i^{o+} M' c_i^o + \sum_n' (\lambda_i^o - \lambda_n^o)^{-1} (c_i^{o+} M' c_n^o)(c_n^{o+} M' c_i^o)$$

and to first order in c_i

$$c_i = c_i^o + \sum_n' (\lambda_i^o - \lambda_n^o)^{-1} (c_n^{o+} M' c_i^o) c_n^o$$

This can be very considerably simplified under the following special conditions: namely that we will take M_o to be a diagonal matrix and M to be a matrix possessing only small, off-diagonal elements. The c_i^o now become very simple in form since all elements of the vector are zero save only the i^{th} element which is unity. Further, the λ_i^o are the diagonal elements of M_o. It is clear, that if M' contains no diagonal element

$$c_i^o M' c_i^o = 0$$

$$c_i^o M' c_n^o = M'_{in}$$ the in^{th} element of M'

and so

$$\lambda_i = \lambda_i^o + \sum_n' \frac{(M'_{in})^2}{\lambda_i^o - \lambda_n^o}$$

$$c_i = c_i^o + \sum_n' \frac{(M'_{ni}) c_n^o}{\lambda_i^o - \lambda_n^o}$$

We have clearly effected a considerable simplification

in the matrix algebra; thus, consider two orbitals transforming as Γ_k and belonging to the same component (i) of Γ_k . Then, if we assume that $\Gamma_k(1)$, $\Gamma_k(2)$ derive from the same orbital type

$$|\Gamma_k(1)\rangle = (1+\chi_k(1))^{-\frac{1}{2}} \sum_j c_j^k(1)\,|j\rangle$$

$$|\Gamma_k(2)\rangle = (1+\chi_k(2))^{-\frac{1}{2}} \sum_l c_l^k(2)\,|l\rangle$$

$$E_k(1) = \varepsilon_m + \int_m \chi_k(1)$$

$$E_k(2) = \varepsilon_m + \int_m \chi_k(2)$$

The required off-diagonal element is given by

$$\langle \Gamma_k(1)|\mathcal{H}|\Gamma_k(2)\rangle = (1+\chi_k(1))^{-\frac{1}{2}}(1+\chi_k(2))^{-\frac{1}{2}} \sum_{j,l} \bar{c}_j^k(1)\, c_l^k(2) \langle j|\mathcal{H}|l\rangle$$

$$= E_k(1,2)$$

The energies of the states will then be given by the eigenvalues of the following matrix

$$\begin{pmatrix} E_k(1) & E_k(1,2) \\ E_k(2,1) & E_k(2) \end{pmatrix}$$

which are

$$E_k'(1) = E_k(1) + \frac{E_k^2(1,2)}{E_k(1)-E_k(2)} = \varepsilon_m + \int_m \chi_k(1) + \frac{E_k^2(1,2)}{\int_m (\chi_k(1)-\chi_k(2))}$$

and

$$E_k'(2) = \varepsilon_m + \int_m \chi_k(2) - \frac{E_k^2(1,2)}{\int_m (\chi_k(1)-\chi_k(2))}$$

From the discussion above it is clear that $E_k(1,2)$ is proportional to the overlap integral between $|T_k(1)\rangle$ and $|T_k(2)\rangle$ which can be written $S_k(1,2)$ and, if ξ_k is the required proportionality constant we have

$$E_k'(1) = \varepsilon_m + \gamma_{mk}(1) + \frac{\xi_k^2 S_k^2(1,2)}{\Delta_k(1,2)}$$

where $\Delta_k(1,2)$ is the energy difference of the unperturbed orbitals. In actual fact, the same formula can be obtained using Brillouin-Wigner perturbation theory when $\Delta_k(1,2)$ is the difference between $E_k'(1)$ and $E_k'(2)$ and this is probably more accurate.

By simple extension, if we have several orbitals all transforming as T_k, we obtain

$$E_k'(1) = E_k(1) + \sum_n \xi_k^2(1,n) S_k^2(1,n) \Delta_k^{-1}(1,n)$$

Thes formulae suffer from the general faults associated with any simple Huckel theory; it is only a well defined approximation for closed-shell molecules or open-shell systems which can be described by a single determinant, where ε_m may be unambiguously defined. For the more complex systems, the theory will not work in general, since, as for any Huckel theory, electron

repulsion may not be easily included.

The actual ε_m are also difficult to determine, since they are not orbital energies for the isolated ligands, but are corrected for charge and potential effects to give the self-consistent energies of the concomitant MO's. They are usually determined empirically, and much of the interpretation which follows is built up from a knowledge of the values of ε_m needed to account for such simple spectra as acetone and formaldehyde. It is clear that for metal complexes, the problem may be reduced to a pseudo-diatomic situation in which we consider the complete ligand system separately and the metal separately and then permit the two to interact.

We first consider the UV-PE spectra of the simple carbonyls.* Many of these contain the CH_3 fragment whose energy level scheme can be calculated quite simply and will serve to illustrate the algebra above. The hydrogen 1s orbitals transform in C_{3v} as $a_1 + e$, and the required symmetry orbitals are:

$$\varphi_{a_1} = \tfrac{1}{\sqrt{3}}(s_1 + s_2 + s_3) \qquad \chi'_{a_1} = 2S, \quad S = \langle s_1 | s_2 \rangle \text{ etc}$$

$$\varphi_e = \begin{cases} \varphi_e^x \left(\tfrac{1}{\sqrt{6}}(2s_1 - s_2 - s_3) \right) \\ \varphi_e^y \left\{ \tfrac{1}{\sqrt{2}}(s_2 - s_3) \right. \end{cases} \qquad \chi'_e = -S$$

Let S'_σ denote the overlap between the H s-orbital and the carbon p_σ orbital. Define x,y axes as shown in the figure,

* All the experimental IE's are given in table 4A at the end of this chapter.

with their origin at the central carbon, and let α be the semi-vertical angle

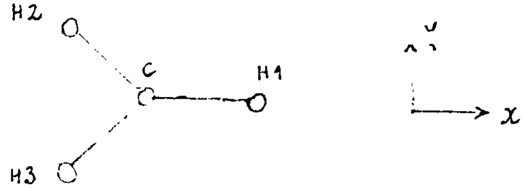

$$\langle \varphi_c^y | p_y \rangle = \sqrt{\tfrac{3}{2}} \sin\alpha \, S_\sigma'$$

$$\langle \varphi_x | p_x \rangle = \sqrt{3} \cos\alpha \, S_\sigma'$$

If we put $\alpha = 70^{\circ}$ (tetrahedral geometry) then we have, for the energy levels:

$$E_e'(C) = E_e(C) + \frac{1.32\, S_\sigma'^2 \beta^2}{E_e(C) - E_e(H)} \qquad E_{a_1}'(C) = E_{a_1}(C) + \frac{0.33\, S_\sigma'^2 \beta_\sigma^2}{E_{a_1}(C) - E_{a_1}(H)}$$

Giving a simple MO picture of the form shown, provided S_σ' is small

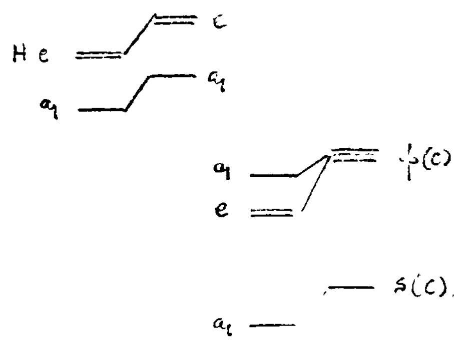

If now we add a fourth hydrogen to make methane, we must add $S_\sigma'^2 \beta^2 / (E_{a_1}(C) - E(H))$ to $E_{a_1}'(C)$, which will, approximately, give a_1 and e degenerate. The approximation arises because we have not considered the interaction of the fourth hydrogen with the other three.

Thus, we have built up a very simple picture of the bonding in the methyl fragment. Of course it is not quantitative and, unfortunately, epr data on CH_3 is not helpful since the isolated radical is apparently planar, though with a very small deformation constant. However it can be seen that the a_1 orbital is the only one greatly affected when methyl bonds in the fourth position and, to a good approximation the bonding e orbital should ionise from compound to compound at much the same energy of about 14 eV. Throughout the above analysis, the influence of the s orbitals on carbon has been neglected. This is because there is known to be a 10 volt gap between the p and s orbital ionisation energies in gaseous methane[37], but there are some circumstances in which the central carbon atom s orbital is strongly destabilised such as in neopentane by inductive effects where the s orbital must be considered as "true" valence orbital.

The main bonding of the CH_3 fragment will be through the a_1 orbital which will be labelled t_σ in the discussion below. The interactions of the e type orbitals of the fragment with the remainder of the molecule will not be considered since evidence suggests that hyperconjugation in the molecules considered is a small effect. It would of course be essential to include this effect in strongly

aromatic systems.

Consider now the formaldehyde molecule, whose UV-PE spectrum is given in fig. 4.1.[1] We have the following orbitals to consider

(i) The H 1s orbitals whose symmetric combination has a_1 symmetry and is given by

$$\varphi_{a_1} = \frac{1}{\sqrt{2}}(1s_1 + 1s_2)(1+S)^{-\frac{1}{2}}$$

and the antisymmetric combination of b_2 symmetry

$$\varphi_{b_2} = \frac{1}{\sqrt{2}}(1s_1 - 1s_2)(1-S)^{-\frac{1}{2}}$$

where S is the overlap integral $\langle s_1 | s_2 \rangle$.

(ii) The p orbitals on carbon and oxygen.

Taking axes as shown

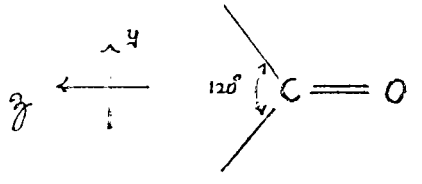

with x running out of the plane of the paper to complete a right handed set, we have p_x, p_y, and p_z transforming as b_1, b_2 and a_1 respectively.

Thus, in toto, we have 3 orbitals transforming as a_1, 3 as b_2 and 2 as b_1. The b_1 orbitals are straightforward, the energy of the bonding b_1 orbital being given by

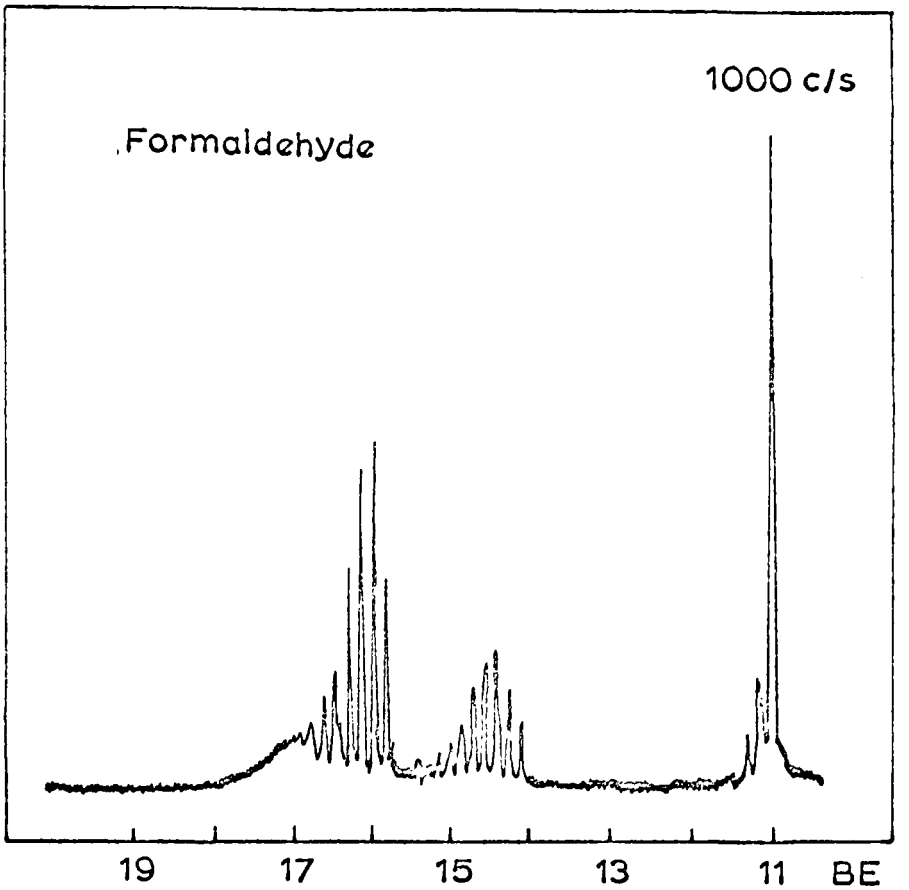

FIGURE 4.1

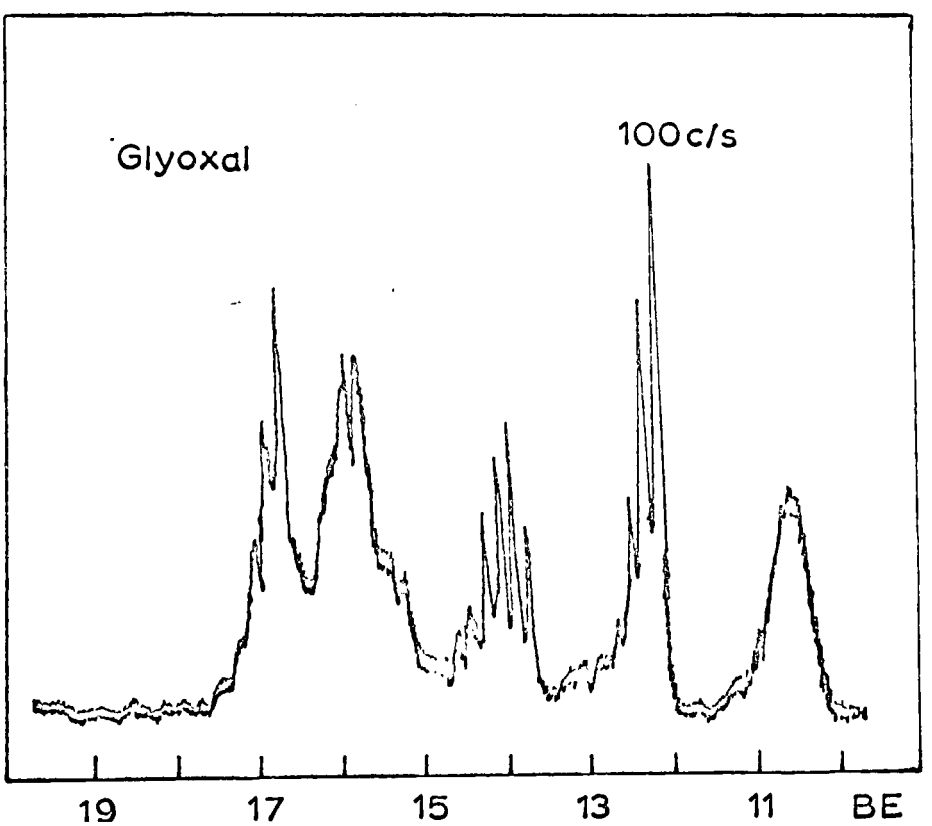

FIGURE 4.3

$$E(b_1) = \varepsilon_C(b_1) + \frac{\beta^2 S^2}{\Delta_{CO}}$$

where $\Delta_{CO} = \varepsilon_C - \varepsilon_O$ and it is assumed that $\varepsilon_C < \varepsilon_O$

Consider now the b_2 orbitals. There are three, whose energies are

$$E_1(b_2) = \varepsilon_C(b_2) + \frac{\beta^2 S^2}{\Delta_{CO}} + \frac{\beta^2 S^2}{2\Delta_{CH}}$$ assuming $\varepsilon_C < \varepsilon_H$

$$E_2(b_2) = \varepsilon_O(b_2) - \frac{\beta^2 S^2}{\Delta_{CO}}$$ assuming that the bonding between oxygen and hydrogen is negligible

$$E_3(b_2) = \varepsilon_H(b_2) - \frac{\beta^2 S^2}{2\Delta_{CH}}$$

Now, independent evidence exists to suggest that the highest occupied level in formaldehyde is a b_2 orbital[1] localised mainly on the oxygen atom. This must be $E_2(b_2)$ and so we know that

$$E_2(b_2) < E_3(b_2)$$

which suggests an ordering

$$\varepsilon_C < \varepsilon_O \lesssim \varepsilon_H$$

There are eight electrons only to be paired up in p-type and H 1s type orbitals, so there is only one occupied a_1 orbital which has an energy

$$E(a_1) = \varepsilon_C(a_1) + \frac{\beta^2 S^2}{\Delta_{CO}} + \frac{\beta^2 S^2}{2\Delta_{CH}}$$

Since S_σ is normally larger than S_π, we would expect

the ordering of levels to be

$$a_1 < b_2 < b_1 < b_2$$

Interestingly, this is precisely the ordering suggested by Turner on the basis of much more elaborate calculations and vibrational assignments. The method of overlap seems to be working quite well.

Turning to the spectrum of acetone (fig. 4.2), it can be seen that the first band has a very similar structure to that in formaldehyde, the splitting being about 1200 cm^{-1} suggesting that the C-C stretch or C-H bending modes have been excited. The excitation probability is obviously greater in the case of acetone suggesting a larger degree of delocalisation of the lone pair. It is also notable that the ionisation energy of this b_2 orbital in acetone is 1.1 eV lower in energy than the corresponding orbital in formaldehyde. The remainder of the spectrum is much less well-resolved save for a curious band at about 18 volts. Comparison of this band with bands in other hydrocarbons suggests two possibilities

(a) It is the predominantly C $2p_z$ a_1 orbital whose ionisation has excited a specific C-H bending mode at 1370 cm^{-1}. Such a situation is known for cyclopropane.

(b) It is the predominantly C 2s a_1 orbital, or a strong admixture of this and $2p_z$. Such s-type a_1 orbitals are

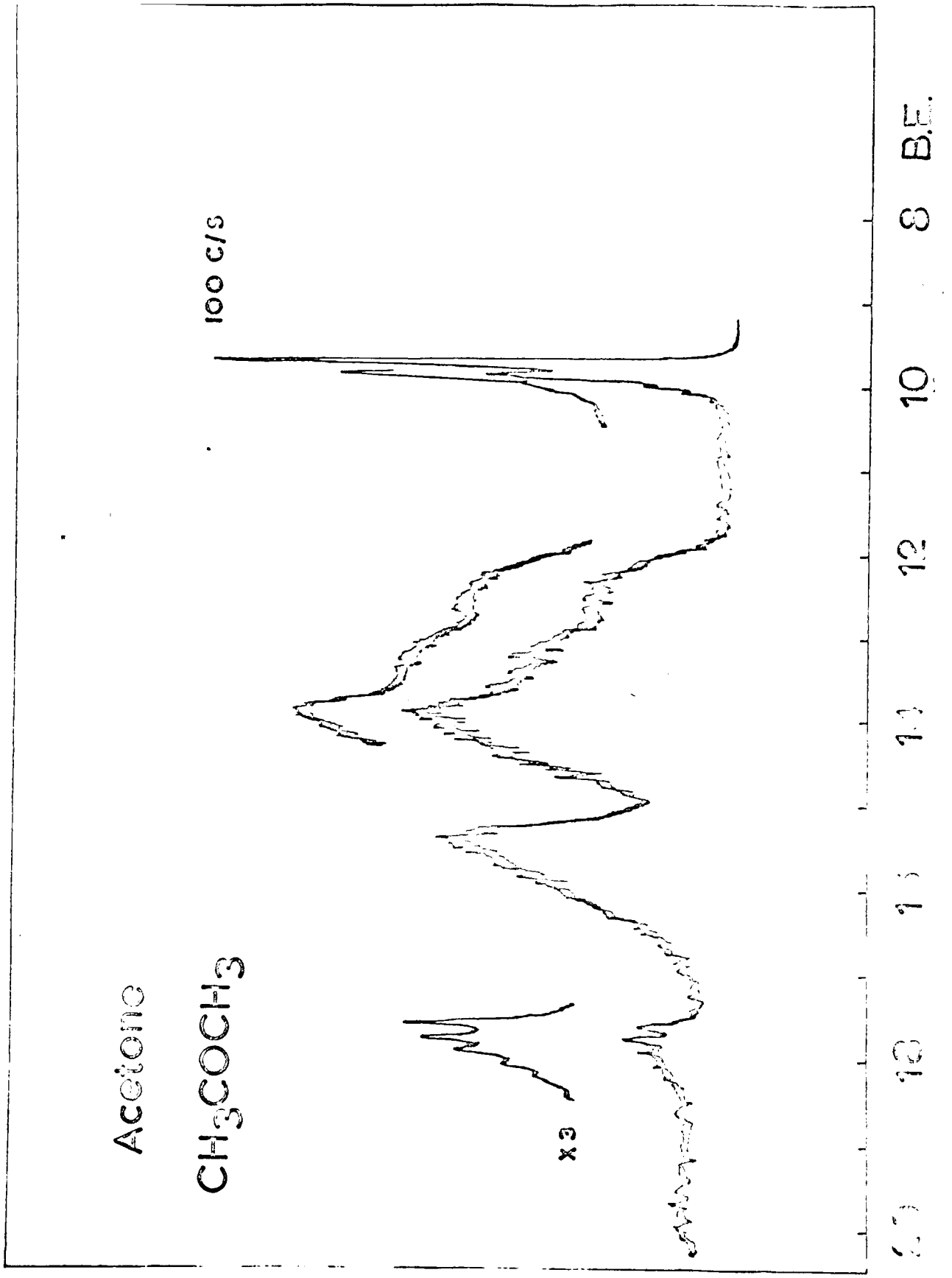

FIGURE 4.2

known to be structured from He II spectra, though it is difficult to see why it should be so destabilised. If possibility (a) is allowed, we must postulate very strong C-C bonding in acetone, since the a_1 orbital in formaldehyde is found at 17 volts.

The strong band at 15.6 eV in the spectrum can probably be assigned to the lowest b_2 bonding orbital which is π skeletal and mainly C-C-C bonding. It is also strong in formaldehyde which again suggests this assignment. The lone pair (b_2)/π-bond (b_1) splitting in formaldehyde is 3.2 eV, and, assuming that this is unaltered in acetone, the π-bond probably ionises to give rise to either the first or second of the three ill-resolved bands between 12 and 14 eV. Since we have assumed that the e orbitals of the two methyl groups do not interact to any great extent either with the framework of the molecule or with each other their most probable assignments are to the two bands at 13.3 and 14.0 eV, leaving the band at 12.6 eV to the π-band. Clearly this is only very approximate; these e orbitals must be split since the overall point group of the molecule is C_{2v}, which contains no degenerate irreducible representations. However we can say with some certainty that the methyl ionisations occur between 12.5 and 14.0 eV in acetone and do not greatly interact with the lone-pair.

More interesting is the consideration of the lone-pair interactions in the spectra of glyoxal and diacetyl. Both molecules have the trans configuration

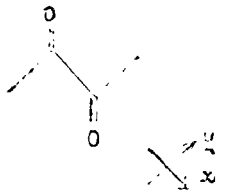

z-axis out of plane to define a right-handed set

The effective symmetry group is C_{2h} and again, in diacetyl, we will assume that the methyl groups bond via a_1 type orbitals which are labelled $t_\sigma(1)$ and $t_\sigma(2)$. The orbitals of the molecule can be partitioned immediately into two subsets: those lying in the x,y plane and those lying perpendicular to it and constituting the π-orbitals. The energy of the carbon π-orbitals is given by

$$\varepsilon_c \pm \gamma_c S_{\pi c}$$

and the levels are

$$E'_{a_u} = \varepsilon_c + \gamma_c S_{\pi c} - \frac{\beta_{co}^2 S_{\pi c}^2}{\varepsilon_c + \gamma_c S_{\pi c} - \varepsilon_o}$$

$$E'_{b_g} = \varepsilon_c - \gamma_c S_{\pi c} + \frac{\beta_{co}^2 S_{\pi c}^2}{-\varepsilon_c + \gamma_c S_{\pi c} + \varepsilon_o}$$

where it is assumed that the two O $2p_\pi$ orbitals do not interact directly with one another. If we assume that $\varepsilon_c < \varepsilon_o$ (in order that the top occupied level by mainly oxygen 'lone pair' in character), and that $|\varepsilon_o - \varepsilon_c| < |\gamma_c S_{\pi c}|$, then the lowest a_u level is pre-

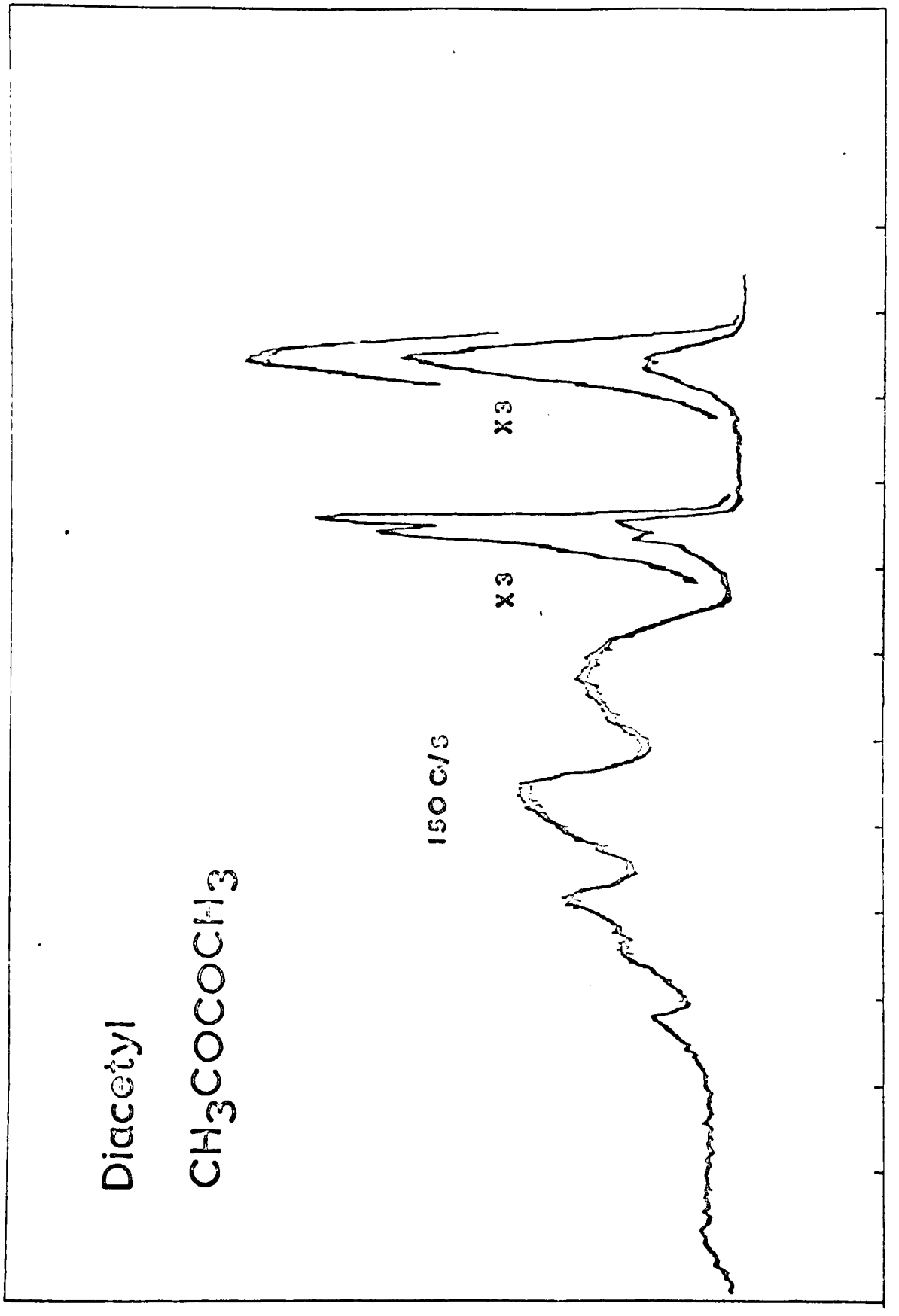

FIGURE 4.4

dominantly carbon in character and the next lowest b_g π level predominantly oxygen in character. That is, we have the π-MO scheme shown

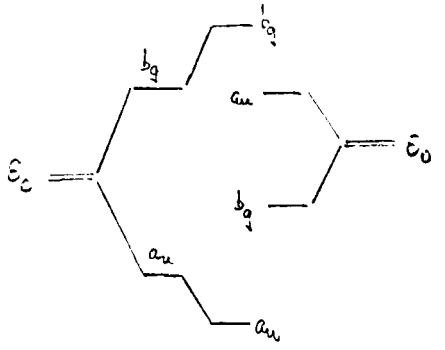

The antibonding a_u level has the orbital energy

$$\varepsilon_0 + \frac{\beta^2 S_{\pi}^2}{(\varepsilon_0 - \varepsilon_c) - \gamma_c S_{\pi c}}$$

and so the first $\pi \rightarrow \pi^*$ transition within the Huckel approximation has the energy

$$\frac{2\gamma_c S_{\pi c} \beta^2 S_{\pi}^2}{(\varepsilon_0 - \varepsilon_c)^2 - \gamma_c^2 S_{\pi c}^2}$$

It should be emphasised that these π-orbitals are quite different in form and energy from the single b_1 carbonyl bond in formaldehyde. Since $\varepsilon_0 > \varepsilon_c$, the lowest one must be primarily a C=C bond with some oxygen character. To preserve electroneutrality, the upper one must primarily be the two isolated O π-orbitals out of phase and bonding

to the π^* C=C bond; alternatively it may be looked on as two b_1 carbonyl bonds out of phase. For this reason, we may, with some confidence, place the energy of this b_g orbital above the b_1 orbital in formaldehyde (ca. 14.3 eV vertical). We shall see that for the spectrum of glyoxal this allows us to make an unambiguous assignment of the band at 12.4 eV to this b_g orbital.

Consider now the σ-framework. The oxygen orbitals may be swiftly dealt with; define local axes as shown:

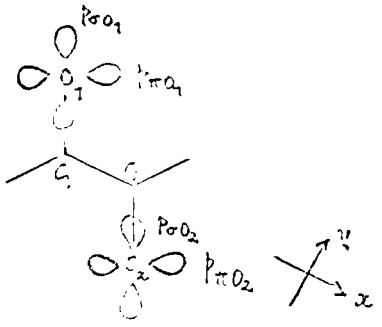

We assume linear combinations of these can be taken, and that the orbitals do not overlap. For the p_π orbitals

$$O_{\pi b_{1a_g}} = \frac{1}{\sqrt{2}}\left(p_{\pi O_1} - p_{\pi O_2}\right)$$

$$O_{\pi b_{1u}} = \frac{1}{\sqrt{2}}\left(p_{\pi O_1} - p_{\pi O_2}\right)$$

and similar combinations for the oxygen p_σ orbitals may be written down. The carbon p orbitals are defined along the x and y axes defined above. We will allow these to interact with each other first before considering interaction with the oxygen orbitals. This first step generates

two bonding orbitals:

$$\psi_{a_g} = \frac{1}{\sqrt{2}}(1+\lambda_\sigma^2)^{-\frac{1}{2}}(\phi_{a_1} - \phi_{a_2}) \qquad \lambda_\sigma = S_{\sigma C}$$

$$\psi_{b_u} = \frac{1}{\sqrt{2}}(1+\lambda_\pi^2)^{-\frac{1}{2}}(\phi_{b_1} + \phi_{b_2}) \qquad \lambda_\pi = S_{\pi C}$$

assuming that $S_{\pi C} < S_{\sigma C}$, we find

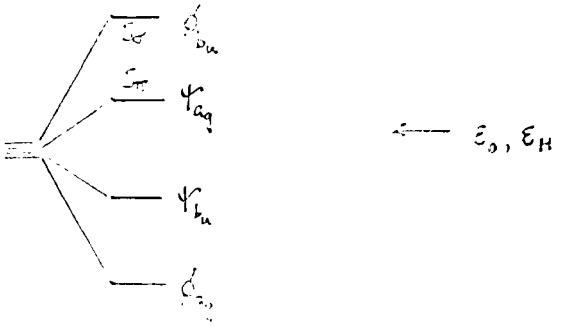

The two hydrogen atoms will not interact directly with each other to any significant extent and, to a good approximation, not with the oxygen atoms, so we have:

$$\left.\begin{aligned} \psi_{a_g} &= \frac{1}{\sqrt{2}}(s_1 + s_2) \\ \psi_{b_u} &= \frac{1}{\sqrt{2}}(s_1 - s_2) \end{aligned}\right\}$$

The main skeletal bonding levels ψ_{a_g} and ψ_{b_u} have energies:

$$E_{\psi_{a_g}} = \varepsilon_C + \beta_C S_{\sigma C} + \frac{(\beta_\sigma^2 + \beta_\sigma^2 S_{\sigma C})\beta_{CH}^2}{4(\varepsilon_C + \beta_C S_{\sigma C} - \varepsilon_0)} + \frac{S_\sigma^2 \beta_{CH}^2}{4(\varepsilon_C + \beta_C S_{\pi C} - \varepsilon_H)}$$

and

$$E_{\psi_{b_u}} = \varepsilon_C + \beta_C S_{\pi C} + \frac{(\beta_\sigma^2 + S_\sigma^2 \beta_{CH})\beta_{CH}^2}{4(\varepsilon_C + \beta_C S_{\pi C} - \varepsilon_0)} - \frac{S_\sigma^2 \beta_{CH}^2}{4(\varepsilon_C + \beta_C S_{\pi C} - \varepsilon_H)}$$

The position indicated for ε_0 follows from a discussion

of the π-framework above. That of ε_H is more doubtful, but the formaldehyde spectrum seems to indicate that $\varepsilon_H \gtrsim \varepsilon_O$.

Consider the π-in plane orbitals of oxygen

$$\varepsilon_{O p\pi a_g} = \varepsilon_O + \frac{3 S_{\pi}^2 \beta_{\omega}^2}{4(\varepsilon_O - \varepsilon_c - \beta_c S_{\pi c})} + \frac{\beta_{\omega}^2 \beta_{\sigma}^2}{4(\varepsilon_O - \varepsilon_c + \beta_c S_{\pi c})}$$

$$\varepsilon_{O p\pi b_u} = \varepsilon_O + \frac{\beta_{\omega}^2 S_{\pi}^2}{4(\varepsilon_O - \varepsilon_c - \beta_c S_{\pi c})} + \frac{3 \beta_{\pi}^2 \beta_{\omega}^2}{4(\varepsilon_O - \varepsilon_c + \beta_c S_{\pi c})}$$

Neither of the π-orbitals is strongly bonding, and we have one of two possibilities:

(i) the band in the glyoxal spectrum at 10.6 eV may be assigned to both the lone pair π_{a_g} and π_{b_u} orbitals

(ii) the bands at 10.6 eV and 12.4 eV are assigned to the π_{a_g} and π_{b_u} orbitals.

We can say with some confidence that $Op_{\pi a_g}$ will be <u>higher</u> in energy than the highest out-of-plane π-orbital of symmetry b_g, as an examination of the energy expressions will show. However, we also saw that the third band of glyoxal at 14.0 eV is too high in IE to be considered as the b_g π-band. The likelihood is, that the πb_g band is 12.4 eV which automatically leads to assignment (i). However, that leaves open the question of the assignment of the band at 14 eV. It is unlikely to be the second π-level a_u and cannot be one of the two strongly σ-bonding

skeletal orbitals. The most likely assignment is to the σ-a_g bonding level, of energy

$$E_{\sigma a_g} = \varepsilon_O - \frac{\beta_{CO}^2 S_\sigma^2}{4(\varepsilon_O - \varepsilon_C - \beta_\sigma S_{\sigma})} - \frac{3\beta_\pi^2 S_{CO}^2}{4(\varepsilon_O - \varepsilon_C + \beta_\pi S_{\pi})}$$

which, assuming reasonable values for S_σ and S_π, will lie lower in energy than the $b_g(\pi)$ orbital. The $a_u(\pi)$ is more difficult to place with confidence. However, if we assume that the carbonyl b_1 orbital in formaldehyde at 14.3 eV has split in glyoxal to yield an antisymmetric combination ionising at 12.4 eV then the symmetric combination should ionise at 16.2 eV. There is indeed a strong band at 16 eV whose general profile resembles that of the 12.4 eV band. This cannot however be assigned to the a_u orbital however, since it is certain that $a_u(\pi)$ must be much less stable than either σ_g or [illegible]. Unless the b_u skeletal bond is strongly destabilised by interaction with the b_u combination of carbon 2s orbitals, which we have not considered, the $a_u(\pi)$ orbital must correspond to the ionisation giving the shoulder at 15.6 eV. There is in fact an orbital at ca. 20 eV in glyoxal, very weak in HeI which might well be the b_u C 2s combination. However the spectrum of the molecule diacetyl shown in fig. 4.4 shows no band higher in energy than 17.4 eV. This orbital

is in some ways reminiscent of that found in acetone and again suggests either very strong C-C bonding or a dramatic destabilisation of the C 2s orbitals. It should also be mentioned in support of this hypothesis that the ESCA spectra of the metallocenes have shown beyond reasonable doubt that there is a carbon 2s band between 16 and 17 eV in the cyclic C_5 grouping so that a very high energy C 2s combination arising from an extended carbon framework may be a quite general phenomenon. The first two bands of diacetyl at 9.5 and 11.5 eV are clearly related to the first two glyoxal bands at 10.6 and 12.4 eV. The difference between the two shifts is not very large but may indicate that the two bands do indeed originate from rather different orbitals as suggested above. Unfortunately, the remainder of the spectrum is diffuse and difficult to understand, the structure of the third band at 14 eV has been completely lost, presumably owing to superimposed ionisations from the methyl groups.

Thus, to summarise, the overlap model has been less successful in the assignment of the glyoxal and diacetyl spectra, though it has enabled us to rule out several alternatives. The ordering of the levels is almost certainly

$$\phi_{a_g}\ (\sigma\text{-bonding}) < \phi_{b_u}\ (\sigma\text{-bonding}) < \pi_{a_u}\ (\pi\text{-bonding})$$
$$< O_{b_g}\ (\sigma\text{-bonding}) < b_g\ (\pi\text{-bonding})$$

$< O_{p\sigma_{g}}$ (in-plane lone-pair) $\lesssim O_{p\text{-}b_u}$ (in-plane lone-pair)

If the band at 12.4 eV is assigned to $O_{p\pi_{g}}$, we must explain why the antisymmetric combination of π-carbonyl bonds is destabilised so very little from the single π-bond of formaldehyde and is also so much more stable than that in acrolein which ionises at 10.9 eV. It is not sufficient to say that the C=C bond in ethylene ionises at 10.7 eV and the C=O bond in formaldehyde at 14.3 eV since we are not dealing with single bonds but with a split Huckel π-system. The correlation of these molecules with butadiene[1] is illustrated below assuming that the oxygen lone-pairs in glyoxal are degenerate, and the upper π-level can be seen to stabilise steadily from 9.2 eV in butadiene through 11.0 eV in acrolein to 12.4 eV in glyoxal.

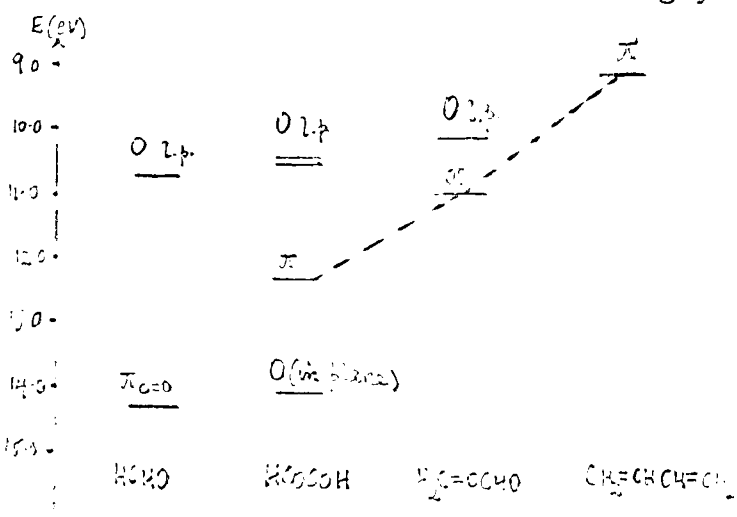

Having now gained some idea of the relative intensities

of π and lone pair orbitals in simple carbonyls, it is possible to make some predictions about the spectra of the β-diketones. The prototype compound, acetylacetone, exists in the vapour phase and in non-coordinating solvents almost entirely in the enol form (fig. 4.5).[38] The six-membered ring is planar, conferring C_{2v} symmetry on the molecule, and, of the other β-diketones studied, where there is less direct structural evidence, hexafluoro-acetylacetone (R=R = CF_3) is known to exist primarily in the enol form even in aqueous solution[39] and will almost certainly exist as such in the vapour phase; trifluoroacetylacetone (R = CF_3, R = CH_3) will presumably follow suit; dipivaloyl-methane (R = R = Me_3C) is more difficult to predict, the alternative keto-type structure also shown

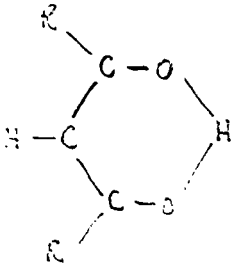

enol

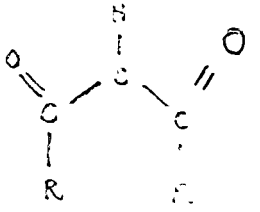

keto

would be expected to be less stable owing to steric interaction between the two bulky tertiary butyl groups and so the enol form would be favoured. The compound trifluorotrimethylacetylacetone (R = CF_3, R = Me_3C) is impossible to predict though the results of Hammond[40] would again suggest an enol form. It is possible however that the very unsymmetrical charge distribution within this

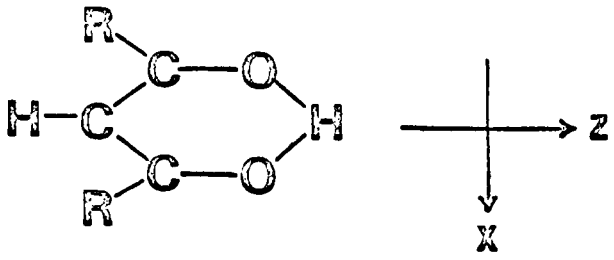

FIGURE 4.5

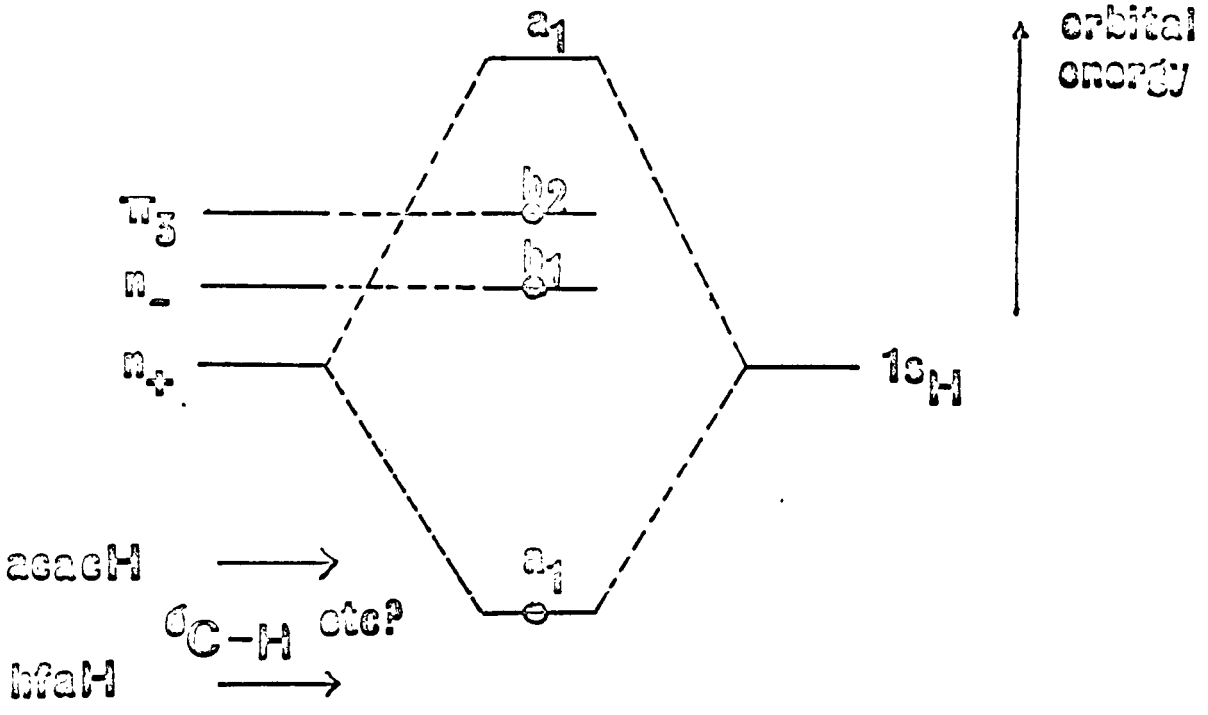

FIGURE 4.7

molecule might lead it to behave in an anomalous fashion and its UV-PE spectrum is very difficult to understand.

The planar ring system will generate a set of π-orbitals which has been extensively discussed.[41] This π-system derives from the out-of-plane p_y orbitals of the three carbon and two oxygen atoms which together transform as $3b_2 + 2a_2$ in C_{2v}. The five π-orbitals are shown in fig. 4.6 and simple Huckel theory leads to an energy ordering $\pi_1 < \pi_2 < \pi_3 < \pi_4 < \pi_5$ and, with the usual choice of parameters, it is found that π_3 is well separated from both π_2 and π_4[41,42] implying that neither of these orbitals will be of great importance as regards the bonding in metal chelates. Fig. 4.6 shows that π_2 may be regarded as an antisymmetric combination of localised C-O π-bonding orbitals and π_3 as a slightly anti-bonding orbital formed from the symmetric combination of the two π-C-O orbitals out of phase with the p πAO on the unique carbon atom. Now the πC-O bonds will certainly not interact to the extent found in diacetyl (IE 11.5 eV) and in fact we would expect the energy of π_2 to be quite close to the value observed in acetone (between 13 and 14 eV). The separation of π_2 from π_3 is very difficult to gauge from the spectra of simple carbonyls but simple Huckel theory suggests a value of 3 - 4 eV, similar to that found for the two

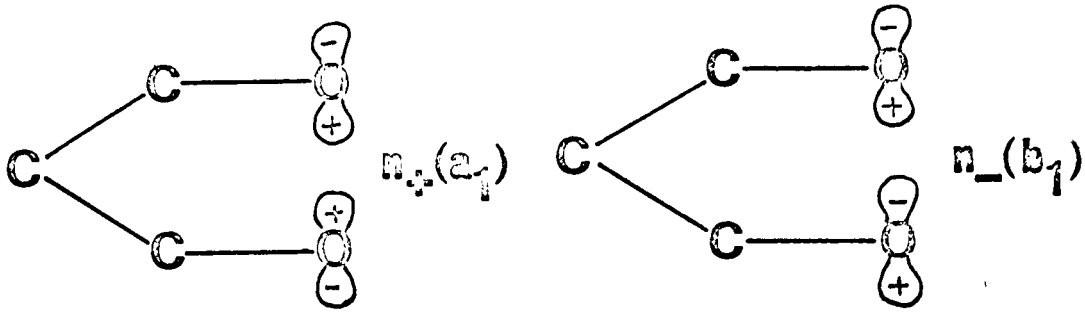

FIGURE 4.6

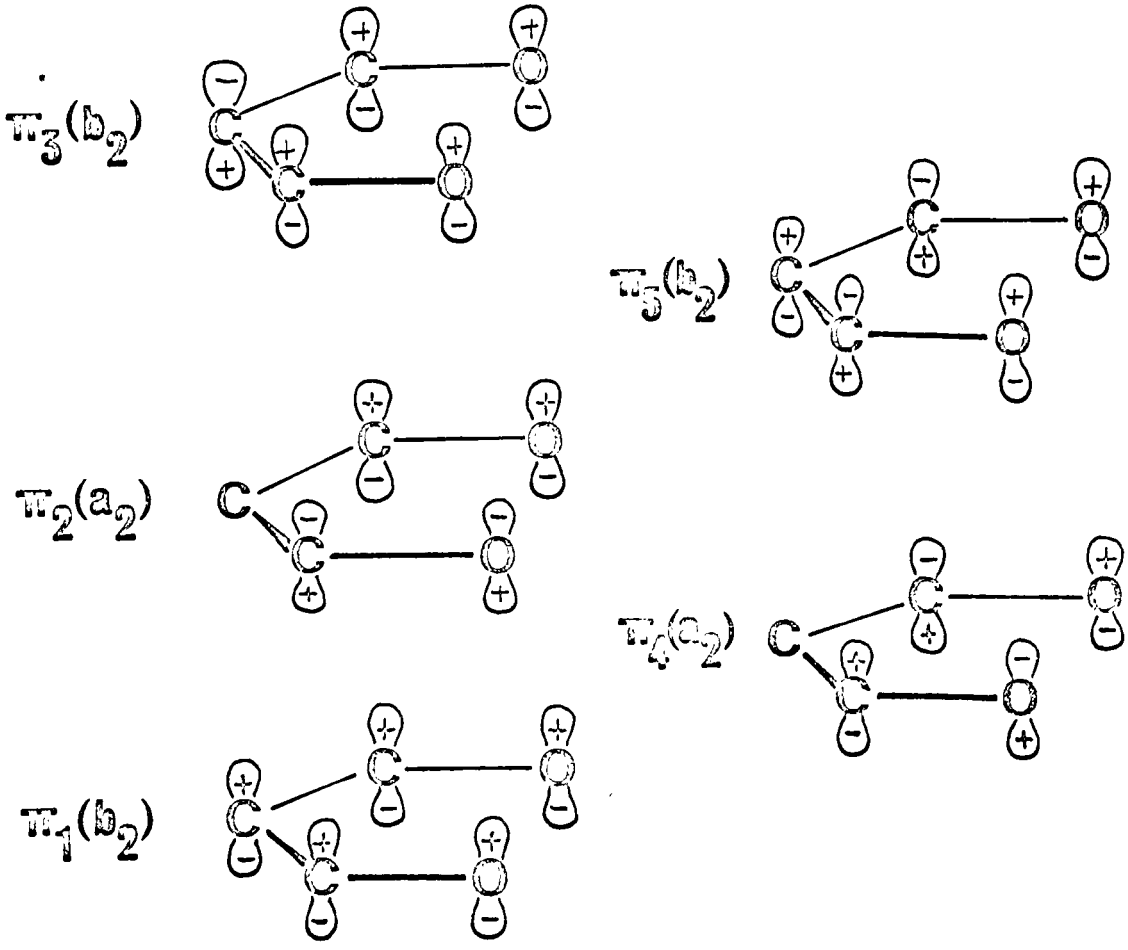

occupied π orbitals in glyoxal. The strong implication must be that this π_3 level will separate from the σ-framework and be seen as a band at low IE.

As with the other ketones, it is also necessary to consider the oxygen non-bonding level. We saw that for glyoxal, the symmetric and antisymmetric (n_+, n_-) oxygen lone-pair combinations, built up from the p_x orbitals in plane and perpendicular to the C-O bond, were not separated by more than a few tenths of an electron volt in energy. Such a situation is not however expected for acetylacetone and other β-diketones in the enol configuration. This is because the symmetric combination $n_+(a_1)$ of the two oxygen p_x orbitals interacts with the hydrogen 1s orbital, this being probably the major source of bonding with the proton. The antisymmetric combination $n_-(b_1)$ is however immediately comparable to the lone pair in acetone. From the above analysis of the acetone spectrum, this ionisation occurs at 9.8 eV and bands in the acetylacetone spectrum are observed at 9.7 and 9.2 eV. Now, through-space interactions would be expected to destabilise n_- slightly, and, though it is very difficult to assess the extent of such interactions, the energy differentiation between n_+ and n_- in the anion $acac^-$ is probably rather small. We neglect through-bond interactions in this analysis since

they are probably small and likely to affect n_+ and n_- in much the same way.[43] It is almost impossible to order n_- and π_3 with the information presented above, and the tentative energy level scheme given in fig. 4.7 which places π_3 above n_- is ultimately defined by the PE spectroscopic information derived from the metal chelates, where there is little doubt as to the ordering.

The remainder of the acetylacetone spectrum (fig. 4.8) is disappointingly diffuse. A 1.5 eV window separates the π_3 and n_- ionisation bands from an edge at 12 eV. A distinct peak can be seen at 12.7 eV which is rather low for the methyl ionisation and there are two possibilities; either it is the ionisation of the second π orbital, π_2, or it derives from the $n_+(b_1)$ orbital. Its intensity would suggest that it probably arises from an orbital similar in type to the one giving rise to the band at 9.74 eV, which we have assigned to the $n_-(b_1)$ ionisation. Hence we may tentatively assign this band to the $n_+(a_1)$ orbital giving a splitting between n_+ and n_- of 2.94 eV, which is not unreasonable as a measure of the hydrogen binding energy (70 kcals/mole).

This assignment is supported by the HeI UV-PE spectrum of hexafluoroacetylacetone fig. (4.9), which exhibits <u>three</u> low energy bands at 10.75 eV, 11.26 eV and 14.03 eV. The

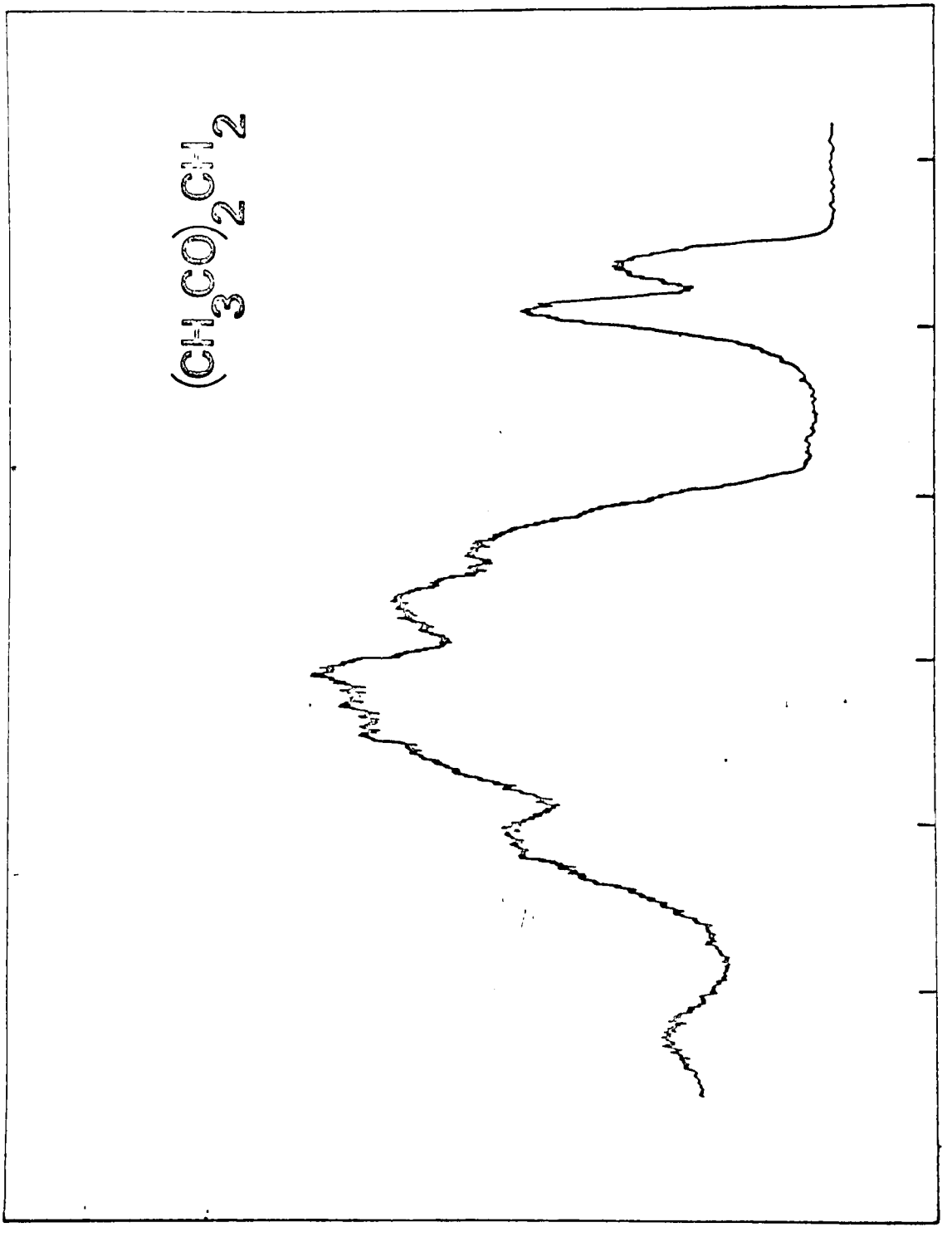

FIGURE 4.8

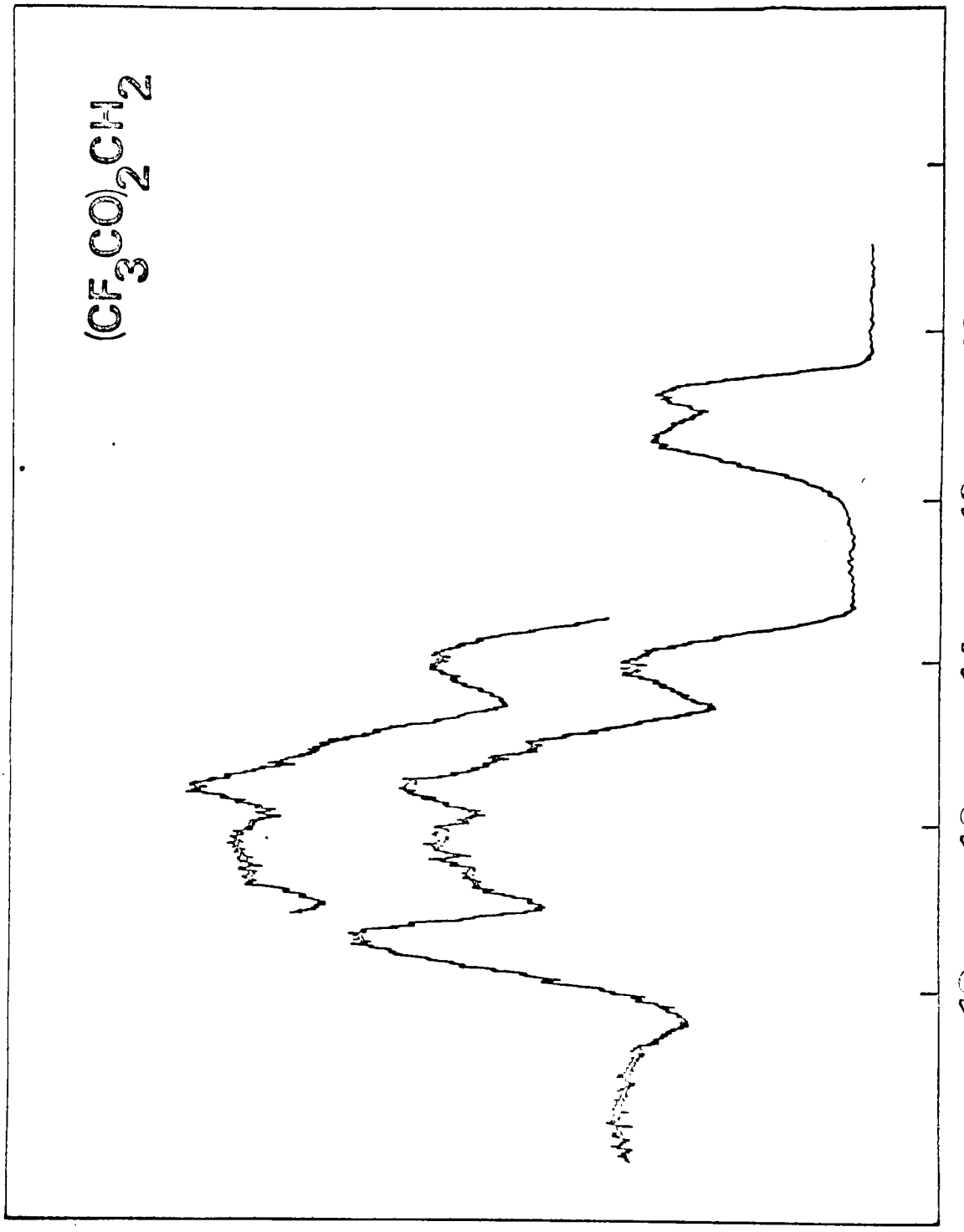

FIGURE 4.9

shifts of the first two bands from acetylacetone are respectively 1.58 eV and 1.52 eV. It might seem strange that the π orbital shifts to a greater extent than the orbital on replacing CH_3 by CF_3 but this is almost certainly a consequence of the very strong π overlap characteristic of fluorine which manifests itself in the theory of aromatic substitution as the fluorine effect.* Thus, CF_3 does not behave chemically in a manner predicted by extrapolation

---

* The fluorine effect should not be confused with the inconveniently named perfluoro-effect.[44] The latter arises from a study of the movement of π-bonds when fluorine atoms are substituted for the olefinic hydrogen atoms: e.g. a comparison of ethylene with C_2F_4 or trans-but-2-ene with trans-2,3, difluoro-but-2-ene. It is found experimentally that, although the σ-bonds are strongly stabilised on fluorination, the π-bonds are hardly affected in energy at all, presumably because of extensive through-bond interactions with the fluorine lone-pairs. The fluorine effect mentioned above is connected with fluorination in the β position,[45] and the standard PE example of this is the comparison between trans-but-2-ene and perfluoro trans-but-2-ene, where both π and σ levels are strongly stabilised on fluorination, but the π level 0.2 eV more than the σ level.

from CCl_3, often exhibiting highly anomalous behaviour. Assuming that the effect of CF_3 substitution on π_2 is at least as marked as on π_3, the possibility that the band at 14.03 eV arises from π_2 may be ruled out since the shift from acetylacetone is only 1.4 eV and the similarity of this shift to that observed for the band we have assigned to n_- is added support. Furthermore, comparison with the formaldehyde spectrum would strongly suggest that π_2 in hexafluoroacetylacetone should be lower than π C-O at 14.3 eV.

Interestingly, in hexafluoroacetylacetone, the separation between n_+ and n_- has been reduced to 2.77 eV suggesting some loss in the bond strength of the hydrogen; this in turn suggests that the major reason for the extensive enolisation of hexafluoro species lies in the availability of the π system in the enol form stabilised by interaction with the CF_3 groups. Since fluorine 2p has a higher cross-section than oxygen 2p, admixing F 2p from the CF_3 groups with π_3 should raise the cross-section of that orbital relative to n_+ and n_- and a glance at the two spectra shows that this is indeed the case, adding further support to our assignment.

In an endeavour to settle the low IE ordering, and to investigate other β-diketones with a view to measuring the

spectra of their complexes, the spectra of dipivaloylmethane (2,2,6,6,tetramethylheptane 3,5-dione: dpmH) fig. 4.10, trifluoroacetylacetone (1,1,1,trifluoropentane 2,4-dione: tfaH) fig. 4.11 and trimethyltrifluoroacetylacetone (1,1,1,trifluoro 5,5,dimethylhexane 2,4-dione: tmtfacH) fig. 4.12 were obtained. The spectra of the first two are fairly easily understood: dpmH exhibits two bands at 8.83 and 9.23 eV, the separation being less than that in acetylacetone presumably since the tertiary butyl groups will tend to destabilise the σ-system more than the π-system. As expected the relative intensities are much closer to those observed in acetylacetone, though they are poorly resolved. The spectrum of tfaH also has two bands in the low IE region, at 9.92 and 10.53 eV. It is difficult to understand at first sight why these two bands are separated by such a large margin; a splitting intermediate between that in acetylacetone and that in hexafluoroacetylacetone would have been expected. One way however in which the result might be explained is by supposing that the unsymmetrical charge distribution in tfaH has given rise to a polarisation of the σ-framework towards the CF_3 group and a reverse polarisation of π_3 and implying that the σ orbitals should be more stable than expected whilst the π orbitals will be less stable. This is, however, not borne out by the position of the $n_+(a_1)$ orbital which is 0.1 eV less

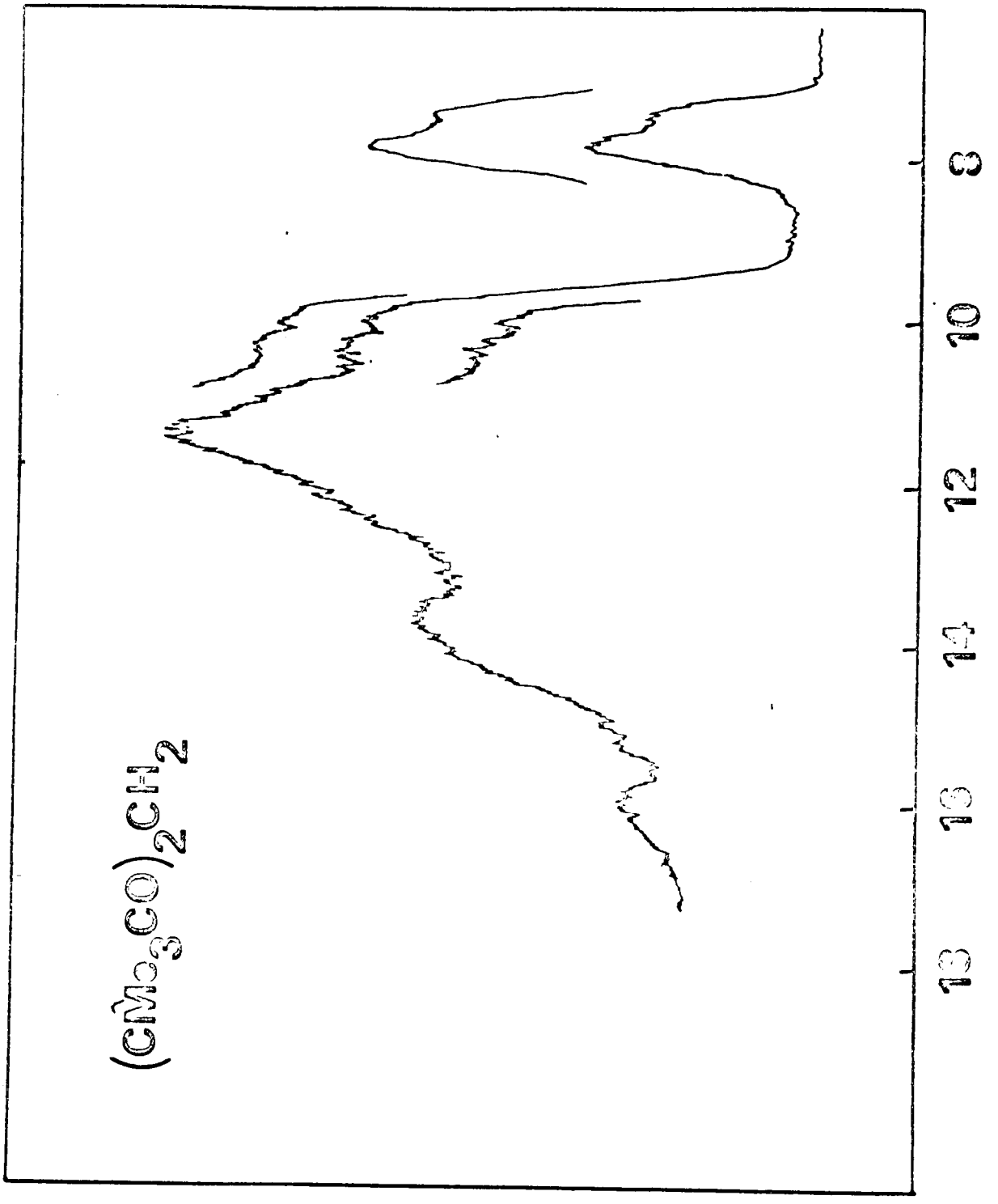

FIGURE 4.10

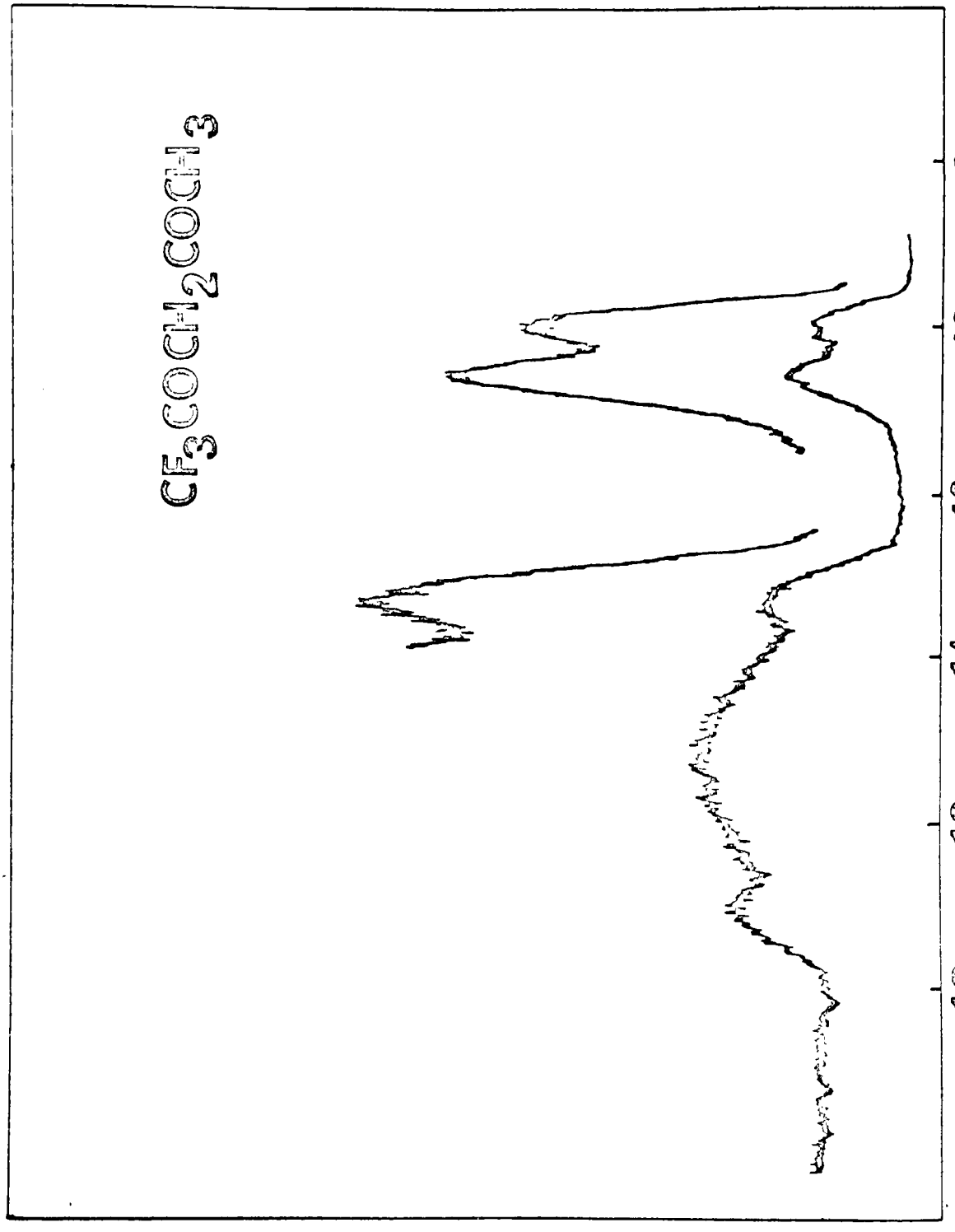

FIGURE 4.11

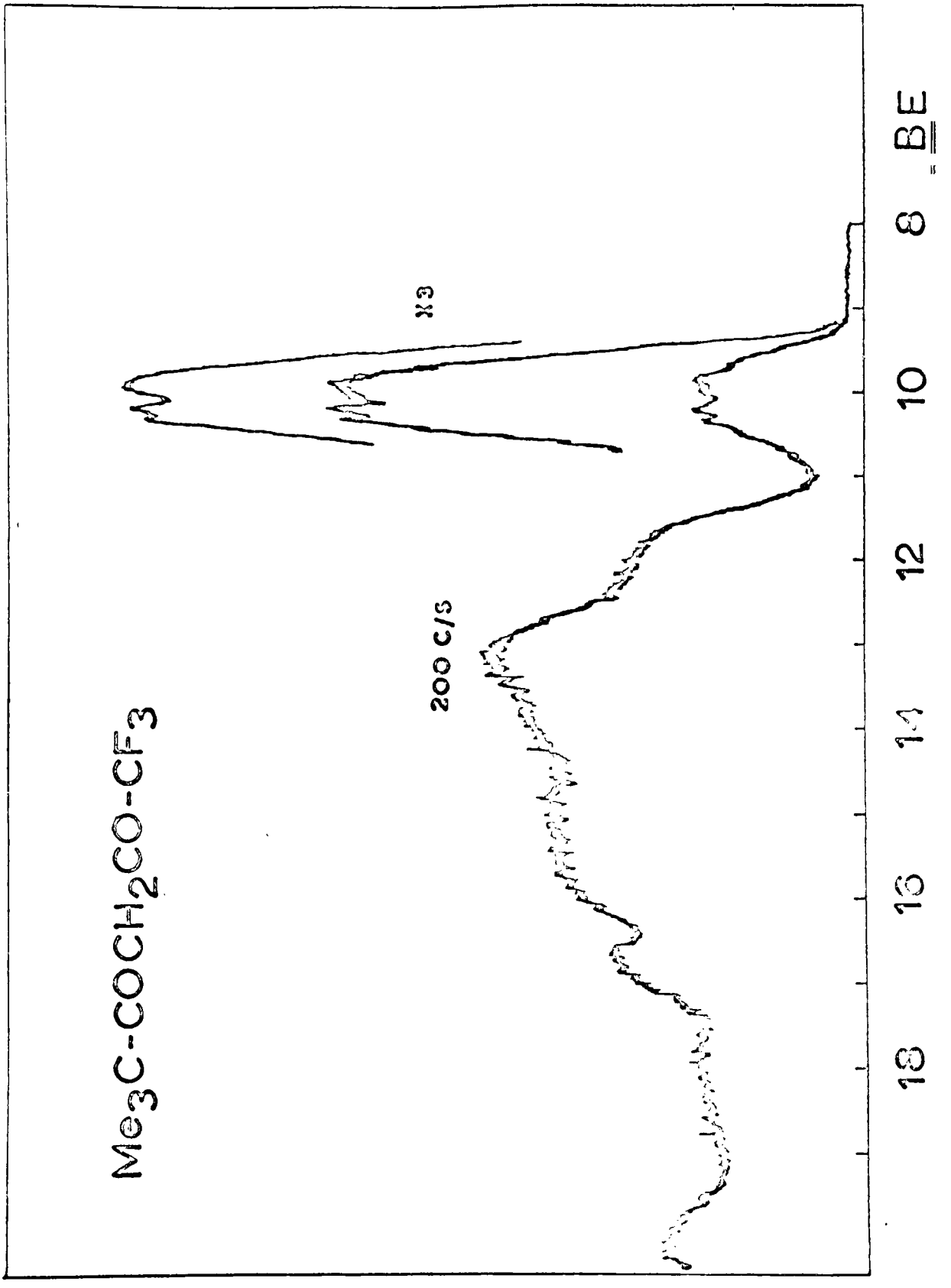

FIGURE 4.12

stable than expected suggesting possibly that through bond interactions may be more important in an unsymmetrical electronic environment.

The low IE region of tmtfacH appears to exhibit three bands, the third being indicated by a poorly resolved shoulder on the high IE side of the second band. The reason for this is not certain, but it may be that the compound is a mixture of keto and enol forms. The spectrum of tmtfacH is altogether rather discouraging as regards the possibility of studying its complexes by PE spectroscopy since there is no window between the first group of bands and the onset of the main region of ionisation. One of the complexes studied, $Al(tmtfac)_3$, appeared to consist of two stereoisomeric forms differing considerably in physical properties, and further investigations into the complexes of this ligand were abandoned.

THE SPECTRA OF THE COMPLEXES

We saw above, that the UV-PE spectra of the β-diketones were intelligible in terms of three types of orbitals in the low IE region of the spectrum. Firstly, an orbital n_+ formed from a symmetric combination of oxygen p_σ orbitals which, in the enol form of the ligand of the ligand, is the major source of bonding to the proton; secondly, an orbital n_- formed from the antisymmetric combination of the same p_σ orbitals, which, in the ligand has little bonding character, and lastly, a π orbital which we have denoted by π_3. We also saw that π_3 was well separated from π_2 and π_4, the former being a major source of bonding in the C-O system, and the latter strongly antibonding.

When three such ligands are brought together to form the tris-chelate framework, the orbitals we discussed above interact with one another. Two forms of through-space interaction may be distinguished; an intra-ligand interaction present in the anion, which tends to destabilise n_- by an amount β_o and to stabilise n_+ by a similar amount. Clearly β_o derives from overlap terms and, in the isolated ligand is given by $\beta_o S_\sigma$. A second type of interaction present is interligand in origin and is of rather smaller magnitude. The effect of these interactions is to split the initially degenerate triplets of π_3, n_- and n_+ apart by small amounts. Simple symmetry arguments

show that the π_3 and n_- triplets each split into a degenerate e doublet and a non-degenerate a_2 level, whereas the n_+ triplet splits into a_1 + e, the group labels referring to the irreducible representations of the overall point group of the molecule, D_3. It follows that there are three e levels which may further interact in second order by an amount proportional to the square of the relevant off-diagonal element and inversely proportional to their energy separation.

These separations and splittings may be related by the model discussed above to the overlaps between the component ligand orbitals. In all the tris-acetylacetonato complexes, the structure is based fairly closely on an octahedral configuration of oxygen atoms about the central metal, and even in the case of $Mn(acac)_3$, the distortion is comparatively small. The coordinate system is defined by the sketch below, with the chelate ligands being numbered (1), (2) and (3) and the oxygen atoms 1 or 2 for each ligand

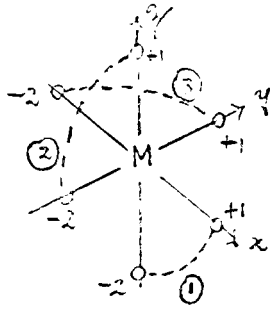

The axes shown are those of an octahedron, and the algebra

is substantially simplified if these are transformed to those of a D_3 system as:

$$\hat{i}' = 1/\sqrt{2}\,(\hat{i} - \hat{j})$$

$$\hat{j}' = 1/\sqrt{6}\,(-\hat{i} + 2\hat{j} - \hat{k})$$

$$\hat{k}' = 1/\sqrt{3}\,(\hat{i} + \hat{j} + \hat{k})$$

and $\hat{k}'$ corresponds to the three-fold axis of rotation in D_3. The inverse transformations are

$$\hat{i} = 1/\sqrt{2}\,\hat{i}' - 1/\sqrt{6}\,\hat{j}' + 1/\sqrt{3}\,\hat{k}'$$

$$\hat{j} = 2/\sqrt{6}\,\hat{j}' + 1/\sqrt{3}\,\hat{k}'$$

$$\hat{k} = -1/\sqrt{2}\,\hat{i}' - 1/\sqrt{6}\,\hat{j}' + 1/\sqrt{3}\,\hat{k}'$$

For the p orbitals of the central atom we have at once:

$$p_x' = 1/\sqrt{2}\,(p_x - p_y)$$

$$p_y' = 1/\sqrt{6}\,(-p_x + 2p_y - p_z)$$

$$p_z' = 1/\sqrt{3}\,(p_x + p_y + p_z)$$

and the d-orbital transformations are given in table 4.1a.

TABLE 4.1a

	d_{z^2}'	$d_{x^2-y^2}'$	d_{xy}'	d_{xz}'	d_{yz}'
d_{z^2}	0	$1/2\sqrt{3}$	$1/2$	$-1/\sqrt{2}$	$-1/\sqrt{6}$
$d_{x^2-y^2}$	0	$1/2$	$-1/2\sqrt{3}$	$1/\sqrt{6}$	$1/3\sqrt{2}$
d_{xy}	$1/\sqrt{3}$	$1/3$	$1/\sqrt{3}$	$1/\sqrt{6}$	$1/3\sqrt{2}$
d_{xz}	$1/\sqrt{3}$	$-2/3$	0	0	$-\sqrt{2}/3$
d_{yz}	$1/\sqrt{3}$	$1/3$	$-1/\sqrt{3}$	$-1/\sqrt{6}$	$1/3\sqrt{2}$

Evaluation of group overlaps

A σ M-O bonds. The most general oxygen σ-basis is illustrated below

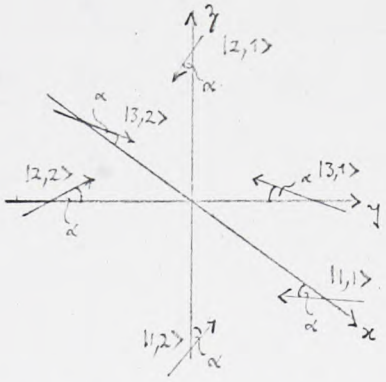

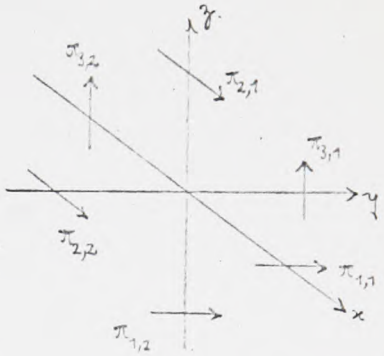

The notation $|x,y\rangle$ will be used to label the p_σ-basis, where x refers to the chelate (1), (2) or (3) and y to the particular oxygen atom 1 or 2. The angle α is indeterminate, since, in the isolated anion it will have the value $\pi/6$ for n_+ and n_-, but cannot be specified in the molecule, though we will assume a value of $\pi/6$ in any numerical illustration.

The simple overlaps are given by

$$\langle 11|12\rangle = \langle 21|22\rangle = \langle 31|32\rangle = -S_\sigma \cos^2\left(\tfrac{\pi}{4}-\alpha\right) - S_\pi \sin^2\left(\tfrac{\pi}{4}-\alpha\right)$$

$$\langle 11|31\rangle = \langle 11|21\rangle = \langle 12|22\rangle = \langle 12|32\rangle = \langle 21|31\rangle = \langle 22|32\rangle$$

$$= \tfrac{1}{2} S_\sigma \cos^2\alpha - \tfrac{1}{2} S_\sigma \cos\alpha\sin\alpha + \tfrac{1}{2} S_\pi \sin^2\alpha + \tfrac{1}{2} S_\pi \sin\alpha\cos\alpha$$

$$\langle 22|11\rangle = \langle 12|31\rangle = \langle 21|22\rangle$$

$$= S_\pi \sin^2\alpha - \tfrac{1}{2} S_\sigma \cos^2\alpha - \tfrac{1}{2} S_\pi \cos^2\alpha$$

The p_σ orbitals generated in D_3 using the usual techniques

of primitive idempotents are given in table 4.1b

TABLE 4.1b

	a_1	a_2	e(1a)	e(1b)	e(2a)	e(2b)
|1,1>	$1/\sqrt{6}$	$1/\sqrt{6}$	$-1/\sqrt{3}$	0	$-1/\sqrt{3}$	0
|1,2>	$-1/\sqrt{6}$	$1/\sqrt{6}$	$-1/\sqrt{3}$	0	$1/\sqrt{3}$	0
|2,1>	$1/\sqrt{6}$	$1/\sqrt{6}$	$1/\sqrt{12}$	$1/2$	$1/\sqrt{12}$	$-1/2$
|2,2>	$-1/\sqrt{6}$	$1/\sqrt{6}$	$1/\sqrt{12}$	$1/2$	$-1/\sqrt{12}$	$1/2$
|3,1>	$1/\sqrt{6}$	$1/\sqrt{6}$	$1/\sqrt{12}$	$-1/2$	$1/\sqrt{12}$	$1/2$
|3,2>	$-1/\sqrt{6}$	$1/\sqrt{6}$	$1/\sqrt{12}$	$-1/2$	$-1/\sqrt{12}$	$-1/2$

The relevant group overlaps are given immediately as:

$$\chi_{a_1} = \tfrac{3}{2}c^2 S_\sigma - cs\,S_\sigma + \tfrac{3}{2}c^2 S_\pi + cs\,S_\pi - s^2 S_\pi + \beta_0$$

$$\chi_{a_2} = \tfrac{1}{2}c^2 S_\sigma - cs\,S_\sigma + \tfrac{c^2}{2} S_\pi + cs\,S_\pi + s^2 S_\pi - \beta_0$$

$$\chi_{e(1)} = -\tfrac{1}{2}(c^2 - cs)S_\sigma - \tfrac{1}{2}(c^2 + cs)S_\pi + \tfrac{1}{4}c^2 S_\sigma - \tfrac{1}{2}(s^2 - \tfrac{1}{2}c^2)S_\pi - \beta_0$$

$$\chi_{e(2)} = -\tfrac{1}{2}(c^2 - cs)S_\sigma - \tfrac{1}{2}(c^2 + cs)S_\pi - \tfrac{1}{4}c^2 S_\sigma + \tfrac{1}{2}(s^2 - \tfrac{1}{2}c^2)S_\pi + \beta_0$$

where $c = \cos\alpha \quad s = \sin\alpha$

$$\beta_0 = \cos^2\left(\tfrac{\pi}{4} - \alpha\right) S_\sigma + \sin^2\left(\tfrac{\pi}{4} - \alpha\right) S_\pi$$

The orientation is such that e(1a) and e(2b) lie in the direction of the y axis and e(1b) and e(2a) in the x direction.

Inter-orbital overlap between the two e orbitals has the value

$$\langle 1a|2b\rangle = \tfrac{1}{4\sqrt{3}}\left(3c^2 S_\sigma - 6(s^2 - \tfrac{1}{2}c^2)S_\pi\right)$$

In a similar way, the π orbitals may be written out. Using the sketch above, which is drawn to the same perspective as that used for the p_σ orbitals, we have to consider both inter- and intra-ligand effects. Actually the latter can be neglected, since they are the same in both neutral molecule and anion and serve only to determine the position of π_3 in the PE spectrum of acetylacetone itself. The interligand effects are, as expected, very small. If we write $\gamma = S'_\sigma + S'_\pi$, where S'_σ, S'_π are p overlaps for the p AO's of π_3

$$\alpha'_{a_2\pi} = -\tfrac{1}{2}\gamma$$

$$\alpha'_{c\pi} = \tfrac{1}{4}\gamma$$

The π_3 and σ orbitals also overlap, and table 4.1c gives the required integrals for the AO's and table 4.2 those for the various MO's.

TABLE 4.1c

π / b_2	π_{11}	π_{12}	π_{21}	π_{22}	π_{31}	π_{32}
|1,1>	0	0	a	b	d	0
|1,2>	0	0	0	d	b	a
|2,1>	d	0	0	0	a	b
|2,2>	b	a	0	0	0	d
|3,1>	a	b	d	0	0	0
|3,2>	0	d	b	a	0	0

where $a = 1/2(s + c)S_{\pi} - 1/2(c - s)S_{\sigma}$

$b = c/2\ S_{\pi} - c/2\ S_{\sigma}$

$d = s\ S_{\pi}$

TABLE 4.2

	e(1)	e(2)	π_e	a_2	π_{a_2}
e(1)	1	$\frac{\sqrt{3}}{4}(c^2 S_\sigma - (2s^2 - c^2)S_\pi)$	$-\frac{\sqrt{3}}{4}(a+b-d)$	0	0
e(2)	$\frac{\sqrt{3}}{4}(c^2 S_\sigma - (2s^2 - c^2)S_\pi)$	1	$\frac{1}{2}(a+b+d)$	0	0
π_e	$-\frac{\sqrt{3}}{4}(a+b-d)$	$\frac{1}{2}(a+b+d)$	1	0	0
a_2	0	0	0	1	$a+b+d$
π_{a_2}	0	0	0	$a+b+d$	1

We first consider the overlap of the σ and π orbitals with a central metal whose main valence orbitals are s and p in character. Tables 4.3 and 4.4 give the overlap integrals in terms of two parameters ϕ and μ, where ϕ is the σ $p_M - p_O$ overlap, and μ the π metal-oxygen overlap.

TABLE 4.3

	ψ'_{p_x}	ψ'_{p_y}	ψ'_{p_z}
a_1	0	0	0
a_2	0	0	$\sqrt{2}(s\mu - c\phi)$
e(1a)	0	$\frac{1}{\sqrt{2}}(s\mu - c\phi)$	0
e(1b)	$\frac{1}{\sqrt{2}}(s\mu - c\phi)$	0	0
e(2a)	$\sqrt{\frac{3}{2}}(s\mu + c\phi)$	0	0
e(2b)	0	$\sqrt{\frac{3}{2}}(s\mu + c\phi)$	0

TABLE 4.4

	ψ_x	ψ_y	ψ_z
π_{a_2}	0	0	$\sqrt{2}\mu$
$\pi_e(a)$	0	$\sqrt{2}\mu$	0
$\pi_e(b)$	$\sqrt{2}\mu$	0	0

Using these figures it is now possible to venture a tentative assignment of the PE spectrum of $Al(hfa)_3$, fig. 4.13. The spectrum is far from simple owing to a series of accidental degeneracies, as will be seen. Consider first the $\pi_3 e + a_2$ levels. Interligand interaction will only cause a small splitting between these two levels and, if bonding can only occur to the s and p orbitals on the central metal, we find that, to a first approximation, the levels will remain almost degenerate. Thus, in $Al(hfa)_3$, we would not expect to resolve the e and a_2 bands derived from π_3 save under the most favourable circumstances. The major overlap between the Al(3p) orbitals and the ligand arises from the σ orbitals, with that to e(2) (derived from n_+) being strongest. The bonding to e(1) is only a quarter the strength of that to $a_{2\sigma}$, though the fact that inter-ligand splitting places e(1) above a_2 will reduce this differential to a certain extent. Thus, we expect a situation in which e(2) is quite strongly stabilised,

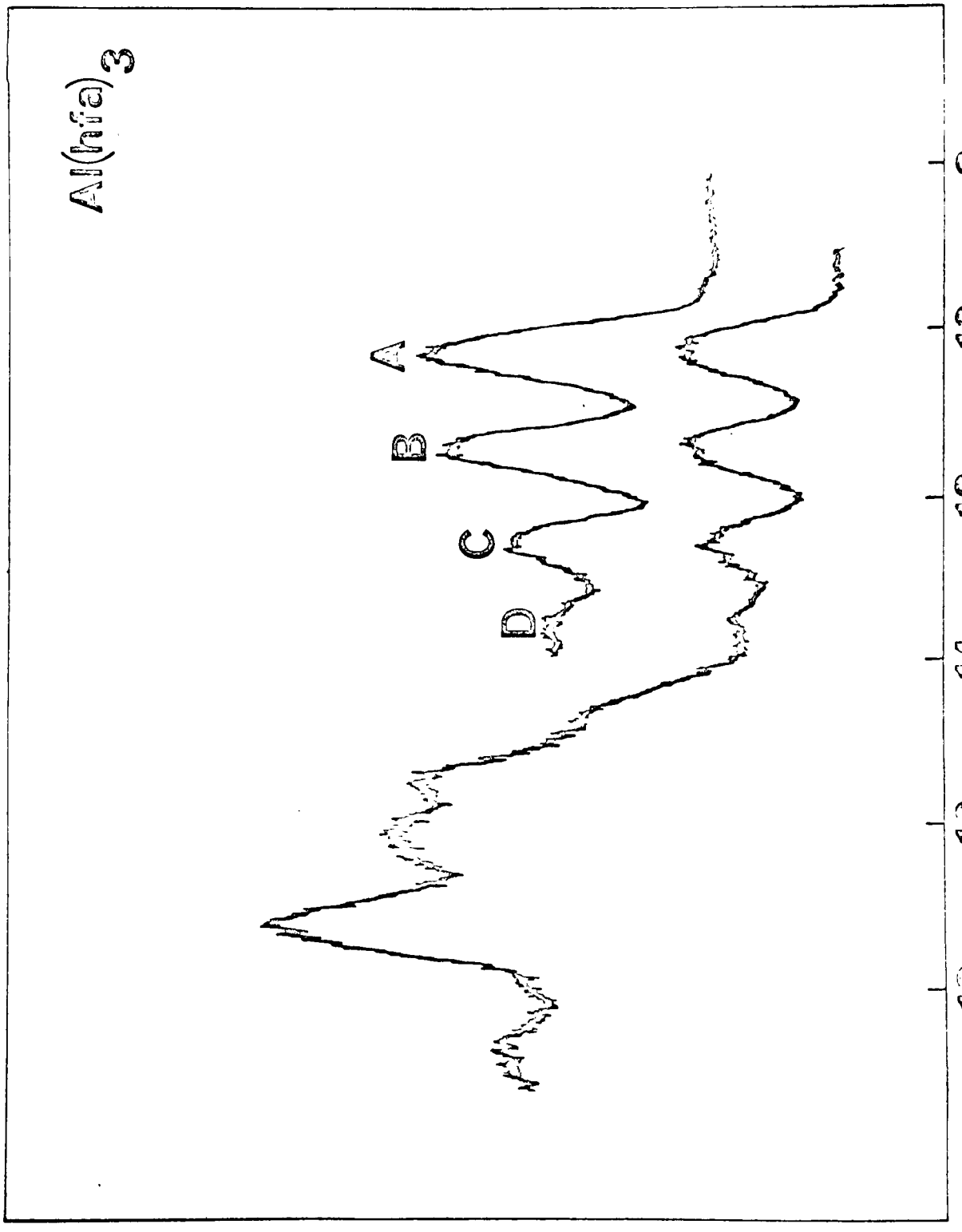

FIGURE 4.13

e(1) and π_3 less so, and $a_{2\sigma}$ lying below e(1). The splitting of e(2) and $a_{1\sigma}$ caused by inter-ligand interaction is quite large as we have seen, and a_1 will bond strongly to the Al(3s) orbital so that it is possible that e(2) and $a_{1\sigma}$ will be resolved in the PE spectrum though it is obviously impossible to say on a priori grounds how this splitting will compare with that expected between e(1) and $a_{2\sigma}$; we can however say that the latter should increase with increasing p_σ bonding, see fig. 4.14.

To explore the possibilities of increasing covalence the spectrum of $Ga(hfa)_3$ fig. 4.15 was also obtained, since it is known that much of the general chemistry of Ga(III) is very difficult to understand except in terms of a greater covalence than that found in the corresponding Al(III) [48] compounds (the so-called alternation effect) [72] which presumably arises from a general contraction across the first transition series akin to the lanthanide contraction. This being so, it is of interest to examine the PE spectrum of $Ga(hfa)_3$ to see if any changes have occurred. There are in fact two main differences: the band B has split, with a low intensity component appearing to high IE, and a new band X has appeared on the high IE side of C. Our provisional assignment of the $Al(hfa)_3$ spectrum given in fig. 4.14 suggests that increasing p_σ bonding to the n_- triplet in $Ga(hfa)_3$ has caused $a_{2\sigma}$

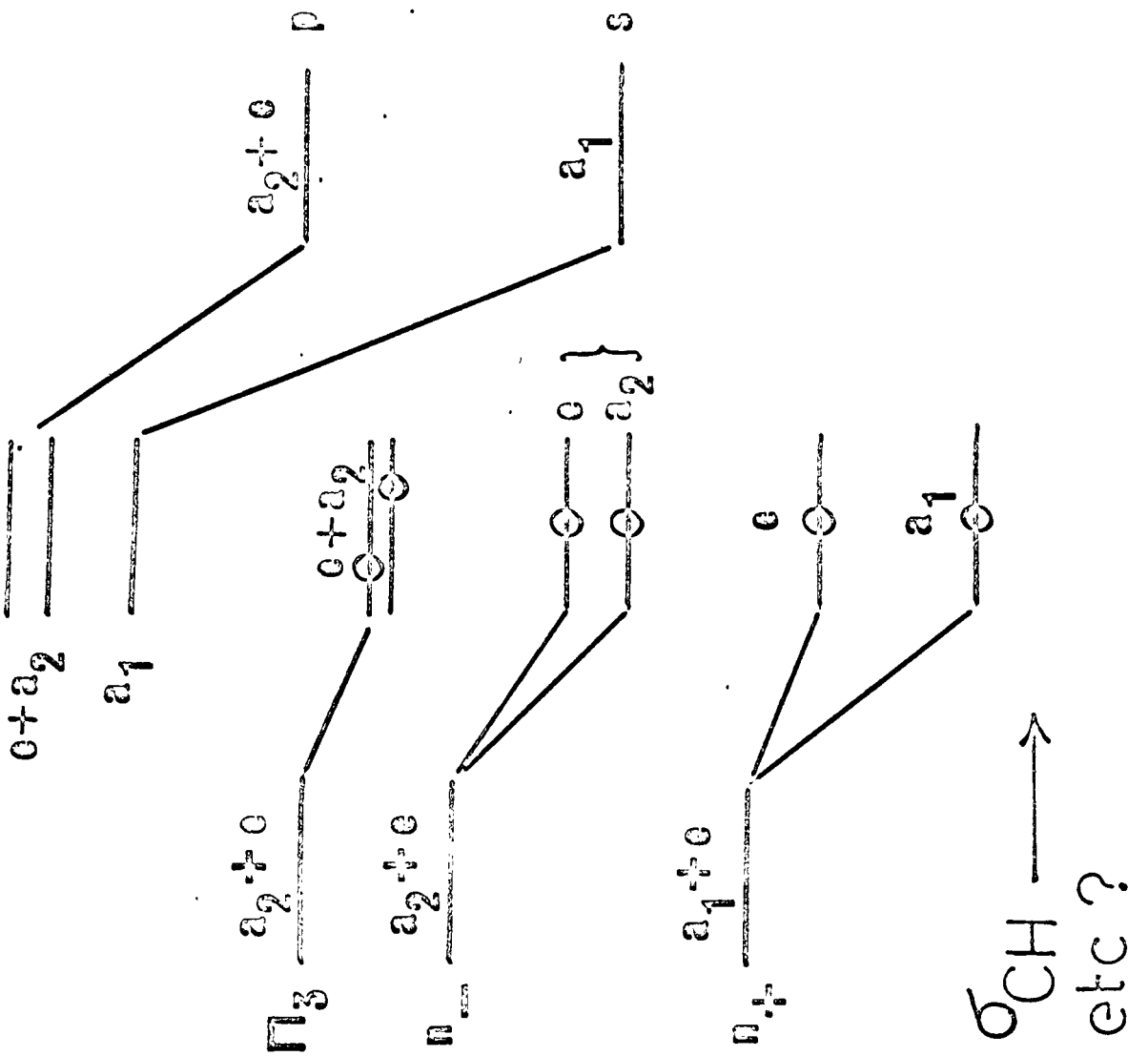

FIGURE 4.14

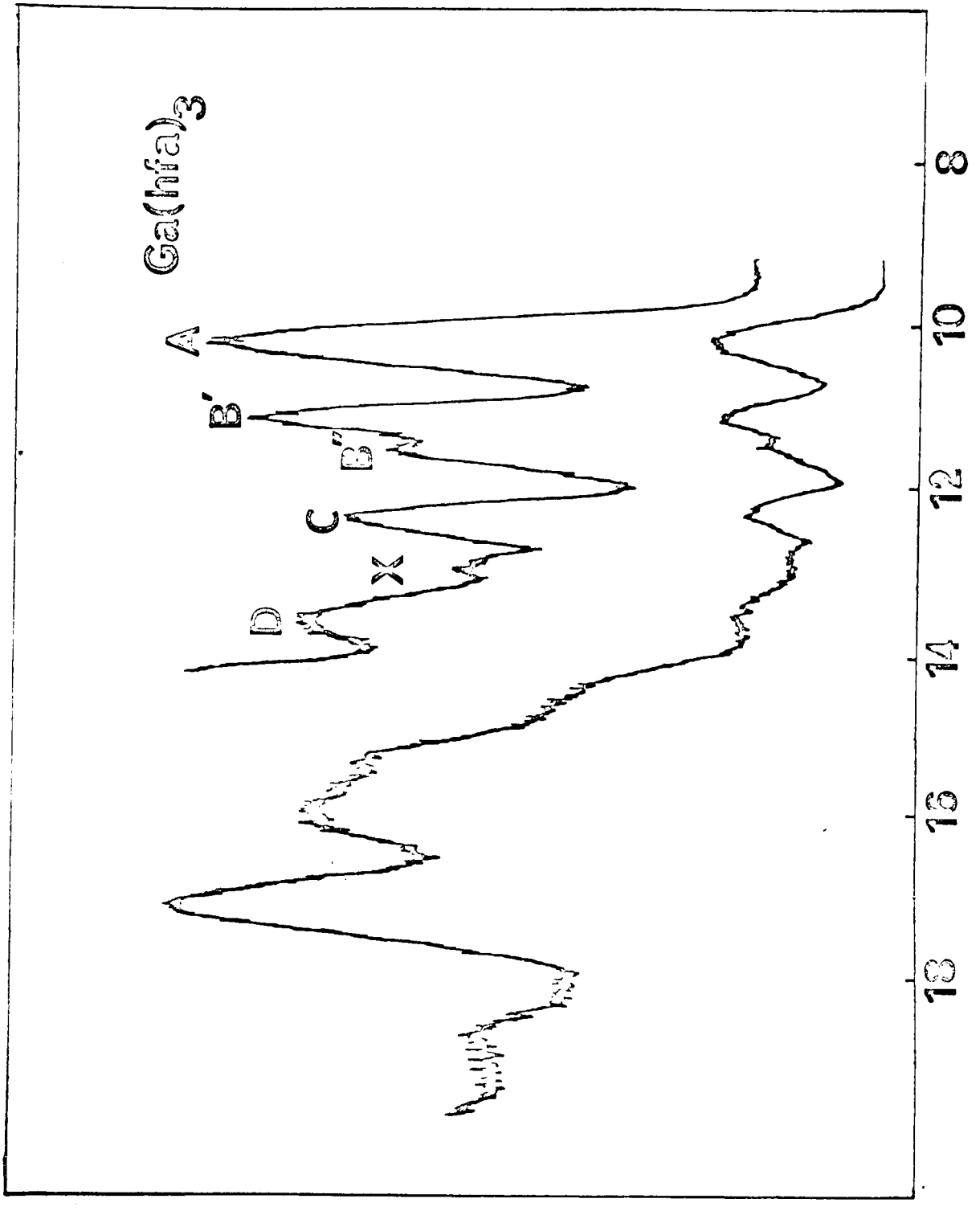

FIGURE 4.15

to separate from e(1). A second possibility is that the gallium 3d orbitals, which lie below the main valence structure have caused the e(1) level to become slightly antibonding. Whilst this latter explanation cannot be absolutely ruled out, a considerable body of evidence is beginning to accumulate that these d-orbitals lie very low in energy (< -21 eV) and their bonding to the ligand is probably very small. Given the first interpretation, there seems little doubt that band B in $Al(hfa)_3$ does indeed arise from the n_- $e(1)/a_2$ triplet. From our arguments above, e(2) will certainly lie below e(1) so the first band in the $Al(hfa)_3$ spectrum, A, must be due to the π_3 ionisations, which, as can be seen, are not split, either in $Al(hfa)_3$ or $Ga(hfa)_3$, as expected. The third band C can be assigned to e(2), at least in part. The appearance of band X in $Ga(hfa)_3$ is difficult to understand at first sight. Its relative intensity and position would suggest that it derives from ionisation of the a_1 orbital, which has been stabilised even more than p_π by covalent interaction. This being so, we must assign band C in $Al(hfa)_3$ to ionisation from both e(2) and a_1. An alternative explanation, namely that band D derives from a_1 can be ruled out on the grounds that if bandX is indeed the a_1 ionisation in the spectrum of $Ga(hfa)_3$, it is extremely unlikely that it should be destabilised relative to its position in the aluminium complex. The

extent to which the 3d orbitals of aluminium should be included in a description of the bonding is of course a thorny problem in theoretical chemistry. The main effect of including 3d orbitals, as we shall see below, is to cause a stabilisation of e(1) relative to a_2 , i.e. to induce a splitting of band B in a direction opposite to that observed in $Ga(hfa)_3$. The absence of any splitting of this band in the spectrum of $Al(hfa)_3$ might suggest that the incipient splitting induced by the p bonding was being annulled by $d_{\sigma,\pi}$ bonding. However, in the absence of any evidence concerning the importance of the 4d orbitals in the bonding of gallium complexes, it is difficult to quantify this argument.

The extent of π bonding in both $Al(hfa)_3$ and $Ga(hfa)_3$ is difficult to estimate. Since our model allows for second order interactions, which are quite large between e(1) and e_π, some π bonding will certainly occur through this mechanism. The absolute values of the various ionisation energies cannot however be taken as an index of the extent of covalence since, although on a simple basis, the more ionic the bonding, the lower the ionisation energy of the mainly ligand orbitals should be, an intense positive field, such as that generated by the very small aluminium ion, will stabilise the ligand orbitals dramatically. Thus, $Al(hfa)_3$ has the highest measured first IE, almost certainly for this reason, and comments about

covalency differences being reflected in the measurement of ionisation energies should be treated cautiously.

A comparison of the spectra of $Al(hfa)_3$ and $Sc(hfa)_3$ shown in fig. 4.16 reveals at first sight fewer differences than might have been expected. The bonding characteristics have however changed dramatically; $a_{2\sigma}$ has now become non-bonding in effect, as has $a_{2\pi}$, since no component of the d orbitals transforms as a_2. The d orbitals transform in an octahedral field as $t_{2g} + e_g$, but when the symmetry is reduced to D_3, $t_{2g} \rightarrow a_1 + e_a$ and $e_g \rightarrow e_b$. Thus a trigonal field can, in effect, scramble the t_2 and e orbitals. In choosing a set of d orbitals which are quantised around the threefold axis, we take the combinations

$$e_a^+ = \sqrt{\tfrac{2}{3}}\, d_{x^2-y^2} + \sqrt{\tfrac{1}{3}}\, d_{yz} \qquad e_a^- = \sqrt{\tfrac{2}{3}}\, d_{xy} + \sqrt{\tfrac{1}{3}}\, d_{xz}$$

$$e_b^+ = -\sqrt{\tfrac{1}{3}}\, d_{x^2-y^2} + \sqrt{\tfrac{2}{3}}\, d_{yz} \qquad e_b^- = -\sqrt{\tfrac{1}{3}}\, d_{xy} + \sqrt{\tfrac{2}{3}}\, d_{xz}$$

These combinations are similar to those given by Ballhausen,[47] with a slight change of axes.

The overlap integrals with the σ and π framework of the ligand are given in tables 4.5 and 4.6.

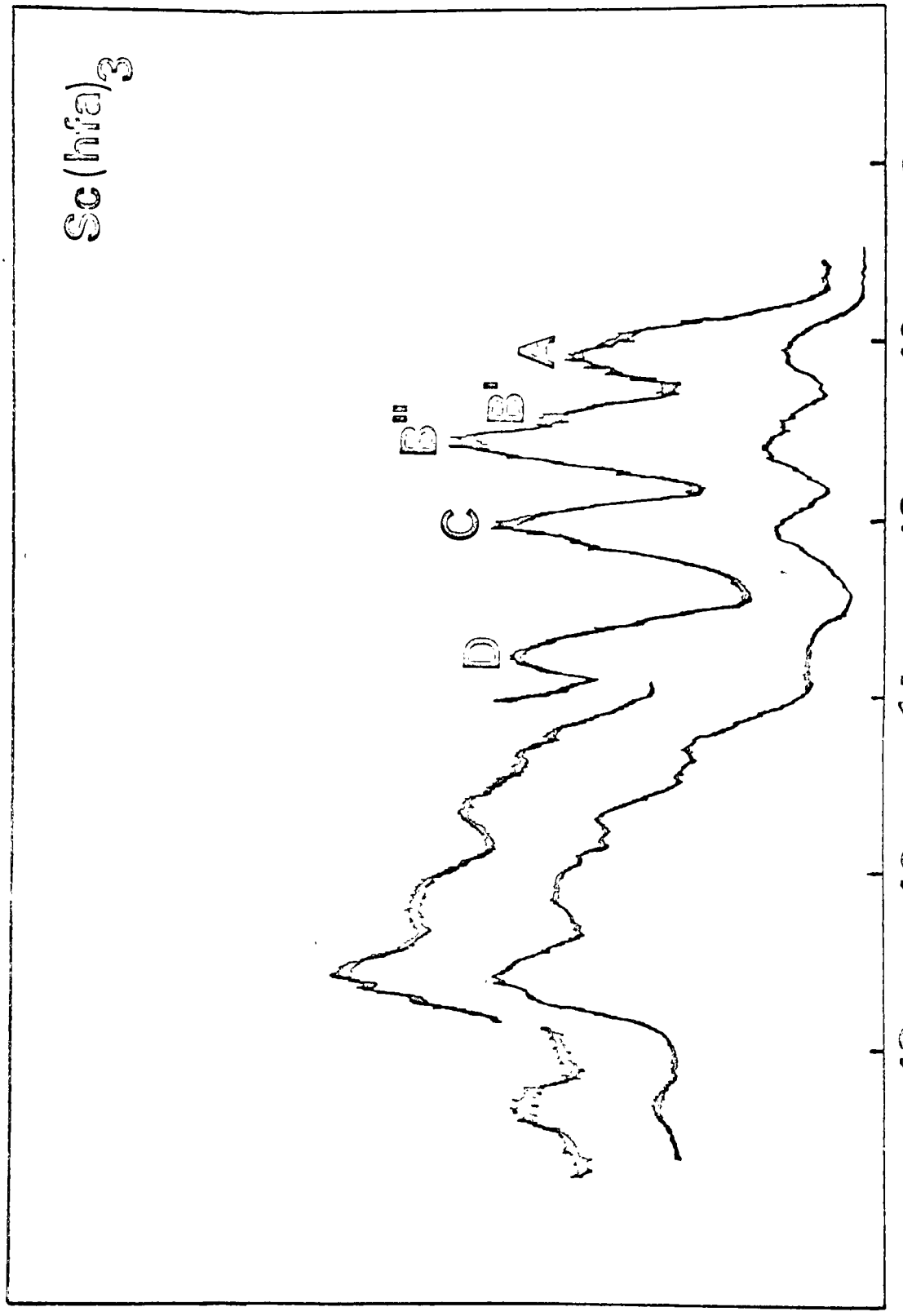

FIGURE 4.16

TABLE 4.5

	d'_{z^2}	e_a^+	e_a^-	e_b^+	e_b^-
a_1	$\sqrt{2}\,xs$	0	0	0	0
a_2	0	0	0	0	0
e(1a)	0	0	0	0	$\sqrt{3}\,\lambda_c$
e(1b)	0	0	0	$\sqrt{3}\,\lambda_c$	0
e(2a)	0	$\sqrt{2}\,xs$	0	$-\lambda_c$	0
e(2b)	0	0	$\sqrt{2}\,xs$	0	$-\lambda_c$

TABLE 4.6

	d'_{yz}	e_a^+	e_a^-	e_b^+	e_b^-
π_{a_2}	0	0	0	0	0
$\pi_e(a)$	0	0	$\sqrt{\frac{3}{2}}\,x$	0	0
$\pi_e(b)$	0	$-\sqrt{\frac{3}{2}}\,x$	0	0	0

where x, λ are the overlap integrals referring to $d_\pi - p_\pi$ and $d_\sigma - p_\sigma$ bonding respectively.

The major source of bonding is now between the e_b^+ orbitals on the central metal, and the e(1) and e(2) orbitals on the ligands. A small amount of d_π / p_π bonding between the $e_a^\pm$ metal orbital and the ligand e_π will also be present. At first

sight however, in spite of this, the only apparent difference between the two spectra is that our sensitive 'barometer,' the middle band, B, has now split in the opposite direction from that found in $Ga(hfa)_3$. This we can understand immediately since e(1) is now strongly stabilised through bonding to the central atom, whereas $a_{2\sigma}$ is now non-bonding. The remainder of the spectrum of $Sc(hfa)_3$ may be assigned easily by analogy with that of $Al(hfa)_3$. Band A must be the π_3 triplet and band C doubtless arises, at least in part, from ionisation of e(2). The position of band a_1 is of some interest since, as can be seen, it is only weakly bonding to the central metal d orbitals, and, if bonding to the Sc 4s orbital is also weak, then it will be little stabilised. It is most likely to be under band C though in principle it could lie under band B. However the considerable inter- and intra-ligand stabilisation of the a_1 orbital would lead to its assignment to band C as being the more likely. The fact that the spectra of the scandium and aluminium complexes are so similar suggests that this assignment also holds for the latter. In addition, since the π_3 band in $Sc(hfa)_3$ has remained unsplit, the extent of π bonding in the scandium complex must be small as, unlike the situation in $Al(hfa)_3$, where the orbitals bond to the same extent, there will be little bonding to $a_{2\pi}$ in the transition metal series, see fig. 4.17.

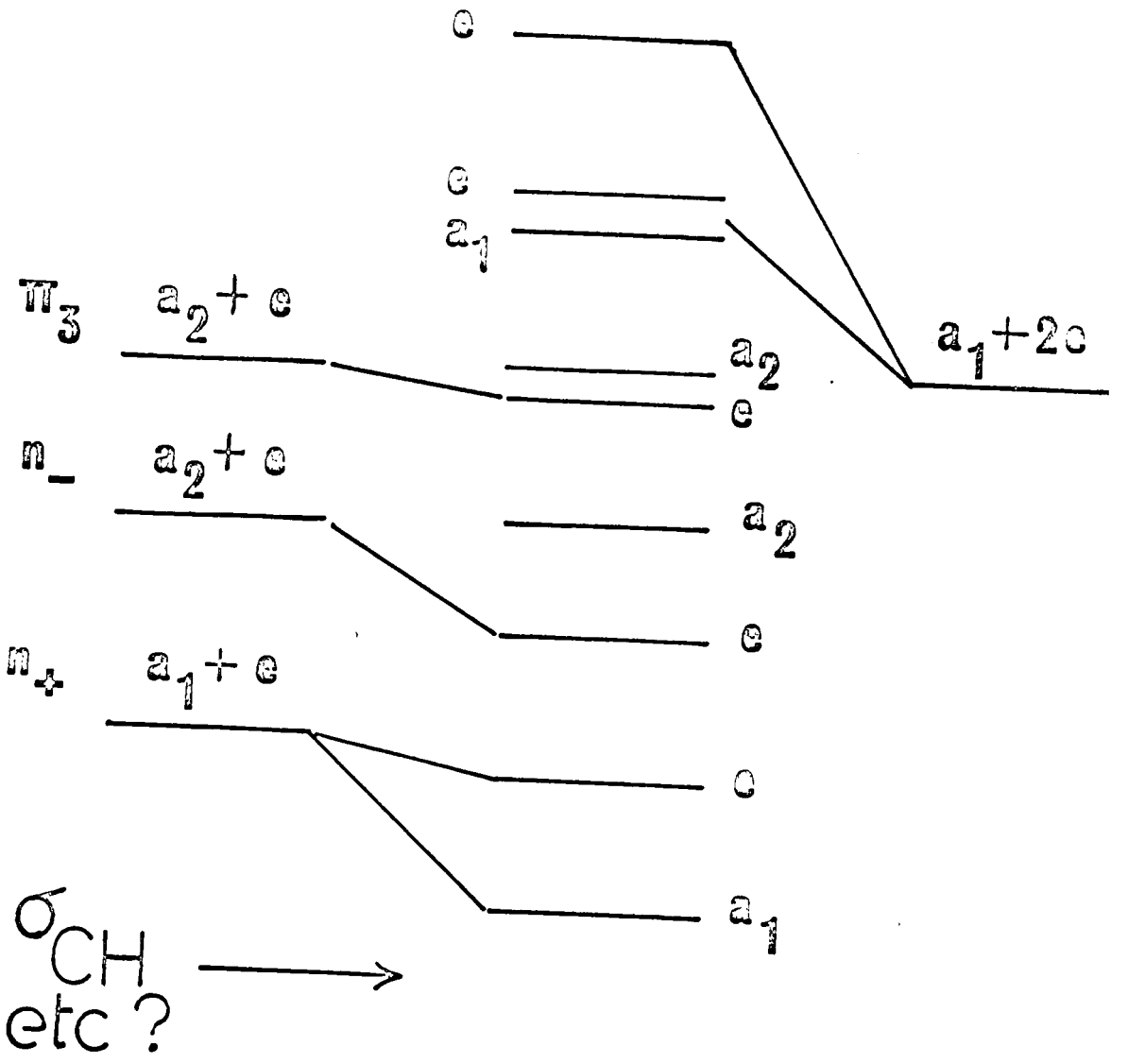

FIGURE 4.17

If we turn now to the t_{2g}^n series of complexes, $Ti(hfa)_3$, $V(hfa)_3$, $Cr(hfa)_3$ and $Co(hfa)_3$, these can be interpreted fairly easily on the above model. We saw that the major difference between $Al(hfa)_3$ and $Sc(hfa)_3$ lay in the splitting of the second band (B) into $a_{2\sigma}$ and e(1) components. Turning to the spectrum of $Ti(hfa)_3$, fig. 4.18, another novel feature appears in the guise of a weak band at 7.93 eV which is quite sharp. Now this must arise from ionisation of the single d electron present in Ti(III) complexes, which might occupy either the $a_1(d_{z^2})$ or $e_a^{\pm}$ orbitals. ESR evidence[5] suggests that a_1 lies below $e_a^{\pm}$, in agreement with our simple model, giving a ground state of $^2A_1$ to $Ti(hfa)_3$. The general MO scheme is illustrated in fig. 4.17. Another feature of interest is the increased splitting of the $a_{2\sigma}$ and e(1) levels as compared to $Sc(hfa)_3$, being 0.28 eV in the latter and 0.39 eV in $Ti(hfa)_3$. This increased splitting is caused by the rapid stabilisation of the d orbitals and concomitantly, as we shall see below, an increase in the relative importance of these, as regards the bonding, compared to the 4s and 4p orbitals.

The spectrum of $V(hfa)_3$ fig. 4.19 is rather interesting in that the d ionisation has now shifted to higher energy and has slightly broadened. The compound is known to be high spin, and the electronic structure could be a_1e_a or e_a^2, and magnetic evidence from $V(acac)_3$[7] suggests a $^3A_2$ ground state implying

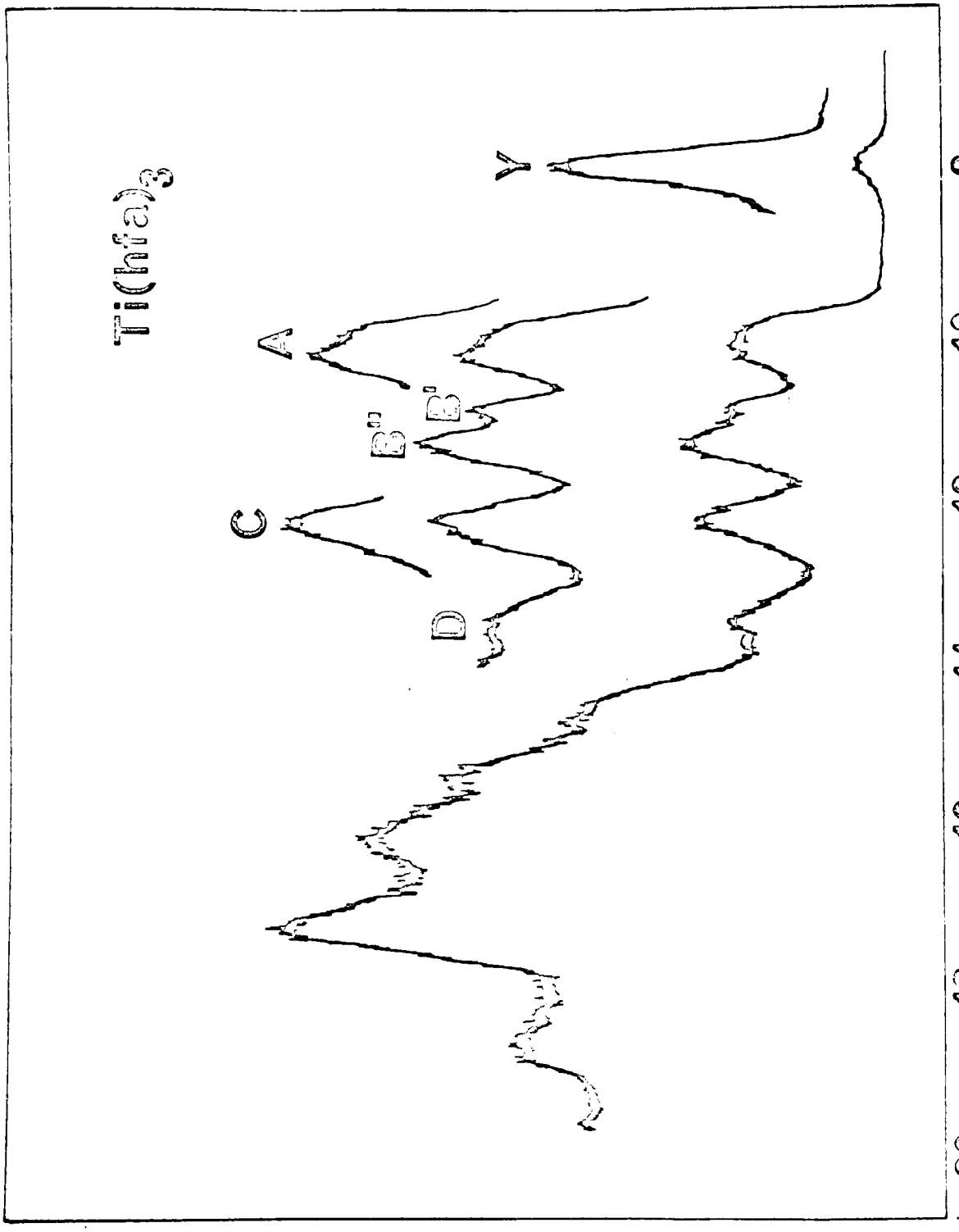

FIGURE 4.18

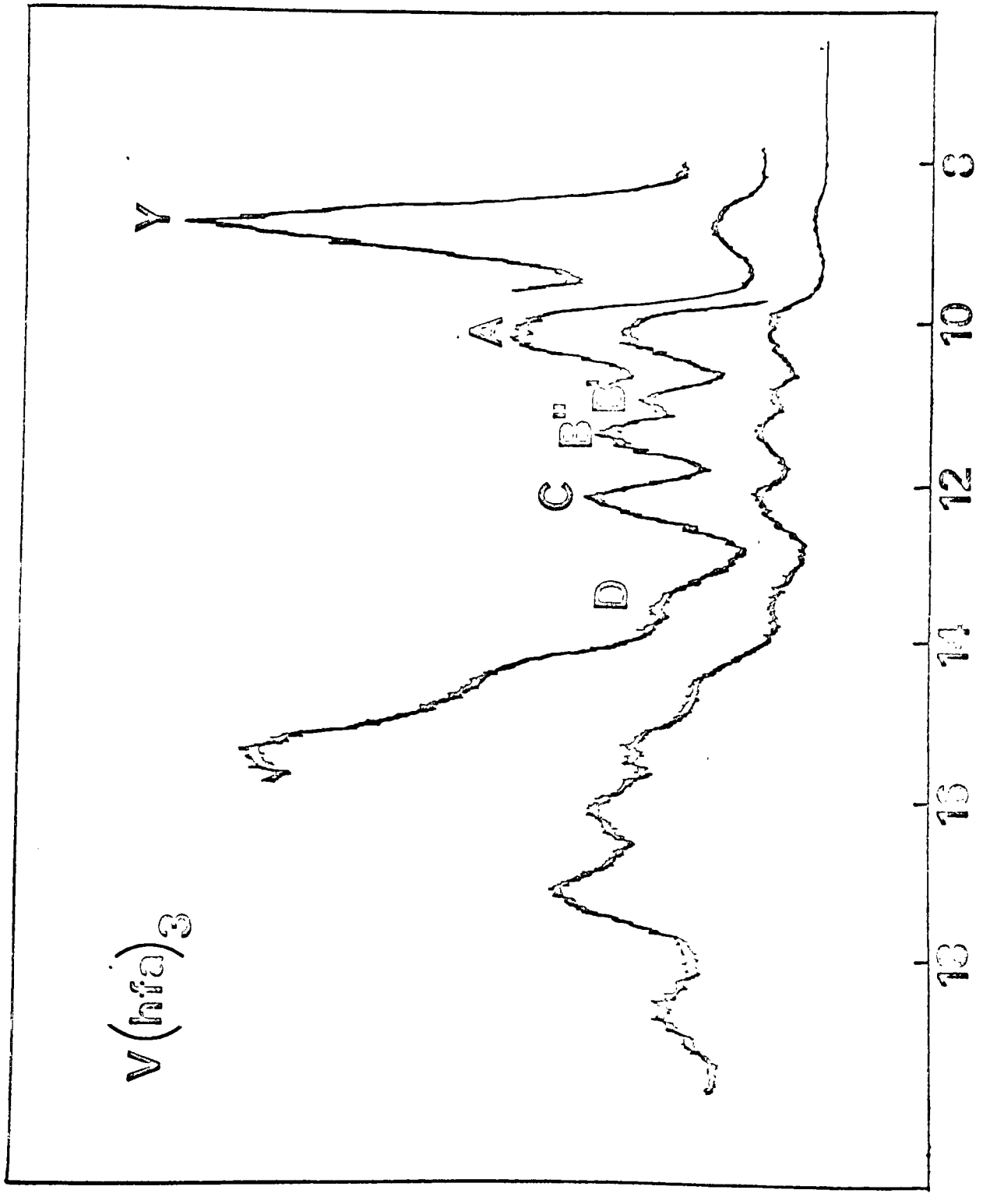

FIGURE 4.19

the latter e_a^2 configuration. This is rather surprising in view of the ground state of Ti(III), but presumably reflects the fact that $J_{e_a^+e_a^-} - K_{e_a^+e_a^-}$ is smaller than $J_{e_a a_1} - K_{e_a a_1}$ owing to the greater bonding characteristics, especially π-delocalisation, of e_a compared to a_1. If the difference in repulsion and exchange integrals exceeds the presumed trigonal splitting Δ_2, then the ordering of one-electron energies would be $a_1 < e_a$ even though the ground state were e_a^2. The additional broadening of the d band in $V(hfa)_3$ might arise from the greater bonding character of the e_a orbital and perhaps also from a small Jahn-Teller induced splitting in the ionised state. Interestingly, ionisation of $V(hfa)_3$ cannot yield the ground state of $V(hfa)_3^+$ which will presumably be a_1^1 since this would involve a two electron process. A further notable point in this spectrum is the increased splitting observed in band B, with the a_{2g} ionisation at 10.96 eV and e(1) at 11.39 eV, which is in accord with the expectation that, as the d orbitals stabilise, their interaction with e(1) will increase.

The spectrum of $Cr(hfa)_3$ fig. 4.20 shows that the d orbital ionisation energy is now almost the same as the ionisation energy of the first ligand band π_3. The ground state of the complex is $^4A_2$ corresponding to the expected ground configuration $a_1 e_a^2$, but the relative ordering of the two

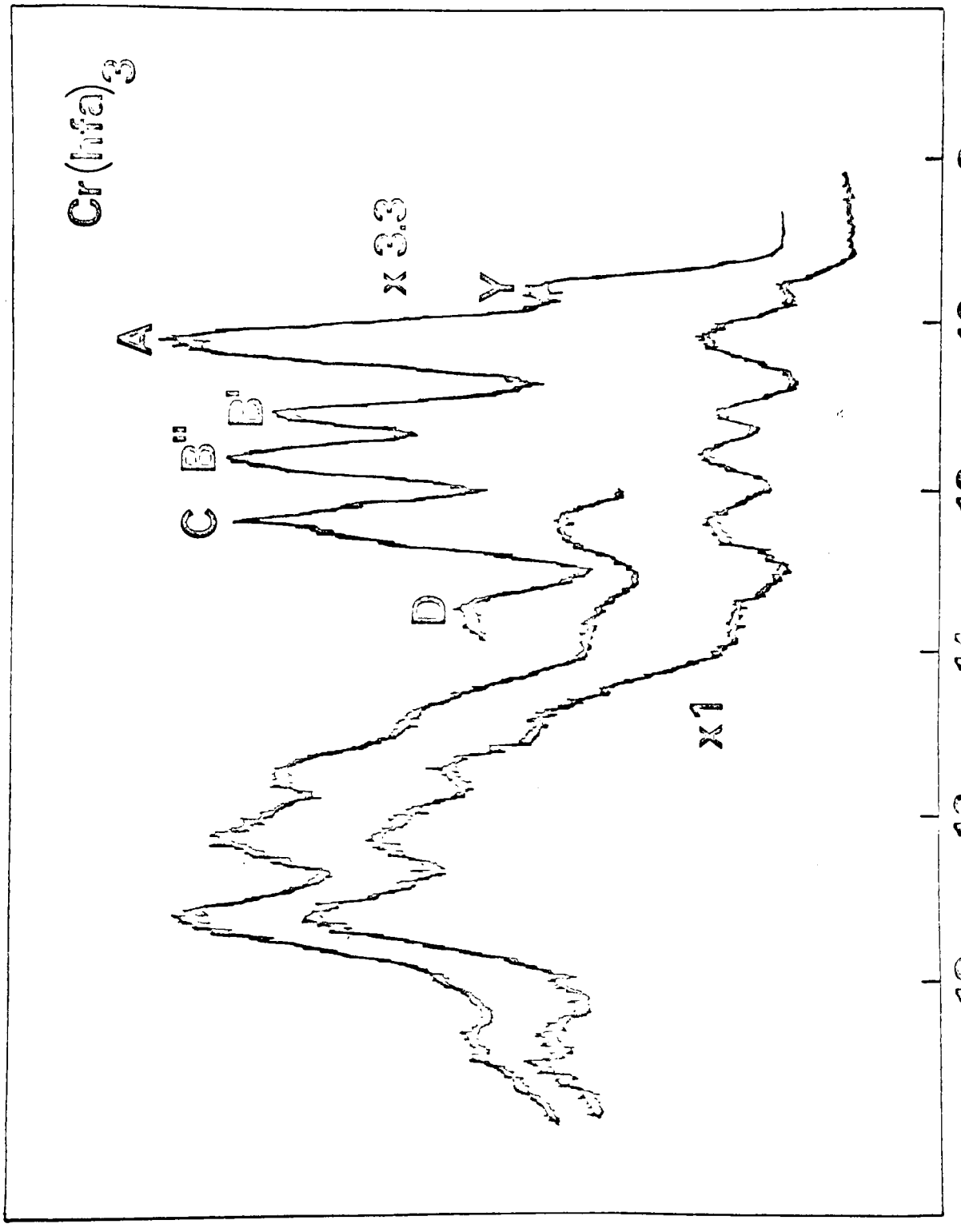

FIGURE 4.20

levels is uncertain. Ligand field analysis[53] tends to support $a_1 < e_a$ as the energy ordering, but this of course is based on the splitting of the excited ^4T states and, as our analysis showed for $V(hfa)_3$, the assumption of equal electron repulsion integrals may be highly misleading in the case of such very small splittings. We would expect, on the basis of d_π covalency, that the repulsion and exchange integrals for e_a^+ will be less than those of a_1 so that, on ionisation, the $^3A_2$, e_a^2 term will be stabilised relative to the $a_1 e_a$ term ^3E. This would have the effect apparently of destabilising the pseudo one-electron orbital energy of a_1. Hence the ligand field ordering may not be reflected in the photo-electron spectrum.* Actually, there appears to be only one d orbital band in the PE spectrum of $Cr(hfa)_3$ indicating that the two effects are cancelling to a certain extent. It is also noteworthy in the spectrum that that the splitting of band B has now increased still further, the $a_{2\sigma}$ and e(1) bands now ionising at 11.12 and 11.61 eV

---

* An extreme example of this effect is found in ferrocene,[54] when the ligand field arguments would place a_1 unambiguously above e_2, but the very large difference in orbital repulsion energies within these two terms even within the ligand field approximation amounts to 20 B, leading to an energy ordering of ion states $^2E_2 < {}^2A_1$.

respectively.

Thus we have assigned on a fairly simple one-electron model, the spectra of the t_{2g}^n series of tris chelate complexes up to $Cr(hfa)_3$; however, a few factors remain to be discussed. Firstly it is apparent that the spectra should show exchange splittings comparable to those discussed for VCl_4[55]. These splittings arise from spin-coupling in the ionised state of the molecule when an electron is removed from one of the filled inner shells. Thus, in $Ti(hfa)_3$, ionisation of the e(2) level of the ligand should give rise to two states, ^1E and ^3E whose energies will differ by twice the exchange integral between the e(2) and metal a_1 levels, K_{ea_1}. It is difficult to estimate the value of such integrals but a comparison of the half widths of bands in the $Ti(hfa)_3$ and $Sc(hfa)_3$ spectra shows that this exchange splitting is not apparently a major source of band broadening. The magnitude of the splitting will increase across the series, being $3K_{e_a e(1)}$ or $V(hfa)_3$ and $4/3\ K_{ea_1} + 8/3\ K_{ee_a}$ for $Cr(hfa)_3$ and, examining the relevant spectra, very little broadening can be detected; indeed, for the a_{2g} band, which will be similarly effected, some sharpening up can be seen in the spectrum of $Cr(hfa)_3$.

A second point to note is that the d ionisation observed is, of course, the lowest ionisation potential corresponding, in Cr(III) complexes to $^3T_1 \leftarrow {}^4A_2$. Neglecting trigonal effects

for the moment, a transition is found in the UV absorption spectrum of $Cr(acac)_3$ at 12,900 cm^{-1} which has been assigned to the $^2E \leftarrow {}^4A_2$ transition.[53,56] Using standard strong-field theory,[57] the ^2E state should lie 9B + 3C in energy above the $^4A_2$ ground state, giving a value for B of 580 cm^{-1}, assuming C = 4.4B, implying a very large nephelauxetic ratio even for the t_{2g} orbitals. Taking this value of B, we can calculate for t_2^3, a spin-randomised ionisation energy for the process $t_2^3 \rightarrow t_2^2$. The correction to our initial value of 9.53 eV for the IP of $Cr(hfa)_3$ is -1,05 volts, implying that the <u>mean</u> d-orbital ionisation energy is 8.48 eV. Unfortunately, it is not possible in V(III) tris-chelates, to distinguish the spin-forbidden intra-t_2 transitions, and values of B given are probably much too high; e.g. Griffith quotes 787 cm^{-1} for B in $V(H_2O)_6^{3+}$ which would give a corrected value for the IP lower than that of the Ti(III) complex. The simplest assumption is that the nephelauxetic ratios for V(III) and Cr(III) are the same which gives a corrected IP of 8.13 eV. These values, together with that of $Ti(hfa)_3$ at 7.93 eV are probably a more accurate representation of the rate at which the d orbitals stabilise. In general spin-randomised ionisation potentials for a given subshell show a smooth increase across a series, though in this case certainly not a linear one, and, as we shall see below, the trend is not sufficiently well-

defined to enable us to predict accurately the d-orbital energies in $Co(hfa)_3$. It can however be seen that it is this trend rather than that of the uncorrected IE's which can be extrapolated to the case of $Co(hfa)_3$.

The mean d-orbital energy calculated in this way is not related in any simple manner to any one-electron orbital energy. Within the Roothaan open-shell formulation, it is not difficult to show, at least for atoms, that our defined spin and orbitally randomised ionisation energy is equal to the negative of the weighted average of the orbital energies corresponding to the available multiplets (assuming Koopmans' theorem). Thus, if we were to calculate the t_2 orbital energy for <u>each</u> of the multiplet states of t_2^3 and then average them by J-weighting, we would expect to obtain the value -8.48 eV. However there is no simple relationship between this and the t_2 orbital energy for the $^4A_2$ state in Roothaan's MO formalism, but it is a well known feature of the atomic Roothaan equations that for a simple single determinant p wave function, where no electron pairing has occurred in the open shell, the orbital eigenvalue is exactly the negative of the observed IP of that shell assuming Koopmans' approximation, and so, we immediately have, for the complexes so far considered, a value for ε_{t_2}. It is for this reason that, within our overlap model, the value taken for ε_d is that observed, and not the spin-randomised

one.

The splitting observed for band B may be explained within the overlap model fairly easily. The strength of bonding to the e(1) level of n_- and the d-orbitals will be given by

$$\Delta = \frac{\xi^2 S^2}{\varepsilon_{e_b} - \varepsilon_{2(1)}}$$

where a Brillouin-Wigner formalism for the perturbation expansion has been assumed. Assuming that the $a_{2\sigma}$ level stays accurately constant and non-bonding then Δ will give the required splitting directly. The main problem is that we do not know the value of ε_{e_b} since the e_b level is not occupied. Empirically however we will assume that the splitting between the e_b and e_a levels remains roughly constant throughout the t_2^n series and so a plot of $\varepsilon_{t_2} - \varepsilon_{e(1)}$ against $1/\Delta$ should be linear. This plot is shown in fig. 4.21 and as can be seen it is approximately linear, giving a value of 0.75 for ξ S. If we extrapolate this to $Sc(hfa)_3$, we obtain a value for $\varepsilon_{t_2} - \varepsilon_{e(1)}$ of 6 volts, and a suggested d-orbital energy of -5 eV. This is remarkably high and other extrapolations suggest a more reasonable value of about -7 eV. This would imply that some other effect must be operating in Sc(III) complexes, presumably bonding to 4s or 4p orbitals

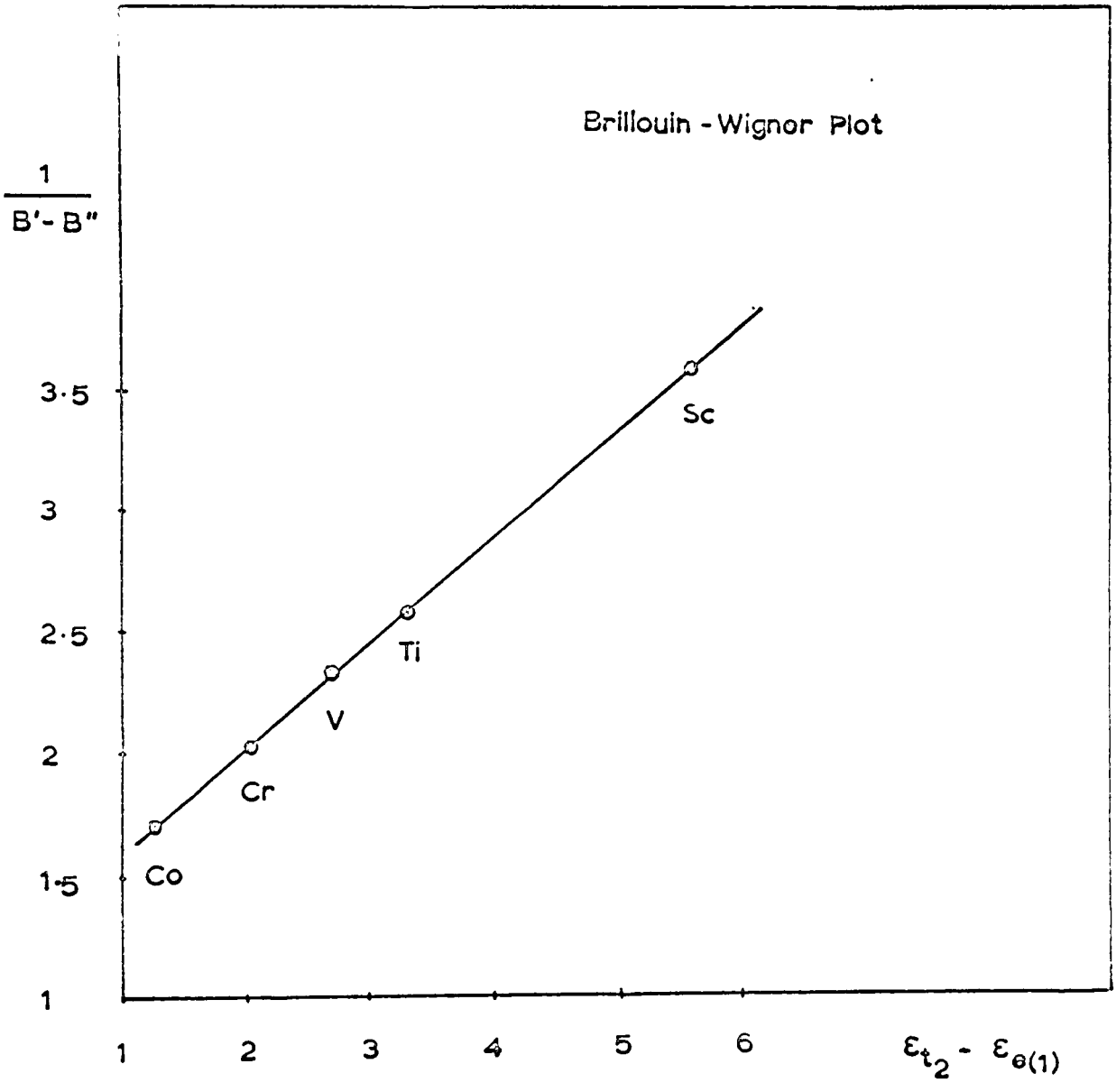
Brillouin - Wignor Plot
1
B' - B"
3·5
3
2·5
2
1·5
1
Co
Cr
V
Ti
Sc
1
2
3
4
5
6
$\varepsilon_{t_2} - \varepsilon_{e(1)}$

FIGURE 4.21

which must be substantial in $Sc(hfa)_3$ and, as we will see below, the ESCA spectrum of $Sc(hfa)_3$ is also anomalous. As we saw in the spectra of $Al(hfa)_3$ and $Ga(hfa)_3$, the effect of bonding to the 4p orbitals will be to cause an inverse splitting of band B with $a_{2\sigma}$ lying lowest. Superposition of such an expected splitting on that caused by interaction with the 3d orbitals will certainly lead to a reduction in the observed splitting of band B which is precisely the effect seen in $Sc(hfa)_3$. The bond lengths in the ternary oxide phase systems also suggest a rapid contraction between Sc(III) and Ti(III) which will increase the value of S in the latter complex. This effect will also lead to an anomalously low splitting of band B in Sc(III) complexes.

At first sight the spectrum of $Co(hfa)_3$, fig. 4.22, is rather complex since there are now <u>six</u> bands in the low IE region. However, we can immediately correlate the bands at 11.15 and 11.75 eV with the bands B'' and B' seen in the earlier members of the t_{2g}^n series, and the band at 12.56 eV clearly corresponds to band C, the $e(2)/a_{1\sigma}$ ionisations. The remaining three bands, labelled K, L and M are much more difficult to assign. There are four possibilities

(i) the band at 9.73 eV corresponds to the e_a and a_1 orbitals on the metal; then, on intensity grounds, L is the e band of T_3 and K the a_2 band.

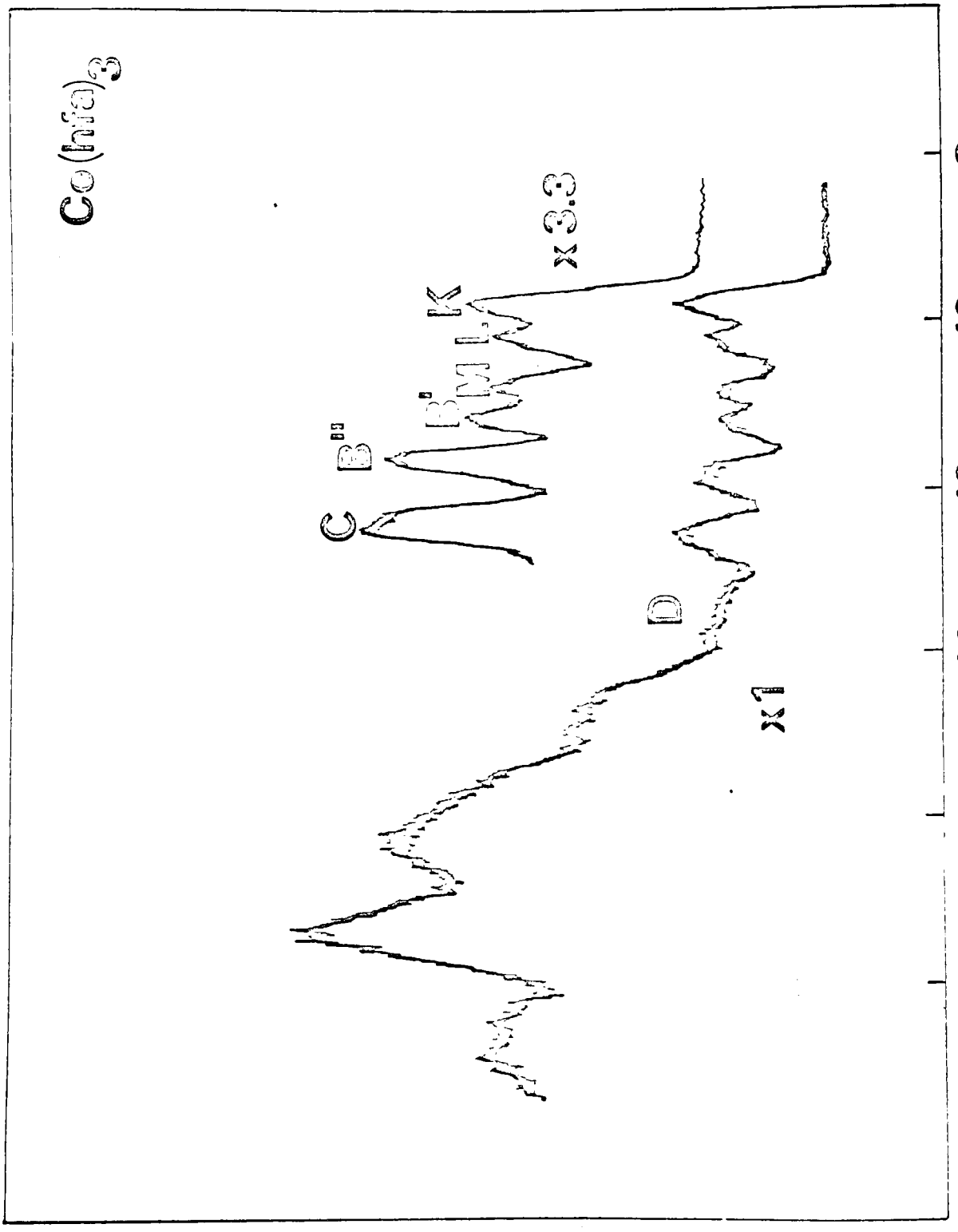

FIGURE 4.22

(ii) the band at 9.73 eV (M) is the e_π and $a_{2\pi}$ components of π_3; then, on intensity grounds, L is the e_a band and K the a_1 band derived from the metal d-orbitals.

(iii) M corresponds to e_π of π_3 only, the $a_{2\pi}$ and a_1 (metal) ionisations both lie under L, and K corresponds to ionisation from metal e_a.

(iv) M corresponds to e_a of the metal only, band L is as (iii) above, and K corresponds to ionisation from e_π.

It is clear that in $Co(hfa)_3$, the t_2 d-orbitals on the central metal lie close in energy to the π_3 level of the ligand, and it is difficult to decide at this stage which of the two lies lower in energy. Since we found above that the e_a orbital on the metal does not bond to e(1) and bonds to e(2) to the same extent as d_{z^2} bonds to a_1, a trigonal splitting of the d-orbitals can only occur in first order by bonding to π_3. If this is so, then the observed splittings of π_3 and the metal t_2 orbitals should be approximately equal, lending support to assignments (iii) and (iv). The simple MO diagram should resemble

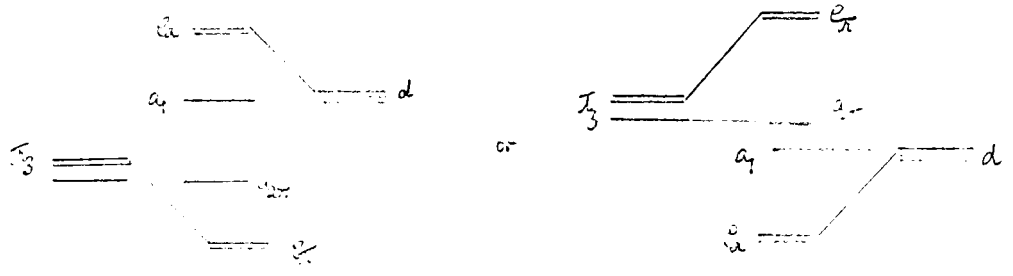

which would lead to $\varepsilon(e_\pi) < \varepsilon(a_{2\pi})$ if $\varepsilon_{\pi_3} < \varepsilon_d$ and $\varepsilon(e_a) < \varepsilon(a_1)$ if $\varepsilon_d < \varepsilon_{\pi_3}$. This would tend to rule out assignments (i) and (ii). Further evidence against (i) is provided by the Brillouin-Wigner plot discussed above. It must be recognised that it is rather a jump from the open shell molecules in the first half of the series to Co(III), but, given a splitting of 0.60 eV a mean t_2 energy of 10.5 eV would be predicted which would strongly support assignment (iii). The assumption in this extrapolation, that the value of 10Dq remains unchanged from $Co(hfa)_3$ to $Cr(hfa)_3$, seems to be borne out by the UV spectra.*

Assignment (ii) corresponds to the situation in which the trigonal splitting of π_3 is negligible, and the observed splitting of e_a and a_1 is entirely due to very strong interaction with e(1) which would destabilise e_a with respect to a_1. This is difficult to rule out absolutely, but since no splitting is observed in $Cr(hfa)_3$ some doubt must still attach to it as an alternative to (iii). Evidence from the UV absorption spectrum of $Co(acac)_3$[59] is inconclusive but would suggest a ligand field splitting of only 0.2 eV, but there

---

* The relevant values of 10Dq for the tris-acetylacetonato complexes are: Ti(III): ca. 18,000 cm^{-1}, V(III): 18,500 cm^{-1}, Cr(III): 17,860 cm^{-1}, Co(III): ca. 19,000 cm^{-1}.

seems little doubt that assignment (i), which is supported by this figure can be ruled out on other evidence. The problem with the ligand field analysis in the case of $Co(hfa)_3$ is that there are no intra- t_2 transitions and indications of the trigonal splitting must be gleaned from an examination of the $t_2 \rightarrow e$ transitions. It is perhaps interesting that the ligand field analysis does predict the a_1 level to lie above the e_a level.

The metal d-orbital cross-section seems to be steadily increasing throughout the t_{2g}^n series, being comparable at $Cr(hfa)_3$ to that of π_3. If this growth in cross-section is maintained, then assignments (ii) and (iii) become the tenable alternatives, and both presuppose that the metal d-orbitals lie <u>below</u> the first ligand level π_3. This is not so surprising as it might appear, since, as we saw above, extrapolation of the spin-randomised ionisation energies of the t_2^n series would suggest a d ionisation energy of between 10 and 11 eV. Of the other assignments, (iv) was suggested by Barnum as best explaining the UV absorption spectrum of $Co(acac)_3$[4]. Caution should however be used in interpreting Barnum's results, since he paid no attention to the σ-framework of the molecule, and his interpretations of other tris-chelate spectra have been challenged by several authors.

To try and resolve the question of the assignment more

satisfactorily, the PE spectra of some other Co(III) chelates were examined. As can be seen however from the spectrum of $Co(acac)_3$ reproduced in fig. 4.23 the low IE regions of this and $Co(hfa)_3$ are very similar. This suggests a rather remarkable phenomenon, namely that both ligand and metal orbitals appear to have moved together on perfluorination of the ligand. No real explanation can be put forward for this effect, though it may be related to the fluorine effect discussed above. A comparison of the shifts observed on perfluorination in $Cr(acac)_3$ and $Co(acac)_3$ are given in table 4.7a

TABLE 4.7a

	Cr^{III}, Δ		Co^{III}, Δ
		M	2·21
Y	2·11	L	2·10
A	2·12	K	2·24
B′	2·14	B′	2·16
B″	2·15	B″	2·21
C	2·18	C	2·22
D	?	D	?

It can be seen that the shifts are both larger on average and more irregular in the cobalt complexes. Thus, in the chromium complexes the π band moves by a similar amount to the σ bands, but in the corresponding cobalt case, band L

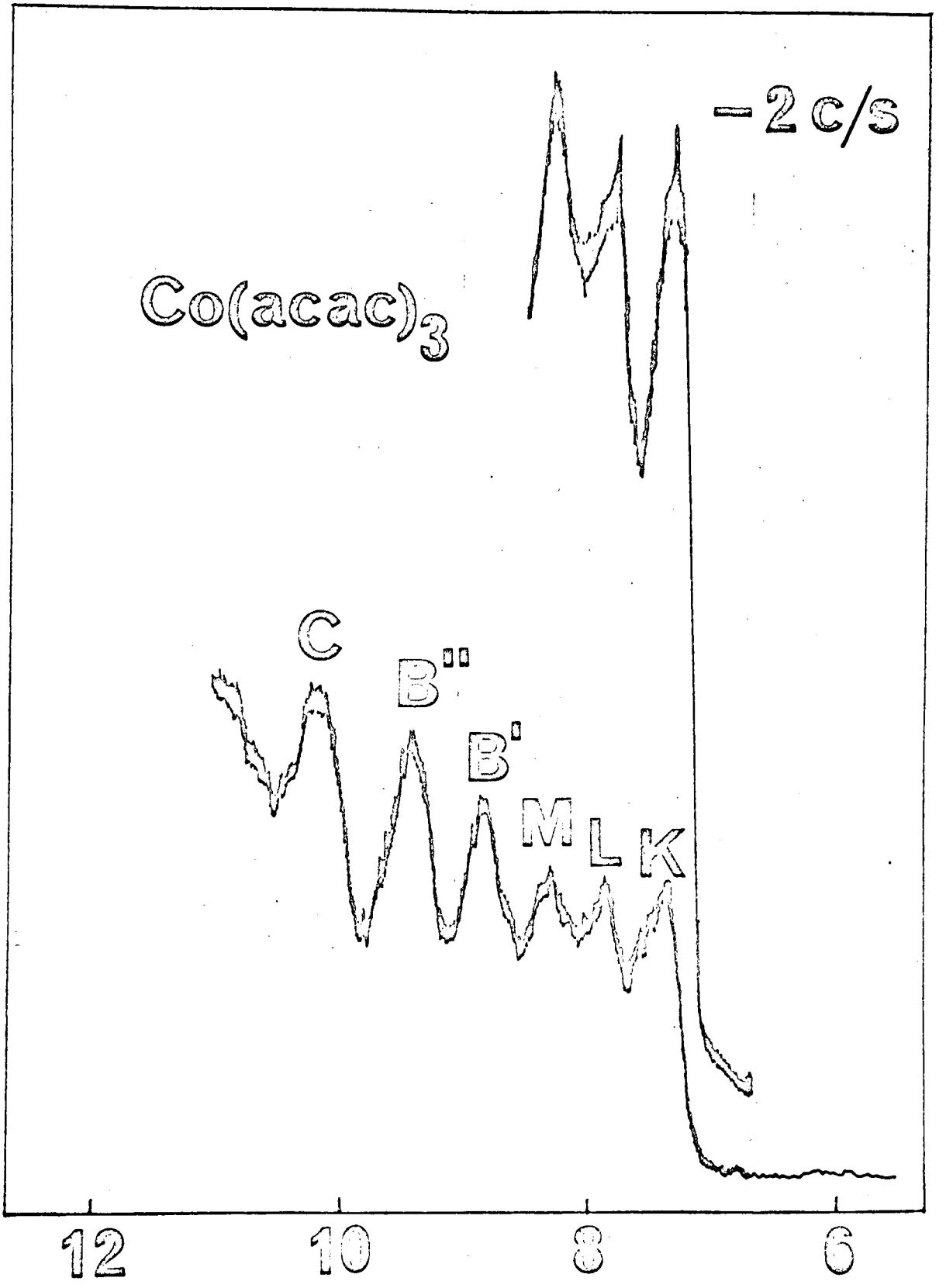

FIGURE 4.23

appears to move rather less. In addition, the splitting between e(1) and $a_{2'}$ is much smaller in $Co(acac)_3$, a fact which is probably not due to smaller overlap since there is no change in the splitting in $Cr(acac)_3$. It is clear that a rather profound change in bonding type has occurred between $Co(acac)_3$ and $Co(hfa)_3$ between that of assignment (iii) in the latter case to possibly that of assignment type (i) or (iv) in the case of $Co(acac)_3$. This leaves Barnum's interpretation of the UV spectrum intact, though the trigonal splitting from the UV is now the wrong sign. If this is indeed the case, the result is especially interesting as showing how finely balanced the metal and ligand energy levels are in Co(III) complexes.

Finally, in this section we consider the UV-PE spectra of the first row transition-metal high-spin complexes. It proved very difficult to obtain a satisfactory spectrum of $Mn(hfa)_3$ owing to the side-effects discussed above. At first sight the spectrum bears little resemblance in the low IE region to those considered above and a general lack of definition is apparent. This could in principle be caused by a dramatic increase in exchange splitting, since measurements on analogous Mn(III) chelates strongly suggest a high spin configuration in the ground state: $a_1 e_a^2 e_b$. The delocalisation of the e_b orbital would naturally lead to a rather larger value of the exchange

integral. Another possibility is that the ^5E ground state distorts through the Jahn-Teller effect so as to reduce the overall molecular symmetry from D_3, but owing to the topological restrictions imposed by the chelating rings, little distortion of the metal environment from a pure octahedron is in fact found crystallographically.[69] It is perhaps surprising that the distortion is so small since halo-complexes of Mn(III) suffer severe distortions giving five-coordinate species.

Ionisation of the ^5E state can give rise to quartet states only, by virtue of the fact that photo-ionisation is a one-electron process; ionisation of the e_b electron leads to $a_1e_a^2$ $^4A_2$ state, and ionisation of the a_1 and e_b electrons leads in a pure octahedral geometry to $^4T_1$ and $^4T_2$ both of which are split by both trigonal and Jahn-Teller effects, giving rise to a complex series of ionisation processes. To evaluate the relative intensity of the three bands, we must calculate the fractional parentage coefficients arising from $|t_2^3(^4A_2)e(^2E)\rangle$, $|t_2^2e(^3T_1)a_1(^2E)\rangle$ and $|t_2^2e(^3T_2)a_1(^2E)\rangle$ for the ^5E state. These were obtained using tables A 20 and A 24 in Griffith[55] and have the values 1/2, $-\sqrt{6}/4$ and $-\sqrt{6}/4$ respectively giving the relative intensities of the bands as 1/4, 3/8, 3/8. The total intensity will be proportional to the number of electrons, so, relative to the π_3 band having an intensity of 6, that of $^4A_2$ will be one, and those of $^4T_1$, $^4T_2$ will be 3/2 each. It should be

noted that these intensities differ from those predicted by the simple multiplet theory; this is because $^4T_1$ and $^4T_2$ ionisations effectively share the ionisation intensity from the t_2^3 sub-shell.

Another way of regarding the PE spectrum of $Mn(hfa)_3$ is as the energy level sequence found for $Mn(hfa)_3^+$, a six-coordinate Mn(IV) complex. This is of course iso-electronic with $Cr(hfa)_3$, and so the UV spectrum of the latter should be of value in interpreting the PE spectrum of $Mn(hfa)_3$. Unfortunately, the UV spectrum of $Cr(acac)_3$[56] does not show the $^4T_1 \leftarrow {}^4A_2$ transition clearly, apparently because it is swamped by the $\pi \rightarrow \pi^*$ and $n \rightarrow \pi^*$ excitations. It is thus necessary to examine the UV spectrum of $Cr(H_2O)_6^{3+}$.[51] If we neglect CI with the $^4T_1$ term derived from t_2e^2 (which can be shown to be comparatively small), the $^4T_1$ term will lie at 10Dq + 12B above the $^4A_2$ ground state, and the $^4T_2$ term exactly 10Dq above $^4A_2$. Thus, if we know B for $Mn(hfa)_3$ we can predict the observed separation of $^4T_1$ and $^4T_2$ in the PE spectrum quite accurately. However the UV spectra of Mn(III) chelates have been the subject of considerable controversy.[50,52] Taking that of $Mn(acac)_3$ as an example, bands at 8,890 cm^{-1} and 18180 cm^{-1} are found. The second is almost certainly the spin allowed $^5T_2 \leftarrow {}^5E$ transition, of energy 10Dq. The first band might be assigned to the $^3T_1 \leftarrow {}^5E$ transition, but its very large

oscillator strength suggests a spin-allowed band, and Fackler et al., having examined the UV spectra of a number of substituted tris-chelates of Mn(III), found the band to be solvent dependent to an extent apparently incompatible with a basically d → d transition.[62a] Piper and Carlin[71] have argued that the band is a d → d transition whose intensity arises because of spin-delocalisation and Jahn-Teller coupling. If the band at 8,890 cm^{-1} is indeed the $^3T_1 \leftarrow {}^5E$ band, then its energy is given in strong field theory by 6B + 5C - 10Dq[57] and, since 10Dq = 18,180 cm^{-1} = 2.25 eV, we obtain a value of 965 cm^{-1} for B, a value which is rather high, bearing in mind the large nephelauxetic ratios found in many tris-chelate complexes. Taking these values of 10Dq and B the separation of the three PE bands $^4A_2$, $^4T_2$ and $^4T_1$ should be 2.25 and 1.44 eV respectively. The separation of $^4T_1$ and $^4T_2$ calculated in this way, 11,600 cm^{-1}, is very much larger than that observed in Cr(III) complexes, e.g. in $Cr(H_2O)_6^{3+}$ it is 7,180 cm^{-1}. Thus the suggestion must be that the band at 8,890 cm^{-1} in $Mn(acac)_3$ is not a d → d transition. Of course, in the same way, the PE spectrum of $Fe(hfa)_3$ should give the energy levels of a d^4 chelate system, and there, the separation between $^5E(\pi_3^6 t_2^3 e_b)$ and $^5E(\pi_3^5 t_2^3 e_b^2)$ is certainly very small and may well be negative (see below). Thus, it is likely to be quite small in $Mn(acac)_3$[62a] suggesting that this intense low

energy band in the UV spectrum may even be charge transfer $\pi_3 \rightarrow e_b$. Jørgensen[24] has placed this band at 25,000 cm^{-1}, but in the light of the above discussion this seems unlikely.

Thus, if the band at 8,890 cm^{-1} is not the $^3T_1 \leftarrow {}^5E$ transition, there is no way in which we can directly evaluate B for the Mn(III) complex. It does seem likely however that its value will be greater than in Cr(III) complexes even if it is less than 960 cm^{-1}, so that the separation of $^4T_1$ and $^4T_2$ will presumably be intermediate between 1.0 and 1.5 eV. Turning now to the details of the PE spectrum, the first band we expect to see in the low IE region will arise from ionisation to the $^4A_2(t_2^3)$ state, and, compared to band A, we expect it to be very weak (ca. 1/6 intensity). A clearly resolved band is not observed either in $Mn(hfa)_3$ or in the PE spectrum of $Mn(acac)_3$, but a broad and anomalous tailing is seen to the low IE side of band A, apparently corresponding to the expected ionisation. The high IE of the e_b electrons (9.2 eV) is rather surprising, but it should be remembered that we have a situation in which very considerable spin stabilisation of the state has occurred. If we spin randomise the t_2^3 shell, assuming the usual strong field theory, we must subtract 6B + 2C from the ionisation energy to obtain a measure of the average d energy as we showed for Cr(III) complexes above, and the corresponding stabilisation energy for Mn(III) is 9B + 3C

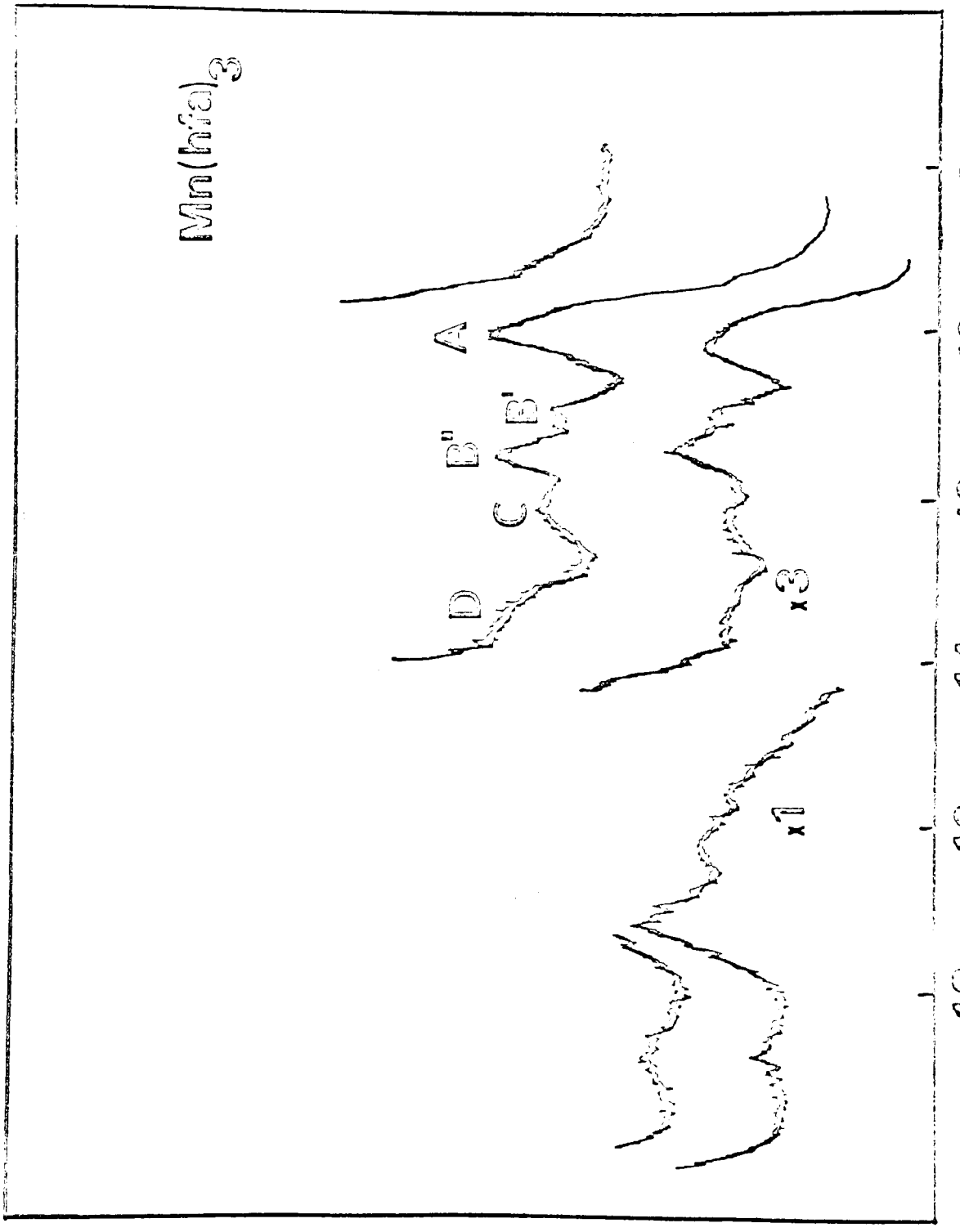

FIGURE 4.24a

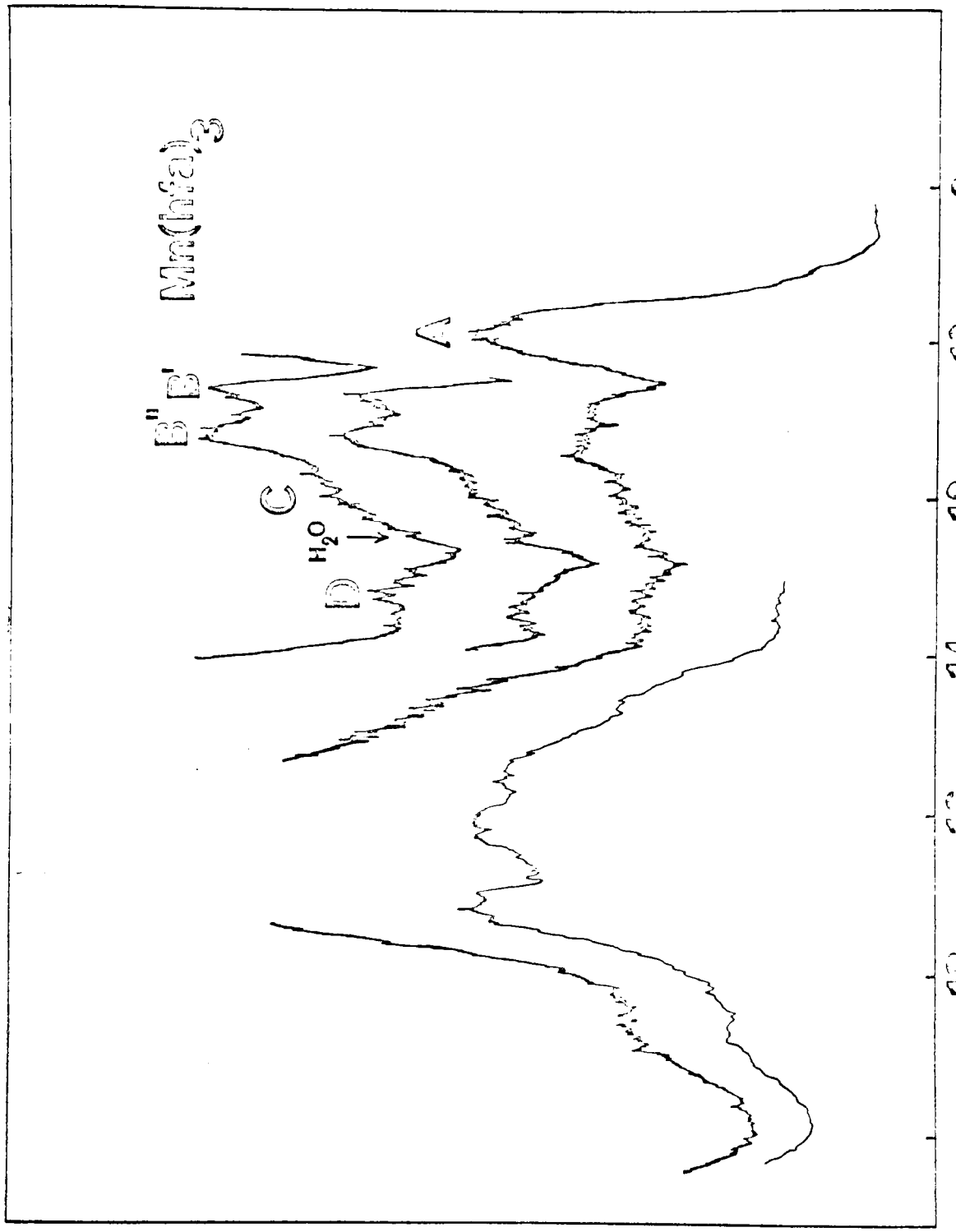

FIGURE 4.24b

which, for reasonable values of B will certainly be larger than 2 eV. Chemically, this is a rather more satisfactory energy for the e_b electron, but the analysis does re-emphasise the fact that in the PE spectrum of high-spin complexes we are going to see results which bear very little resemblance to traditional MO pictures.

Assuming that the band at 9.2 eV does arise from the $^4A_2 \leftarrow {}^5E$ ionisation, band A, at 10 eV will be, without doubt, due to ionisations yielding the various spin-coupled states of π_3 and cannot, assuming the above treatment to be numerically reasonable, arise from any transition involving the metal t_2 electrons. If the figure of 2.25 eV is taken for 10Dq, the next d-orbital band, $^4T_2$, should occur at 11.42 eV. That there is a band at 11.41 eV is undoubtedly fortuitous, since we have not considered the effects of Jahn-Teller and trigonal splittings, both of which may be of the order of 2,000 cm^{-1} in these complexes.[62] The bands labelled B′ and B″ in these complexes are doubtless mainly the $a_{2\sigma}$ and e(1) ionisations respectively, but the e(2) ionisation appears to have substantially altered in intensity, broadened and split. The main peak at 12.3 eV is probably e(2) and the shoulder at 11.8 may well be a component of the expected $^4T_2$ state. Probably a_1 lies under e(2), possibly on the high IE side. Band D is also split into a peak at ca. 13.1 eV and a broad mound at ca. 13.5 eV. If

the band at 11.8 eV arises from $^4T_2$ and that at 13.1 eV from $^4T_1$, then we have a value of 2.6 eV for 10Dq and 875 cm^{-1} for B, both of which are very reasonable.

It is clear that in order to interpret the PE spectrum of $Mn(hfa)_3$ we have had to depart substantially from a simple orbital model. Indeed there is no way in which the essentially one-electron model could predict the existence of two available states from the ionisation of the t_2^3 subshell. It might be argued that the very high IE of the t_2^3 shell would imply that the partially filled t_2 orbitals lie below the filled ligand shells. This is only true in the one-electron model however, and the fact that spontaneous charge transfer does not occur from ligand to metal is explicable on the grounds that the spin-pairing energy within t_2 will greatly exceed that recouped from transferring an electron from one of the upper filled ligand levels. If we had used the open shell formalism of Roothaan, the predicted orbital energies of the t_2 and e levels would lie above those for the filled ligand levels, but Koopmans' theorem is not obeyed in general in the Roothaan formalism and we must correct for various electron repulsion terms to obtain the observed ionisation energies. This is not to say that the Roothaan method will generate a picture physically more familiar to the transition-metal chemist, since the ligand field parameter 10Dq is not related in any simple

way to the difference between the orbital energies of e and t_2; it is possible, at least in principle, for these to have opposite signs.

The UV-PE spectrum of $Fe(hfa)_3$ is very strange indeed, and, from the controversy surrounding the interpretation of the UV absorption spectrum of $Mn(hfa)_3$ discussed above, little concrete information can be gained by considering a d^4 system. The UV spectrum of $Mn(hfa)_3$, like that of $Mn(acac)_3$, contains two bands, a low energy band at 11,600 cm^{-1}, which has substantially shifted from that in $Mn(acac)_3$ and whose energy would seem to rule out absolutely the possibility that it is the cited d → d transition, and a band at 18,700 cm^{-1} which is presumably the value of 10Dq in this complex. The mystery surrounding the first band has not been dissipated by a spate of recent papers which have appeared, all with different explanations. In 1962, Dingle[52] suggested that it might be the transition between the A and B components of ^5E split by a Jahn-Teller distortion; not only would this distortion be exceptionally large at 1.5 eV for an octahedral molecule (though distortions of this size can occasionally be seen in tetrahedral species) but the X-ray structure of $Mn(acac)_3$, published by Morosin and Brathovde in 1964 showed that the molecule was in fact only slightly distorted. Fackler et al. in 1965[53] suggested that $e_b \rightarrow \pi_4$ or $n \rightarrow t_2$,e were possibilities

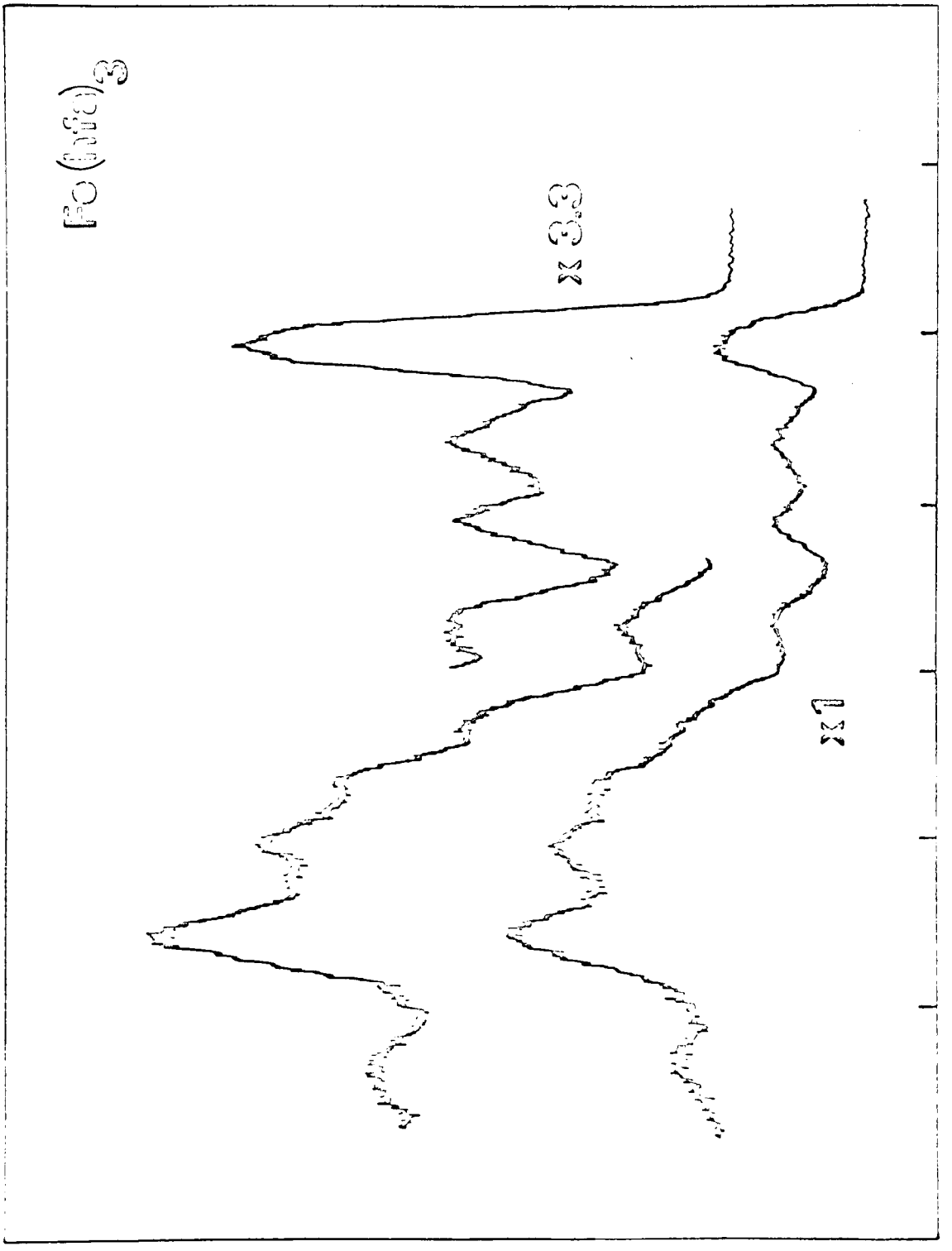

FIGURE 4.25

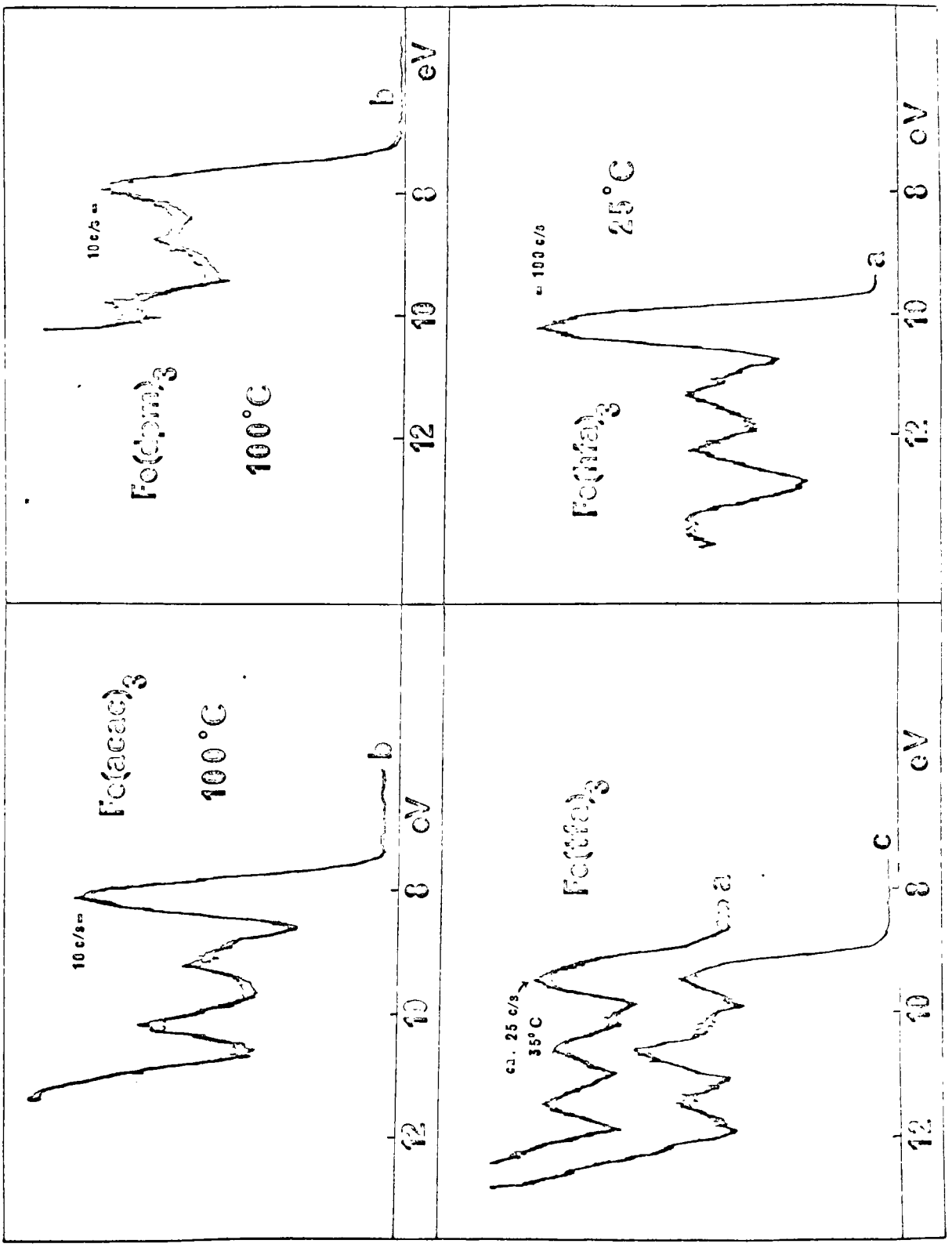
Fe(acac)3
100°C
10 c/s
b
12
10
8
eV
Fe(dpm)3
100°C
10 c/s
b
12
10
8
eV
Fe(tfa)3
ca. 25 c/s
35°C
a
c
12
10
8
eV
Fe(hfa)3
25°C
100 c/s
a
12
10
8
eV

FIGURE 4.26

since the band was found to be strongly influenced by hydrogen bonding solvents. However, in 1968 these authors substantially revised their interpretation in the light of further work on Mn(III) chelates.[6] A comparison with Mn(III) complexes which do show large static distortions from octahedral symmetry showed that the intense low-energy band was also encountered in these latter types, and the authors suggested that a dynamic Jahn-Teller effect operated in these systems, perhaps a pseudorotation. However the very large change in energy of this band between $Mn(acac)_3$ and $Mn(hfa)_3$ is difficult to reconcile with this theory, and suggests a more direct involvement of the ligand in this transition. Since the π band is probably altered in <u>character</u> more than the σ-system, by interaction with CF_3, a charge transfer band involving π_3 or π_4 would seem most likely. The fact that the band at 18 kK is far less affected by changing acac for hfa is rather strong evidence for this conclusion. Furthermore, the fact that such a transition is not observed in $Fe(acac)_3$ in the UV suggests that it is probably π_3 - d, since this transition in $Fe(hfa)_3$ and $Fe(acac)_3$ would involve spin-pairing and in consequence have a much higher energy.

If we return to the UV spectrum of $Cr(acac)_3$ and try to assign it using the UV-PE spectrum of $Mn(hfa)_3$, it is immediately apparent that we must shift the <u>relative</u> energies

of d and ligand levels quite substantially, as might be expected, so as to place the $^4T_2$ state above π_3 (since $^4T_2 \leftarrow {}^4A_2$ is the first uv transition seen). If we regard the band at 25,770 cm^{-1} in $Cr(acac)_3$ as the first charge transfer band arising from $\pi_3 \rightarrow e_b$, then the charge transfer $a_2 \rightarrow e_b$ should occur at 33,000 cm^{-1} and $e(1) \rightarrow e_b$ at 36,800 cm^{-1} and $e(2) \rightarrow e_b$ at 44,000 cm^{-1}. The spectrum of $Cr(acac)_3$ does indeed show a band at 33,760 cm^{-1} and a shoulder at 36,900 cm^{-1} which might well correspond to these processes. The transitions corresponding to $d \rightarrow \pi^*$ or $\pi \rightarrow \pi^*$ cannot be seen in UV-PE spectroscopy since π^* is not occupied. Barnum[21] assigned the bands at 26,320 cm^{-1} and 29,850 cm^{-1} in the UV spectrum of $Cr(acac)_3$ to $d \leftarrow \pi^*$, but the bands at 33,900 and 36,720 cm^{-1} to $\pi \rightarrow \pi^*$. DeArmond and Foster[56b] pointed out that additional $\pi \rightarrow \pi^*$ transitions which were inter-ligand in character might occur, though in effect these are transitions between the trigonal components of π and π^* which Barnum had already considered, and their assignment of all the bands in $Cr(acac)_3$ between 23,000 and 39,000 cm^{-1} to $\pi \rightarrow \pi^*$ transitions can be ruled out absolutely by a glance at the UV-PE spectrum. Piper and Carlin[57] could rule out the possibility of the 26,000 cm^{-1} band arising from $^4T_1 \leftarrow {}^4A_2$ on polarisation grounds and suggested e(1) or $a_2 \rightarrow \pi^*$. However, the separation of a_2 and π_3 in the PE spectrum of $Mn(hfa)_3$ would seem to

rule out the possibility of $n \rightarrow \pi^*$ transitions at such low energies.

Since we had to shift the d and ligand orbital energies relatively by 2.4 eV in comparing $Mn(hfa)_3$ and the UV spectrum of $Cr(acac)_3$; if we assume that the 1.5 eV band in the UV spectrum of $Mn(hfa)_3$ is indeed the $\pi_3 \rightarrow e_b$ charge transfer band, we would expect that in the UV-PE spectrum of $Fe(hfa)_3$, the ionisation energy for the first metal transition $^5E \leftarrow {}^6A_1$, would be HIGHER than that giving rise to the π_3 ionisation bands themselves, a result which is reinforced by a consideration of the increased spin-randomisation energy correction for the sextet state. The absence of the expected splitting between the e(1) and $a_{2\sigma}$ levels may in fact result from this, since if the d-stabilisation is comparable to that observed in $Mn(hfa)_3$, then the first expected d-orbital ionisation should be close to the $a_{2\sigma}$ orbital giving an unresolved triplet. Interestingly the spectrum of $Fe(tfa)_3$ does show a splitting between e(1) and $a_{2\sigma}$ and a glance at the UV-spectrum of $Mn(tfa)_3$ suggests that the reason may be the anomalous position of the first band, which we have assigned to a $\pi_3 \rightarrow$ d charge transfer process, which is at lower energy than either that in $Mn(hfa)_3$ or $Mn(acac)_3$. It is possible that in $Fe(tfa)_3$ the first d ionisation has dropped under e(1), allowing the $a_{2\sigma}$ peak to be resolved. The other main feature of the

$Fe(hfa)_3$ spectrum is the sharp band at 13.5 eV which can be assigned to the $^5T_2$ state arising from ionisation of the t_2 orbital, giving a value of 20,000 cm^{-1} for 10Dq.

The PE spectra of $Ru(hfa)_3$ and $Os(hfa)_3$.

These compounds, whilst formally similar to $Fe(hfa)_3$, are both low-spin t_2^5 complexes and are best considered together. Magnetic studies on $Ru(acac)_3$ by Figgis et al.[63] over a range of temperatures suggested a substantial trigonal distortion, but subsequent work using temperature dependent magnetic anisotropy effects[64] has indicated that the trigonal effect amounts at most to ca. 500 cm^{-1}, and the earlier results could be explained as a result of an unfortunate and fortuitous cancellation of opposing trends. Unfortunately, no data is available for $Tc(acac)_3$, so that it is not possible to say with certainty that trigonal effects are also very small in t_2^4 systems, but if we assume that they are not much larger than those found for $Ru(acac)_3$, then the observed splitting of band Y in the PE spectrum of $Ru(hfa)_3$ cannot arise from the trigonal splitting of the ground state of t_2^4, $^3T_1$.

Ionisation of the t_2^5 configuration can give rise to all the possible states of t_2^4 and the relative intensities and ligand-field energies are given in table 4.7½.

TABLE 4.7½

	L.F. Energy	Relative Intensity
$^3T_1$	6A − 15B + 5C	9
$^1T_2$	6A − 9B + 3C	3
^1E	6A − 9B + 3C	2
$^1A_1$	6A + 10C	1

It can be seen that, within the ligand field approximation, $^1T_2$ and ^1E are degenerate. Assuming a value of B for Ru(III) of ca. 500 cm^{-1} and that C = 4B, the separation of the two degenerate singlet states from the ground state will be ca. 4,000 cm^{-1}, i.e. ca. 0.8 eV, and the separation of the $^1A_1$ state from $^3T_1$ will be ca. 2.0 eV.

Examination of the spectrum reveals, rather surprisingly, that the band Y is apparently split by 220 mV, with the less intense component at lower IE. Unless the ground state of t_2^4 is a singlet, which seems extremely unlikely, then this splitting cannot be explained in any simple manner from the ligand field energies listed above. If the splitting is indeed due to ^1T and ^1E terms ionising only 0.2 eV above the ^3T term then we must postulate significant CI between the various singlet terms of t_2^5, and t_2^4e. This effect has in fact been observed in the spectrum of $V(CO)_6$.[65]

However, a second effect is also in operation, namely the spin-orbit coupling which will cause a splitting of $^3T_1$ into four states whose energies are given in table 4.8.

TABLE 4.8

State	Energy
A_1	$-\zeta$
T_1	$-\frac{1}{2}\zeta$
E	$+\frac{1}{2}\zeta$
T_2	$+\frac{1}{2}\zeta$

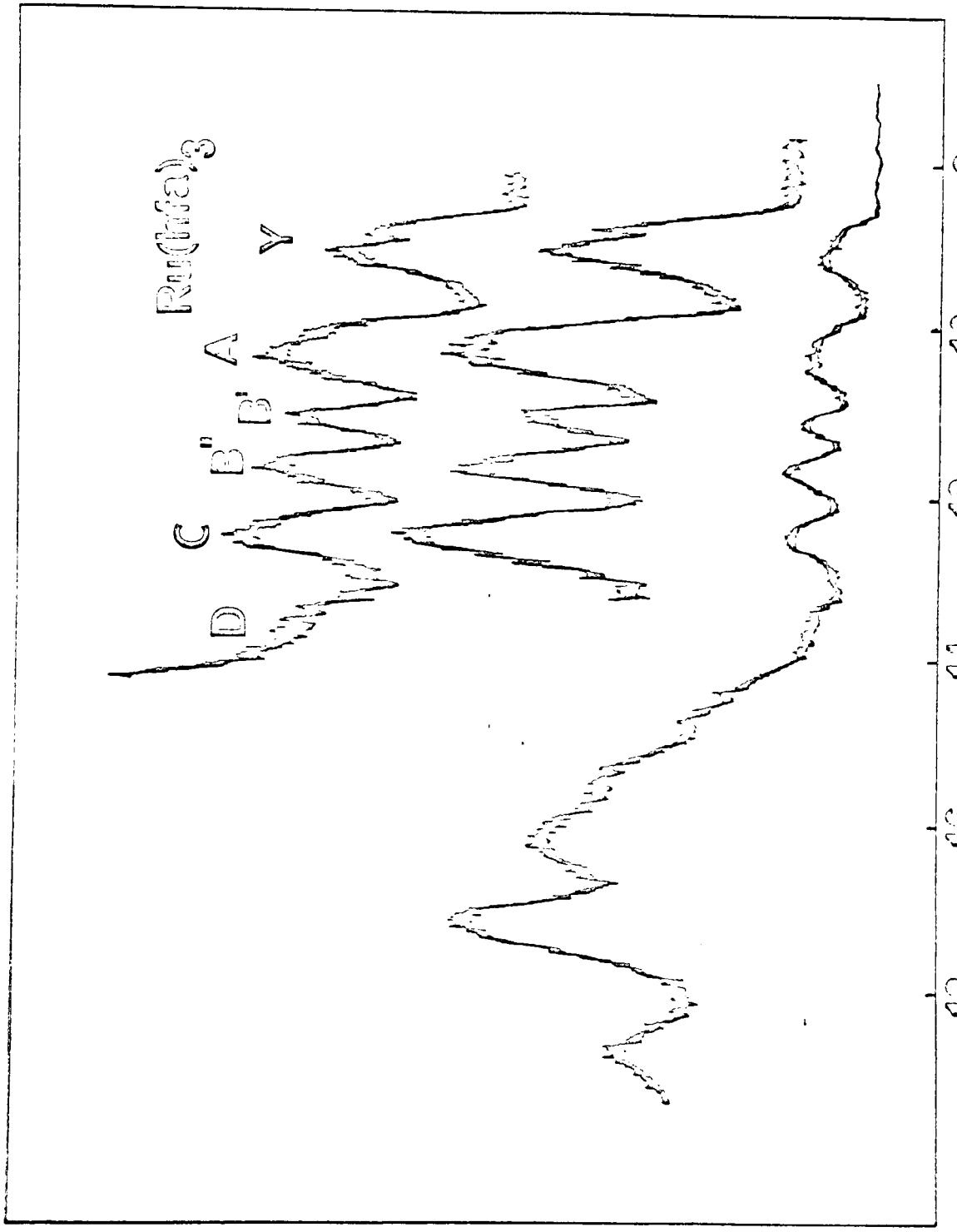

FIGURE 4.27

The off-diagonal matrix elements between the E and T_2 states and those derived from $^1T_2$ and ^1E are both $8/\sqrt{2}$. To evaluate the relative intensities of these states in the PE spectrum the full theory of Cox and Orchard[11] must be used and to this purpose the wave-functions for all the states are listed in table 4.9, in terms of the spherically quantised d orbitals.

TABLE 4.9

STATE	WAVE FUNCTION
$\lvert A_1 a_1\rangle$	$-\frac{1}{\sqrt3}\lvert 1^2-1^+\rho_1^+\rangle - \frac{1}{\sqrt6}\lvert 1^--1^+\rho_1^2\rangle - \frac{1}{\sqrt6}\lvert 1^+-1^-\rho_1^2\rangle - \frac{1}{\sqrt3}\lvert 1^--1^2\rho_1^-\rangle$
$\lvert E\epsilon\rangle$	$-\frac{1}{\sqrt2}\lvert 1^+-1^2\rho_1^+\rangle - \frac{1}{\sqrt2}\lvert 1^2-1^-\rho_1^-\rangle$
$\lvert E\theta\rangle$	$-\frac{1}{\sqrt6}\lvert 1^2-1^+\rho_1^+\rangle + \frac{1}{\sqrt3}\lvert 1^+-1^-\rho_1^2\rangle + \frac{1}{\sqrt3}\lvert 1^--1^+\rho_1^2\rangle - \frac{1}{\sqrt6}\lvert 1^--1^2\rho_1^-\rangle$
$\lvert T_1 1\rangle$	$\frac{1}{\sqrt2}\lvert 1^+-1^+\rho_1^2\rangle + \frac{1}{2}\lvert 1^--1^2\rho_1^+\rangle + \frac{1}{2}\lvert 1^+-1^2\rho_1^-\rangle$
$\lvert T_1 0\rangle$	$-\frac{1}{\sqrt2}\lvert 1^2-1^+\rho_1^+\rangle + \frac{1}{\sqrt2}\lvert 1^--1^2\rho_1^-\rangle$
$\lvert T_1 -1\rangle$	$-\frac{1}{2}\lvert 1^2-1^-\rho_1^+\rangle - \frac{1}{2}\lvert 1^2-1^+\rho_1^-\rangle - \frac{1}{\sqrt2}\lvert 1^--1^-\rho_1^2\rangle$
$\lvert T_2 1\rangle$	$-\frac{1}{2}\lvert 1^2-1^-\rho_1^+\rangle - \frac{1}{2}\lvert 1^2-1^+\rho_1^-\rangle + \frac{1}{\sqrt2}\lvert 1^--1^-\rho_1^2\rangle$
$\lvert T_2 0\rangle$	$-\frac{1}{\sqrt2}\lvert 1^+-1^2\rho_1^+\rangle + \frac{1}{\sqrt2}\lvert 1^2-1^-\rho_1^-\rangle$
$\lvert T_2 -1\rangle$	$-\frac{1}{\sqrt2}\lvert 1^+-1^+\rho_1^2\rangle + \frac{1}{2}\lvert 1^--1^2\rho_1^+\rangle + \frac{1}{2}\lvert 1^+-1^2\rho_1^-\rangle$
$\lvert {}^1T_2 1\rangle$	$\frac{1}{\sqrt2}\lvert 1^2-1^+\rho_1^-\rangle - \frac{1}{\sqrt2}\lvert 1^2-1^-\rho_1^+\rangle$
$\lvert {}^1T_2 0\rangle$	$\frac{1}{\sqrt2}\lvert -1^2\rho_1^2\rangle - \frac{1}{\sqrt2}\lvert 1^2\rho_1^2\rangle$
$\lvert {}^1T_2 -1\rangle$	$-\frac{1}{\sqrt2}\lvert 1^--1^2\rho_1^+\rangle + \frac{1}{\sqrt2}\lvert 1^+-1^2\rho_1^-\rangle$
$\lvert {}^1A_1\rangle$	$-\frac{1}{\sqrt3}\lvert 1^2-1^2\rangle - \frac{1}{\sqrt3}\lvert 1^--1^+\rho_1^2\rangle + \frac{1}{\sqrt3}\lvert 1^+-1^-\rho_1^2\rangle$
$\lvert {}^1E\theta\rangle$	$\frac{2}{\sqrt6}\lvert 1^2-1^2\rangle - \frac{1}{\sqrt6}\lvert 1^--1^+\rho_1^2\rangle + \frac{1}{\sqrt6}\lvert 1^+-1^-\rho_1^2\rangle$
$\lvert {}^1E\epsilon\rangle$	$\frac{1}{\sqrt2}\lvert 1^2\rho_1^2\rangle + \frac{1}{\sqrt2}\lvert -1^2\rho_1^2\rangle$

The ground state of t_2^5 is E whose two components can be written

$$E''(\alpha'') = \tfrac{1}{\sqrt{3}}|0\alpha'\rangle - \sqrt{\tfrac{2}{3}}|1\beta'\rangle = -\tfrac{1}{\sqrt{3}}|1^2-1^2\rho_{-1}^{+}\rangle + \sqrt{\tfrac{2}{3}}|1^{-}-1^2\rho_{1}^{2}\rangle$$

$$E''(\beta'') = \sqrt{\tfrac{2}{3}}|-1\alpha'\rangle - \tfrac{1}{\sqrt{3}}|0\beta'\rangle = \sqrt{\tfrac{2}{3}}|1^2-1^{+}\rho^{2}\rangle + \tfrac{1}{\sqrt{3}}|1^2-1^2\rho_{-1}^{-}\rangle$$

where

$$\rho_1 = i|1\rangle = \tfrac{1}{\sqrt{2}}[d_2 + d_{-2}]$$

From these tables the relevant fractional parentage coefficients can be shown to be

STATE	INTENSITY
$^1A_1$	1/15
^1E	2/15
$^1T_2$	1/5
$A_1\rho_1$	1/45
E	1/9
T_1	1/6
T_2	7/30

If we assume that band Y arises only from ionisation to the $^3T_1$ state, then the interpretation of the splitting is now straightforward. The E and T_2 components, of total intensity 31/90 are separated by $\frac{5}{4}\rho$ from the A_1 and T_1 components, whose

relative intensity is given as 23/90. As we expect the latter two to lie lower in energy we predict an intensity ratio for the components of band Y of 4:3, which is very close to that observed.

A corollary of this assignment is that the ionisations to ^1E and $^1T_2$ will lie under the first ligand band A. This band is indeed much broader than π-bands found in the first row though no definite splitting can be observed. Further evidence for this assignment comes from the ESCA spectrum of $Ru(hfa)_3$ discussed below, which places the mean d-energy at ca. 9.5 eV, and from the UV-PE spectrum of $Os(hfa)_3$ which is shown in fig. 4.28. The basic structure closely resembles that of $Ru(hfa)_3$ save that band Y is now split by 0.5 eV. Assuming the same assignment as that given for the ruthenium complex, this leads to a spin-orbit coupling constant for Osmium of ca. 0.4 eV entirely consistent with the rather sparse experimental data on the atom.[5] The corresponding figure derived for ruthenium is ca. 0.17 eV which is a little large for ruthenium, and suggests that there may be other contributions to the splitting, perhaps trigonal or vibronic in nature.

A second noteworthy feature of the spectrum is the splitting of band B which we discussed at length for the first transition series. The large splitting in both $Ru(hfa)_3$ and $Os(hfa)_3$ of 0.6 eV is comparable to that found in $Co(hfa)_3$

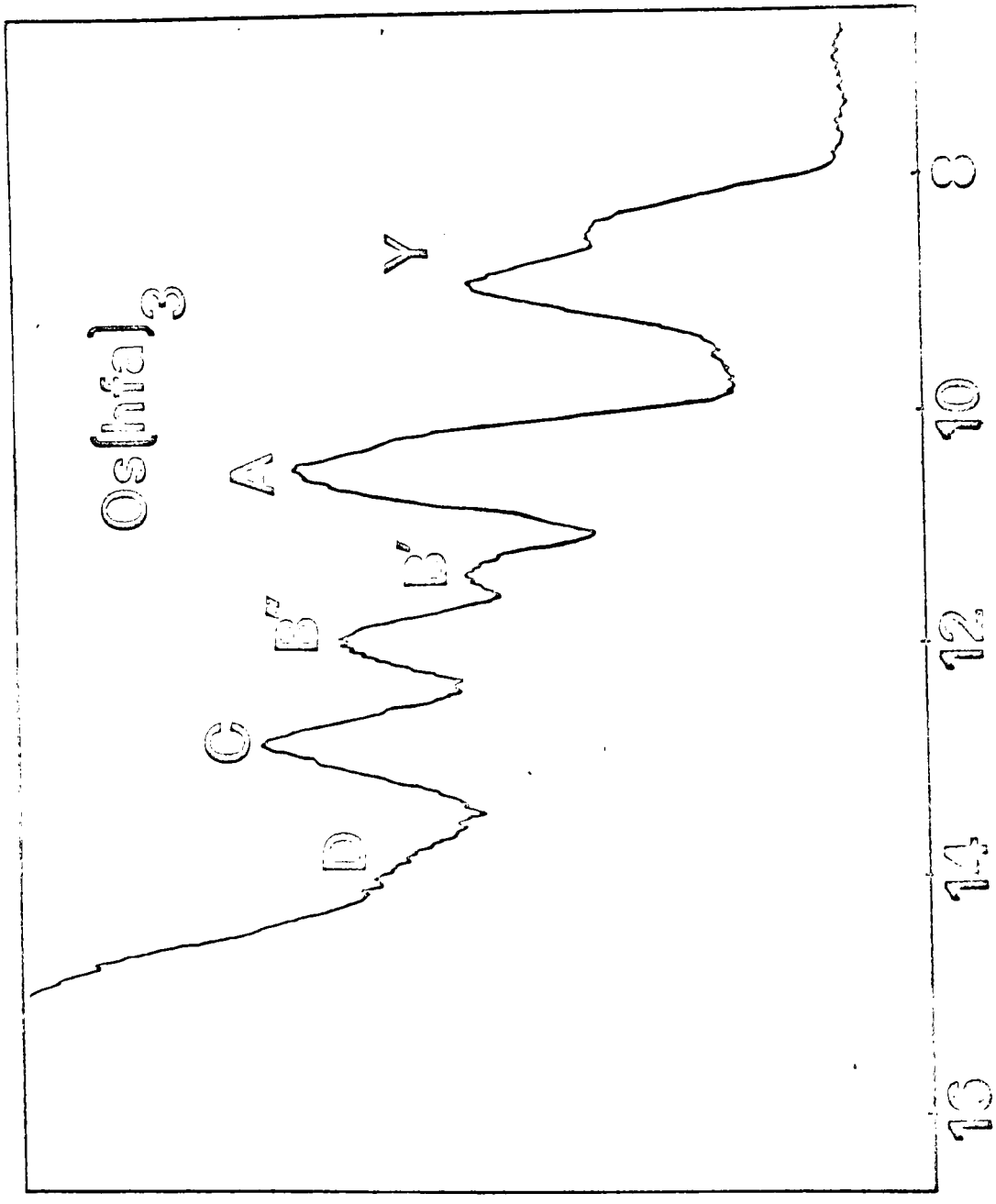

FIGURE 4.28

whose d-electrons are much closer in energy to the ligand orbitals. This leads to the inevitable conclusion that the overlap integrals between 4d or 5d orbitals and the ligand orbitals are much larger than those found in the first row.

Ionisation energy data for the UV-PE spectra

TABLE 42

AcacH	dpmH	hfaH	tfaH	tmtfaH
9·18	8.86	10.74	9·92	9.87
9·74	9·23	11.25	10.53	10.19
				(10.29)
12.68	11.37	14.03	13·27	11.95
	11.79			13.14
13·27	12.78	15.07	15.23	(14.0)
14.18	(13.66)	15.58		(15.24)
14.8	15.07	16.3	16.99	
16.1	(16.55)	17.42		16.8
18.8	17.32	19.3		
		20.92		

Shoulders are indicated by parentheses.
Abbreviations are explained in the text.
The IE data given in this and the following tables is accurate to ± 0.07 eV for the sharper bands. The figures labelling the spectra are intended to be no more than indicative, and accurate values for the IE's should be taken from these tables.

The main group tris-chelates.

PE band	$Al(tfa)_3$	$Al(hfa)_3$	$Sc(hfa)_3$	$Ga(hfa)_3$
A	9·22	10.33	10.13	10.19
B	10.35	11.47	10.82(B′)	11.13(B′)
			11.12(B″)	11.47(B″)
C	11.49	12.64	12.05	12.37
				12.99(X)
D		13.62	13.52	13.63
	14.7	14.81	14.6	14.7
		15.58	15.3	15.5
	16.6	16.20	16.2	16.14
		17.25	17.1	17.24
		18.75	18.5	18.8

Ionisation energy data for the two bis-chelates of beryllium

PE band	$Be(hfa)_2$	$Be(acac)_2$
A	10.39	8.41
B	11.66	9.67
C	12.96	(10.86)
		11.13
	13.4 - 14.3	13.0 -14.7
	(15.1)	
	(15.7)	
	16.3	15.8
	17.4	
	18.9	

Ionisation energy data for some transition-metal tris-chelates

PE band	$Ti(hfa)_3$	$V(hfa)_3$	$Cr(hfa)_3$	PE band	$Co(hfa)_3$
Y	7.94	8.68	9.57	K	9.73
A	10.24	10.10	10.16	L	10.13
				M	10.73
B′	10.87	10.96	11.10	B′	11.15
B″	11.28	11.39	11.61	B″	11.75
C	12.24	12.20	12.44	C	12.56
D	13.50	13.59	13.47	D	13.5
	14.6	14.6	14.86		14.8
	15.39	15.41	15.42		15.5
	16.10	16.16	16.27		16.27
	17.18	17.12	17.24		17.36
	18.65	18.60	18.8		18.56

Ionisation energy data for some tris-chelates of Cr(III) and Co(III)

PE band	$Cr(acac)_3$	$Cr(tfa)_3$	PE band	$Co(acac)_3$
Y	7.46	8.58	K	7.52
A	8.06	9.12	L	8.01
			M	8.49
B′	8.96	10.01	B′	8.99
B″	9.48	10.54	B″	9.54
C	10.26	11.40	C	10.34

Ionisation energy data for some tris-chelates of Mn(III)

$Mn(hfa)_3$		$Mn(acac)_3$
A	B	C
(9.2)	(9.2)	(7.32)
10.1	10.03	8.14
	10.94	
	11.41	
ca.12.3	12.31	
ca.13.1	13.3	
	14.7	
	15.3	
16.2	16.2	
17.2	17.1	
	18.7	

A: measured on the spectrometer of ref.

B: measured on a PS 15 spectrometer

C: measured on a Perkin-Elmer spectrometer using a heated inlet at 132°C.

Ionisation energy data for some tris-chelates of Fe(III)

$Fe(hfa)_3$	$Fe(tfa)_3$	$Fe(acac)_3$	Fe(dpm).
10.13	9.18	8.10	7.92
	(9.92)	(8.93)	
11.30	10.40	9.22	8.76
12.25	11.26	10.16	9.87
13.5		11.4	
14.7		13.2	
15.43			
16.18			
17.22			
18.8			

Ionisation energy data for $Ru(hfa)_3$ and $Os(hfa)_3$

PE band	$Ru(hfa)_3$	$Os(hfa)_3$
Y	8.85	8.28
	9.07	8.69
A	10.30	10.33
B′	11.06	11.24
B″	11.65	11.81
C	12.50	12.72
	13.55	(13.94)
	(14.7)	
	(15.4)	
	16.1	
	17.1	
	18.7	

Owing to difficulties in calibrating the spectrum of $Os(hfa)_3$, the figures quoted are only relatively meaningful. Their absolute accuracy is probably ca. 0.2 eV.

Chapter five
Interpretation of the ESCA spectra

Never had any mother? What do you mean? Where were you born?

Never was born, persisted Topsy; Never had no father, nor mother, nor nothin'. I was raised by a speculator.

Do you know who made you?

Nobody as I knows on, said the child with a short laugh.....
I 'spect I just growed.

Harriet Beecher Stowe
Uncle Tom's Cabin

ASSIGNMENT OF THE ESCA SPECTRA AND PRELIMINARY INTERPRETATION

In many respects, the assignment of ESCA spectra, especially in the core region, is considerably simplified by the very large energy separations between different ionisation bands. As can be seen from the spectra, the core regions of all the hexafluoroacetylacetonato complexes look very similar, with the exception of certain small bands which are listed in table 5.1 together with the assignment based on Siegbahn's[3] tables. The kinetic energy of these peaks has been measured relative to that of the strongest of the three C 1s signals, which was found, in a separate experiment in the case of $Cr(hfa)_3$ to be at 1191 eV KE relative to gold. Since this peak is derived from the $\underline{C}F_3$ carbon 1s orbital it is assumed not to vary significantly in KE throughout the series of hexafluoroacetylacetonato complexes, an assumption which is justified in more detail below. Table 5.2 shows the M $2p_{\frac{1}{2},\frac{3}{2}}$ and M 3s,3p energy separations for the $M(hfa)_3$ series and table 5.3 the main core orbital KE's.*

It can be seen that the F 1s level changes very little (at least relative to $\underline{C}F_3$) across the series, such variation as is observed being well within experimental error, with a mean KE of 797.5 eV, corresponding to an observed BE of 689.1 ± 0.5 eV. Similarly, the F 2s level has a constant BE of 38.3 eV. A much larger variation in the O 1s level can

* These tables are printed at the end of the chapter

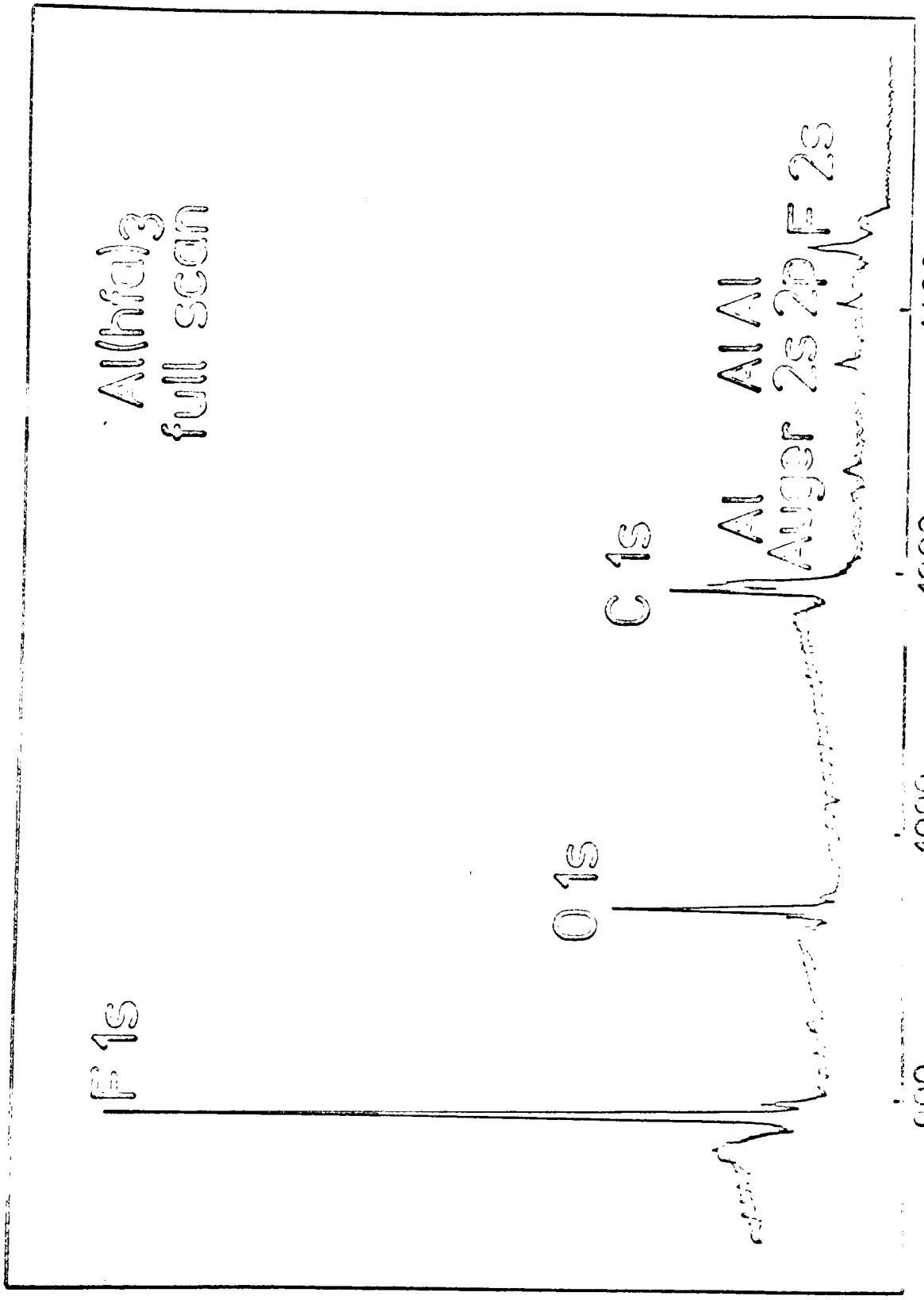
AlNiAl3
full scan
F 1S
O 1S
C 1S
Al Al Al
Auger 2s 2p F 2s
800
1000
1200
1400
K.E.

FIGURE 5.1a

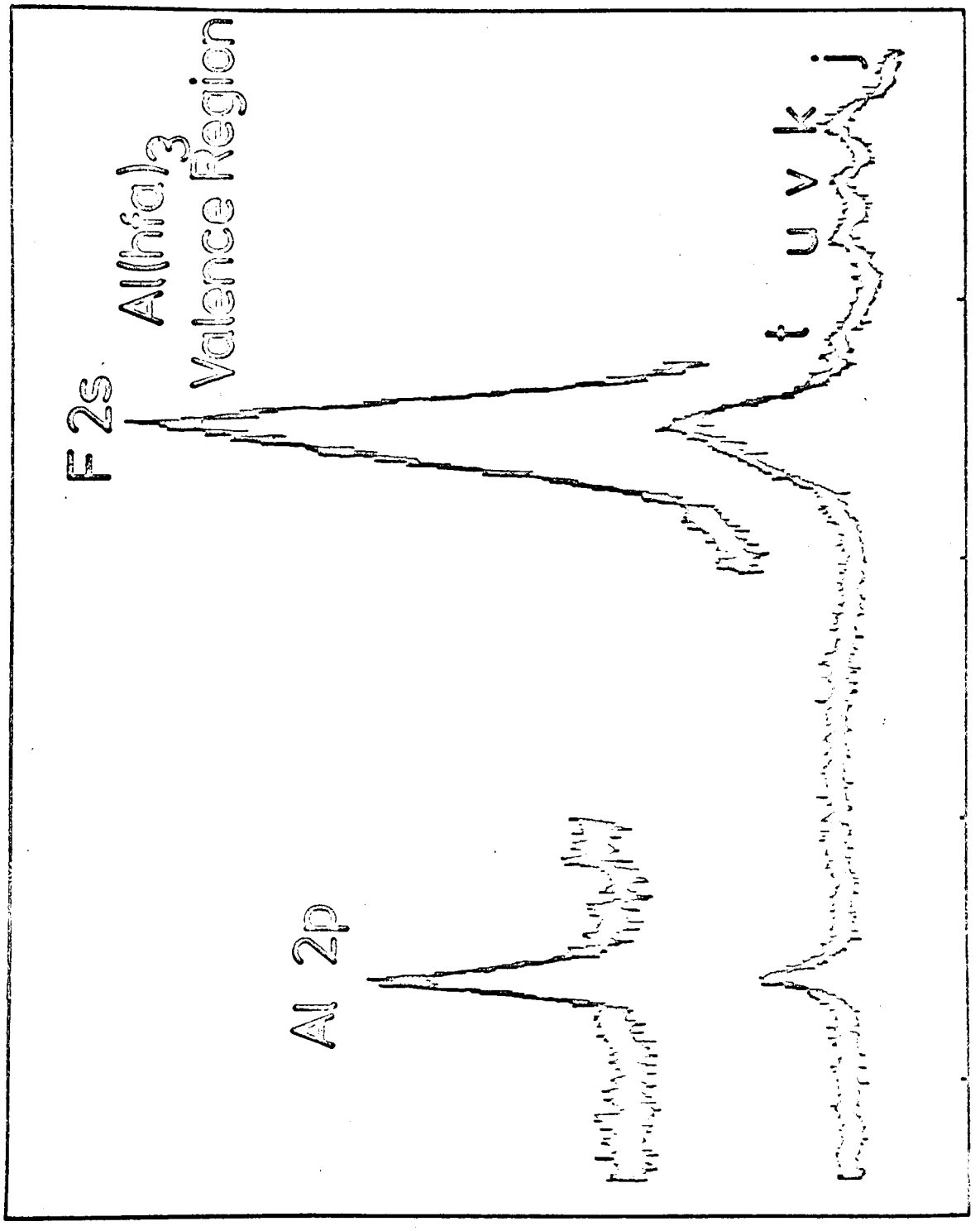

FIGURE 5.1b

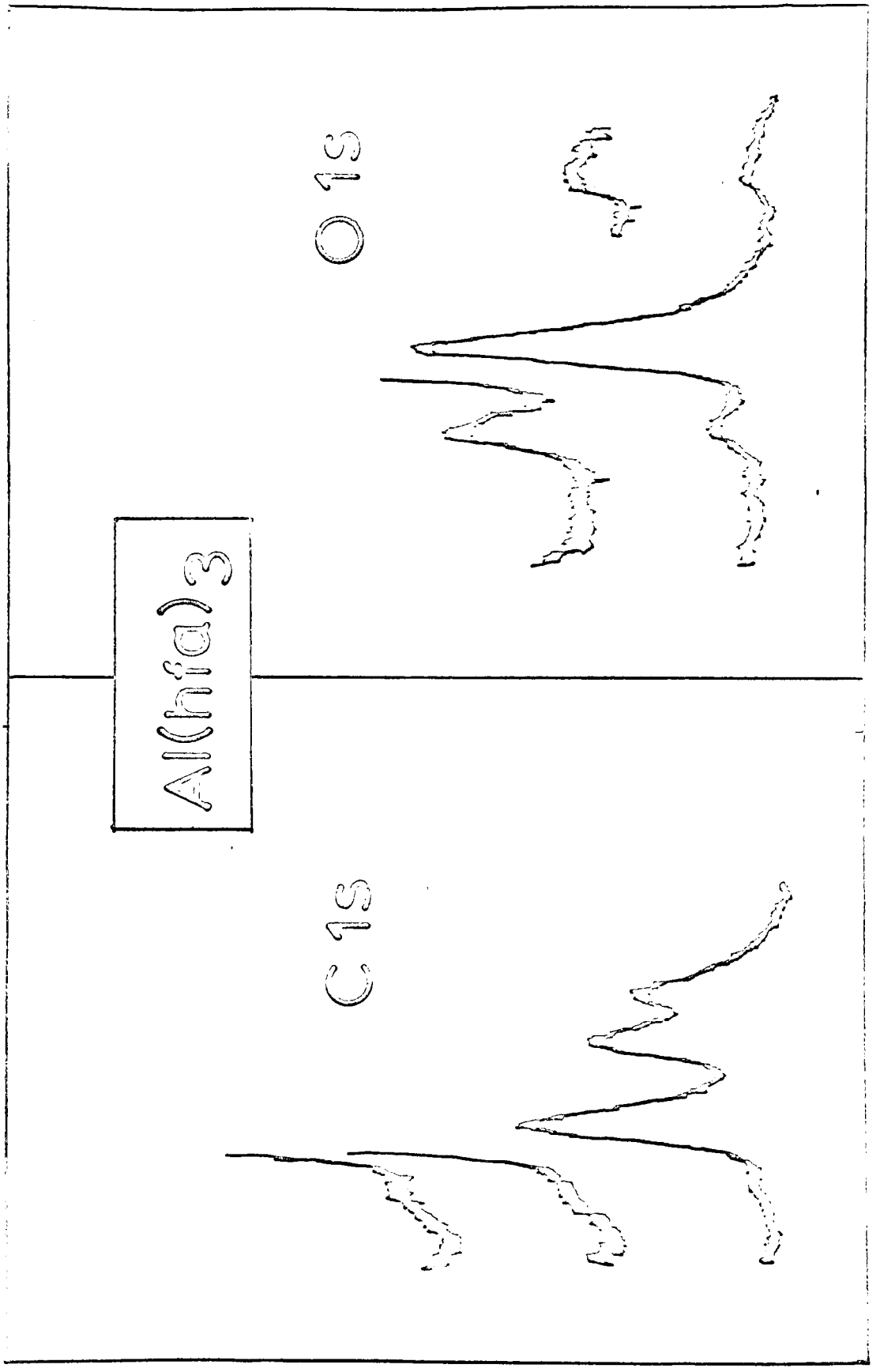

FIGURE 5.1c

however be seen, the BE diminishing steadily from scandium to chromium. At first sight, this trend is the reverse of that expected on simple charging grounds, since we might expect that increasing covalency across the series, as evidenced by the UV-PE spectra, would lead to a less negative charge on oxygen, so <u>increasing</u> the O 1s binding energy. However, the parallel between effective atomic charge and shift, which is found to hold good for organic systems in general, will not work for metal complexes where intramolecular potential effects are often dominant. Let us assume, following Siegbahn et al., that the core shift may be represented by an equation of the form

$$\Delta E_A = k \Delta q_A + \Delta V_A$$

for atom A, where Δq_A is the change in charge on atom A and ΔV_A the change in potential at atom A due to charge shifts on other atoms of the system. Let us also consider a model for the metal tris chelates in which all the charge is either on the oxygen atoms or on the metal atom. Let the charge on each oxygen atom increase by $\frac{2\delta e}{3}$ where e is the electronic charge. The charge on the metal will then decrease by $2\delta e$. Assuming octahedral coordination about the metal, and denoting the metal-oxygen distance by

$$\Delta E_A = \frac{k 2\delta e}{6} + \left(-\frac{2\delta e}{r} - \frac{\quad}{\quad} + \frac{\quad}{\quad} \right) = \frac{\quad}{3} - \frac{\quad}{r}$$

If r is expressed in Ångströms and ΔE_A in electron volts

$$\Delta E_A = \frac{}{} - \frac{}{} \delta q e$$

and, for $r = 2\text{Å}$, if $k < 22$ volts/electron charge, $\left(\frac{\partial \Delta E_A}{\partial r}\right)_r$ will be negative. In actual fact r will not be a constant, though the bond lengths in the mixed oxide phases $LaMO_3$ suggest an approximate constancy between Ti^{3+} and Fe^{3+}, but a sharp contraction between Sc^{3+} and Ti^{3+}. Mn^{3+} is expected to show substantial deviation from the idealised octahedral symmetry as a consequence of Jahn-Teller forces and may be an exceptional case. Actually, a crystal structure of $Mn(acac)_3$ (later refined by Fackler et al.) showed that, although the Mn-O bond lengths are indeed irregular, with one Mn-O distance being larger than the other five, the distortion is not very marked and the mean Mn-O bond length is very similar to that observed in $Cr(acac)_3$ and $Fe(acac)_3$. For this reason the ESCA spectrum of $Mn(hfa)_3$ will be treated as the others from an interpretative standpoint.

The model described above would be inadequate even for an examination of simple oxide phases, and is quite insufficient for a discussion of the chelates. This is shown most clearly on examination of the movement of the various C 1s ionisations. The $\underline{C}F_3$, $\underline{C}O$ and $\underline{C}F_3$, $\underline{C}H$ separations as a function of atomic number are shown in fig. 6.9.* It can be seen at once that the $\underline{C}H$ carbon, which is the most remote carbon in the chelate

* p. 240

ring from both metal and oxygen, destabilises more rapidly than the $\underline{C}O$ carbon in the first part of the series. This observation (based on the assumption that changes in the $\underline{C}F_3$ core energy are at most second order) would strongly suggest that electron density shifts within the π orbitals are involved, at least in part, and this information, coupled with that concerning the O 1s shifts leads to a rather interesting model of the bonding in these chelate systems. We saw that the He(I) UV-PE spectra indicated a steady increase in d_σ interaction from Ti → Cr suggesting a general polarisation of the molecule as shown

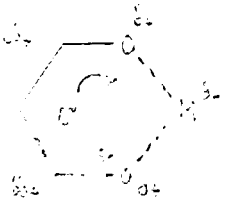

However, as we traverse the first transition series, the occupancy of the d_π orbitals progressively increases. The electrons in the t_{2g} type orbitals are known, from spectroscopic evidence, to have quite low nephelauxetic ratios, suggesting that some $d \rightarrow \sigma,\pi$ delocalisation has occurred. It is not immediately obvious from a consideration of the He(I) spectra whether $\pi \rightarrow M$ delocalisation is greater or less than back $d \rightarrow \pi$ transfer i.e. whether the net effect of π interaction is to increase or decrease the charge on the metal, but we can invoke a simple model to try to distinguish the

possibilities. Let the σ polarisation reduce the metal charge by an amount δ_σ e. Then certainly most of this charge will be derived from the oxygen to which we must add, for each atom, a charge $\frac{\delta_\sigma}{5}$ e. Let the total charge delocalised to the π-framework be $x\delta_\sigma$ e. If this is distributed uniformly in the three chelate rings $-\frac{x\delta_\sigma}{15}$ must be added as charge to each atom. The oxygen shift will be

$$\Delta E_O = \frac{k_O \delta_\sigma e}{5} - \frac{k_O x \delta_\sigma e}{15} - \frac{\delta_\sigma e}{r_{OM}}(1 - [illegible]) + \frac{\delta_\sigma e}{5}[illegible]\frac{1}{r_{OO}\sqrt{2}} - \frac{x\delta_\sigma e}{15 r_0} - \frac{x\delta_\sigma e}{15 r_1} - 2K\delta_\sigma e$$

where r_{OO} is the oxygen-oxygen distance, r_{OM} the metal oxygen bond length, r_0 the C-O bond length, and r_1 the distance between O and $\underline{C}$H. Putting some appropriate values in, we obtain, for $k_O = 30$

$\Delta E_O = (-2.1 + 3.4x + 2K)\,\delta_\sigma$ e

here K represents the effect of the neighbouring ligands.

For the $\underline{C}$H carbon

$$\Delta E_{CH} = -\frac{k_C \delta_\sigma x e}{15} - \frac{2\delta_\sigma x e}{15 r_2} + \frac{2\delta_\sigma e}{r_1}\left(\frac{1}{5} - \frac{x}{15}\right) - \frac{\delta_\sigma e}{r_3}(1 - x) + K'\delta_\sigma$$

where r_2 is the C-C distance and r_3 the $\underline{C}$H-metal distance.

Putting $k_C = 20$ we obtain

$E_{\underline{C}H} = (-2.2 - 0.3x)\,\delta_\sigma$ e + $K'\delta_\sigma$ e

and for the CO carbon

$$E_{CO} = (-1.3 + 0.6x)\,\sigma_{+}\,e + K''\sigma_{+}\,e$$

It can be seen that the model, crude as it is, does successfully predict that the movement of CO will be substantially less than that of CH (for simplicity, the CO-metal distance has been put equal to r_3 and K', K'' assumed to be approximately equal).

Since the 1s energy shifts of CH and CO are approximately equal, and $K > K'$, we predict that $x < 0$. Thus the ESCA spectrum would seem to indicate that π-bonding also involves ligand-metal charge donation, and the destabilisation of CH can be seen to be a consequence of the falling potential on the metal, and the fact that $k_c < k_o$.

Let us consider these ESCA trends in more detail. For $Sc(hfa)_3$ two effects will operate. The UV-PE spectrum (and the observed bond length) indicate that bonding to the 4s and 4p orbitals is more important in scandium than in later members of the series and secondly, there is probably a substantial contraction in bond length between scandium and titanium. In addition to this contraction, which will have a general stabilising effect on all the ligand orbitals, there will, at least judging by the UV-PE data, be a substantial increase in σ-covalency which will operate in the reverse direction, destabilising the ligand orbitals. However, the

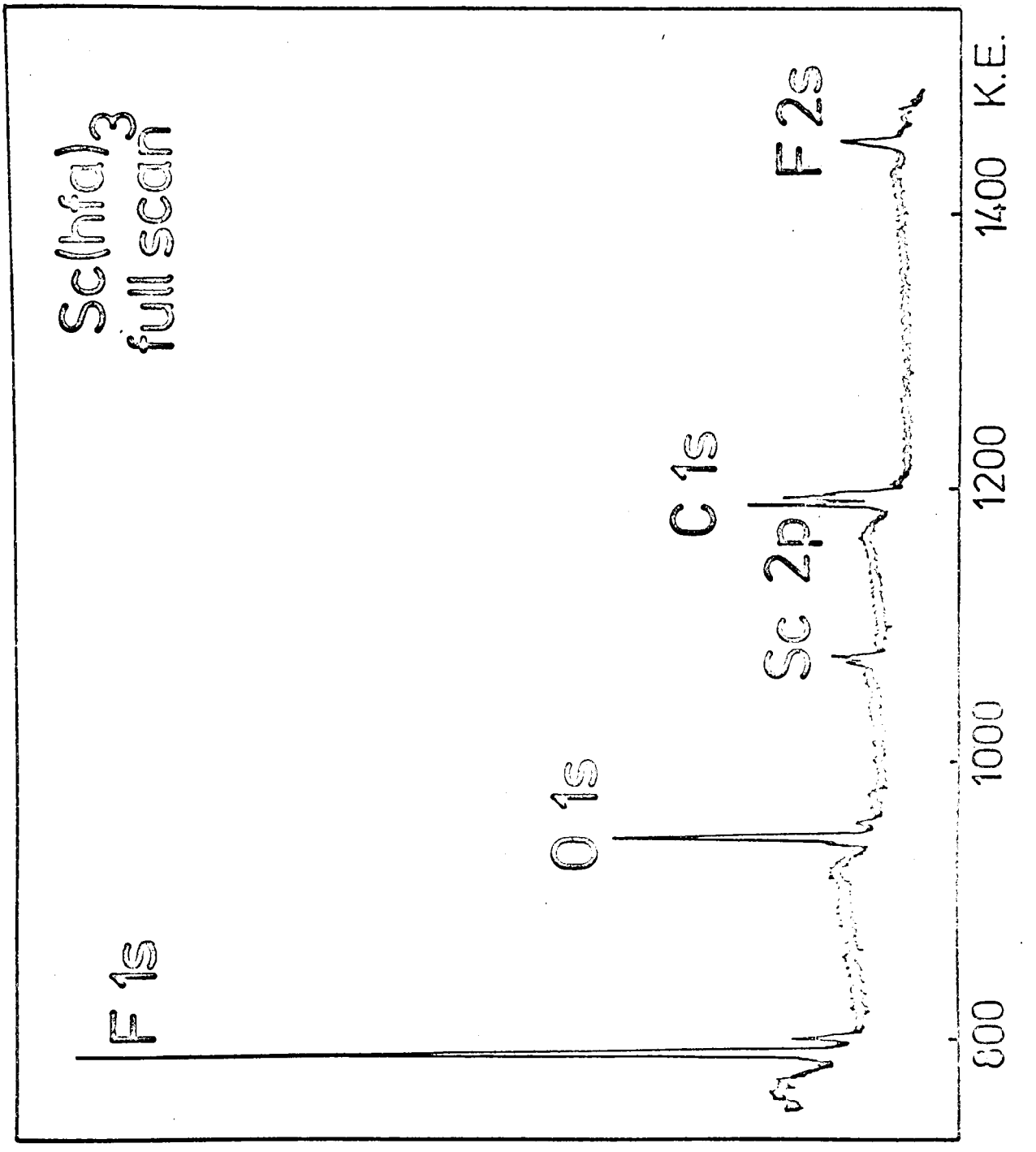

FIGURE 5.2a

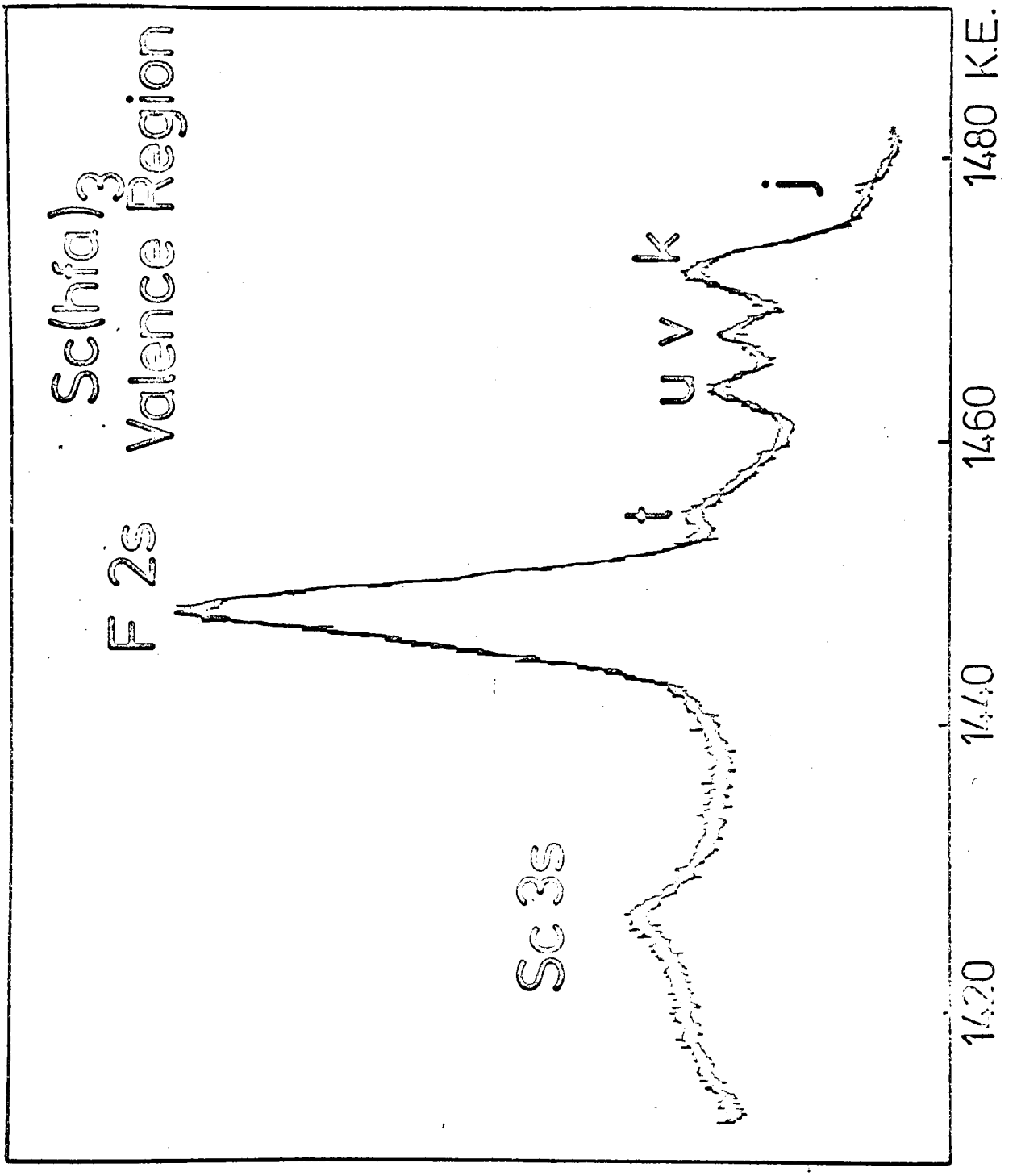

FIGURE 5.2b

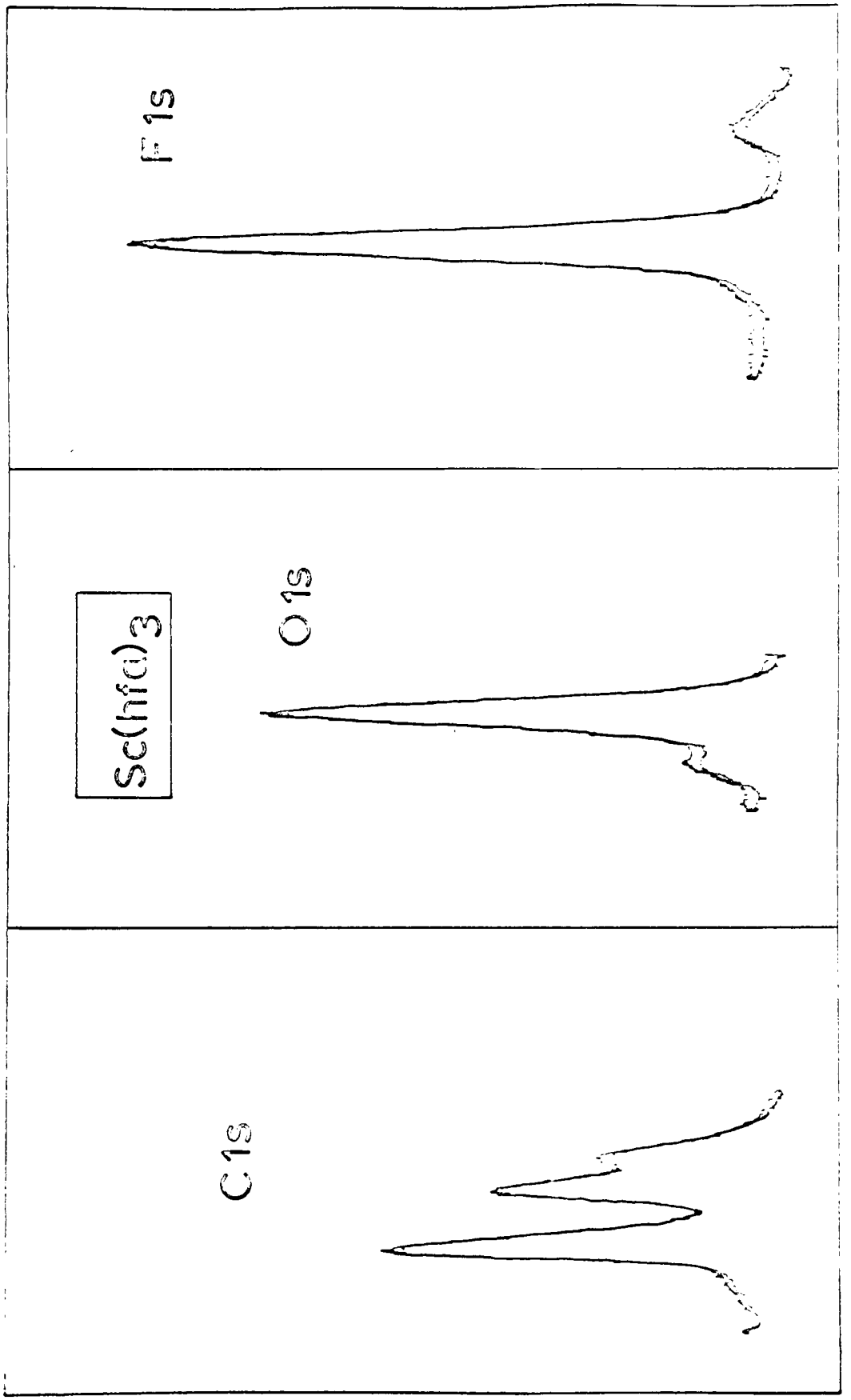

FIGURE 5.2c

ESCA spectrum shows that the net effect of replacing Sc^{3+} by Ti^{3+} is to stabilise the CH and CO 1s orbitals relative to CF_3 and to destabilise the O 1s. Our model cannot easily account for this behaviour since, if the stabilisation of the O 1s orbital on contraction of the M-O bond is V volts, then that of CH will be $V/3$ volts, whereas increasing the covalency will affect both in the same way and to the same extent. The simplest possibility is that the contraction in bond length has lead to a very substantial π and σ polarisation of the ligand framework towards the central metal, of the form:

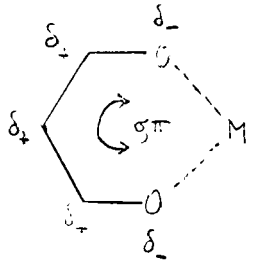

The effect of this will be to stabilise the O 1s by an amount

$$q\frac{\partial r}{r^2} - k\delta_- + V(\delta_+)$$

where the first term is the stabilisation due to the bond contraction δr, and $V(\delta_+)$ is the (positive) potential charge due to the denuded carbon region. If $\delta_+ = -\frac{2}{3}\delta_-$, $q \sim 2$, $r \sim 2.2$ and $\delta r \sim 0.2$, we must add $1.3 - 2\delta_-$ eV to the oxygen 1s energy and, for the CH energy $1\delta_- + 0.5$ eV should be added. Let the destabilisation of both levels arising from increasing covalency

be y volts, then

$$-y + 1.3 - 21\delta_{-} = -0.3$$

$$-y + 13\delta_{-} + 0.5 = +0.4$$

which solve to give $\delta_{-} \sim 0.02$ and y = +0.6 eV; that is, the covalency increase calculated on this simple model is substantially greater than the mean increase between Ti(III) and Cr(III). This again points to a qualitative change in the type of bonding, though uncertainty as to the value of σ makes this only speculative; a value of $\sigma \sim 1$ leads to y ≈ +0.45 volts. Actually this latter value fits very well with the UV-PE data since, if we take the separation of bands B′ and B″ as a measure of covalency, then the increase in this splitting between $Sc(hfa)_3$ and $Ti(hfa)_3$ is about 50% larger than the mean increase between $Ti(hfa)_3$ and $Cr(hfa)_3$.

If we consider the next three complexes in the series, some interesting irregularities are observed. Essentially, $V(hfa)_3$ is less covalent than might have been expected by extrapolation from Ti to Cr. Thus, the destabilisation of both the O 1s and CH 1s orbital energies is less than that predicted assuming a uniform increase in covalency, that of the O 1s especially so (though the error in this measurement is fairly large), and the splitting of band B in the UV-PE spectrum is also small. This trend is reflected in the sum of the first three ionisation potentials of the free atoms which are

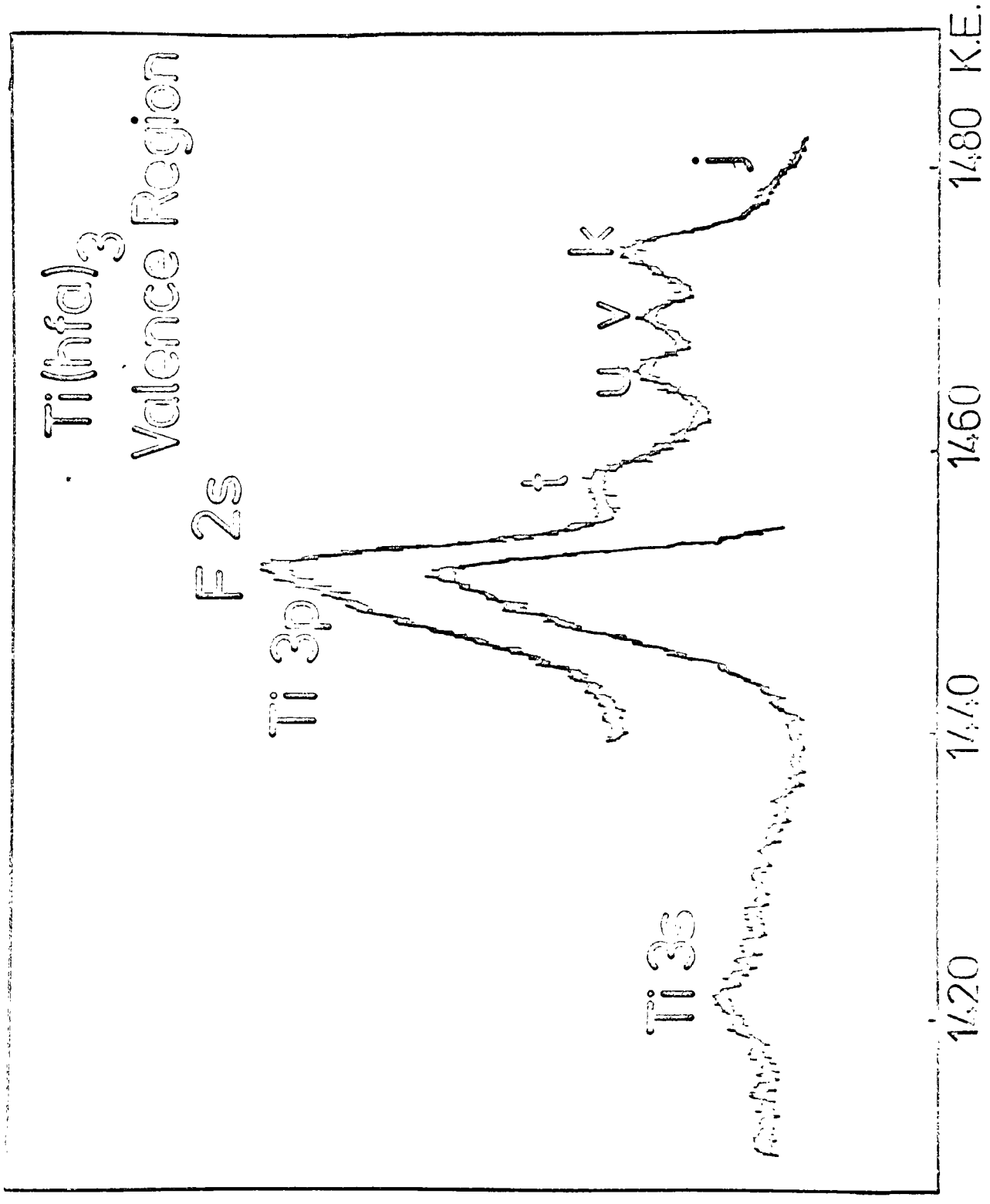

FIGURE 5.3a

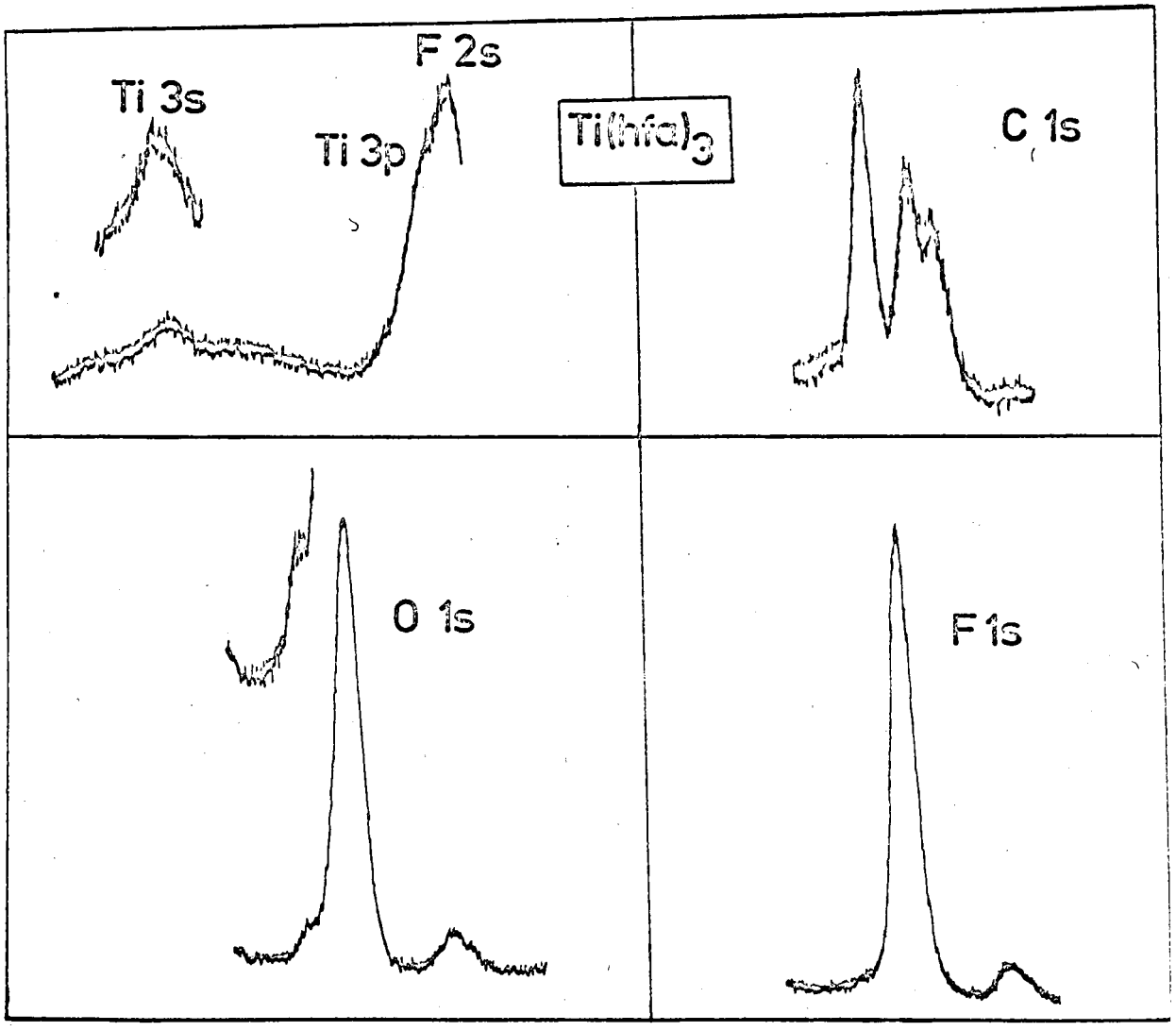

FIGURE 5.3b

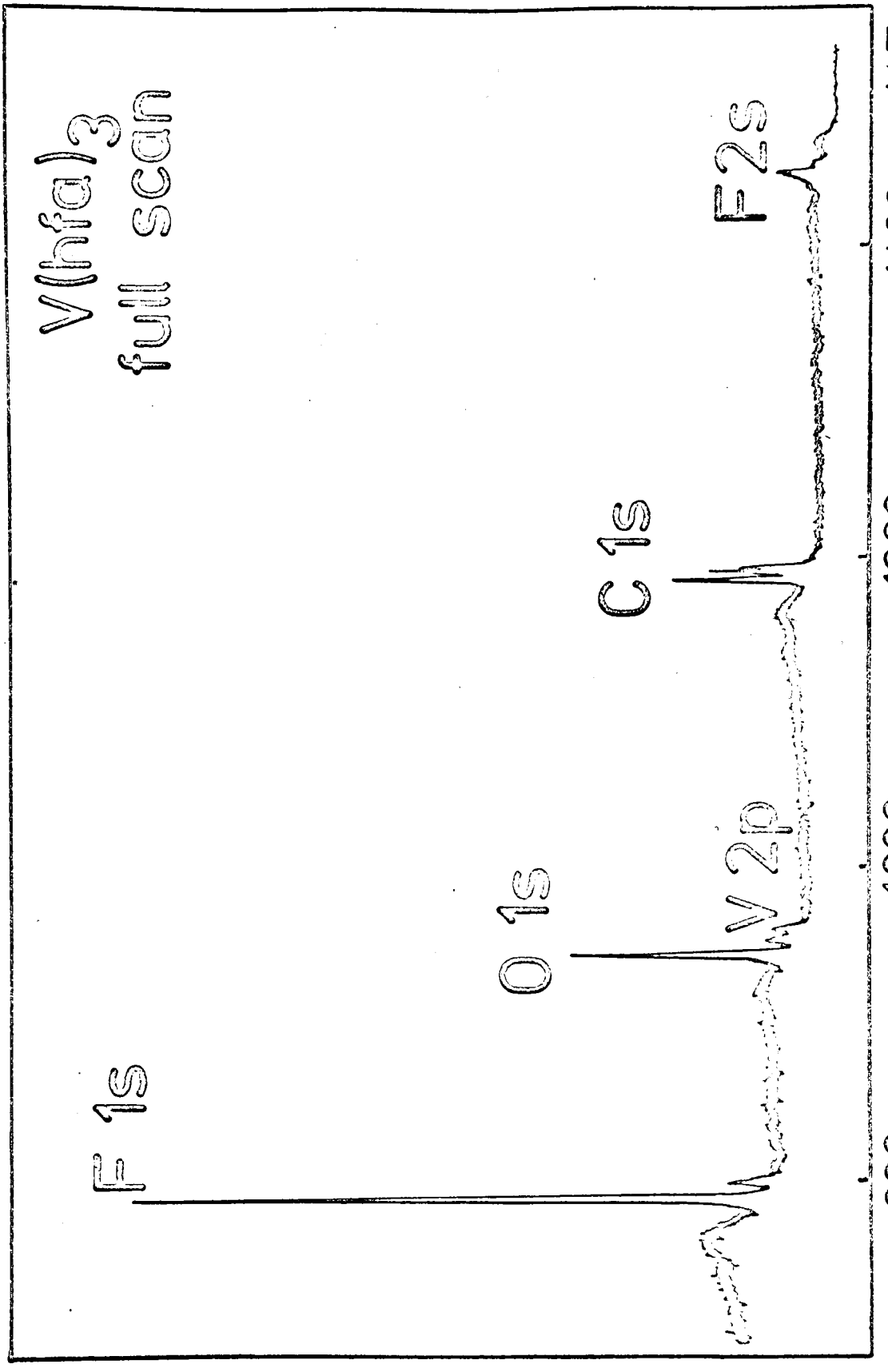

FIGURE 5.4a

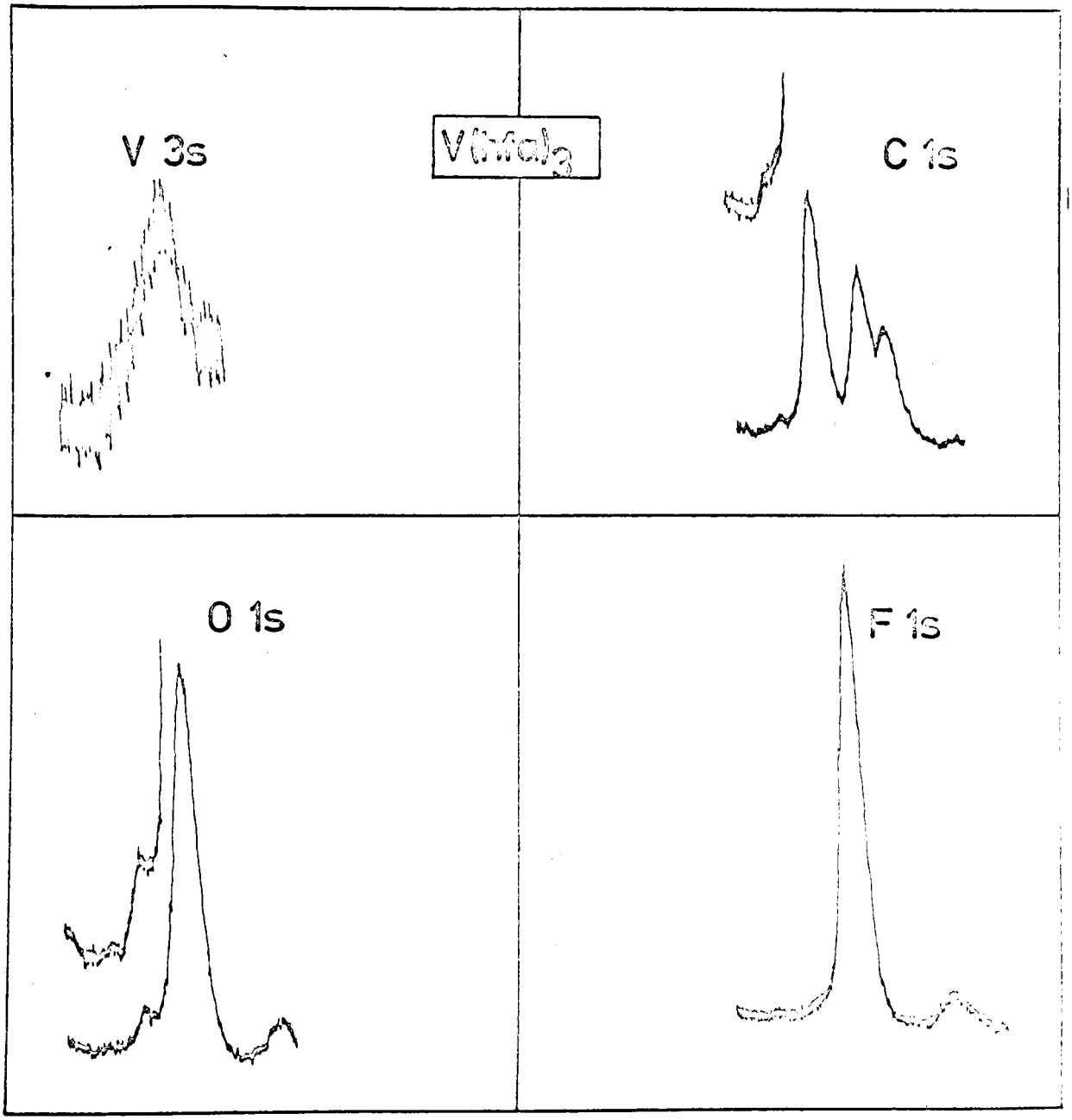

FIGURE 5.4b

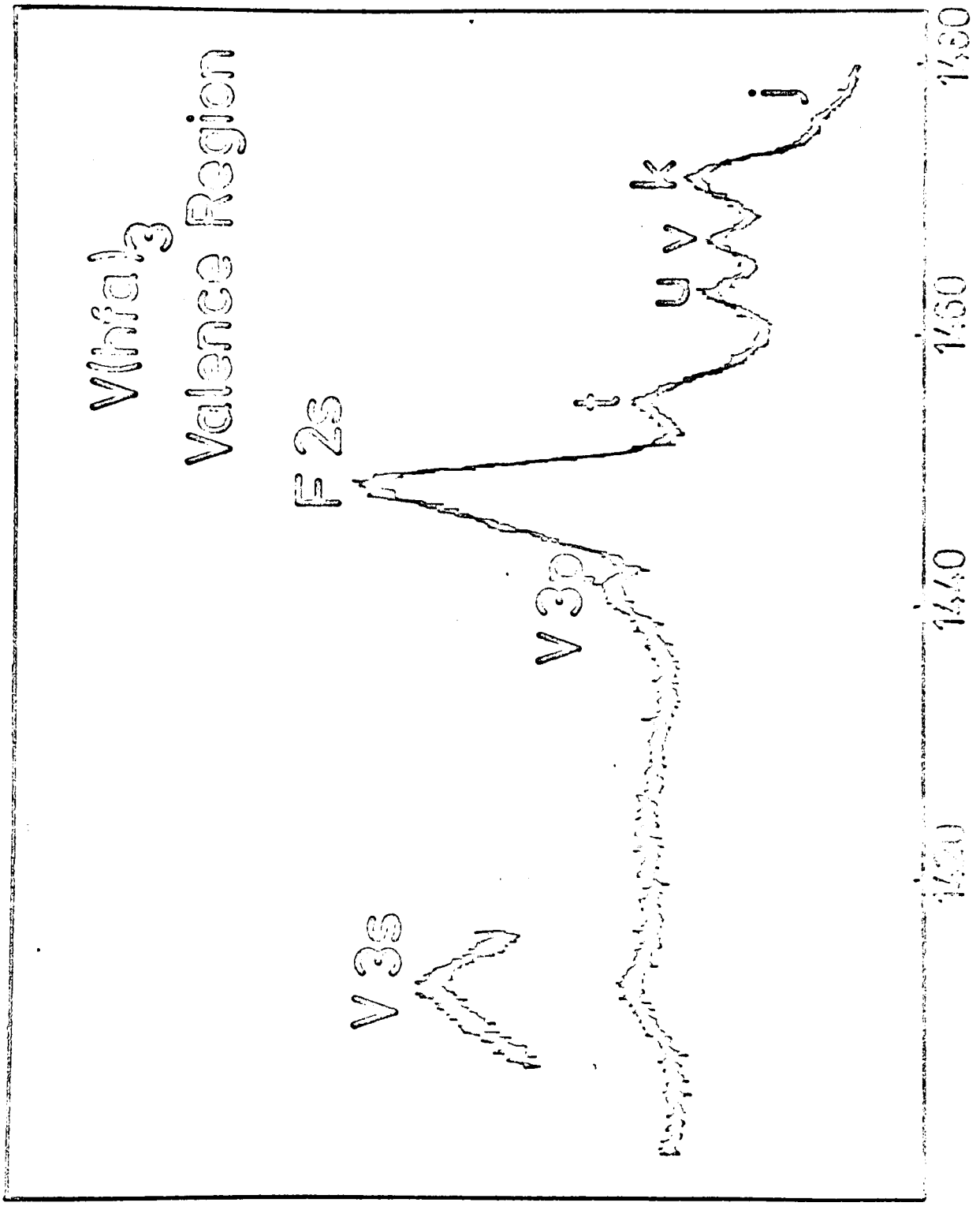

FIGURE 5.4c

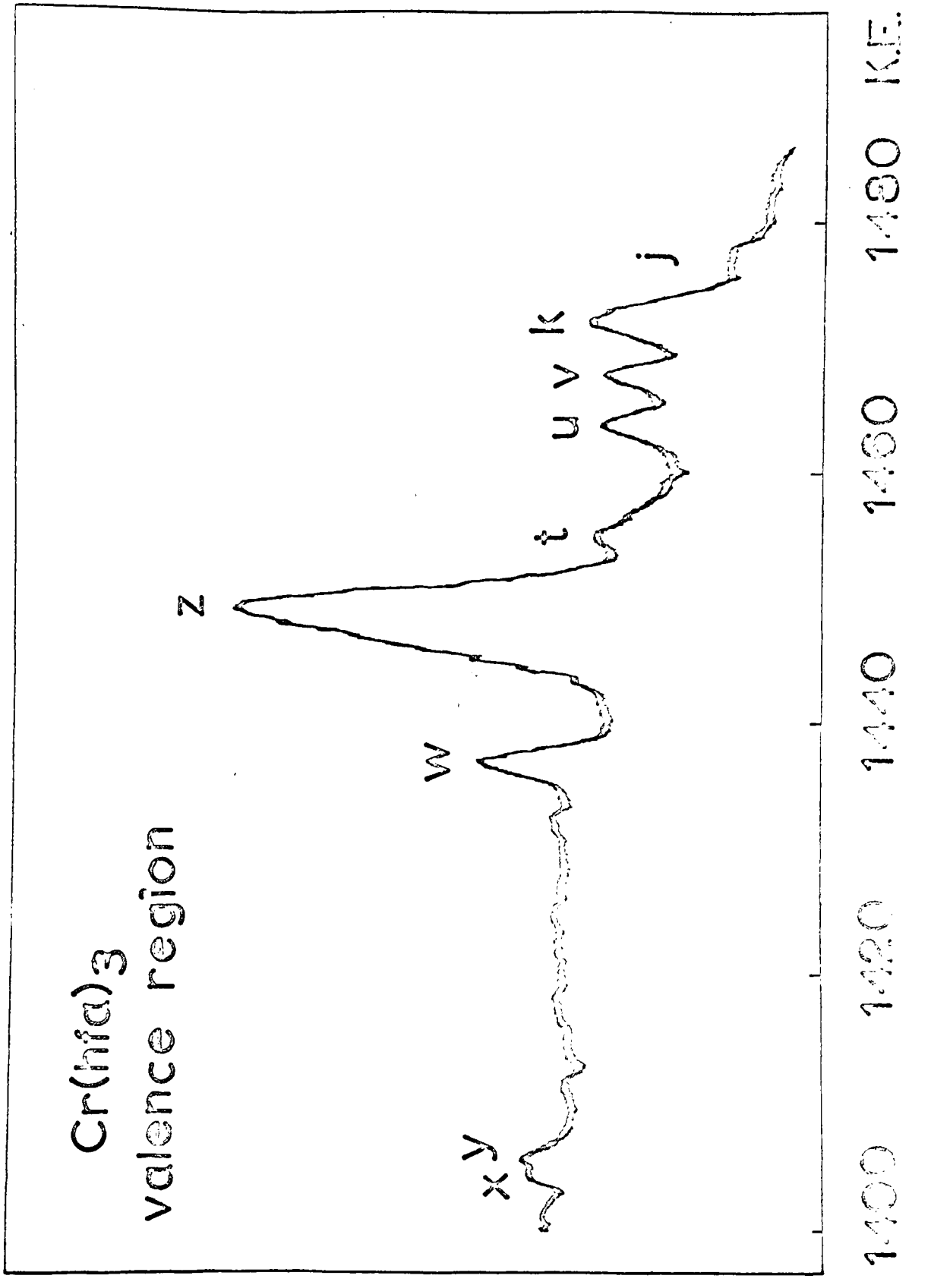
Cr(hfa)3
valence region
x
y
w
z
t
u
v
k
j
1100
1120
1140
1160
1180 K.E.

FIGURE 5.5a

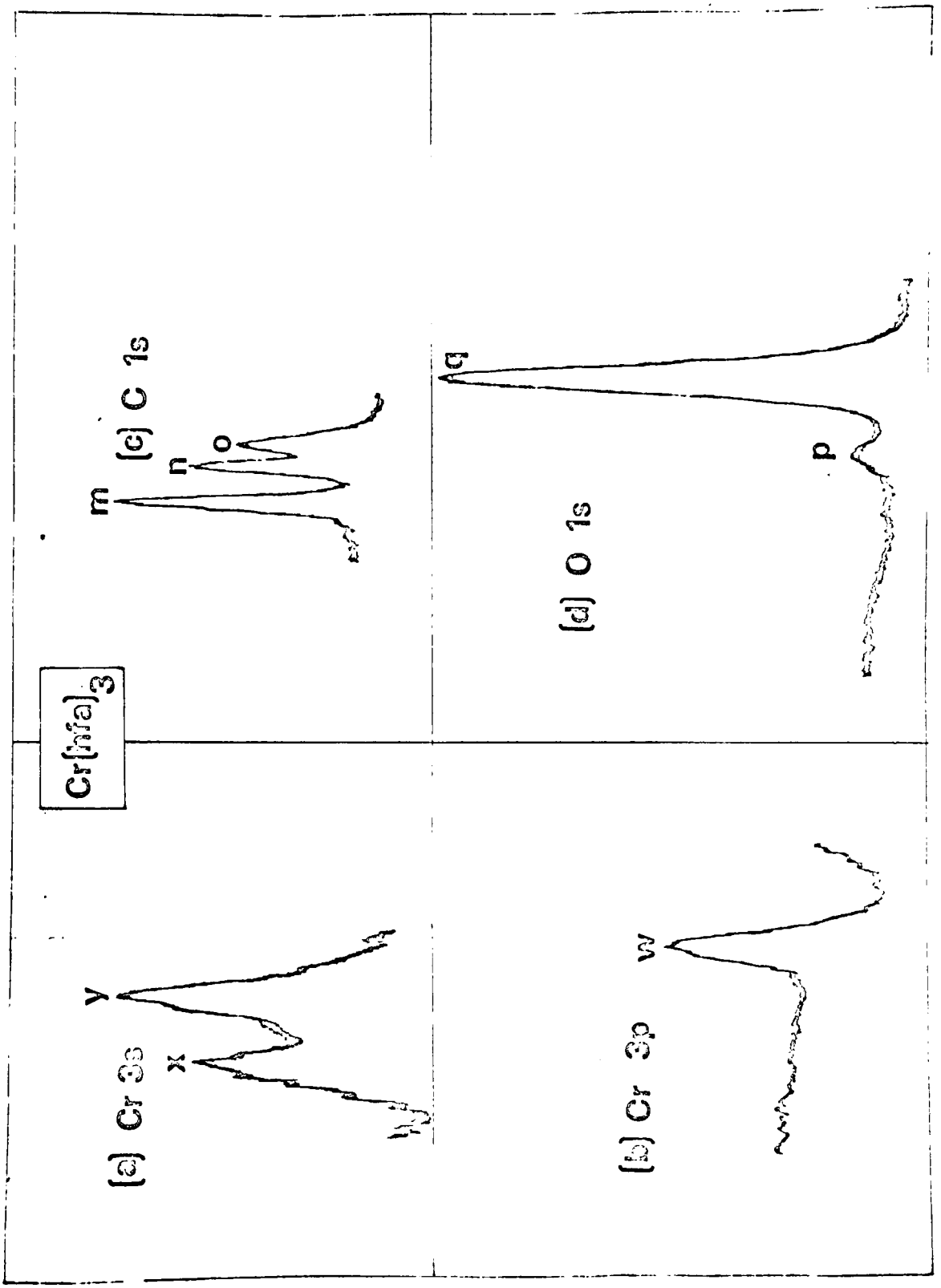

FIGURE 5.5b

44.1 eV for Sc(III), 47.9 eV for Ti(III), 50.7 eV for V(III) and 54.3 eV for Cr(III). In the ternary oxide phases $LaMO_3$, there is, in addition, a small increase in bond length between Ti and V which will contribute to both the observed ESCA and UV-PE trends (if it is reflected in the tris-chelate bond lengths). The origin of these effects probably lies in the changes in π-bonding, the extent of $\pi_3 \rightarrow t_{2g}$ donation being less for vanadium since we have two distinct effects - a stabilisation of the t_{2g} orbitals across the series, which leads to an increase in t_{2g}/π interaction, and an increase in occupancy of these t_{2g} orbitals, which, for a given extent of interaction, will have the effect of increasing back π-donation to the ligand. It appears that this second effect is more important in vanadium(III) than in either Ti(III), where the t_{2g} occupancy is too low, or in Cr(III), where the increasing electron affinity of the t_{2g} orbitals has offset the larger occupancy effect. Passing from $V(hfa)_3$ to $Cr(hfa)_3$, there is probably a slight bond contraction whose net effect would be to stabilise certainly the CH carbon and possibly the O 1s orbital, but these effects are substantially overshadowed by a large increase in covalency probably involving both σ and π donation to the central metal atom.

The irregularity found at $Mn(hfa)_3$ might be a manifestation of the Jahn-Teller distortion of the tris-chelate. However

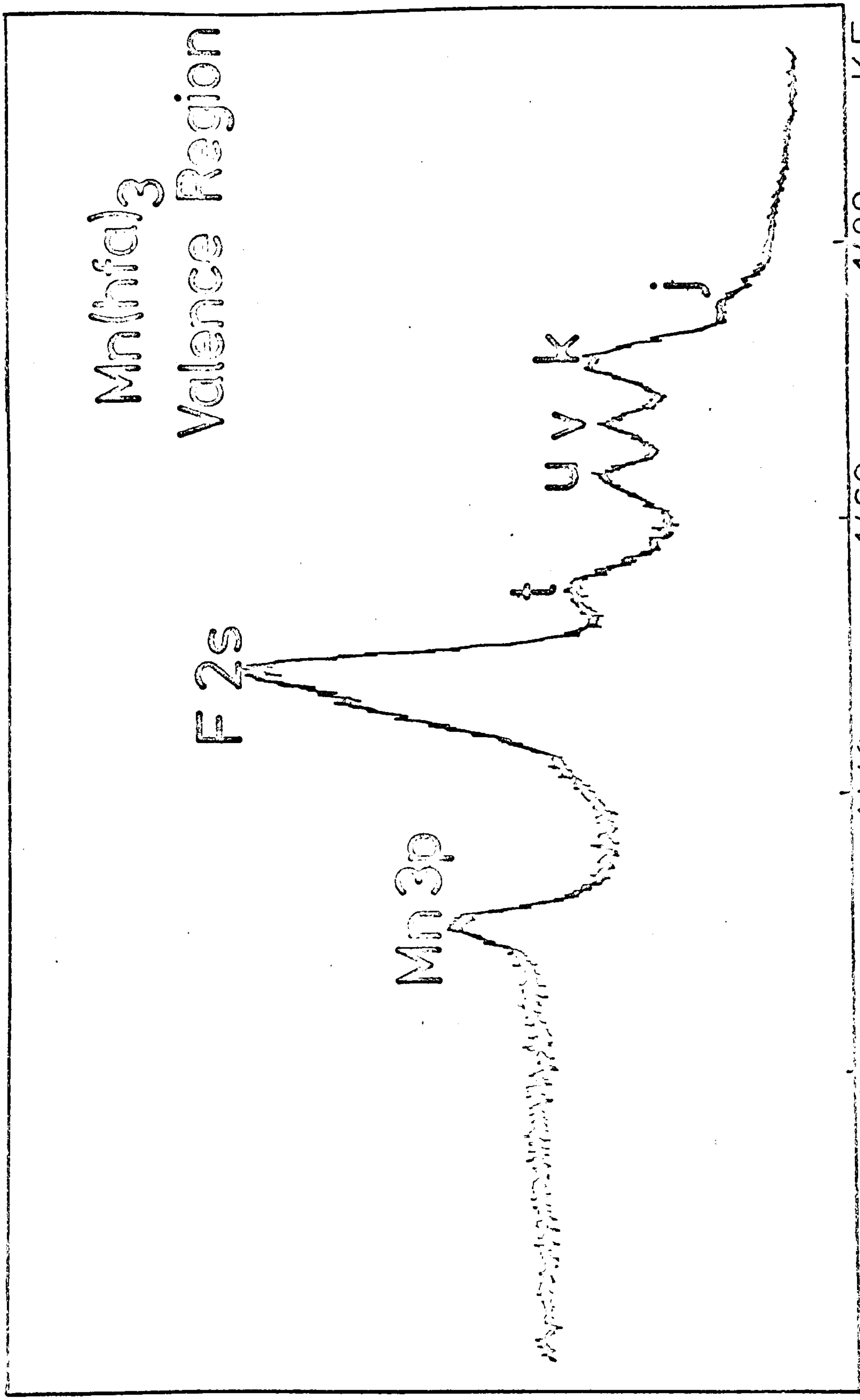

FIGURE 5.6a

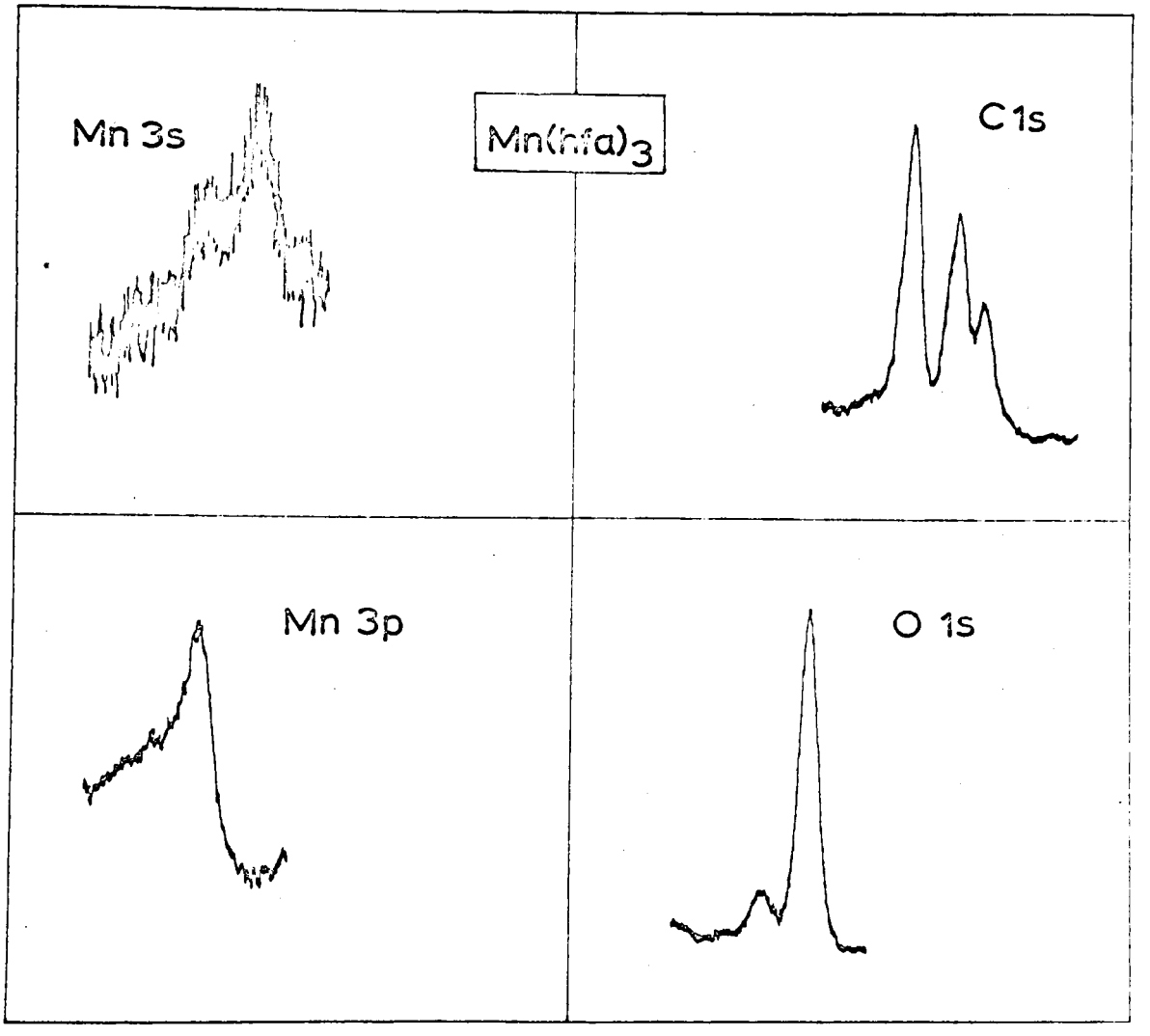

FIGURE 5.6b

the oxygen 1s peak is not noticeably broadened in comparison with the other chelates and a more likely explanation is that for the first time as we traverse the series, the main d-antibonding level e^*_g has become occupied. This orbital is very much more delocalised over the ligand than is the t_{2g} orbital, and the result will be, in effect, to lead to a more "ionic" complex than might have been expected. This is analogous to the explanation of the behaviour of V(III) put forward above, though the effect is magnified considerably by the form of the e^*_g orbital. The only band to show significant movement between $Cr(hfa)_3$ and $Mn(hfa)_3$ is the CH 1s orbital which has stabilised, suggesting that some back donation from the e^*_g orbital to ligand π_4^* (mainly C-O anti-bonding) has occurred, since this orbital has a node on CH which will therefore not be directly destabilised by charge shift mechanisms.

The expansion of bond length for open-shell d^5 systems is not very marked in the tris-chelate series, though it will lead to a slight destabilisation of all the levels. Increasing σ-covalence will also destabilise the ligand levels, and this, when coupled with the increased electron affinity of the d-orbitals in Fe(III), is presumably a major source of O 1s destabilisation as compared with $Mn(hfa)_3$. The comparative immobility in the carbon levels is more difficult to explain,

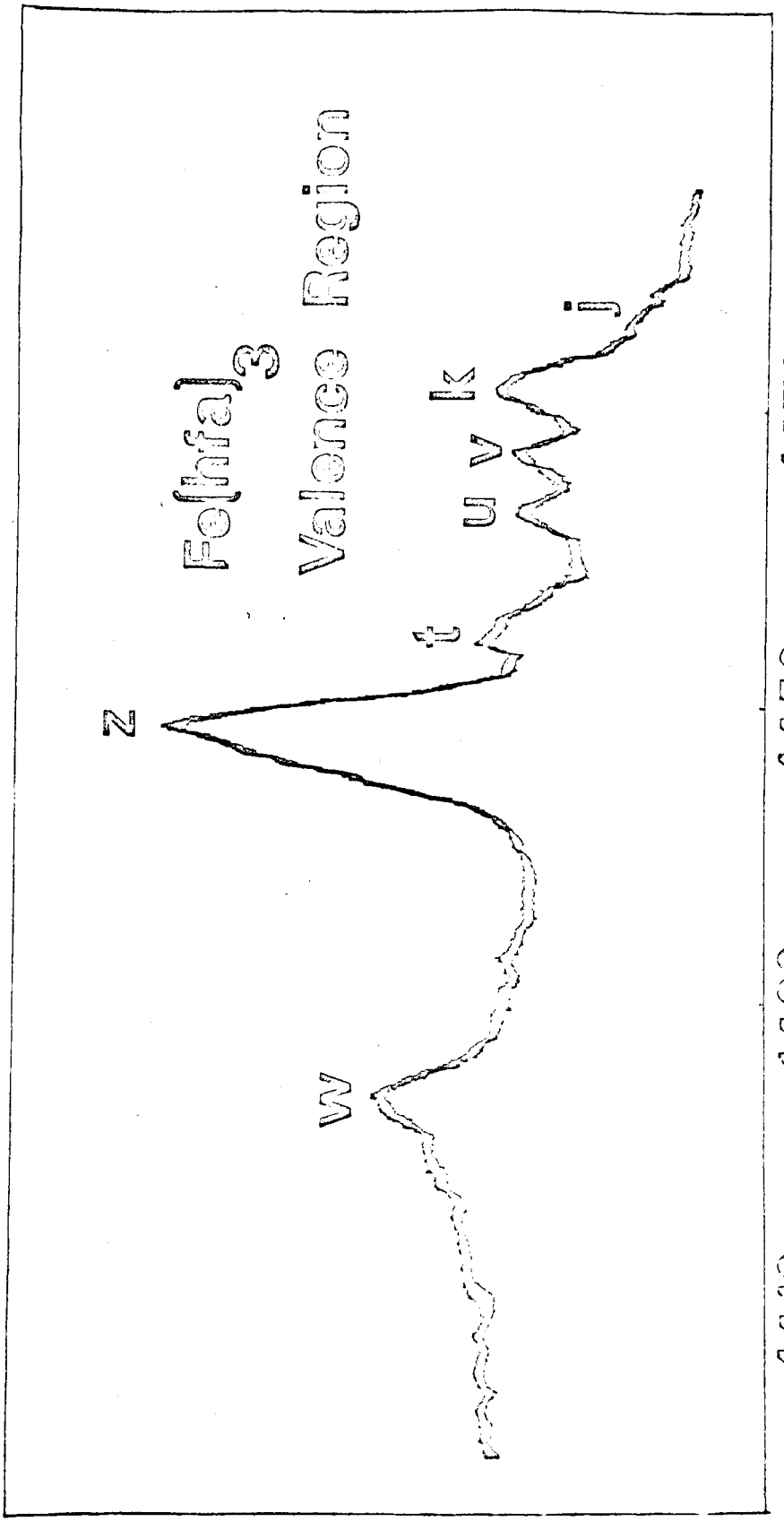

FIGURE 5.7 a

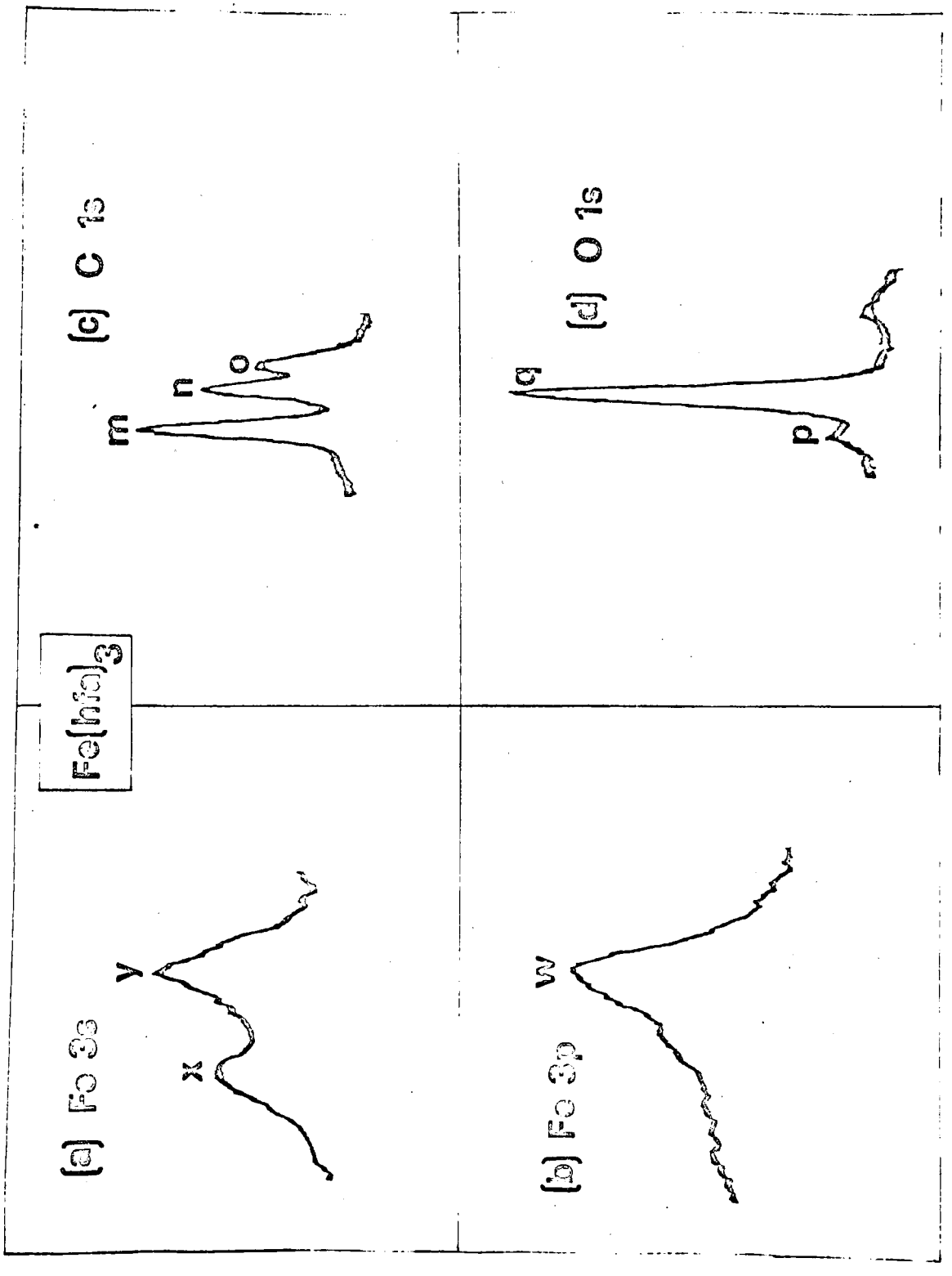

FIGURE 5.7b

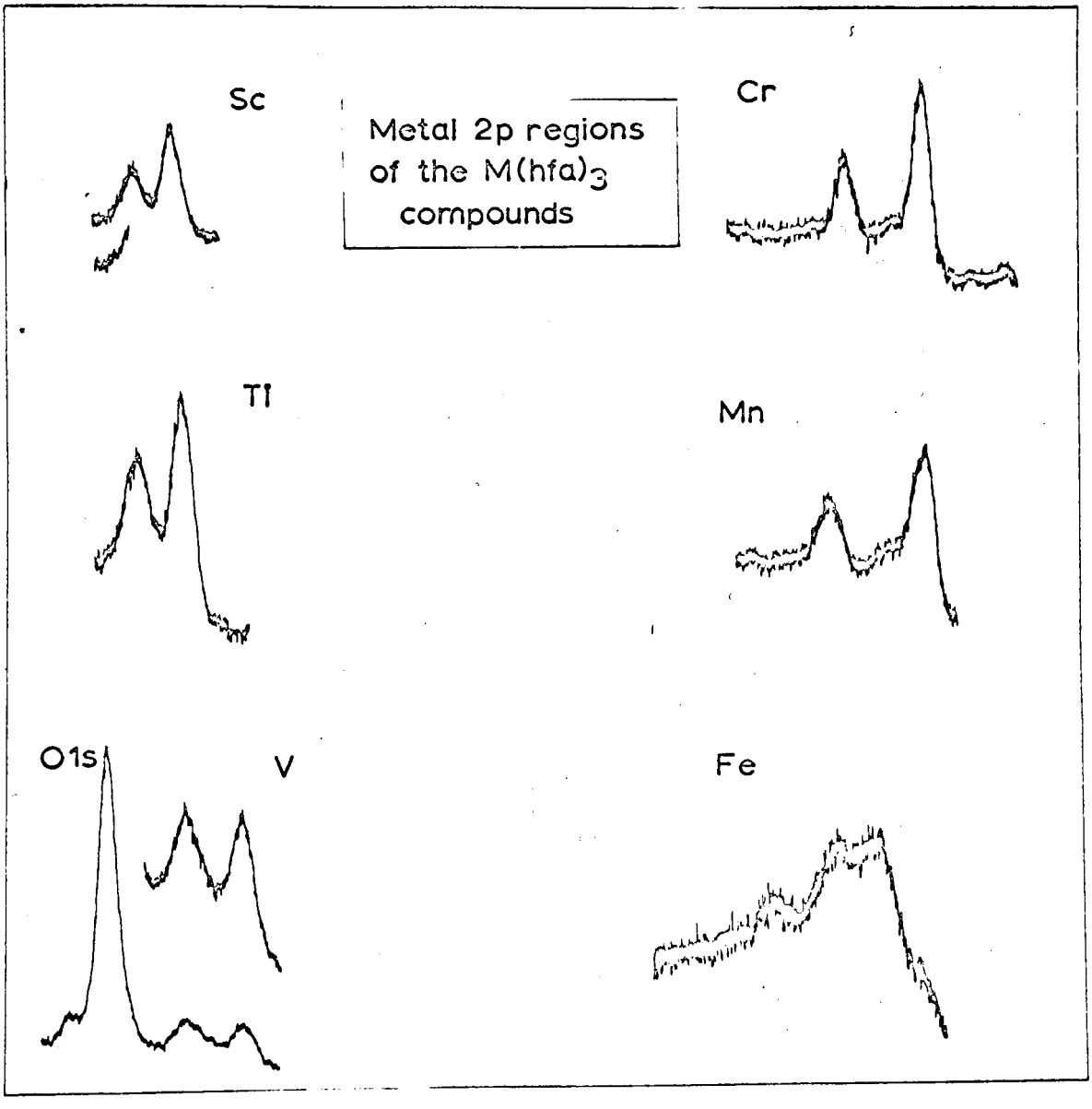

FIGURE 5.8

but is probably compounded of the decrease in potential from the central metal (which will be quite large) and an extensive charge polarisation in the ligand towards the metal, caused by depletion of σ electron density at the oxygen atoms (which, as we saw above, will tend to stabilise the carbon atoms). Since the delocalisation of the e^*_{1g} electrons will cause the metal potential to decrease at a rate less fast than expected, the ligand polarisation effect becomes more significant than for earlier members of the series, where it was swamped by the covalency effect. The substitution of suitable parameter values into the model discussed above supports these qualitative deductions very well.

If we now consider the valence region above 1448 eV KE, it can be seen to be very similar in all the first row complexes. The initial observation that the M 3d electrons had apparently only a very low cross-section in ESCA was somewhat surprising. Subsequently, several studies have indicated that the M 3d cross-section is in fact strongly dependent on the ligand. Thus, the metallocenes all show a strong 3d signal which, in the latter half of the transition series dominates the valence region and the signal showed a steady marked decrease in intensity in the iso-electronic series (d^6), $Fe(\pi Cp)_2$, $(\pi Cp)Mn(CO)_3$ and $Cr(CO)_6$. To try to identify the peaks in the valence region, the spectrum of $Ru(hfa)_3$ was also run, and,

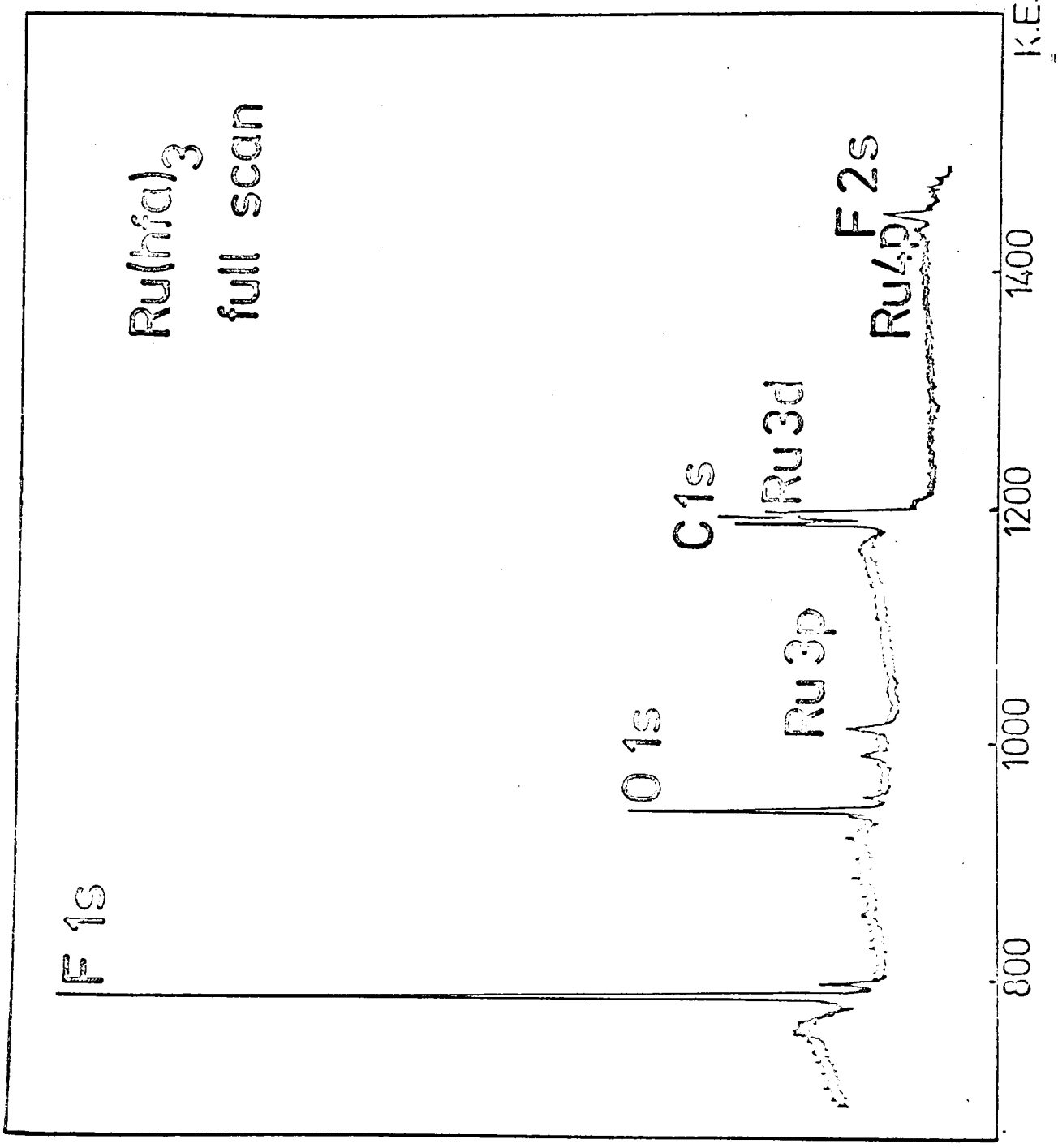
Ru(hfa)3
full scan
F 1S
O 1S
C 1S
Ru 3p
Ru 3d
Ru 4p
F 2S
800
1000
1200
1400
K.E.

FIGURE 5.9a

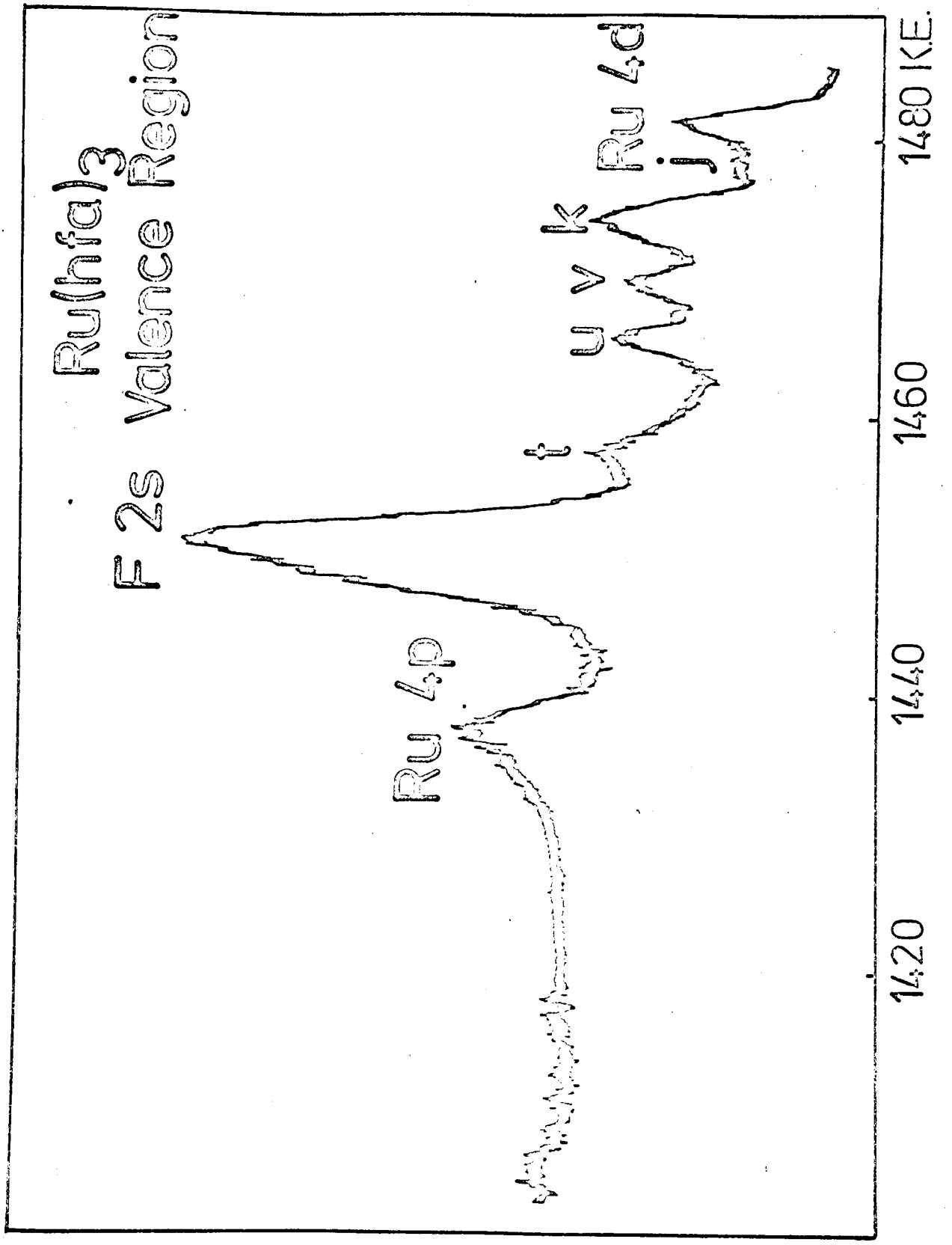
RuNa13
F 2s Valence Region
Ru 4p
+
UVX
Ru 4d
1420
1440
1460
1480 K.E.

FIGURE 5.9b

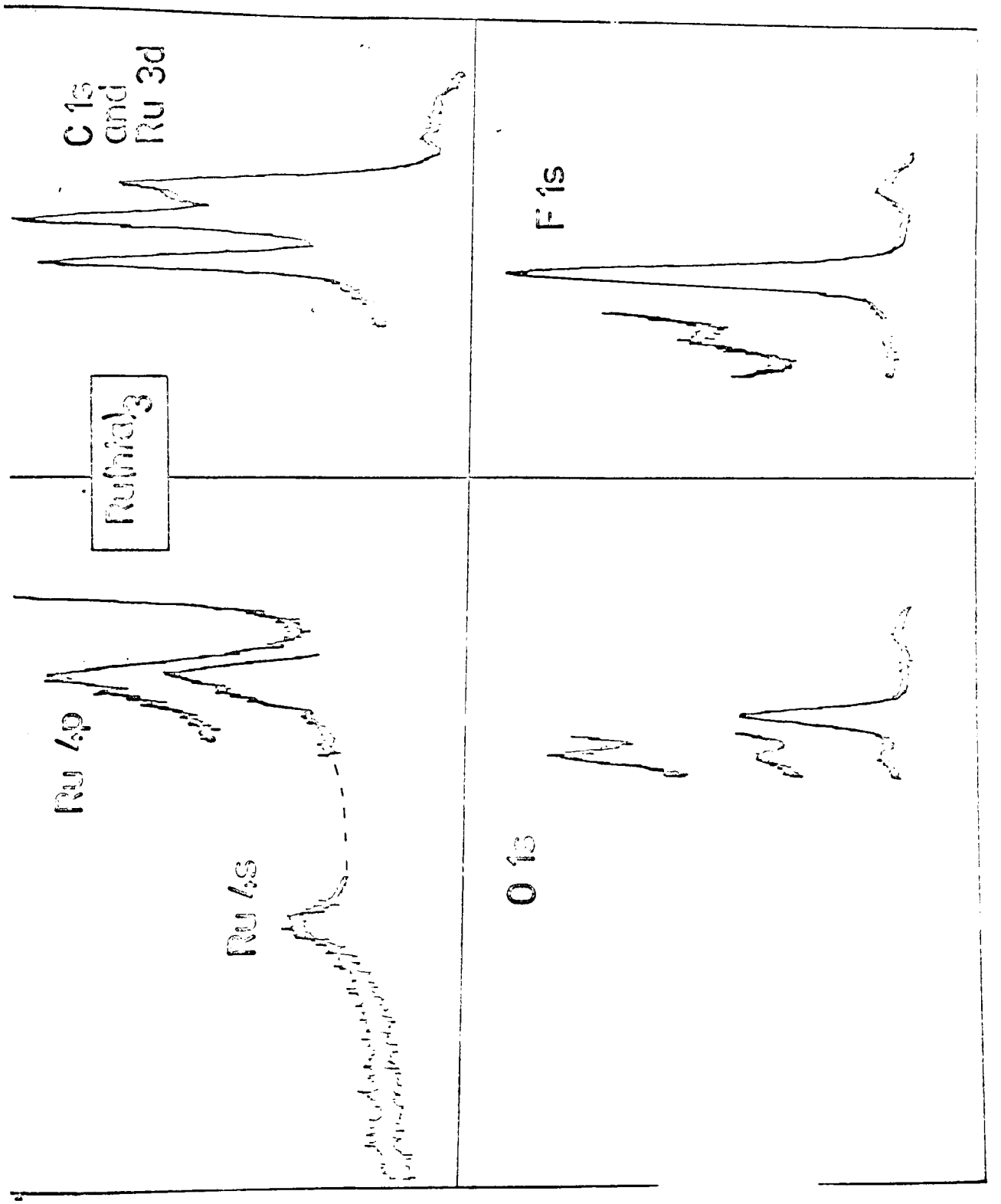

FIGURE 5.9c

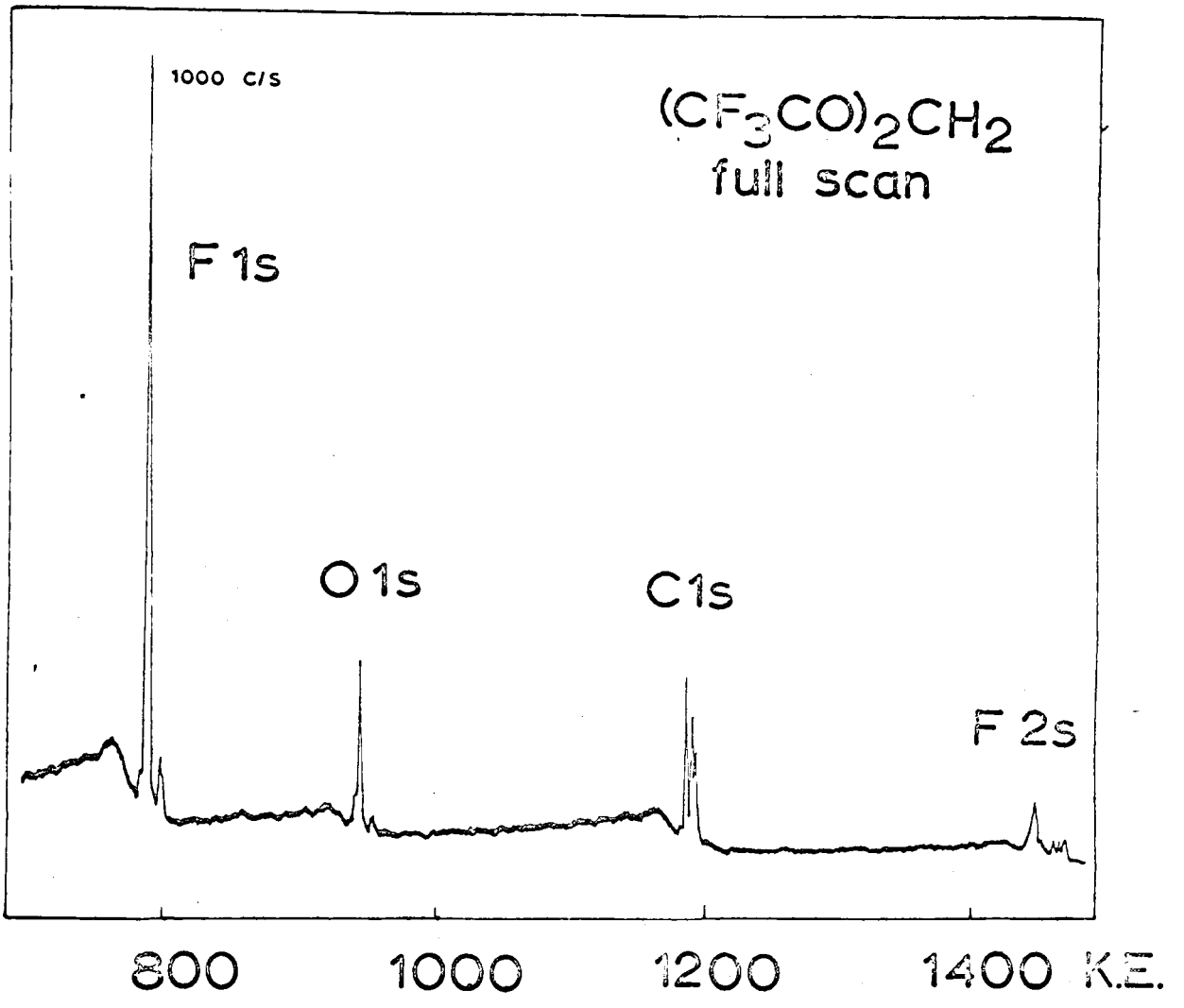
1000 c/s
$(CF_3CO)_2CH_2$
full scan
F 1s
O 1s
C 1s
F 2s
800
1000
1200
1400 K.E.

FIGURE 5.10a

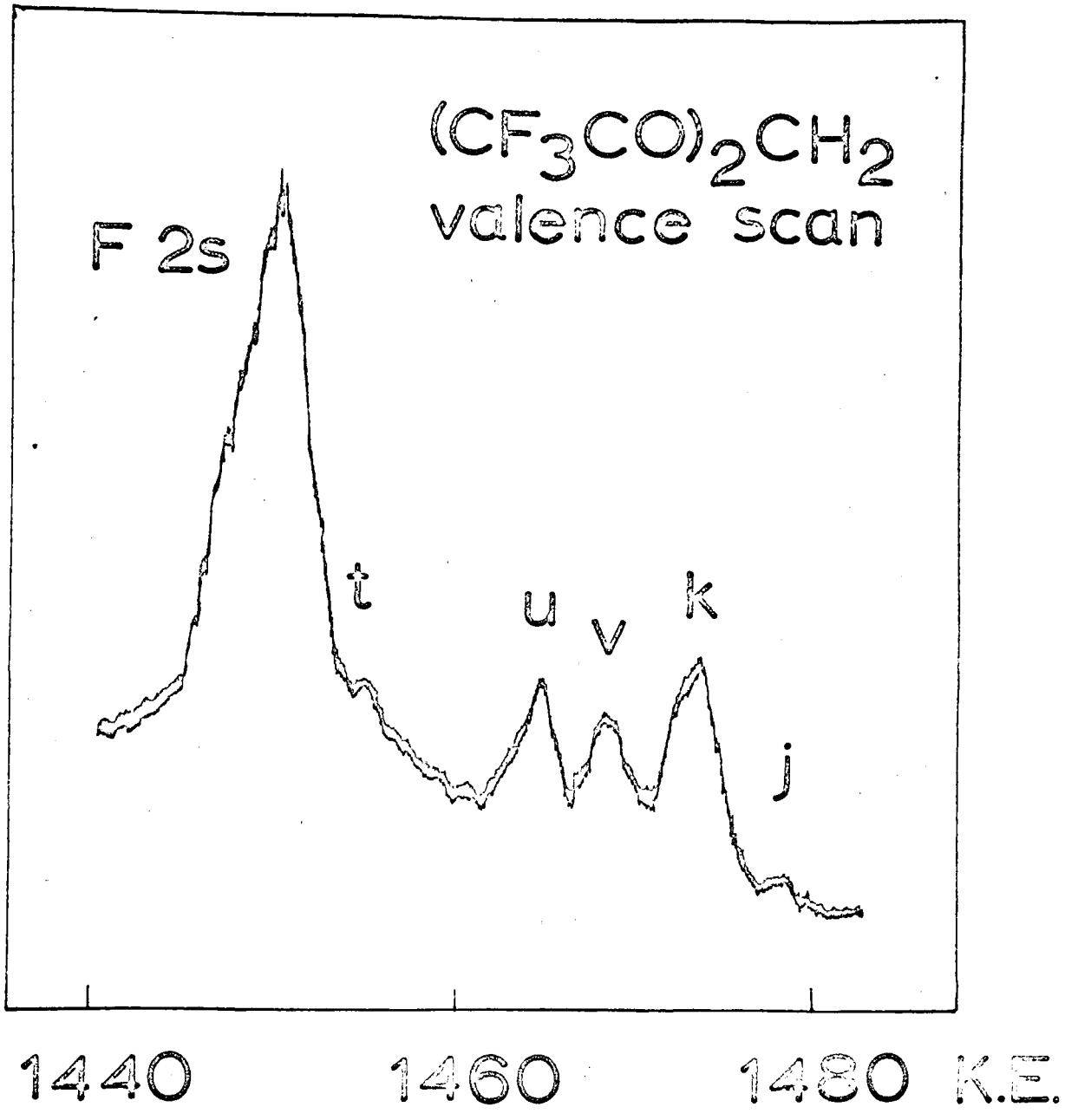

FIGURE 5.10b

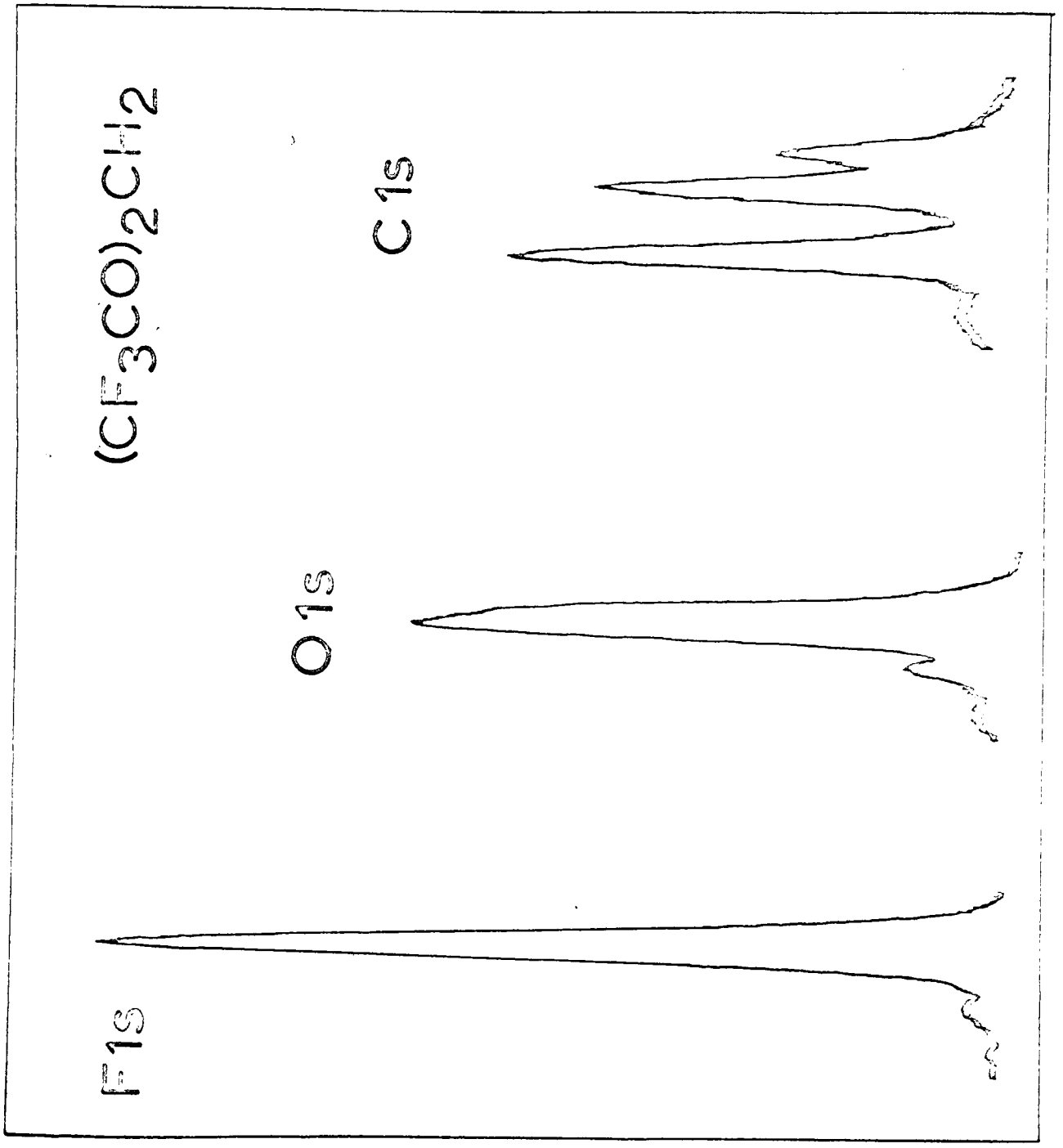

FIGURE 5.10c

as can be seen, the larger cross-section of the M 4d orbitals enables the main d-band to be clearly seen. Comparison with the He(I) spectrum indicates that the peak (k) corresponds most closely in energy to the strong UV-PE band at ~17.2 eV BE. Support for this comes from the observation that the movement in BE of band (k) and the intense UV-PE band at ca. 17 eV parallel one another quite closely through the whole transition series. However, it should be borne in mind that peak (k) will be sensitive to the difference between vapour and solid phases since it almost certainly originates, at least in part, from ionisation from some F 2p non-bonding lone-pair. If we consider the CF_3 grouping in a molecule such as CHF_3, three main peaks may be seen, corresponding to (C2s + F2p$_{\sigma}$), (C2s + F2p$_{\sigma}$), F2p$_{\pi}$. The separation of the first two bands in CHF_3 is 3.9 eV, which corresponds quite well to the separation of peaks (u) and (v) in the ESCA spectra. The band (k) is much broader than either (u) or (v) and its separation from these two bands is rather larger than that between the (a_1 + e) bands and the intense e band at 17.25 eV in the He(I) spectrum of CHF_3. This may be because band (k) includes unresolved C 2s components, and possibly the lower energy F 2p$_{\pi}$ (a_2 + e) components. If this is correct, band (k) will not correspond exactly to the UV-PE band at 17.2 eV in hexafluoroacetylacetonato complexes. Further evidence that this is so comes from an

examination of the free-ligand, which shows an intense UV-PE band at 20.92 eV BE. This must correspond to band (v), and so band (k), separated by 4.5 eV from (v) in the ESCA spectrum of the free ligand, will be at 16.42 eV BE. It follows that the mean Ru 4d BE, as measured from the ESCA spectrum is ~ 9.3 - 9.4 eV, strongly suggesting that band A in the UV-PE spectrum corresponds not only to ionisation from the π_3 orbital but also to the d-ionisations to yield $^1T_2$ and ^1E. This use of the ESCA spectra in assigning UV-PE spectra has proved especially powerful in the case of the metallocenes.

The relative intensities of bands u, v and k are rather difficult to understand. The a_1 band in CHF_3 at ~ 24 eV is probably predominantly C 2s, so that band u presumably corresponds to these two C 2s bands. However, comparison with the ESCA spectra of the metallocenes, discussed below, shows that the C 2s cross-section is rather small and C 2p cross-section negligibly so, in comparison with F 2p and O 2s. It follows that band u must also contain substantial F 2p character, i.e., that there is extensive mixing between C 2s and F 2p in hexafluoroacetylacetone. Now the chain of five carbon atoms will interact to yield, for the C 2s orbitals, five MO's of symmetry 3a + 2b. The b symmetry orbitals interact substantially, generating two energy levels, the lower one of

which will probably be under band u. The other may be obscured by band v, but an examination of the valence region ESCA spectra of the metallocenes suggests that these C 2s interactions can be very large, presumably via through-bond mechanisms, and so the upper b level could equally well be under k. The three a levels, derived as shown in the MO diagrams will interact to generate a low bonding level, presumably also under band (u), a middle level which will be moderately bonding and an upper antibonding level. The complete scheme shown in the MO diagram is speculative but, from an examination of a number of ESCA spectra of simple hydrocarbons, quite reasonable on energetic grounds.

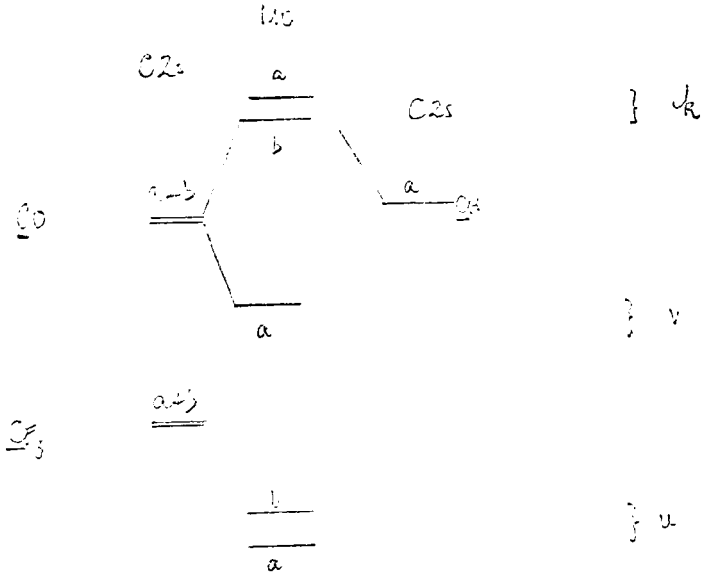

It should be noted in passing here that an orbital interaction model clearly does not provide a suitable rationale for these splittings unless the complete bonding scheme is taken into account; in other words, this splitting cannot be explained on the basis of s-s overlap.

The movements observed in bands (u), (v), (k) and also the He(I) PE bands parallel those observed in π_3 and are discussed in detail below. They provide a remarkable confirmation of the fluorine-effect discussed above. The other valence region orbital, derived from O 2s, is unfortunately a rather ill-defined shoulder which seems to vary somewhat randomly in energy down the series. However, the accuracy of measurement is only $\sim$0.3 eV with respect to F 2s so that further discussion of the band is not warranted at this stage.

EXCHANGE EFFECTS

An examination of the metal 3s region of the transition metal complexes discussed above shows that a distinct splitting of the 3s band into two components may occur, the component at lower binding energy always being the most intense. The phenomenon is restricted to open-shell systems and depends critically on the metal and on the total spin. It was first noted experimentally in the gas-phase spectra of oxygen and nitric oxide and was explained as a spin-coupling effect. As explained in the supplementum, if the total spin of the ground-state molecule is S, and the orbital symmetry Γ', ionisation of an s core electron can generate two states $|S + \frac{1}{2}, \Gamma'\rangle$ and $|S - \frac{1}{2}, \Gamma'\rangle$, by removing respectively the antiparallel and parallel spin electron from the s shell. For simplicity, let us assume that the unpaired electrons in the ground state are all in the same subshell, whose components are γ_i, and consider the situation in which no spin-pairing within the γ_i occurs. Then the ground state may be written

$$\Psi_0 = |s^2 C' \gamma_1^+ \gamma_2^+ \ldots \gamma_n^+\rangle$$

where s^2 is the core s-shell and C' the continued product of the closed-shell orbitals.

The ionised state, of total spin S + $\frac{1}{2}$ has the wave-function

$$\Psi|S+\tfrac{1}{2}\rangle = |s^+ C' \gamma_1^+ \ldots \gamma_n^+\rangle$$

and energy $E_1 = \sum_i^n (J_{\gamma_i S} - K_{\gamma_i S})$ + interaction terms with

$$C' + \sum_{i<j} J_{\gamma_i \gamma_j} - K_{\gamma_i \gamma_j}$$

Similarly, the state of total spin $S - \frac{1}{2}$ may be written

$$\Psi | S - \tfrac{1}{2} \rangle = \left\{ n | S^- C' \gamma_1^+ \ldots \gamma_n^+ \rangle - \sum_i | S \gamma_i C' \gamma_1^+ \ldots \gamma_i^- \ldots \gamma_n^+ \rangle \right\} \frac{1}{\sqrt{n-1}} \times \frac{1}{\sqrt{n}}$$

and its energy is $E_2 = \sum_i^n (J_{\gamma_i S} - K_{\gamma_i S})$ + interaction terms with

$$C' + \sum_{i<j} J_{\gamma_i \gamma_j} - K_{\gamma_i \gamma_j} + \frac{n+1}{n} \sum_i K_{\gamma_i S}$$

Now, since the S orbital has spherical symmetry within the point group, it follows that $K_{\gamma_i S}$ has the same numerical value for all γ_i, and so

$$E_2 = E_1 + (n+1) K_{\gamma_S} = E_1 + (2S+1) K_{\gamma_S} \qquad (5.1)$$

since $n = 2S$. Trivially, the same expression can be shown to hold for a more than half-filled shell. If we have two partly filled shells, of spins S and S′, and symmetries γ and μ, then the expression becomes[6]

$$E_2 = E_1 + \left\{ 2S + \frac{S}{S+S'} \right\} K_{\gamma_S} + \left\{ 2S' + \frac{S'}{S+S'} \right\} K_{\mu_S} \qquad (5.2)$$

Consider the value of $K_{\gamma s}$; it may be written

$$\iint s(1)\,\gamma^*(2)\,\frac{1}{r_{12}}\,\gamma(1)\,s^*(2)\,d\tau_1\,d\tau_2$$

where the spins have been integrated out. Since $|\gamma\rangle$ is a valence MO, it may be written as a linear combination of metal and ligand orbitals, taking the general form

$$|\gamma\rangle = a_1|d\rangle + a_2|\ell\rangle$$

where $|\ell\rangle$ is a linear combination of ligand orbitals of Γ symmetry. It follows that

$$K_{\gamma s} = |a_1|^2 K_{ds} + |a_2|^2 K_{\ell s} + a_1^* a_2 \iint s(1)\,d^*(2)\,\frac{1}{r_{12}}\,\ell(1)\,s^*(2)\,d\tau_1\,d\tau_2 + a_2^* a_1 \iint s(1)\,\ell^*(2)\,\frac{1}{r_{12}}\,d(1)\,s^*(2)\,d\tau_1\,d\tau_2$$

and, if we assume that the cross-terms and $K_{\ell s}$ are small, then we have

$$K_{\gamma s} = |a_1|^2 K_{ds}$$

so that the measured exchange splitting gives a direct measure of covalency. There are, however, some cautionary observations we must make;

(i) it may be that the cross-terms are not negligible, and the effect of neglecting them will depend on the relative phases of ligand and metal orbitals.

(ii) the basis orbitals used in such an LCAO method are not identical to the orbitals found in free atoms. (Now the difference may not be very great since nephelauxetic ratios observed for simple metal complexes are rarely

very different from unity. In the simplest possible formalism of course, a_1^2 should be equal to the square-root of the nephelauxetic ratio, but this will only be true if metal-ligand exchange integrals are negligible compared to those observed in d/d exchange terms).

Two mechanisms for the reduction of such exchange integrals from the observed free-ion values have been suggested. The covalent delocalisation discussed above, which Jørgensen termed "symmetry-restricted covalency" and a second, rather more subtle effect, "central field covalency", which arises because, as the charge on the central metal ion is reduced by covalency, radial expansion of the d-orbitals occurs, to which K_{ds} will be especially sensitive, far more so, in all probability, than K_{dd}. Thus, our results may not bear any close quantitative relationship to such methods as super-hyperfine coupling, which only measure symmetry-restricted covalency.

Table 5.4 lists the exchange splittings for the compounds studied in this thesis, and for a few others for comparison.

TABLE 5.4

COMPOUND	CONFIGURATION	S	ORBITAL EXAMINED	SPLITTING	K_{ds}
$V(\pi C_5)_2$	$a_1^2 e_2^2$	3/2	V 3s	2·8 eV	0·70
$Cr(\pi C_5)_2$	$a_1^2 e_2^3$	1	Cr 3s	2·5 eV	0·83
$Cr(hfa)_3$	t_2^3	3/2	Cr 3s	4·0 eV	1·00
CrF_3	t_2^3	3/2	Cr 3s	4·2 eV	1·05
$Mn(\pi C_5)_2$	$a_1^2 e_2^2 e_1^2$	5/2	Mn 3s	4·3 eV	0·89
MnF_2	$t_2^3 e^2$	5/2	Mn 3s	6·5 eV	1·08
MnO	$t_2^3 e^2$	5/2	Mn 3s	5·7 eV	0·95
$Mn(hfa)_3$	$t_2^3 e$	2	Mn 3s	5·0 eV	1·00
$Fe(hfa)_3$	$t_2^3 e^2$	5/2	Fe 3s	5·5 eV	0·91
FeF_3	$t_2^3 e^2$	5/2	Fe 3s	7·0 eV	1·17

Owing to the very poor S/B ratios for the metal 3s bands, the figures are accurate only to ± 0.2 eV. It can be seen from the table that the largest exchange splittings are obtained with the trifluorides, where $K_{ds} \sim 1.1 - 1.2$ eV; the hexafluoroacetylacetonates have exchange splittings in the range 0.9 - 1.0 eV and the cyclopentadienyl complexes 0.7 - 0.8 eV, which is the expected order of covalency. However, comparing these values with those calculated for the

free ions, the results are very much more surprising, since for both Fe^{III} and Mn^{III}, K_{ds} values for the free ions are ca. 2.5 eV. Clearly, symmetry restricted covalency can be calculated from hyperfine-splitting data, and, for the first row fluorides, the value of a_1^2 (S.R.) is 0.8 to 0.9, indicating that K_{γ_s} should be about 2.0 - 2.3 eV. The very large difference between this value and those actually observed must then be a central-field covalency effect. The reason why K_{ds} should be so sensitive to this is not difficult to see, since we know that for the free ion, the 3d orbitals should show pronounced sensitivity to external charge. Since the 3s orbital is relatively contracted and concentrated about the nucleus, the extent to which its charge distribution overlaps with that of the 3d function will increase very much more rapidly as the 3d orbital contracts than do the inter-electronic repulsion integrals within the d-subshell themselves. Unfortunately, the calculation of such multiplet splittings is extremely difficult in molecules, since they are hole-state calculations depending for their success on the absence of significantly overlapping states of the same symmetry which can be generated using the given basis.[11] However, it would be interesting even within the RHF framework, to calculate K_{ds} for various oxidation states of the metal, to see if a pronounced variation is seen in its value.

If we examine the actual values obtained for the hexafluoroacetylacetonates, confirmation of our deductions concerning the covalency of these chelates can be obtained. If we assume that the major reduction in the exchange integral is a central field effect, then it is not surprising that the average exchange integral observed for $Cr(hfa)_3$ and $Mn(hfa)_3$ is about the same, and is significantly larger than that for $Fe(hfa)_3$, where the charge on the central metal is known to be less. It would be very difficult to explain, on the basis of symmetry restricted covalence alone, why, for $Mn(hfa)_3$, $K_{t_2s} \approx K_{es}$, whilst K_{es} is apparently much reduced in the case of $Fe(hfa)_3$. However, an even more cogent argument for central-field covalence comes from the metallocenes. It will be observed that the splitting of the V 3s band in $V(\pi Cp)_2$ is only slightly larger than that of the Cr 3s band in $Cr(\pi Cp)_2$. If we assume that the electron configuration of $Cr(\pi Cp)_2$ is $a_1e_2^3$, then, using equation 5.2, we obtain the values

$$K_{a_1 s} = 1.8 \text{ eV}, \quad K_{e_2 s} = 0.15 \text{ eV}$$

and, for $Mn(\pi Cp)_2$, using the equation

$$\Delta = \left\{2S + \frac{S}{S+S'+S''}\right\} K_{a_1 s} + \left\{2S' + \frac{S'}{S+S'+S''}\right\} K_{e_1 s} + \left\{2S'' + \frac{S''}{S+S'+S''}\right\} K_{e_2 s}$$

we find that $K_{e_1 s} = 0.95$ eV.

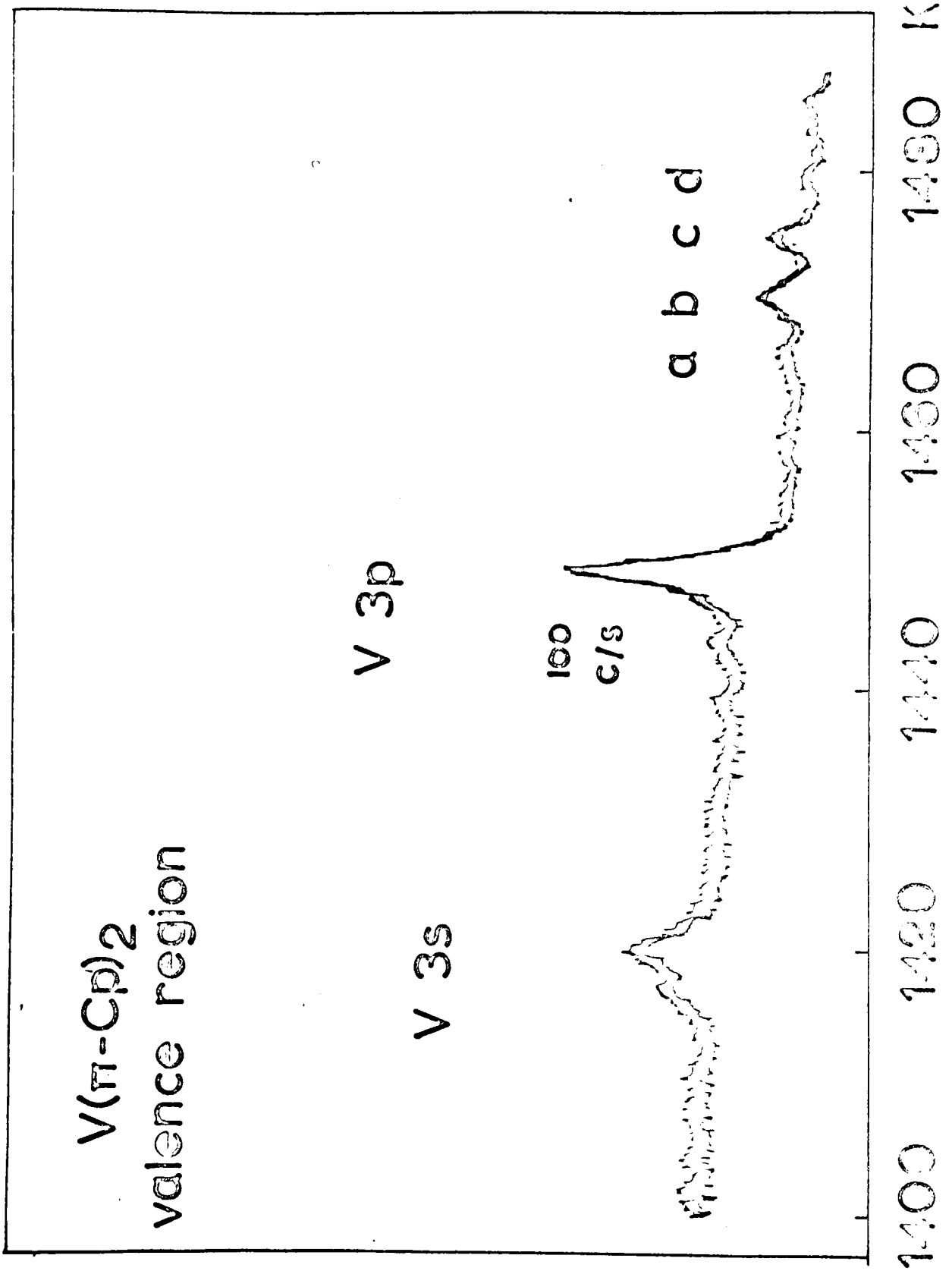
V(π-Cp)2
valence region
V 3s
V 3p
100
c/s
a b c d
1400
1420
1440
1460
1480
K.E.

FIGURE 5.11a

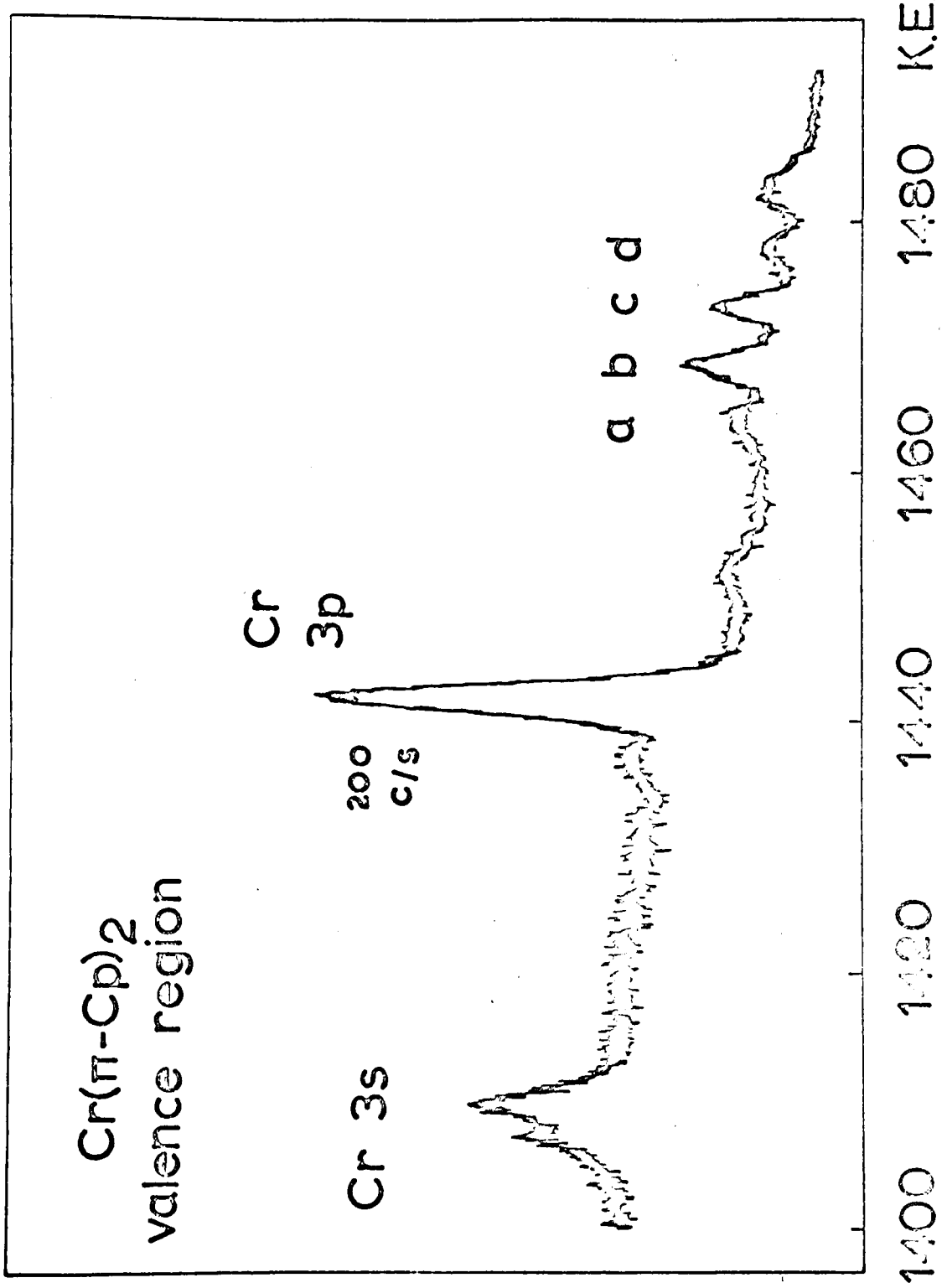
Cr(π-Cp)2
valence region
Cr 3s
Cr 3p
200 c/s
a b c d
1400
1420
1440
1460
1480
K.E.

FIGURE 5.11b

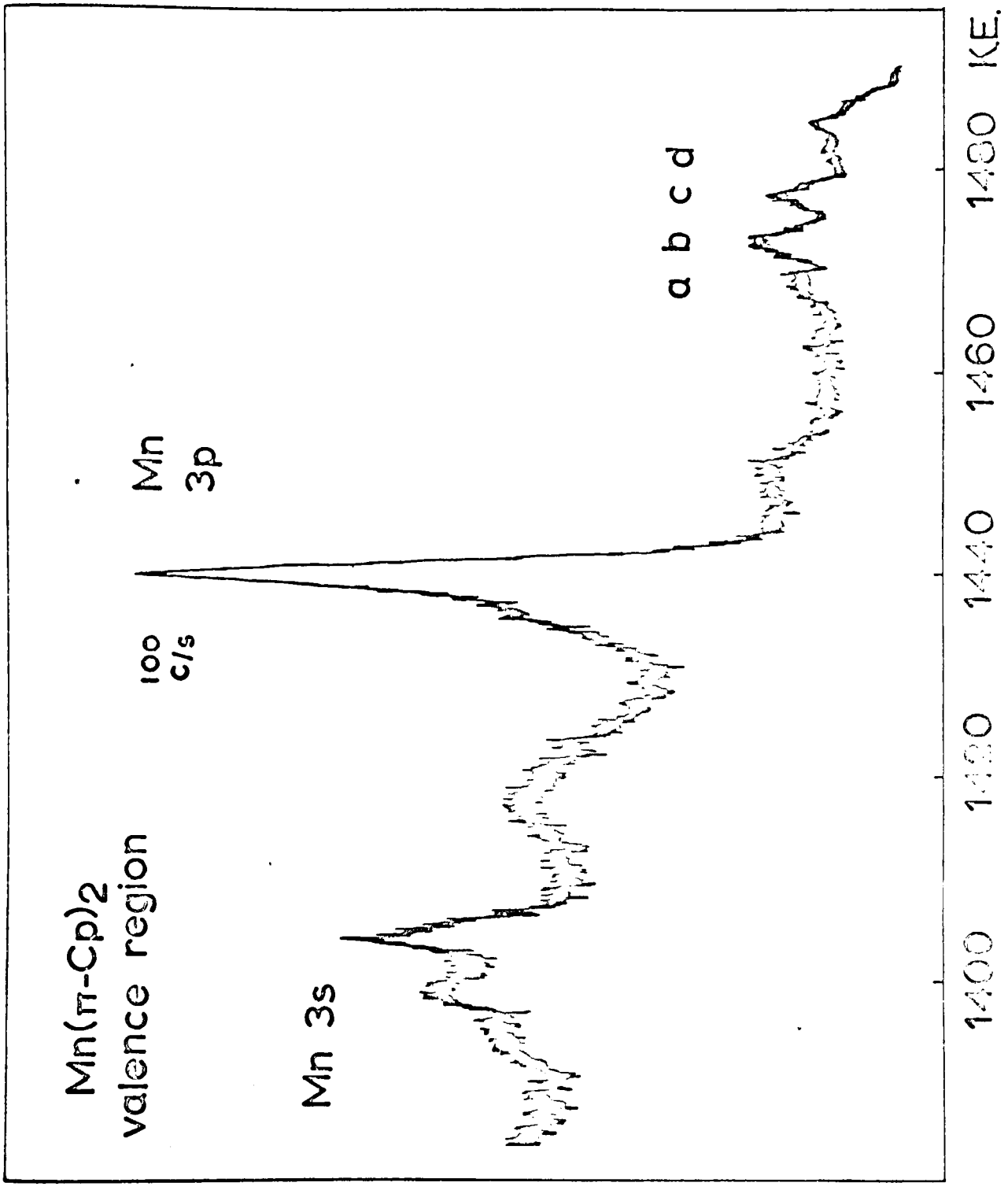
Mn(π-Cp)2
valence region
Mn 3s
100
c/s
Mn
3p
a b c d
1400
1420
1440
1460
1480 KE.

FIGURE 5.12a

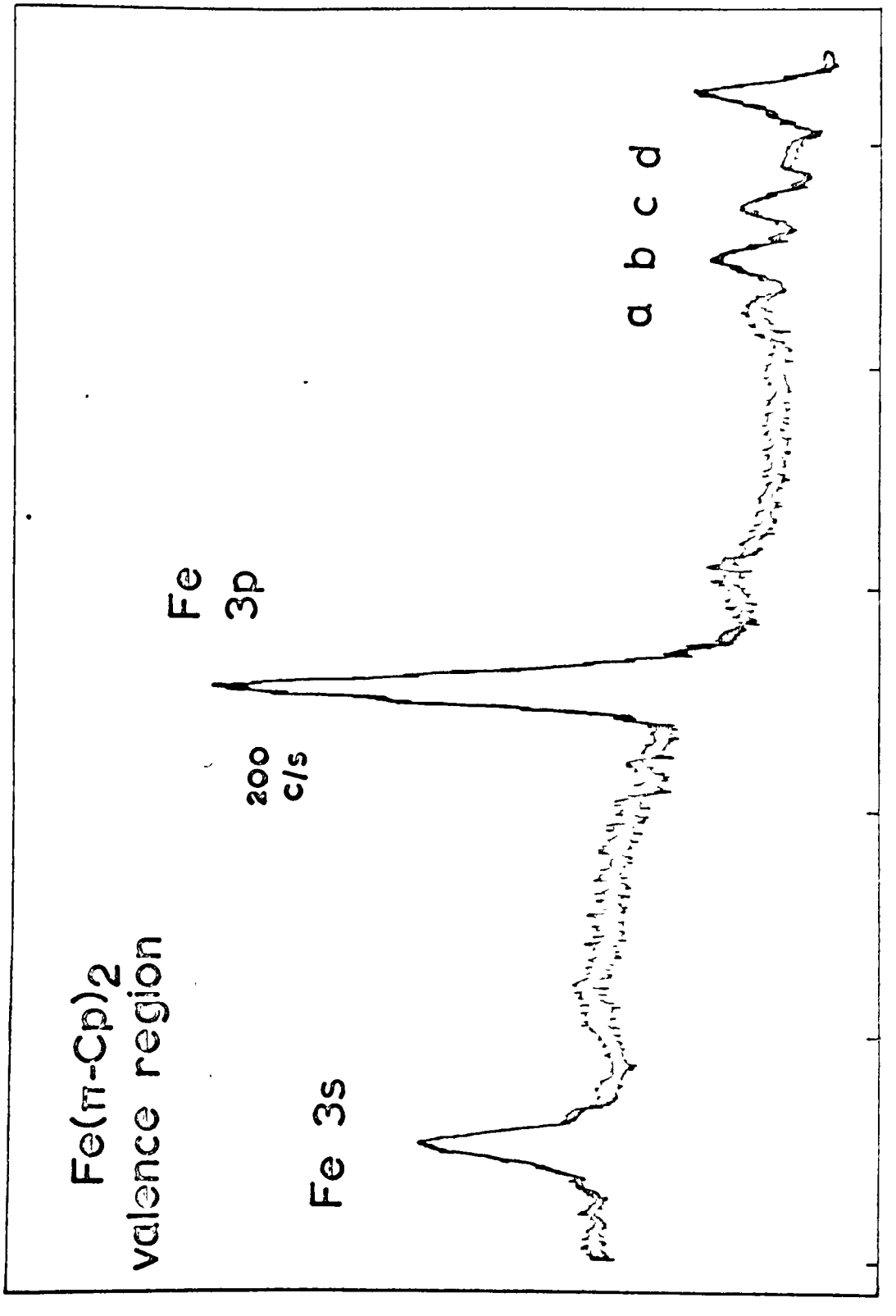
Fe(π-Cp)2
valence region
Fe 3s
200 c/s
Fe 3p
a b c d
1380
1400
1420
1440
1460
1480 K.E.

FIGURE 5.12b

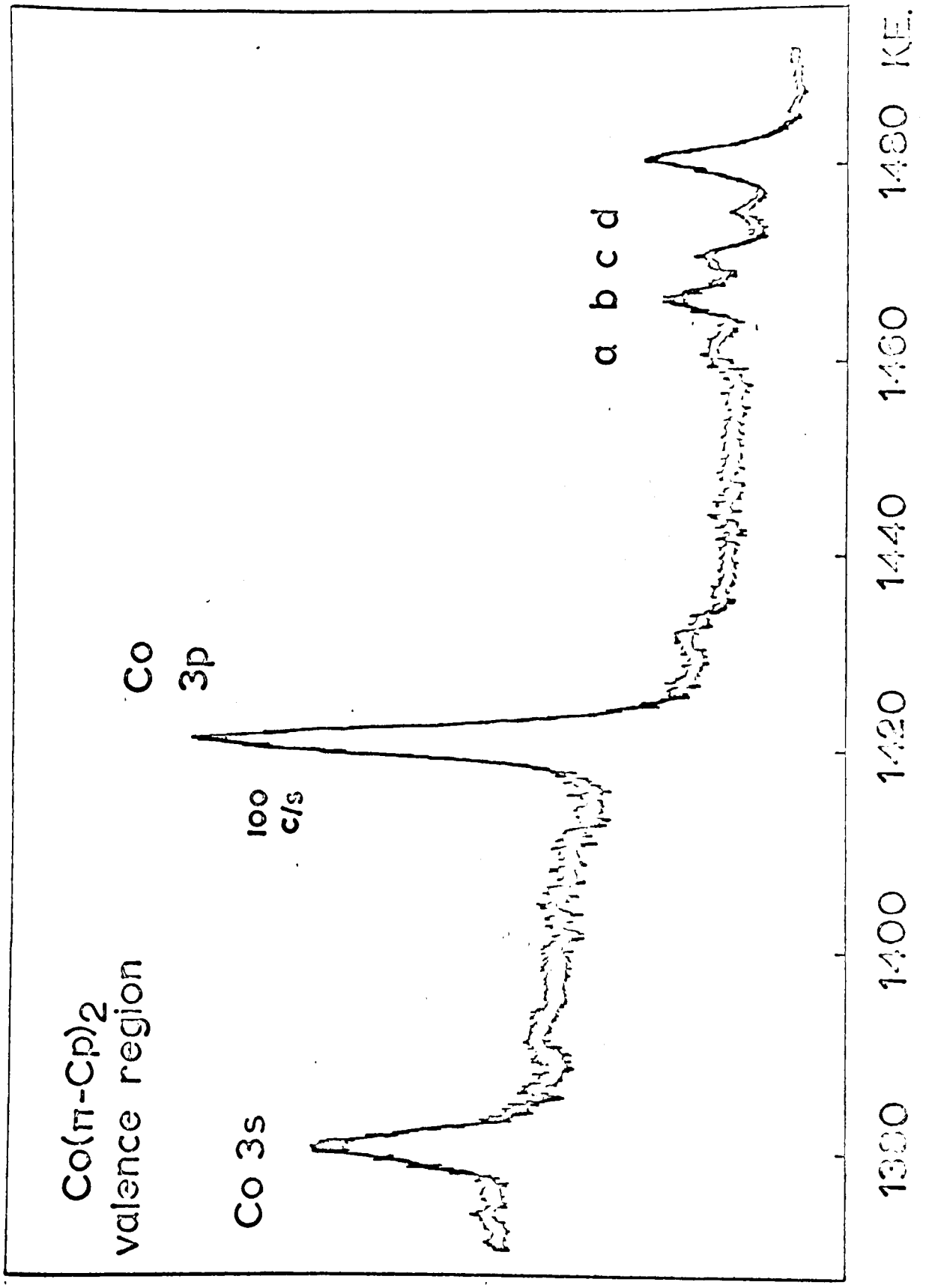
Co(π-Cp)2
valence region
Co 3s
100 c/s
Co 3p
a b c d
1380
1400
1420
1440
1460
1480 KE.

FIGURE 5.13a

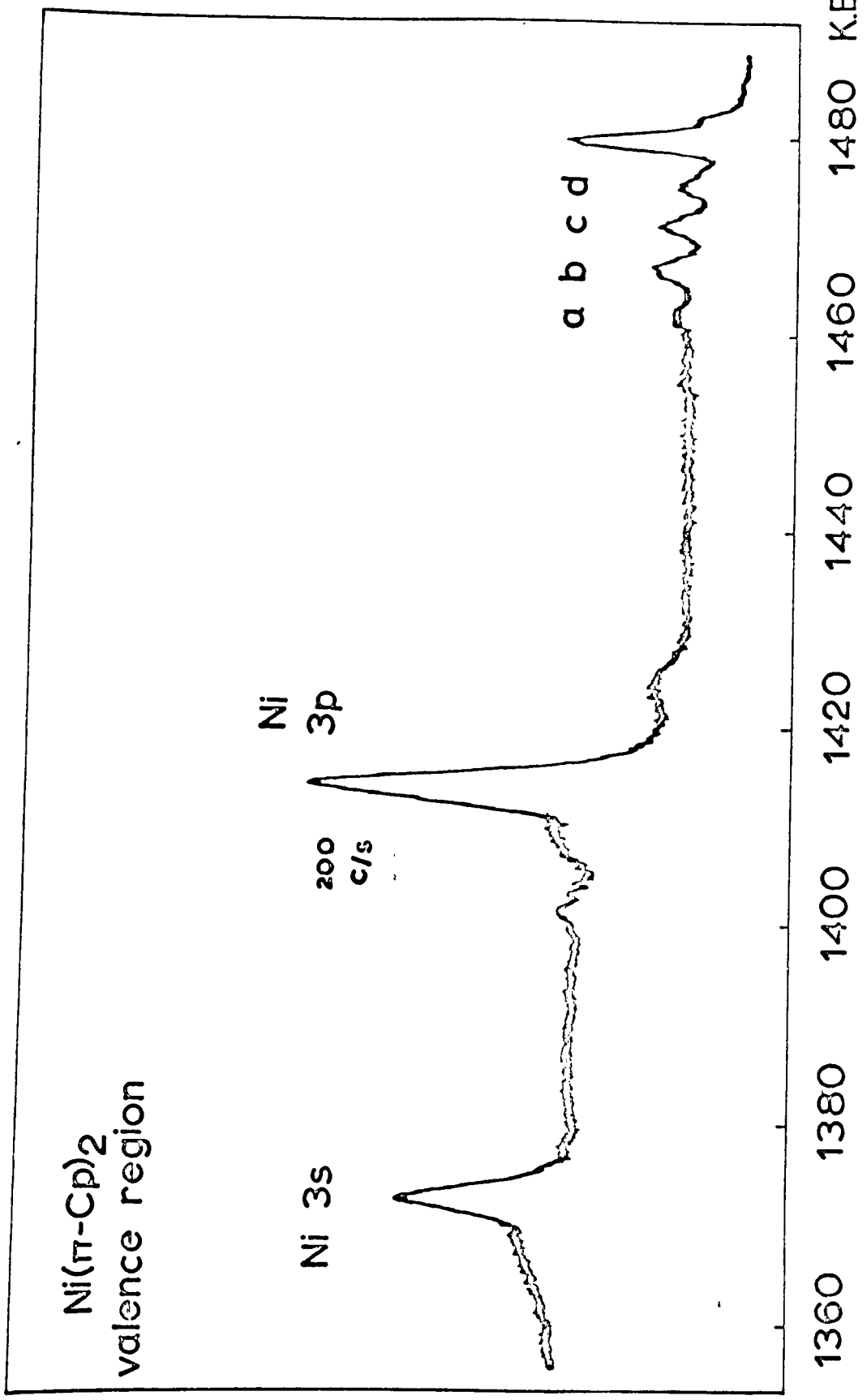
Ni(π-Cp)2
valence region
Ni 3s
200
c/s
Ni
3p
a b c d
1360
1380
1400
1420
1440
1460
1480
K.E.

FIGURE 5.14a

These extraordinary results have been confirmed by other research groups[72], with slightly less extreme values, and are clearly incomprehensible within the symmetry-restricted covalency model, since the $e_1^*(d)$ orbital is known to be that chiefly involved in the bonding, and hence most delocalised over the ligand, a result strongly supported by the ESCA shift data discussed below. Furthermore, the value derived for $K_{e_1 s}$ of 0.95 eV should lead to a clearly resolved splitting of ca. 3 eV in $Ni(\pi Cp)_2$; however, there is strong evidence, from the observed shake-up structure (see below) that $Mn(\pi Cp)_2$ is quite ionic compared to both $Cr(\pi Cp)_2$ and $Fe(\pi Cp)_2$, suggesting that within the central field effect, the apparent value of $K_{e_1 s}$ is enhanced. There still however remains the problem of the smallness of $K_{e_2 s}$ for which two explanations may be suggested

(i) some cooperative effect is operating so as to reduce the splitting in $V(\pi Cp)_2$ or, alternatively, increase that in $Cr(\pi Cp)_2$. Little seems to be known about the magnetism of condensed phases of the metallocenes, but it <u>is</u> certain that $Mn(\pi Cp)_2$ is an antiferromagnet in the solid state at room temperature. The fact that notwithstanding this, the observed splitting is quite consistent with a spin-free complex, suggests that such cooperative effects have little influence on the local

exchange integrals.

(ii) Radial expansion of both the $a_1(d\sigma)$ and $e_1(d\pi)$ orbitals on the metal is constrained by geometrical and overlap considerations, but, owing to the "sandwich" shape of these molecules, there is no such constraint on the $e_2(d\delta)$ orbital, which may differentially expand in such molecules, providing a large measure of the central-field covalency. If this is correct, then such sandwich molecules are indeed strange, and further evidence from UV and magnetic work will have to be sought.

In both cases, there is nothing to explain the apparent total absence of exchange splitting in $Ni(Cp)_2$. Measurements of the width of the Co 3s band of $Co(\pi Cp)_2$ (where no splitting is observed) and the Ni 3s band of $Ni(\pi Cp)_2$ showed that the latter was only ~ 0.4 eV broader. If 0.95 eV is an upper limit for $K_{e_1 s}$, a lower limit from this measurement would be 0.4 eV. However it should be remembered that $Ni(\pi Cp)_2$ is very covalent (even the LF nephelauxetic ratio is less than 0.6) and the 3s orbital at 100 eV binding energy is probably very small, leading to a much smaller exchange integral with the valence d-orbitals.

Satellite structure

It has been observed throughout a wide range of ESCA spectra that the main core binding peaks are always accompanied by smaller satellite peaks on the low BE side and frequently also on the high BE side.[8] The former type of satellite is easy to account for, since an examination of the energy distribution of the exciting Al K_α radiation shows the presence of low intensity, high energy components arising from the 2p $\longrightarrow$ 1s transition in multiply charged aluminium atoms. Thus, fig. 5.17 shows these satellites for the Hg 4f bands, and the so-called K_{α_3} and K_{α_4} satellites can clearly be seen.

However, the high BE satellites cannot be explained in this way, since their energies and relative intensities vary from band to band, and hence are apparently an inherent part of the ESCA spectrum of the compound concerned. Fig. 5.15b* shows these satellites for the C 1s band of $Ni(\pi Cp)_2$ and considerable structure can be seen at once in this spectrum. The first satellite spectrum to be exhaustively investigated was that of Ne 1s in the gas phase[8], where three types of transition can be distinguished:

(i) Discrete energy loss processes; an electron ionised from atom A is scattered inelastically by a different atom B, inducing a transition of the form 2p $\longrightarrow$ 3s in B and losing itself the corresponding energy. Such

*p. 186

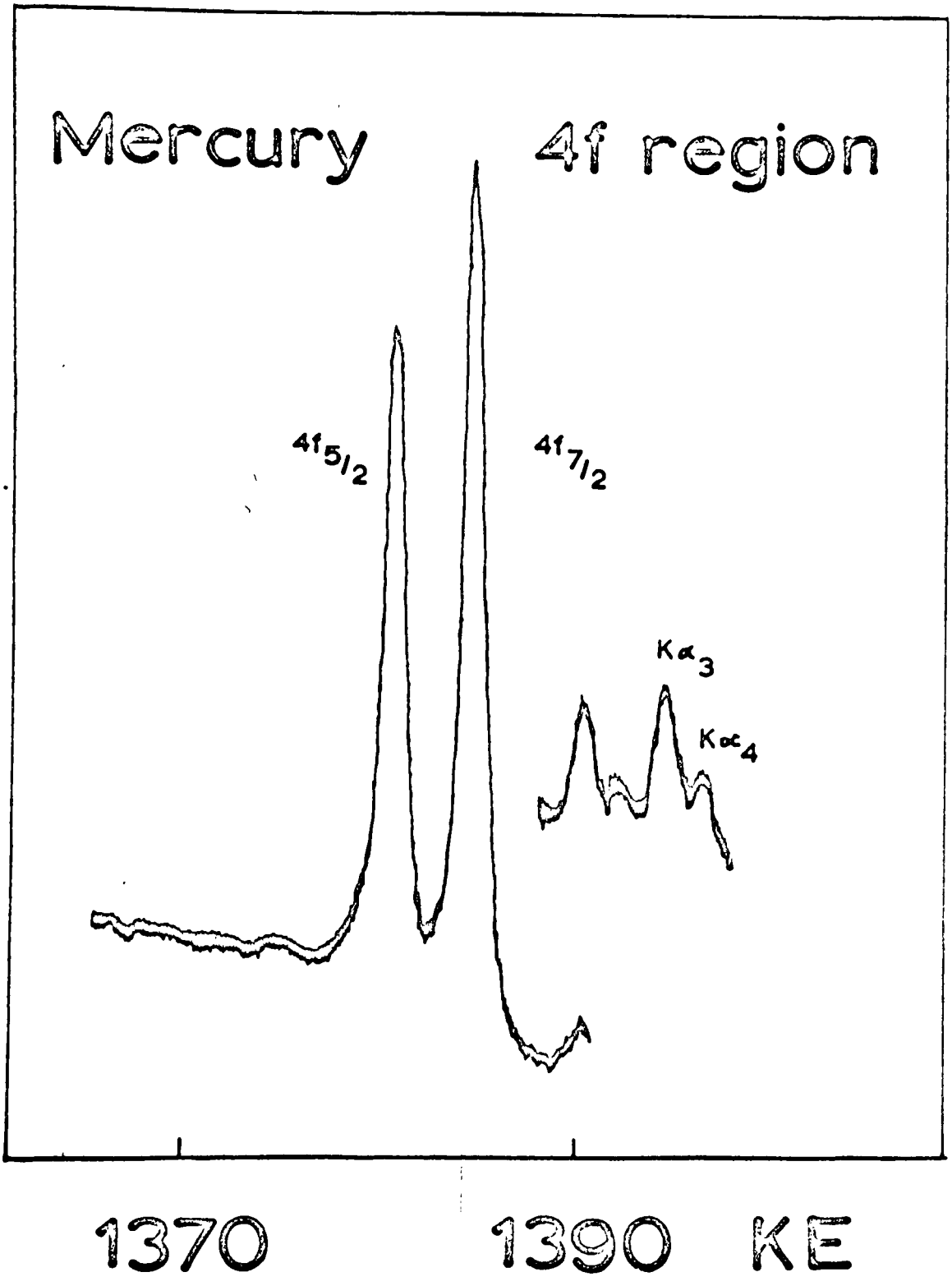

FIGURE 5.17

transitions are easily characterised in the gas phase by varying the pressure, but may be very difficult to distinguish in the solid state from types (ii) and (iii) below.

(ii) Shake-up processes; interaction of the atom with a photon may lead, with rather small probability, to a two electron process of the form

$$Ne(1s^2 2s^2 2p^6) + h\nu \longrightarrow Ne^+(1s2s^2 2p^5 3p) + \epsilon^-$$

where the energy of the electron is given by $h\nu - I_{1s} - E(2p \rightarrow 3p)$, and $E(2p \longrightarrow 3p)$ is the energy necessary to induce the $2p \longrightarrow 3p$ transition.

(iii) Shake-off processes; these clearly resemble type (ii) but involve the simultaneous ionisation of both the core electron and a valence electron as

$$Ne(1s^2 2s^2 2p^6) + h\nu \longrightarrow Ne^{2+}(1s2s^2 2p^5) + 2\epsilon^-$$

Both types (ii) and (iii) are pressure independent.

Investigation of such satellite bands in the solid-state is more complex since cooperative phenomena can also give rise to inelastic scattering. Thus, many core orbitals in metal phases show extensive satellite structure due to plasmon processes.[73] A positive hole created in an electron sea causes the rapid relaxation of the sea towards the hole. However, this relaxation tends to overrun the neutralisation point creating a sort of negative hole from which the sea is repelled.

In this way, a harmonic oscillation is set up in the electron gas, the associated waves being termed plasmons by analogy with the similar oscillatory behaviour observed in plasmas. Certain crystals can also set up rapidly moving exciton waves, especially on or near the surface, which, although probably of very short duration, may interact with outgoing electrons.

The only way to determine whether such cooperative effects are significant is to examine a sequence of iso-structural compounds; if only one or two exhibit extensive satellite structure, then the most probable origin of this is intra- rather than inter-molecular. In the latter case it becomes of some importance to find a suitable mechanism whereby such two-electron processes can occur, which, in turn, raises the question of how rapidly electron relaxation actually occurs in core ionisation. No clear-cut answer to this question can be given at present and, for this reason, the theoretical analysis below is unavoidably speculative. Elementary considerations[74] suggest that valence electrons will relax much more rapidly than core orbitals however, and Snyder,[75] and later Bagus and Schaefer[76] suggested that the best description of core ionisation would be to generate, at least over the time scale of the ionisation process, a localised core hole. In other words, the very concept of a Koopmans' ionisation from a molecular orbital cannot be applied to core ionisations, since

the localised orbital will not, unless the atom is unique, be a symmetry adapted eigenfunction of the total molecular Hamiltonian. This implies that core ionisation will in general destroy the symmetry of the molecule, permitting mixing between otherwise orthogonal occupied and unoccupied valence orbitals.

Taking this as a reasonable physical basis, three possible mechanisms can be formulated, all of which may be important in any given core ionisation. They are the "sudden approximation", internal scattering and various CI (configuration-interaction) mechanisms.

(i) The sudden approximation.[77]

Consider a wave-function $\Psi_0(x_1 \ldots x_n)$ and suppose that the N^{th} electron is suddenly removed as a photo-electron. Then, as the photoelectron recedes, the wave-function alters in such a way as to take on the form of an eigenstate of $N-1$ electrons. If this is denoted by $\phi_n(x_1 \ldots x_{N-1})$ we may expand the wave-function as

$$\Psi_0(x_1 \cdots x_{N-1}, x) = \sum_n \int a_n(\underset{\sim}{k}') \upsilon(\underset{\sim}{k}', x) \phi_n(x_1 \ldots x_{N-1}) \, d\underset{\sim}{k}'$$

where x is the coordinate of the photoelectron, $\upsilon(\underset{\sim}{k}', x)$ its wave-function and $a_n(\underset{\sim}{k}')$ the coefficient of the expansion into the complete set of functions $\upsilon\phi_n$.

If we put

$$\tilde{\Psi}_0 = \int \upsilon^*(k, x) \Psi_0(x_1 \cdots x_{N-1}, x) \, dx$$

and assume that ν is suitably normalised, then

$$|a_n|^2 = P_n(k) = |\langle \tilde{\Psi}_0 | \phi_n \rangle|^2$$

Normally, the approximation is made that

$$\Psi_0(x_1 \ldots x_N) = \sqrt{\frac{1}{N}} \sum_{i=1}^{N} (-)^i u_\lambda(x_i) \chi(x_1 \ldots x_{i-1}, x_{i+1} \ldots x_N)$$

where χ is some suitable function. Then

$$\tilde{\Psi}_0 = \chi \langle \nu | u_\lambda \rangle$$

and

$$P_n(k) = |\langle \chi | \phi_n \rangle|^2 |\langle \nu | u_\lambda \rangle|^2$$

Clearly, there will be one term, ϕ_0, in the expansion which is very close in form to χ; this is the ground-state term, and for this $P_0(k)$ will be close to unity. The probability of any shake-up occurring is then $1 - P_0(k)$, and the remaining ϕ_n may contain one or more valence electrons excited into previously unoccupied orbitals. The theory suffers from some disadvantages however, the major one being the physical difficulty experienced in understanding the time-ordering of the problem. Clearly, the approach will work best if $|\underset{\sim}{k}|$ is large, when the selection rules will be those for monopole transitions. However, if we ionise a core-electron from one of a set of equivalent atoms, then such monopole selection rules do not apply, and we can obtain

formally forbidden transitions, as Hillier et al. have pointed out. Perhaps because of ease in computation, the sudden approximation has been extensively investigated, and, as a result, is no longer regarded (save for individual atoms) as more than indicative.[45] Quantitative agreement has not been very satisfactory in the study of molecules both in the prediction of the positions of shake-up bands, and in the calculation of their relative intensities.

(ii) Internal scattering.

An electron ionised from a core orbital will travel outwards from the centre of the atom, and, on its way out, may interact inelastically with the valence cloud of electrons, losing itself a quantum of energy. According to the first Born approximation,[71] the probability that the outgoing electron can induce a transition from state $|m\rangle$ to state $|n\rangle$ is given by

$$I_{mn} \propto k_{mn}/k \left| \iint V(r, R) \exp\left\{ i(k_{mn} r_1 - k n_0) \cdot R \right\} \psi_n^*(r) \phi_m(r) \, dr \, dR \right|^2$$

where V(r, R) is the interaction potential $e^2/|r - R|$, k is the initial momentum of the electron in direction n_o and k_{mn} the final momentum, having induced a transition $m \rightarrow n$. Since we have assumed a plane-wave form for the photoelectron, which is grossly approximate, the energy

conservation law tells us that

$$\frac{\hbar^2 k^2}{2m} = \frac{\hbar^2 k_{mn}^2}{2m} + (E_n - E_m)$$

However, for X-ray photoelectron scattering, we have, in general, $|E_n - E_m| \ll k, k_{mn}$, so approximately

$$k - k_{mn} = \frac{m(E_n - E_m)}{\hbar^2 k} = \frac{\alpha}{k} \qquad \text{(say)}$$

and if the scattering angle is very small

$$I_{mn} \propto \frac{k_{mn}}{k} \left| \iint \frac{e^2}{|\underset{\sim}{r} - \underset{\sim}{\rho}|} \exp\left(\frac{-i\alpha \underset{\sim}{R}\cdot\underset{\sim}{n}}{k}\right) \phi_n^*(\underset{\sim}{r})\,\phi_m(\underset{\sim}{r})\, d\underset{\sim}{r}\, d\underset{\sim}{\rho} \right|^2$$

$$\propto \frac{k^2 k_{mn}}{\alpha^2} \left| \int \exp\left(\frac{-i\alpha \underset{\sim}{r}\cdot\underset{\sim}{n}}{k}\right) \phi_n^*(\underset{\sim}{r})\,\phi_m(\underset{\sim}{r})\, d\underset{\sim}{r} \right|^2$$

If we now expand the exponential in a multipole series, we obtain

$$I_{mn} \propto \frac{k^2 k_{mn}}{\alpha^2} \left| \langle n|m\rangle - \frac{i\alpha}{k} \langle n| \underset{\sim}{r}\cdot\underset{\sim}{n} |m\rangle + \cdots \right|^2$$

$$\propto \frac{k^2 k_{mn}}{\alpha^2} \left[|\langle n|m\rangle|^2 + \frac{\alpha^2}{k^2} |\langle n| \underset{\sim}{r}\cdot\underset{\sim}{n} |m\rangle|^2 + \cdots \right]$$

and the first term can be seen to be related to the first term of the sudden approximation, and the second term is a dipole contribution to the scattering. Clearly, the derivation is inadequate since, from the discussion of time dependency above, ϕ_n and ϕ_m are strongly varying functions of the time. It might be justified to expand ϕ_m in terms of the initial wave functions and ϕ_n in terms of eigenfunctions of the ion state, leading to a very general formulation of satellite problem intermediate between that of the sudden approximation, and the CI mechanisms discussed below. However, one very important consequence of the scattering formula should be noted; namely, even if relaxation is very small, so that the integral $\langle \phi_n | \phi_m \rangle$ vanishes by orthogonality, shake-up may still occur by a dipole mechanism, which may be equally important in magnitude as the normal shake-up mechanism, since, within the CGS system of units, $\alpha/k \approx 10^7$ and the integral will be non-zero over a few angstroms, having the value $\sim 10^{-8}$.

(iii) Multiple CI mechanisms.

The wave-function for the ground state will not, in general, be adequately represented by a single Slater determinant, but should be written as a sum of such determinants

$$\underline{\Psi} = \underline{\Psi}_0 + \Sigma_i c_{i0} \underline{\Psi}_{i0}$$

where $\underline{\Psi}_0$ is the uncorrelated wave-function. Consider ionisation of a core orbital c, leading to a wave-function $\underline{\Psi}^+$, which again may be written as a linear combination of the stationary states of the ionised system

$$\underline{\Psi}^+ = \underline{\Psi}^+_{0s} + \Sigma_i c_{is0} \underline{\Psi}^+_{is0}$$

The dipole induced transition probability between these two states is given by the usual dipole matrix element. However the discrete state $\underline{\Psi}^+_{is}$ is given by a similar expansion

$$\underline{\Psi}^+_{is} = \underline{\Psi}^+_{is0} - c_{is0}\underline{\Psi}^+_{0s} + \sum_{j\neq 0,i} c^j_{is}\underline{\Psi}^+_{js0}$$

where we have ensured that $\underline{\Psi}^+_{is}$ is orthogonal to the ground state. Then,

$$|\langle \underline{\Psi}_0 | \hat{\mu} | \underline{\Psi}^+_{is}, v_k \rangle = \left(\langle \underline{\Psi}_0 | \underline{\Psi}^+_{is0} \rangle - c_{is0} \langle \underline{\Psi}^+_0 | \underline{\Psi}^+_{0s} \rangle \right) \langle c | \hat{\mu} | v_k \rangle$$

which compares to the sudden approximation value of $|a_i|^2 |\langle c | \hat{\mu} | v_k \rangle|^2$ assuming that $\underline{\Psi}^+_{0s}$ has unit overlap and $\underline{\Psi}^+_{is0}$ zero overlap with $\underline{\Psi}^+_0$. If this is not so, we obtain

$$\langle \underline{\nu}_0 | \hat{\mu} | \underline{\nu}_{is}^{+}, \nu_k \rangle = \left(\langle \underline{\nu}_0^{+} | \underline{\nu}_{is}^{+} \rangle - c_{is0} \langle \underline{\nu}_0^{+} | \underline{\nu}_{\alpha s}^{+} \rangle \right) \langle c | \hat{\mu} | \nu_k \rangle$$

$$\left| \langle \underline{\nu}_0 | \hat{\mu} | \underline{\nu}_{is}^{+}, \nu_k \rangle \right|^2 = \Big\{ \left| \langle \underline{\nu}_0^{+} | \underline{\nu}_{is}^{+} \rangle \right|^2 + \left| c_{is0} \right|^2 \langle \underline{\nu}_0^{+} | \underline{\nu}_{\alpha s}^{+} \rangle |^2$$

$$- c_{is0} \langle \underline{\nu}_0^{+} | \underline{\nu}_{\alpha}^{-} \rangle \langle \underline{\nu}_{is0}^{+} | \underline{\nu}_0^{+} \rangle$$

$$- c_{is0}^{*} \langle \underline{\nu}_{\alpha s}^{+} | \underline{\nu}_{\alpha}^{-} \rangle \langle \underline{\nu}_0^{+} | \underline{\nu}_{is0}^{+} \rangle \Big\} \times$$

$$\times \left| \langle c | \mu | \nu_k \rangle \right|^2$$

where, the sudden approximation term is seen as the first term of the series. In other words, at this higher level of approximation, the configuration interaction theory automatically contains the quantity a_n discussed above.

Certain symmetry arguments are apparent from the above discussion. Firstly, it is clear that $|\underline{\nu}_0^{+}\rangle$ and $|\underline{\nu}_{is0}^{+}\rangle$ must have the same symmetry for the leading term of the sudden approximation not to vanish identically. This leads to the somewhat unfortunately named monopole selection rules[8] of Siegbahn et al., derived originally for the limiting case of very weak orbital coupling between core and valence levels. Thus, in the case of neon, where coupling is unimportant,

removal of the 1s orbital to generate σ^{+} gives a ^2S state, and, monopole selection rules demand that all states attained by shake-up, will also be ^2S, arising from excitation of the 2p orbital into an np orbital. Should any state such as $1s2s^22p^53s$ (^2P) arise, this must be treated, within the sudden approximation, as 2p ionisation, followed by shake-up of the 1s electron. That this particular picture is not especially physically likely goes without saying, and such states are perhaps better considered as arising from a dipole scattering picture or possibly, as we shall see below, a ground state CI mechanism.

If, however, an orbital not of s symmetry is ionised, the shake-up structure obtained will depend strongly on the magnitude of orbital interaction between core and valence shells. In the limit of zero interaction, valence monopole selection rules will be obeyed, but, if interaction becomes significant, a more general type of possibility can arise. Consider the gas, Argon. Ionisation of the 2p orbitals can generate $^2P_{3/2}$ and $^2P_{\frac{1}{2}}$ states, whose wave functions take the form

$$\chi_{\frac{3}{2}} = \left|\tfrac{3}{2},\tfrac{3}{2}\right\rangle = \left|p_{+1}^2 p_0^2 p_{-1}^{+}\right\rangle$$

$$\chi_{\frac{1}{2}} = \left|\tfrac{1}{2},\tfrac{1}{2}\right\rangle = \sqrt{\tfrac{2}{3}}\left|p_{+1}^2 p_0^{+} p_{-1}^2\right\rangle + \sqrt{\tfrac{1}{3}}\left|p_{+1}^2 p_0^2 p_{-1}^{-}\right\rangle$$

Consider now shake-up arising from valence-region transitions. We saw that, for ionisation of an s orbital, shake-up arising from p $\rightarrow$ p transitions could occur, giving $|p^5, np\rangle$ $^{1,3}S$ which coupled with the ^2S hole state to produce two ^2S states. For ionisation of a core p-orbital, the p $\rightarrow$ p transition can generate $^{1,3}S$, P and D, all of which can couple to the ^2P hole, generating, in all, six ^2P states. These correspond to the true "monopole" processes p $\rightarrow$ np, but consider the p $\rightarrow$ s transition, generating $^{1,3}P$. This also, on coupling to the ^2P hole, can generate two ^2P states, the overall transition obeying monopole type selection rules, though it would appear, at first sight, to be induced by a dipolar mechanism. It is important to note that we have implicitly assumed strong spin-coupling throughout this section.

Within the sudden approximation, the extent of this orbital angular momentum coupling effect can be seen fairly easily if we partition the valence excitation into the monopole allowed transitions for the valence shell and those only allowed by coupling with the core shell. In the former case we obtain, for argon, only those p $\rightarrow$ p transitions which are $^1S \rightarrow ^{1,3}S$. This can be seen from the form of the wave-functions for $^{1,3}D$, P and S

$$^3D(2) = |p_{+1}^2 p_0^2 p_{-1}^+ \cdot p_{+1}^+\rangle$$

$$^3P(1) = \left(|p^2_{+1} p^+_0 p^2_{-1} \cdot p^+_{+1}\rangle + |p^2_{+1} p^2_0 p^+_{-1} \cdot p^+_0\rangle \right)/\sqrt{2}$$

$$^3S(0) = \left(|p^+_{+1} p^2_0 p^2_{-1} \cdot p^+_{-1}\rangle + |p^2_{+1} p^+_0 p^2_{-1} \cdot p^+_0\rangle + |p^2_{+1} p^2_0 p^+_{-1} \cdot p^+_{+1}\rangle \right)/\sqrt{3}$$

If these are coupled with core orbitals, and interacted with $\frac{1}{r_{12}}$, only in the case of the ^2S state do we not need to permute core and valence orbitals to obtain a non-zero overlap. In other words, to obtain shake-up to $^{1,3}S$ states derived from the $p \rightarrow p$ excitation, the sudden approximation coefficients are derived from integrals of the form

$$\langle \bar{p}_{+1}(\omega e) \cdot p^+_{+1} \bar{p}_{+1} \mid \bar{p}'_{+1}(\omega e) \cdot p'^+_{+1} \cdot \bar{p}'_{+1} \rangle \qquad (A)$$

where the primes refer to stationary orbitals in the ion state. For the other states nominally accessible by sudden approximation excitation, integrals of the form

$$\langle \bar{p}_{+1}(\omega e) \cdot p^+_{+1} \bar{p}_{+1} \mid \bar{p}'_{+1} \cdot p'^+_{+1}(\omega e) \cdot \bar{p}'_{+1} \rangle \qquad (B)$$

must be evaluated. As these are dependent on overlap between core and valence orbitals, they are presumably substantially smaller numerically than those of type (A). Thus, although such states as ^2P(p(core); $^{1,3}D$(valence)) are accessible, the sudden approximation suggests that they will not be realised

with any significant probability as a general rule. Within a CI framework, the conclusion would be that correlation involving excitation of core orbitals is substantially less important than that involving valence orbitals, a conclusion borne out by calculation.

Thus, save in highly exceptional cases, the monopole selection rules should apply to the valence shell <u>in isolation</u> and it is in this form that it will be used.

A shake-up mechanism which may prove important in a limited number of cases is that through ground-state CI. If this is significant, the ground-state will be written

$$\underline{\Psi} = \underline{\Psi}_0 + \Sigma_i c_{is} \underline{\Psi}_{is}$$

Consider ionisation to a state $\underline{\Psi}^+_{iso}$ from orbital c

$$\langle \underline{\Psi} \| \underline{\Psi}^+_{iso}, \nu_k \rangle = \langle \underline{\Psi}^+_0 + \Sigma_i c_{is} \underline{\Psi}^+_{is} \,|\, \underline{\Psi}^+_{iso} \rangle \langle c | \hat{\mu} | \nu_k \rangle$$

and the probability is

$$\langle \underline{\Psi}^+_0 + \Sigma_i c_{is} \underline{\Psi}^+_{is} \,|\, \underline{\Psi}^+_{iso} \rangle|^2 \approx |\langle \underline{\Psi}^+_0 | \underline{\Psi}^+_{iso} \rangle + c_{is} \langle \underline{\Psi}^+_{is} | \underline{\Psi}^+_{iso} \rangle|^2$$

$$= |\langle \underline{\Psi}_0 | \underline{\Psi}^+_{iso} \rangle|^2 + |c_{is}|\langle \underline{\Psi}^+_{is} | \underline{\Psi}^+_{iso} \rangle|^2$$

$$+ c_{is} \langle \underline{\Psi}^+_{is} | \underline{\Psi}^+_{iso} \rangle \langle \underline{\Psi}^+_{iso} | \underline{\Psi}^+_0 \rangle$$

$$+ c^*_{is} \langle \underline{\Psi}^+_{iso} | \underline{\Psi}^+_{is} \rangle \langle \underline{\Psi}^+_0 | \underline{\Psi}^+_{iso} \rangle$$

If now, relaxation is unimportant, $\langle \Psi_0^+ | \Psi_{iso}^+ \rangle \approx 0$ and the probability of ionisation is

$$|\langle \Psi_{is}^+ | \Psi_{iso}^+ \rangle|^2 |c_{is}|^2 \approx |c_{is}|^2$$

One point must be made about this formalism; it is that only under very particular conditions can it be of paramount importance. In closed-shell molecules, Brillouin's theorem[80] will operate and the mechanism can, for core ionisations, only give doubly excited shake-up structure; secondly, for core ionisation, unless the molecule has undergone relaxation, the integrals will vanish in any case, since, under these circumstances, the ion state attained will be $\Psi_{is}^+ = \Psi_{iso}^+ - c_{is}\Psi_0^+$ and

$$\langle \Psi_0^+ + c_{is}\Psi_{is}^+ | \Psi_{iso}^+ - c_{is}\Psi_{so}^+ \rangle = \langle \Psi_0^+ | \Psi_{iso}^+ \rangle - c_{is}\langle \Psi_0^+ | \Psi_{so}^+ \rangle + c_{is}^*\langle \Psi_{is}^+ | \Psi_{iso}^+ \rangle - |c_{is}|^2 \langle \Psi_{is}^+ | \Psi_{so}^+ \rangle$$

and since relaxation has not occurred, this integral vanishes. Thus, the mechanism is only likely to be significant, in closed-shell species, if ionisation actually occurs from an orbital involved in the CI, and will hence be of primary importance in valence region ionisation.

An interesting test case is provided by the UV-PE spectrum

of mercury vapour, illustrated in fig. 5.18. The ground state is $5d^{10}6s^2$, and strong mixing under CI with the ^1S state derived from $5d^{10}6p^2$ can be expected, giving a ground state wave function of the form

$$\Psi_0 = [d^{10}]s^2 + c_p[d^{10}]p^2$$

Now, photoionisation may yield the states $5d^{10}6s;^2S_{\frac{1}{2}}$ and $5d^96s^2;^2D_{\frac{3}{2}},^2D_{\frac{5}{2}}$ directly, but, as the spectrum shows, there are two further bands, not attributable to additional lines in the helium lamp, or to any obvious impurities, which are found at energies corresponding exactly to the $5d^{10}6p;^2P_{\frac{1}{2}},^2P_{\frac{3}{2}}$ states of Hg^+ as given by Moore. It is difficult to explain this easily by CI in the ion state, since the $^2P_{\frac{1}{2},\frac{3}{2}}$ terms cannot mix directly with the $[d^{10}]s\ ^2S_{\frac{1}{2}}$ ground state of Hg^+, and would therefore be expected to have only extremely small coefficients, and so we postulate a mechanism of the form above, the relevant matrix element being

$$\langle \Psi_0 | \hat{r} | [d^{10}]6p, \nu_k \rangle = c_p \langle [d^{10}]6p | [d^{10}]6p \rangle \langle p | \hat{\mu} | \nu_k \rangle$$

Note the difference in form of this integral from the usual CI matrix element, in that the dipole part does not involve the orbital (ionised) from which we have reckoned the shake-up. An oddity about this mechanism is that the intensity ratio for the two satellite peaks, which should be as the

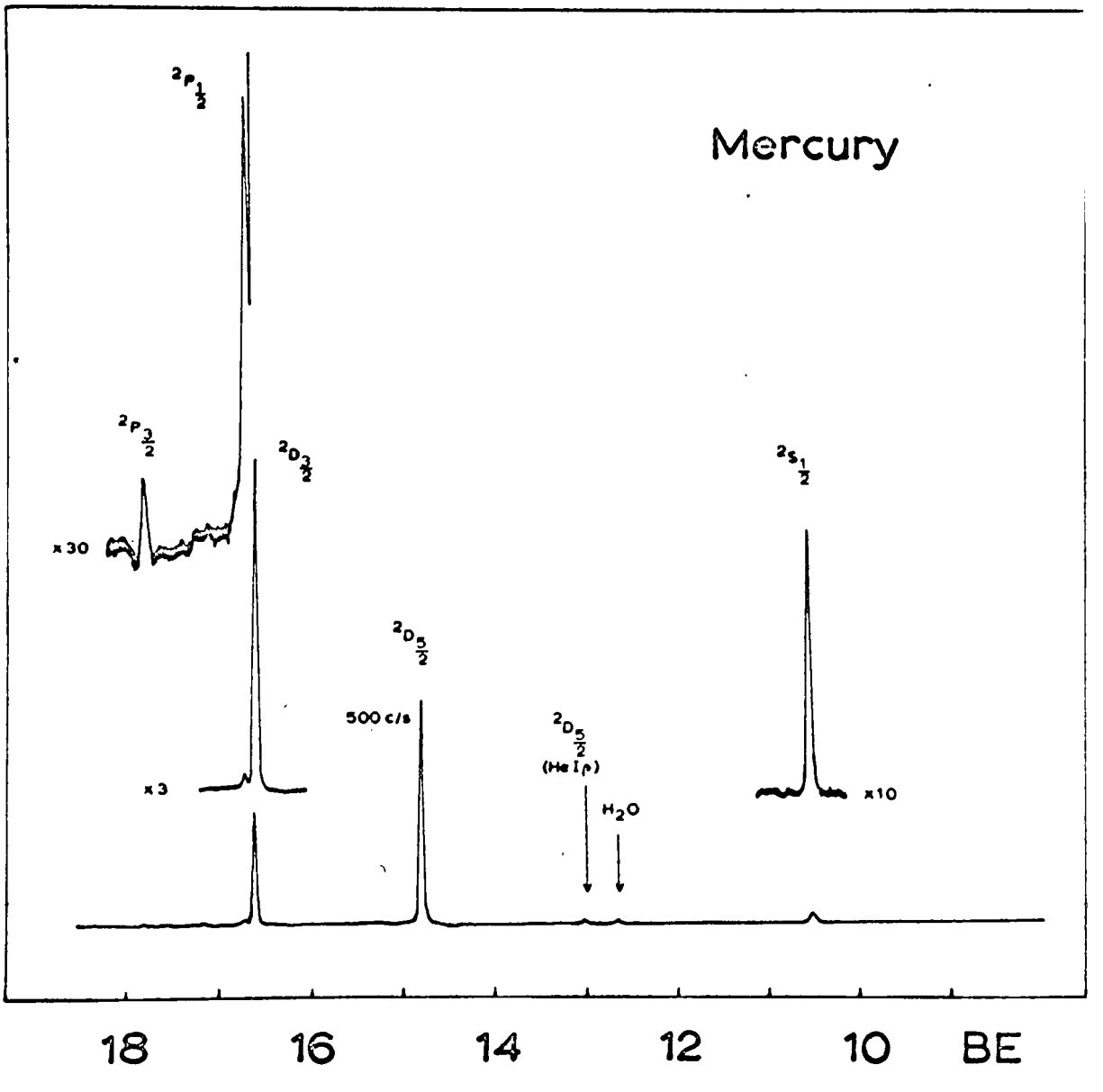
Mercury
$^2P_{\frac{1}{2}}$
$^2P_{\frac{3}{2}}$
$^2D_{\frac{3}{2}}$
$^2D_{\frac{5}{2}}$
$^2D_{\frac{5}{2}}$ (He I ρ)
$^2S_{\frac{1}{2}}$
H2O
x30
x3
500 c/s
x10
18
16
14
12
10
BE

FIGURE 5.18

j -degeneracies, is experimentally inverted. However, although no interaction is possible in first order between the $^2P_{\frac{1}{2}}$ and $^2D_{\frac{1}{2}}$ states, their extraordinary proximity in energy, coupled even by weak, second-order interactions arising from the electromagnetic field, may enable some intensity borrowing to occur, giving the $^2P_{\frac{1}{2}}$ state an anomalously high intensity.

Satellite structure in the metallocenes

Satellite structure on both the metal 2p and carbon 1s peaks can be seen in the metallocenes, the former being found only for Mn, Ni and, weakly for $Co(\pi Cp)_2$, though C 1s shake-up is observed for all the compounds examined. The essential qualitative difference between the two types of atoms is that asymmetrical relaxation may occur around the carbon atom 1s hole, as this probably behaves as if it were localised.[75,76] The result is to substantially lower the molecular symmetry permitting, even within the sudden approximation, shake-up to states not having the symmetry of the ground state. For ionisation from the metal orbitals however, the number of possible transitions is severely limited within the sudden approximation since the molecular symmetry is retained. In an isostructural set of molecules we can assume that symmetry restrictions on shake-up intensities will remain constant across the series so that we can make meaningful comparisons between the different members.

The details of the satellite behaviour are given in table 5.5.

TABLE 5.5

COMPOUND	CARBON 1s	METAL 2p	METAL 3p	CONFIGURATION
$Mg(\pi Cp)_2$	8eV	-	-	π^{12}
$V(\pi Cp)_2$	7.4eV, ~11.5eV	(?~8eV)	5.0eV (~10eV?)	$\pi^{12} a_{1g}^2 e_{2g}^2$
$Cr(\pi Cp)_2$	7.2eV	-	4.7eV	$\pi^{12} a_{1g}^2 e_{2g}^3$
$Mn(\pi Cp)_2$	6.4-7.0 eV (?~11.7eV)	4.6-6.1eV	ABSORPTIONS, br.	$\pi^{12} a_{1g}^2 e_{2g}^2 e_{1g}^{*2}$
$Fe(\pi Cp)_2$	6.5eV, 10.5eV	(?~8eV)	-	$\pi^{12} a_{1g}^2 e_{2g}^4$
$Co(\pi Cp)_2$	4.5eV, 6.3-11.0eV)	~15.0eV	-	$\pi^{12} a_{1g}^2 e_{2g}^4 e_{1g}^{*}$
$Ni(\pi Cp)_2$	3.7eV, 7.9eV, 11.0eV	4.7-6.5eV	5.8eV, ?~13.0eV	$\pi^{12} a_{1g}^2 e_{2g}^4 e_{1g}^{*2}$

The following points may be noted:

(i) The metal 2p peaks exhibit shake-up only when the anti-bonding d-orbital, e_{1g}^* is occupied. This suggests that the induced transition is $e_{1g}^* \rightarrow \phi$, where ϕ is some excited orbital, presumably $\pi^*(e_{2u} + e_{2g})$, or else, if the transition is ligand localised, that the e_{1g}^* orbital is strongly delocalised over the ligand. A third possibility is that the M 2p ionisation is shaking up a d-d transition, though it is difficult to see why this does not occur for the cases when e_{1g}^* is unoccupied. If the process is $e_{1g}^* \rightarrow \pi^*$, then all such transitions within the sudden approximation are forbidden. The mechanism could be excited state CI however, or some form of scattering or possibly a discrete-energy loss process caused by inelastic scattering in the solid state (the

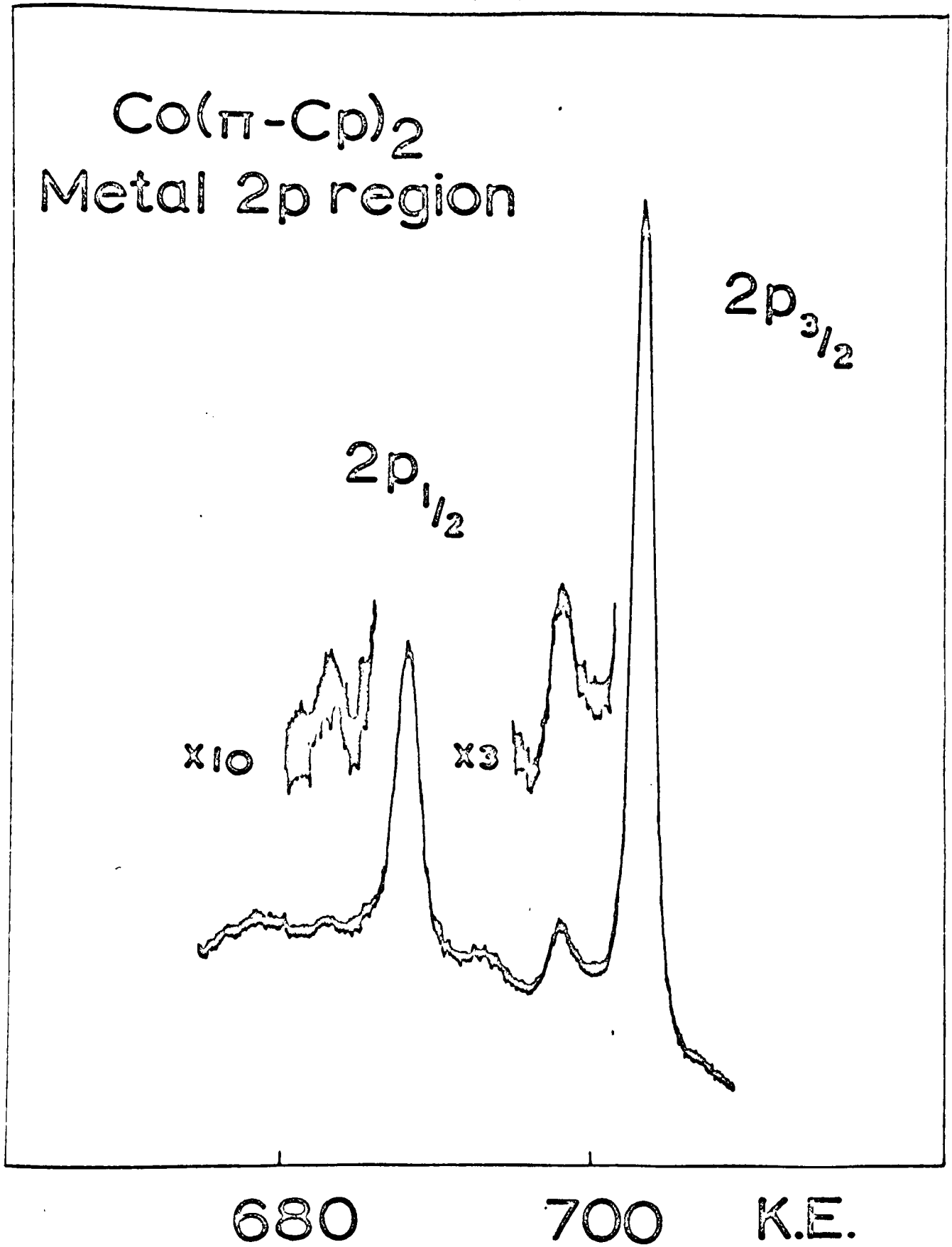

FIGURE 5.13b

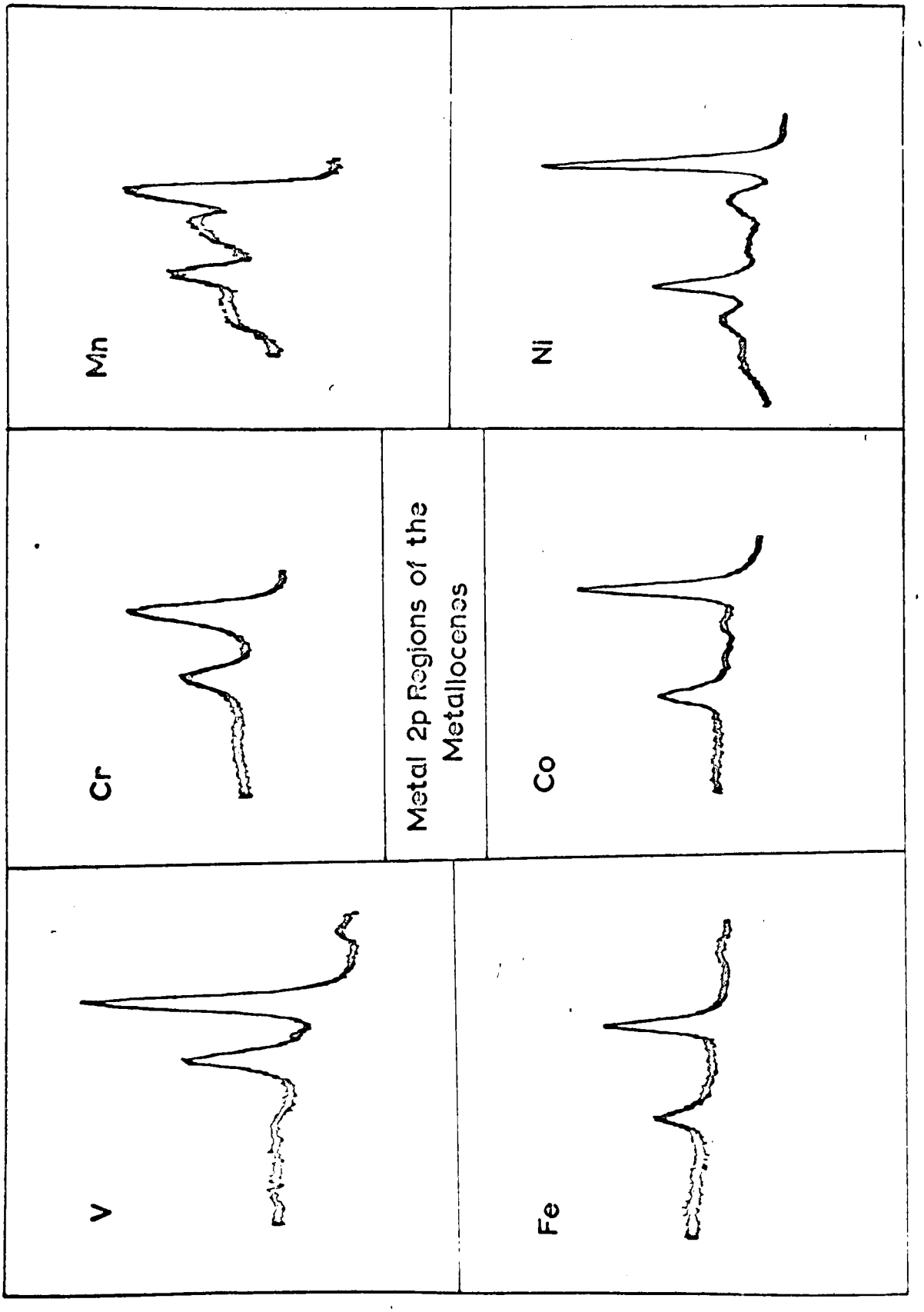

FIGURE 5.15a

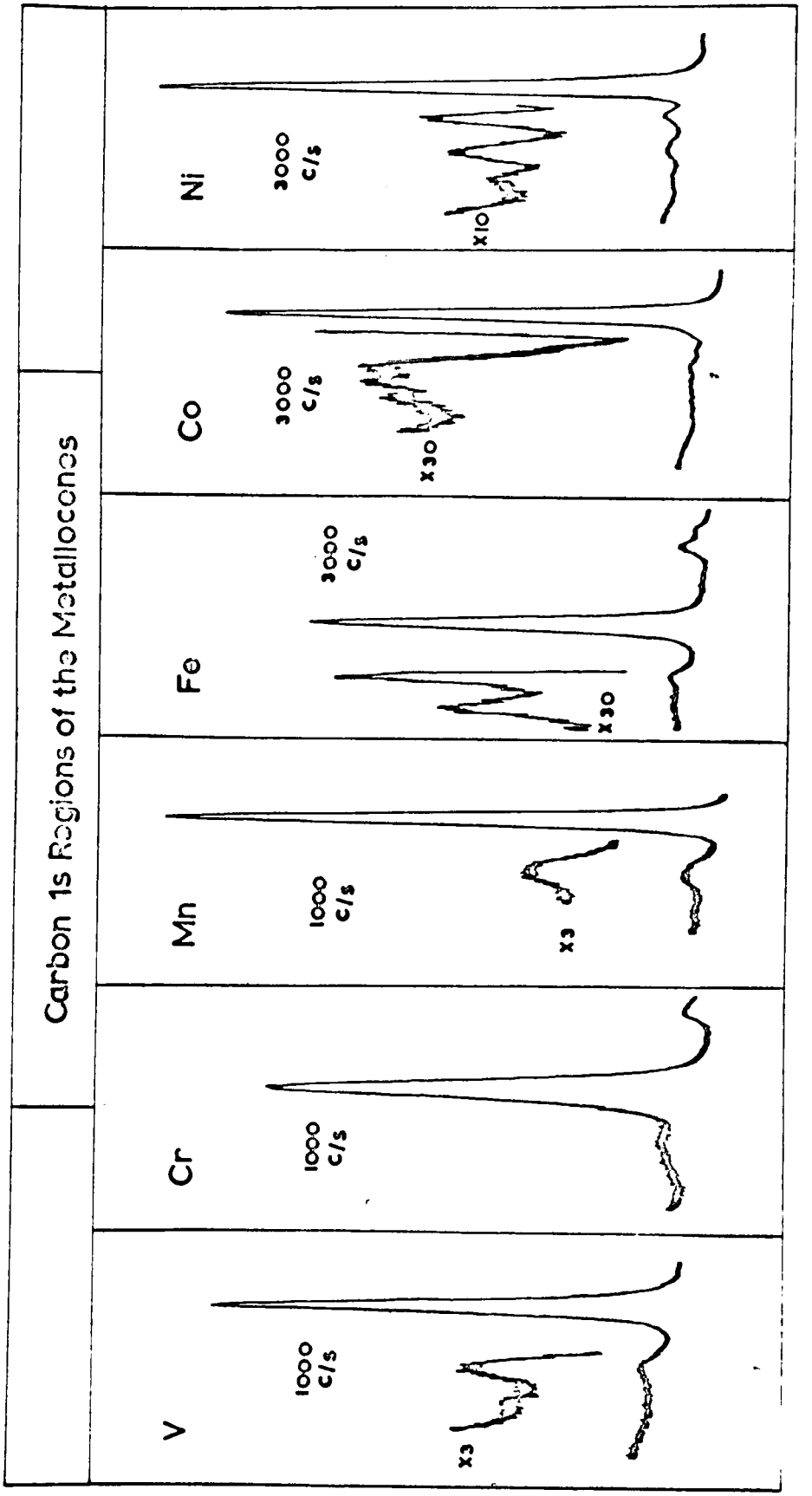
Carbon 1s Regions of the Metallocenes
V
1000 c/s
x3
Cr
1000 c/s
Mn
1000 c/s
x3
Fe
3000 c/s
x30
Co
3000 c/s
x30
Ni
3000 c/s
x10

FIGURE 5.15b

latter could, in principle, be tested by examining the gas-phase ESCA spectrum, but technical difficulties have prevented this). Both scattering mechanisms, especially that involved in an intermolecular process, involve dipole mechanisms, depending on integrals of the form $\langle \pi^* | r | e^*_{1g} \rangle$ which are likely to be large only if e^*_{1g} is delocalised over the ring, a possibility which is, however, strongly supported by the chemical shift data discussed below. If, on the other hand, the mechanism is CI, then the coefficients will be determined through integrals of the form $\langle 2pe^*_{1g} \| 2p\pi^* \rangle$, which again will be large only if there is significant delocalisation of the e^*_{1g} orbital. Actually, for $M(C_5H_5)_2$, CI with the high spin forms will involve only exchange integrals of the form $\langle 2pe^*_{1g} | \pi^* 2p \rangle$[81] which are presumably rather small, so it may be that only spin-uncoupled shake-up is significant in this case.

On this basis, the high intensity of the shake-up in manganocene is a consequence of the extensive delocalisation of the e^*_{1g} electrons in this compound onto the ring. This would possibly explain some of the peculiar features of the chemistry of manganocene. It is clear, for example, that this delocalisation of essentially metal electrons will lead to an apparently high ionicity as

compared to its low-spin neighbours $Cr(\pi Cp)_2$ and $Fe(\pi Cp)_2$ where the metal electrons are in non-bonding or bonding orbitals.[33,34] This delocalisation does not require vacant acceptor orbitals on the ligand, but is simply a consequence of electron sharing as a means of chemical bonding. This large delocalisation also leads to a large nephelauxetic effect, which, together with the larger spin-pairing energy in manganocene, as compared to chromocene, is apparently just sufficient to enable the compound to go high spin. However in the solid state manganocene is an anti-ferromagnet, even at room temperature, though in the absence of a reliable crystal structure it is perhaps unduly speculative to suggest that antiferromagnetic interactions may occur via the spin density delocalised onto the ring.

(ii) The carbon shake-up lines in $V(\pi Cp)_2$, $Cr(\pi Cp)_2$ and $Fe(\pi Cp)_2$ show a steady trend to lower energy which would tend to eliminate shake-off processes from the metal as a possible origin, and also, presumably, metal to ligand transitions. We are then left with either $\pi \rightarrow \pi^*$ or $\pi \rightarrow e^*_{1g}$ transitions, both of which might occur in this energy region.[35] The former correspond to $e_1 \rightarrow e_2$ processes, giving, for $V(\pi Cp)_2$ the states $^{4,6}E_1$ and $^{4,6}E_2$ all of which are inaccessible within the sudden

approximation, though the loss of symmetry through localisation of the hole will enable the symmetry restrictions to be lifted. However, the $\pi \rightarrow e^*_{1g}$ transition is allowed even within the sudden approximation formalism which might suggest that this origin is to be preferred. If so, then the fact that such a transition is observed again supports the conclusion that the e^*_{1g} orbital is substantially delocalised.

(iii) For manganocene an intense shake-up band is observed at 6.4 - 7.0 eV. If this is a $\pi \rightarrow e^*_{1g}$ transition, then it is a little surprising that it occurs so close in energy to those observed for the other metallocenes discussed above. On the other hand, its intensity must be coupled with the greater delocalisation of the metal electrons presumed for $Mn(\pi Cp)_2$ so that it is difficult to avoid the inference that the antibonding metal d-orbitals play a significant part in the shake-up.

(iv) Both $Co(\pi Cp)_2$ and $Ni(\pi Cp)_2$ exhibit very complex C 1s shake-up structure. Both are characterised by a filled set of lower energy d-orbitals with partially occupied antibonding $d(e^*_{1g})$ orbitals. Consider first the 3.7 eV shake-up in $Ni(\pi Cp)_2$. If this is a $\pi \rightarrow \pi^*$ transition, it is difficult to understand why such a transition should not occur in the earlier members of the series. An

examination of the UV spectrum of $Ni(\pi Cp)_2$, as compared to $Fe(\pi Cp)_2$, shows that there is a band at ca. 33,000 cm^{-1} which has been assigned to $d \rightarrow \pi^*$ or $d \rightarrow p$. The latter seems to be rather unlikely on the basis of known atomic data and, if the shake-up is due to the $d \rightarrow \pi^*$ transition, it is difficult to understand why there is not a corresponding band in $Co(\pi Cp)_2$ at ca. 2.5 eV. The effect of considering the C 1s hole as localised will split both π and π^* into symmetry adapted components of the local C_{2v} point group, though the extent of this splitting is impossible to estimate without calculation. However it might be quite large, so that it is possible in $Ni(\pi Cp)_2$ that the two bands at 3.7 and 7.5 eV are components of the $\pi \rightarrow \pi^*$ or $\pi \rightarrow e^*_{1g}$ excitation, or possibly $d \rightarrow \pi^*$. If this latter suggestion is correct, then we must postulate that the lower component of this splitting in $Co(\pi Cp)_2$ is actually of so low an energy as to be unresolved from the main carbon 1s band.

(v) The shake-up structure on the metal 3p bands is very interesting. The fact that the shake-up energies differ substantially from those on the 2p bands would suggest that intermolecular scattering processes probably play little part in determining such structure in the metallocenes. Shake-up bands are clearly observed for

$V(\pi Cp)_2$, $Cr(\pi Cp)_2$ and $Ni(\pi Cp)_2$ suggesting that either the shake-up process does not involve the e^*_{1g} orbitals, or that the induced transition is d $\rightarrow$ d in nature. If this latter is true, the mechanism is presumably CI since, although the repulsion and exchange integrals (rather surprisingly) are, if anything, rather larger between 3d and 2p than 3d and 3p orbitals, the 3p orbitals are much closer in energy to the valence shell, giving rise, on a simple perturbation model of CI, to larger CI coefficients. The absence of such satellites in ferrocene and cobaltocene is however rather strange.

Satellite structure in the hexafluoroacetylacetonato-complexes.

The ESCA spectra of most carbonyls show very strong shake-up structure on the C 1s and O 1s bands, usually between 5 and 6 eV from the parent peak. By analogy, we would expect the complexes of hexafluoroacetylacetone to show similar structure, though interestingly, the splitting is now 4.5 to 5 eV on O 1s. The satellite on the carbon 1s derived from $\underline{C}O$ cannot however be seen and may only be postulated by inference, since the $\underline{C}F_3$ carbon 1s band is also 4 - 5 eV displaced from the $\underline{C}O$ band, but is rather more intense than can easily be accounted for on the basis of equal C 1s cross-sections. Thus, it is likely that some of its intensity is due to a $\underline{C}O$ satellite, though this is speculative. It should be noted that this intensity pattern differs somewhat from the published spectrum of Clark et al. though extremely careful checks on my own data and spectra have not shown in any of the hexafluoroacetyl-acetonates an intensity pattern resembling Clark's. I cannot therefore account for the discrepancy.

Table 5.6 shows the oxygen 1s satellite bands.

TABLE 5.6 [41, 51, 56, 59, 88]

COMPOUND	O 1s SATELLITE	$\pi - \pi^*$
$Al(hfa)_3$	5.0 eV	
$Sc(hfa)_3$	4.7eV	4.2eV
$Ti(hfa)_3$	4.4eV	4.0eV
$V(hfa)_3$	4.6eV	4.3eV
$Cr(hfa)_3$	4.9eV	4.6eV
$Mn(hfa)_3$	4.4eV	4.5eV
$Fe(hfa)_3$	4.9eV	4.5eV

The general trends in the oxygen 1s satellite energies follow the movements in the $\underline{C}F_3$- $\underline{C}H$ splitting quite closely, and we saw above that these were sensitive to changes in the electrons constituting the π-framework. Thus, the O 1s satellite almost certainly involves the π_3 orbital, probably as $\pi \rightarrow \pi^*$, since the trends observed are the reverse of those expected for ligand to metal transitions. They are compared in the table with the $\pi \rightarrow \pi^*$ energies found by Barnum[41] from the UV spectra of the acetylacetonates, and it should be borne in mind here that Barnum's values are for the lowest $\pi \rightarrow \pi^*$ transition, and a mean $\pi \rightarrow \pi^*$ energy would be slightly higher. It can be seen that, apart from $Mn(hfa)_3$, the trend is very much in keeping with the O 1s satellite splitting, and it is again noteworthy that the scandium complex occupies an

irregular position, strongly supporting the suggestion that the τ_3 orbital is involved. The general increase from titanium to chromium in the transition energy correlates with increasing covalence, which tends to stabilise τ_3 and destabilise τ_4. $Mn(hfa)_3$ appears to be rather exceptional, though the shake-up band is ill-resolved in this molecule. In addition the ultra-violet spectrum was obtained by Barnum using absolute ethanol as solvent, whereas chloroform had been used for the other chelates. $Mn(hfa)_3$ is also unusual in that shake-up structure is also observed on the metal 2p band. From the discussion of the metallocene shake-up structure above, this would be most naturally assigned to an $e_g \rightarrow \pi^*$ process, and the fact that such satellites are not observed for the t_{2g}^n series of complexes strongly suggests that the e_g orbital is substantially more delocalised, a supposition supported, as we have seen, by the ESCA shift data. Unfortunately, the Fe 2p region is very indistinct owing to the fact that it is "swamped" by non-quantum scatter from the F 1s peak. However, its very indistinctness is suggestive of extensive shake-up. The energy of the metal 2p shake-up in $Mn(hfa)_3$ is 5.0 eV, which is slightly larger than that of the O 1s satellite, and suggests that Barnum's assignment may be incorrect; perhaps the 4.5 eV band should be assigned to $d \rightarrow \pi^*$ and the 4.0 eV band to $\pi \rightarrow \pi^*$ transitions. This would also have the merit

of restoring the parallel between the O 1s satellite and $\pi \rightarrow \pi^*$ energies in table 5.6.

The valence regions of the metallocene ESCA spectra

The Esca valence regions of the metallocenes show a very interesting set of progressions which will be briefly discussed. The metal levels and occupancies are given in table 5.8 and the relevant ligand levels have been discussed for ferrocene by Evans et al.[54] In fig. 5.19, the ESCA and UV-PE spectra of ferrocene are compared on the same energy scale and the correspondence can easily be seen. Two especially noteworthy facts emerge; firstly the cross-section of the metal 3d orbitals has substantially increased (relatively) and those of the p_σ orbitals lowered, and, secondly, the carbon 2s ionisations, which correspond to bands a, b and c in fig. 5.12a have become very large in comparison with the $2p_\sigma$ framework, labelled band d in the ESCA spectrum corresponding, as can be seen, to the major UV-PE band between 12 and 14 eV.

The levels are given in table 5.7 and these are derived from assuming that band a remains constant in energy. The BE of this band has been fixed from the UV-PE spectrum of ferrocene.

TABLE 5.7

COMPOUND	a	b	c	d	π	METAL
$V(\pi Cp)_2$	26·5	21·3	17·1	12·5	8·7	6·7
$Cr(\pi Cp)_2$	26·5	21·3	17·2	12·3	8·3	2·3, 5·7
$Mn(\pi Cp)_2$	26·5	22·1	17·7	13·2	?	10·6, 8·2
$Fe(\pi Cp)_2$	26·5	21·3	17·2	12·9	9·2	7·0
$Co(\pi Cp)_2$	26·5	21·3	17·2	12·4	?	7·6, 5·8
$Ni(\pi Cp)_2$	26·5	21·3	17·2	13·4	?	5·6, 6·2±0·3

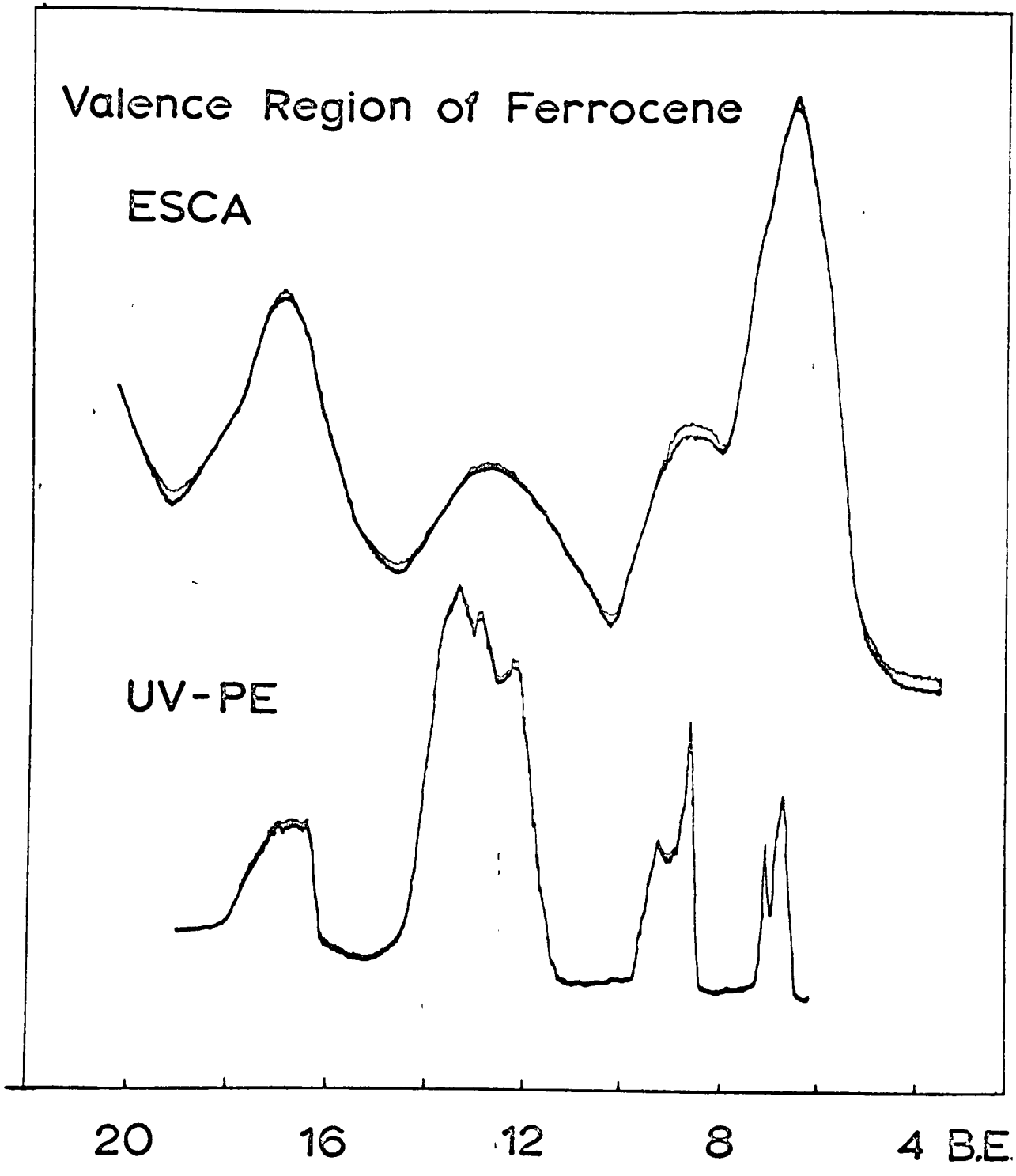

FIGURE 5.19

On the whole these figures agree remarkably well with the UV-PE results of Evans.[5] The main differences arise in the spectrum of $Mn(\pi Cp)_2$ where the ESCA valence region shows an indistinct shoulder on the low IE side of what appears to be a predominantly metal ionisation at 10.6 eV. The UV-PE spectrum of $Mn(\pi Cp)_2$ is extremely difficult to interpret but it does seem likely that metal d-ionisations at ca. 10 - 10.5 eV, presumably arising from the a_1 and e_2 orbitals can be distinguished from the surrounding ligand structure. That the ESCA spectrum of manganocene, obtained at -150°C should differ radically from the gas-phase UV-PE spectrum is not very surprising since the compound is known to be an anti-ferromagnet even at room temperature, as was pointed out in the discussion of satellite structure above. Perhaps the spectrum can only be explained in terms of a rather more sophisticated picture than the one we will use here.

The interpretation of the origin of the various d-ionisation bands is fairly difficult and, in appendix 3, are given the necessary coupling coefficients and fractional parentage coefficients for the metallocenes. Table 5.8 lists the ground states of the molecules,[51,95] the only doubtful cases being chromocene and manganocene. In the former case, the ground state chosen is that consistent with magnetic measurements and the UV-PE spectrum,[5] whilst in the latter case it is

that deduced from magnetic measurements in dilute solution.[89]

TABLE 5.8

COMPOUND	GROUND STATE
$V(\pi Cp)_2$	$a_1e_2^2$ $^4A_2$
$Cr(\pi Cp)_2$	$a_1e_2^3$ $^3E_2$
$Mn(\pi Cp)_2$	$a_1e_2^2e_1^2$ $^6A_1$
$Fe(\pi Cp)_2$	$a_1^2e_2^4$ $^1A_1$
$Co(\pi Cp)_2$	$a_1^2e_2^4e_1^*$ $^2E_1$
$Ni(\pi Cp)_2$	$a_1^2e_2^4e_1^{*2}$ $^3A_2$

The energies of the ion states which are accessible by d-orbital ionisation are listed in table 5.9 in terms of the Racah parameters.

TABLE 5.9

COMPOUND	STATE AND ENERGY
$V(\pi Cp)_2$	a_1e_2 ($^3E_2$) $\Delta_1 + A - 8B$; e_2^2 ($^3A_2$) $2\Delta_1 + A + 4B$
$Cr(\pi Cp)_2$	$a_1e_2^2$ ($^4A_2$) $2\Delta_1 + 3A - 12B$; ($^2A_1$) $2\Delta_1 + 3A - 8B + 5C$; ($^2A_2$) $2\Delta_1 +$
	$3A + 3C$; ($^2E_1$) $2\Delta_1 + 3A - 3B + 3C$; e_2^3 ($^2E_2$) $3\Delta_1 + 3A + 12B + 4C$
$Mn(\pi Cp)_2$	$a_1e_2^2e_1$ ($^5E_1$) $2\Delta_1 + \Delta_2 + 6A - 21B$, $a_1e_2e_1^2$ ($^5E_2$) $\Delta_1 + 2\Delta_2 + 6A - 21B$;
	$e_2^2e_1^2$ ($^5A_1$) $2\Delta_1 + 2\Delta_2 + 6A - 21B$
$Fe(\pi Cp)_2$	$a_1^2e_2^3$ ($^2E_2$) $3\Delta_1 + 15A - 20B + 10C$; $a_1e_2^4$ ($^2A_1$) $4\Delta_1 + 15A + 10C$
$Co(\pi Cp)_2$	$a_1^2e_2^4$ ($^1A_1$) $4\Delta_1 + 15A - 28B + 15C$; $a_1^2e_2^3e_1$ ($^3E_1$) $3\Delta_1 + \Delta_2 + 15A - 26B + 12C$;
	($^3E_2$) $3\Delta_1 + \Delta_2 + 15A - 32B + 12C$; $a_1e_2^4e_1$ ($^3E_1$) $4\Delta_1 + \Delta_2 + 15A - 13B + 12C$
$Ni(\pi Cp)_2$	$a_1^2e_2^4e_1$ ($^2E_1$) $4\Delta_1 + \Delta_2 + 21A - 31B + 13C$; $a_1^2e_2^3e_1^2$ ($^4E_2$) $3\Delta_1 +$
	$3\Delta_2 + 21A - 43B + 14C$; $a_1e_2^4e_1^2$ ($^4A_2$) $4\Delta_1 + 2\Delta_2 + 21A - 31B + 7AC$

An assignment consistent with these figures is only possible if Δ_1, the ligand field energy difference between a_1 and e_2 is negative: i.e. the one-electron ligand-field ordering is $e_2 < a_1$. The UV-PE spectrum of ferrocene on the other hand shows quite clearly that the orbital energy ordering is $e_2 > a_1$. The difference, as was discussed for the spectra of the hexafluoroacetylacetonates, arises from the radically different electron repulsion parameters for the e_2 and a_1 orbitals even within the ligand field framework. With this proviso in mind, the assignment of the d-ionisations is given in table 5.10, together with the values of Δ_1 and Δ_2 estimated assuming a nephelauxetic ratio of 0.6.

TABLE 5.10

COMPOUND	WEVEL	ASSIGNMENT	Δ_1	Δ_2
$V(\pi Cp)_2$	6·7	$^3E_2$, $^3A_2$	-0·6eV	-
$Cr(\pi Cp)_2$	5·7	$^4A_2$	?>-1·0	-
	7·3	$^2A_1$, $^2A_2$, $^2E_1$, ? $^2E_2$	eV	
$Mn(\pi Cp)_2$	8·2	$^5E_1$	-	+2·4eV
	10·6	$^5E_2$, $^5A_1$		
$Fe(\pi Cp)_2$	7·0	$^2A_1$, $^2E_2$	-1·5eV	-
$Co(\pi Cp)_2$	5·8	$^1A_1$	-	+2·2eV
	7·6	$^{1,3}E_1$, $^{1,3}E_1$, $^{1,3}E_2$		
$Ni(\pi Cp)_2$	6·3	$^2E_1$	-	+3·7eV
	8·6	$^{2,4}E_1$, $^{2,4}A_2$		

The assignments given in table 5.10 are not very different from those given by Evans[5], save in the case of $V(\pi Cp)_2$ where

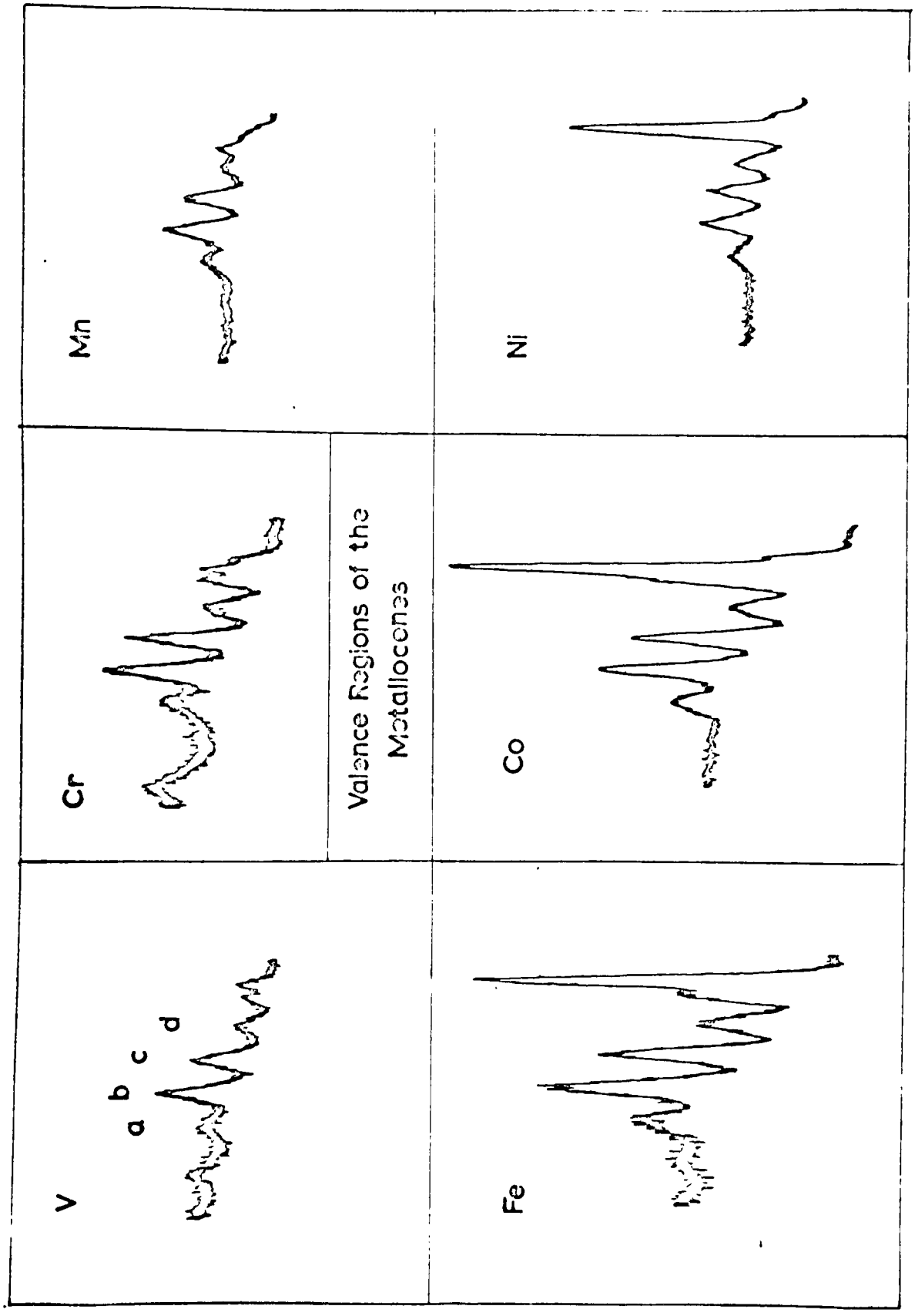

FIGURE 5.16

a sharp band at 8.40 eV in the UV-PE spectrum was assigned to the a_1 ionisation. Several reasons may be adduced against this assignment:

(i) The ESCA spectrum is not consistent with this assignment, in that the metal d-ionisation is well resolved from the main π-ionisations, whose median energy is some 2 eV higher. It is probable that the "d" band at 8.4 eV would not be resolved from the main d-band at 6.8 eV if there were such a band.

(ii) On theoretical grounds, the value derived for Δ_1 using Evans' assignment is larger than that observed in ferrocene and of opposite sign, whereas that derived by assuming that all the d-ionisations occur at 6.8 eV is very similar to the ferrocene value.[95]

(iii) The relative intensities of π and d-ionisations in the UV-PE spectrum strongly support the assignment of all the d-ionisations to the band at 6.8 eV. The assignment of Evans would suggest that the cross-section of the d-orbitals halves between vanadocene and ferrocene. If this is correct, it shows a trend completely opposite to that observed in the hexafluoroacetylacetonates and the ESCA spectra of the metallocenes themselves.

On similar grounds, a slight reassignment of the $Cr(\pi Cp)_2$ spectrum has been made, the band at 5.7 eV corresponding only

to the $(^4A_2)a_1e_2^2 \leftarrow (^3E_2)a_1e_2^3$ ionisation. Again there are several reasons for this:

(i) The cross-section of the metal d-ionisations on Evans' assignment lead in the simplest arguments to a negative cross-section for the a_1 orbital.

(ii) The value of Δ_1 derived using Evans' assignment is now of the same sign as that found in ferrocene, but over twice as large. If this is correct it represents a much larger variation in a ligand field splitting than is usually found in isostructural materials.

Assuming the changes discussed here are accepted, and leaving aside any consideration of manganocene, a plot of d-orbital energy against atomic number is shown in fig. 5.20. It can be seen at once that there is a general stabilisation of the d-orbitals across the series as expected, but that the stabilisation is much less marked than that shown for the chelate complexes in fig. 5.21. In other words it does seem, in these molecules, that the cyclopentadienyl ligand is acting as an electron buffer, with covalency presumably increasing dramatically across the series. In order to examine the effects of covalency a careful study of the core shifts of the metallocenes was then made whose results are discussed in the next section.

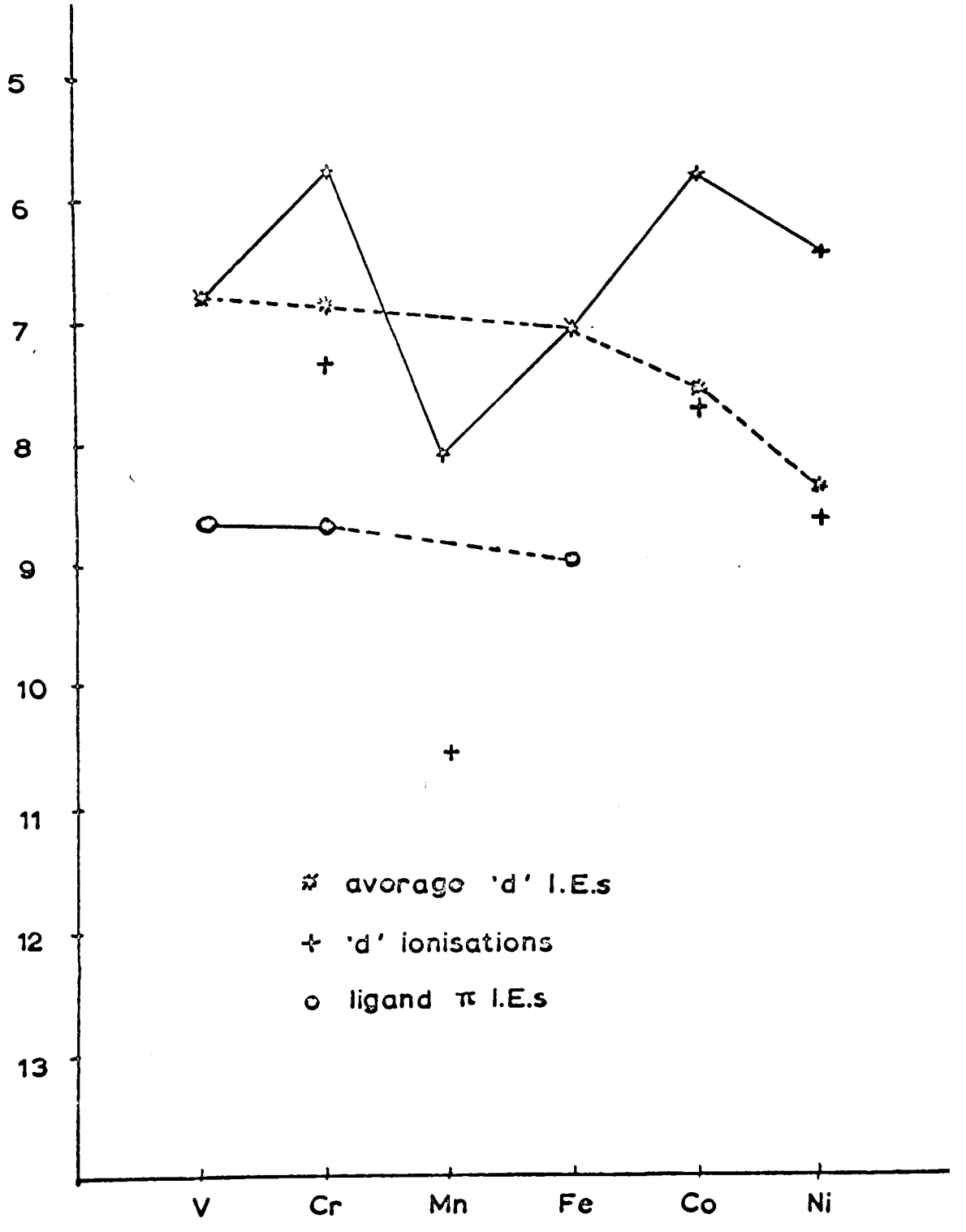
5
6
7
8
9
10
11
12
13
V
Cr
Mn
Fe
Co
Ni
average 'd' I.E.s
'd' ionisations
ligand π I.E.s

FIGURE 5.20

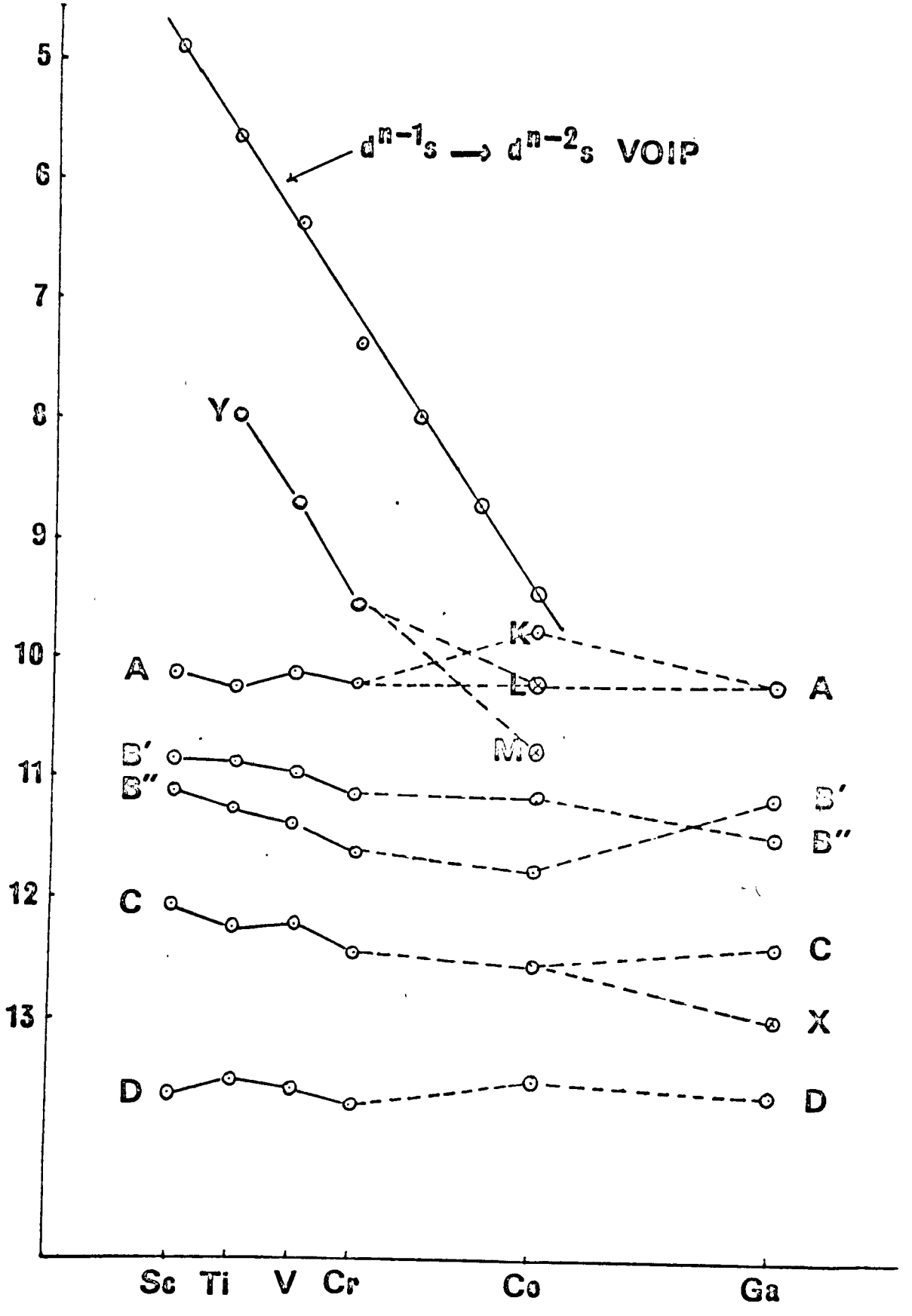
5
6
7
8
9
10
11
12
13
$d^{n-1}s \longrightarrow d^{n-2}s$ VOIP
Y
K
L
M
A
B′
B″
C
D
A
B′
B″
C
X
D
Sc
Ti
V
Cr
Co
Ga

FIGURE 5.21

Core region of the metallocenes

To examine the effects of covalency, the carbon 1s binding energies of the metallocenes were measured relative to the $\underline{C}F_3$ carbon of the calibrant gas $CF_3C \equiv CCF_3$. They are reproduced in table 5.11.

TABLE 5.11

Compound	Carbon 1s
$V(\pi Cp)_2$	9.7(2)
$Cr(\pi Cp)_2$	9.7(5)
$Fe(\pi Cp)_2$	9.3(3)
$Co(\pi Cp)_2$	9.5(0)
$Ni(\pi Cp)_2$	9.5(9)

for comparison, the carbon 1s signal in benzene is 9.95 eV to lower BE

all figures are given to ± 0.1 eV

A fascinating parallel with the O 1s and C 1s binding energies of the tris-chelate complexes can be seen. A steady destabilisation of the C 1s level to ferrocene with a discontinuity at cobaltocene is apparent, and the explanation is very similar. A general increase in $d_{\pi} - Cp_{\pi}$ bonding across the series to ferrocene is expected, leading to a gradual decrease in the negative charge on the ring and positive charge on the metal. As we saw, an expression of the form

$$\Delta E = k\,\Delta q + \Delta V$$

can be used to represent the shifts in BE, and as before we anticipate that the change in potential, ΔV, will be given by

$\delta q/r$. Hence, for the carbon 1s level we have

$$\Delta E = \frac{k}{10}\delta q - \delta q/r_{Mc} + 2\delta q/10r_{cc}$$

whence

$$\partial\Delta E/\partial\delta q = \frac{k}{10} - \left(\frac{1}{r_{Mc}} - \frac{1}{5r_{cc}}\right)$$

Clearly, $\partial\Delta E/\partial\delta q$ is negative for the cyclopentadienyls considered here, and we have at once an explanation for the discontinuity at cobaltocene. The presence of an electron in the e^*_{1g} orbital which is significantly delocalised over the ring, allows the ligand to become more negative. Thus, $\delta q < 0$ and $\Delta E > 0$, that is, the carbon 1s level will stabilise, which is the trend observed. For the case of $Ni(\pi Cp)_2$, the rapidly increasing polarising power of the cation leads to a rapid increase in δq as compared to $Co(\pi Cp)_2$. It should be noted that this interpretation is in accord with the expectations of bonding in the metallocenes, as derived from previous studies and the discussion above. A simple MO scheme is shown below:

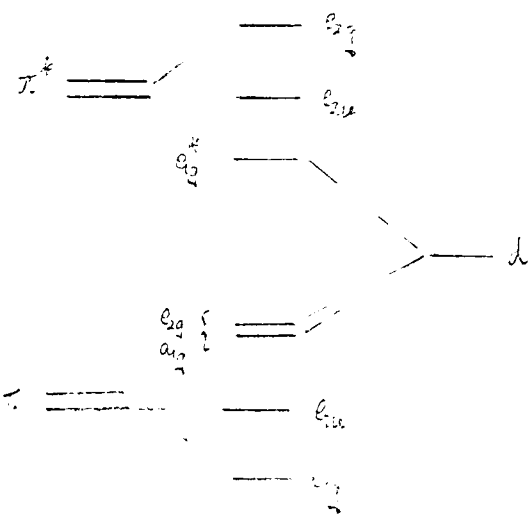

In MO terms, it is clear that as the d-orbitals stabilise, the interaction of the e_{2g} and π^* orbitals will diminish, i.e. there will be less $d \rightarrow \pi^*$ donation, and δq will fall in absolute magnitude. In addition, interaction between e_{1g}^* and $e_{1g}(\pi)$ will increase,[91] and, up to ferrocene (leaving aside manganocene) this will be a purely $\pi \rightarrow d^*$ donation, also causing δq to drop. However, occupation of the e_{1g}^* orbital will allow $d^* \rightarrow \pi$ donation, and the extent to which this occurs will clearly be a function of the binding energy of this d-electron to the central atom. The low IE of cobaltocene, and the stability of $Co(\pi Cp)_2^+$ salts both argue that the d* electron in $Co(\pi Cp)_2$ is probably extensively delocalised over the ligand. However, the considerable stabilisation of the d* electron between $Co(\pi Cp)_2$ and $Ni(\pi Cp)_2$ suggests that such $d^* \rightarrow \pi$ donation will be substantially reduced, and this, coupled with the certainly very small $d \rightarrow \pi^*$ donation in $Ni(\pi Cp)_2$ results in a rapid drop in charge separation between $Co(\pi Cp)_2$ and $Ni(\pi Cp)_2$, and, judging by the figures, Nickelocene and ferrocene are the most covalent of the metallocenes.

To quantify this discussion, we have, for the bond lengths in ferrocene,

$$\partial E / \partial q \approx k/10 - 14.5/2.0 + 14.5/[illegible] \pm 14.5/11.3 + 14.5/[illegible] \simeq k/10 - 2.15$$

Unfortunately, different groups have derived rather different values for k, though experiment does suggest a value of less than 21.5 for π-electrons, and we will take a mean value of 20, so that, at any rate, the result is fairly encouraging. However, the particular mode of stacking of the crystals leads to some uncertainty for the potential part, so that accurate analysis is not possible.

The results for benzene, where V and q are presumable zero, suggest a shift of 9.95 eV from $\underline{C}F_3$ so taking this value as the zero, and k as 20, we obtain for $V(\pi Cp)_2$

$$q = 0.27/0.15 = 1.8$$

and, for ferrocene

$$q = 0.09/0.15 = 0.6$$

This would suggest a very rapid increase in covalency across the series, though it must be emphasised that the figures are only indicative. This rapid increase in covalency is supported by the much slower stabilisation of the d-electrons in the metallocenes as compared to the tris-chelate complexes.

A remarkable confirmation of the above analysis is found in the ^{13}C nmr spectra of the metallocenes.[43] For $V(\pi Cp)_2$ and $Cr(\pi Cp)_2$, the spin density on the rings was found to be negative, whereas for $Co(\pi Cp)_2$ and $Ni(\pi Cp)_2$ it was found to be positive. This is easily explained on the above MO treatment since, for the first two molecules, the main bonding effects,

as we have seen, can be described by increasing $\pi \rightarrow d^*$ transfer. Clearly, the spin delocalised onto the metal by this process will be α-type by Hund's first rule, and so we would expect β-spin to be left on the rings. However, we saw that for $Co(\pi Cp)_2$ the steady $\pi \rightarrow d^*$ trend was offset by a reverse direct $d^* \rightarrow \pi$ donation which will delocalise α-spin onto the ring. At $Ni(\pi Cp)_2$, although this effect is substantially reduced, and $\pi \rightarrow d^*$ probably dominant, since no more α-spin density can be accommodated on the central metal by Pauli's principle, only β-spin may be donated to the nickel, leaving α-spin on the rings.

It should of course be emphasised that nmr measures spin density movements in paramagnetic systems, whereas ESCA measures electron density, so that to a certain extent the techniques complement one another. Diamagnetic shifts in nmr work, arising from electron shielding, bear a complex relationship to ESCA shifts, since the latter are dependent on both charge and potential effects, and the former on the availability of excited states about which PE spectroscopy, in its simplest forms, has little to say.

ESCA ionisation energy data for the tris-chelate complexes

The data were all obtained using AlK_α radiation and are quoted in electron volts AS THE ELECTRON KINETIC ENERGY. To obtain the binding energies, the figures given in the tables below should be subtracted from 1486.6 eV. The KE's have been calculated assuming that the $\underline{C}F_3$ carbon 1s core level has a kinetic energy of 1191 eV.

The main core levels of the tris-hexafluoroacetylacetonato complexes

Band	Al	Sc	Ti	V	Cr	Mn	Fe
F 1s	797.5	797.5	797.5	797.5	797.5	797.5	797.5
O 1s	952.0	951.1	951.4	951.5	952.0	952.0	952.6
$\underline{C}F_3$ 1s	1191.0	1191.0	1191.0	1191.0	1191.0	1191.0	1191.0
$\underline{C}O$ 1s	1195.8	1196.0	1195.7	1195.8	1195.9	1195.9	1195.8
$\underline{C}H$ 1s	1198.5	1198.6	1198.2	1198.5	1198.9	1198.6	1198.7
F 2s	1448.9	1448.9	1448.3	1448.3	1448.3	1448.3	1448.3
O 2s	1455.2	1455.0	1455.0	1455.0	1455.0	1455.0	1455.0
F 2p(k)	1471.5	1471.9	1471.4	1471.5	1471.3	1471.2	1471.2

The metal core levels of the tris-hexafluoroacetylacetonato complexes

Spectrum	Band	Assignment
$Al(hfa)_3$	1364	Al 2s
	1408	Al 2p
$Sc(hfa)_3$	1080	Sc 2p
	1076	Sc 2p
	1428	Sc 3s
	?	Sc 3p
$Ti(hfa)_3$	1026	Ti 2p
	1020	Ti 2p
	1420	Ti 3s
	(1447)	Ti 3p
$V(hfa)_3$	961	V 2p
	968	V 2p
	1413	V 3s
	1442	V 3p
$Cr(hfa)_3$	896	Cr 2p

Spectrum	Band	Assignment
$Cr(hfa)_3$	906	Cr 2p
	1406	Cr $3s^3$
	1437	Cr 3p
$Mn(hfa)_3$	829	Mn $2p^5$
	841	Mn $2p^5$
	1396	Mn $3s^3$
	1431	Mn 3p
$Fe(hfa)_3$	?	Fe $2p^{2,5}$
	?	Fe $2p^{2,5}$
	1387	Fe $3s^3$
	1424	Fe 3p

Notes

1. Approximately degenerate with F 2s
2. Lost under the scatter from the F 1s signal
3. Highest component of a doublet
4. Approximately degenerate with the $K\alpha_{3,4}$ satellite of the O 1s line
5. Satellite structure observed on the Mn 2p and possibly Fe 2p
6. Strong KLL Auger transition observed at 1283.8 eV.

The M $2p_{\frac{1}{2},\frac{3}{2}}$ and M 3s,3p separations for the $M(hfa)_3$ series

Metal	M 2p	M 3s,3p
Sc	4.9	-
Ti	5.5	26.7
V	ca.6.9	28.9
Cr	9.6	30.6
Mn	11.8	34.7
Fe	-	37.6

Chapter six

THE BONDING IN THE CHELATE COMPLEXES

Urbem excoluit adeo, ut iure sit
gloriatus marmoream se relinquere,
quam latericiam accepisset.

Suetonius
Augustus.

THE BONDING IN TRIS-CHELATE COMPOUNDS

The conclusions we have reached from a consideration of both UV-PE and ESCA data may be summarised briefly as follows:

(i) There is a rapid stabilisation of the d-orbital energy across the series within both the t_{2g} and e_g subshells.

(ii) There is a fairly steady increase in covalency across the series from scandium to chromium, the increase being large between scandium and titanium, and between vanadium and chromium, but the vanadium complex is rather more ionic than might have been expected.

(iii) The main bonding is through the σ-framework, and only in $Co(hfa)_3$ is π-bonding significant enough to split the t_{2g} shell, presumably because the one-electron orbital energies for π_3 and t_{2g} differ very little, and the molecular dimensions are also somewhat smaller.

(iv) The main anti-bonding σ orbital e_g^* is very much more delocalised over the ligand than the t_{2g} orbital, and $Mn(hfa)_3$ is therefore more ionic than might have been expected by extrapolation from chromium.

(v) On coordination, the free-ligand π_3 orbital is strongly polarised towards the central metal, a polarisation which increases as the M-O bond length decreases.

The information about charge movements obtained by

photoelectron spectroscopy can be seen to be extremely detailed and of comparable importance to that derived from magnetic resonance techniques. Examination of the nmr of some acetylacetonato complexes by Eaton revealed large shifts of both the unique (γ) proton, and of the CH_3 protons. Assuming that Q_{CH} is negative for π-interaction and Q_{CCH_3} positive, the earlier members of the series give a spin distribution within the π-framework of the classic alternating sort:

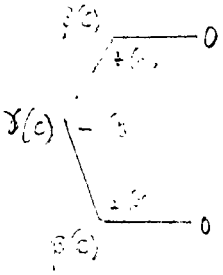

The spin on oxygen could not be observed, since ^{17}O nmr spectra can only be obtained apparently for $Mn(acac)_3$, which, surprisingly, indicated a positive spin on oxygen, almost certainly not representative of the other members of the series. Eaton explained his results entirely in terms of π-bonding to the central metal, but, as we have seen, σ-bonding is much more important, especially early in the series. Now, σ-bonding to the empty e_g orbitals will probably leave an excess of β-spin on the oxygen (that is, spin anti-parallel to the central metal) which will polarise π_3 in just the

direction indicated. However, some σ-bonding also occurs to the $e_a(t_{2g})$ orbitals of the metal and the main effect of this will be difficult to estimate, since back σ-donation from the metal would place α-spin on the oxygen. In addition there are a second set of direct mechanisms involving the π_3 and π_4 orbitals which Eaton suggested and which other workers have discussed. This involves $\pi_3 \rightarrow$ d electron transfer, which, for a less than half filled t_{2g} shell must leave β-spin on the γ-carbon. There is also the possibility of d $\rightarrow \pi_4$ bonding, which, if it is at all important, will only be so for the earliest members of the series. The effect of this is to transfer positive spin density onto the CCH_3 carbons. Finally, there may be direct polarisation of the π_3 orbitals by the central metal leading to α-spin on the oxygen and γ-carbon atoms and β-spin on the β-carbon atoms. This latter effect will presumably increase steadily across the series. For clarity, the effects are listed in table 6.1.

TABLE 6.1

Mechanism		Spin: β(C)	γ(C)	Oxygen
σ-interaction	M←L	α(β)	β	β
	M→L	β(α)	α	α
$\pi_3 \rightarrow$ d		α	β	β
d $\rightarrow \pi_4$		α	?β	?α
π-polarisation		β	α	α

Brackets in the first two lines indicate that some σ polarisation of the β-carbons may occur.

At the beginning of the series, σ-interaction will predominate, possibly with some $d \rightarrow \pi_4$ transfer, both of which give a net α-spin on the β-carbons and a net β-spin on the γ-carbons in agreement with Eaton's analysis. It is difficult to gauge the relative magnitudes of the transfer and σ-induced spin polarisations, since the simple McLachlan and Hückel treatments refer to a half-filled π_3 orbital whereas we are considering polarisation of a filled orbital. The increasing importance of direct π_3 polarisation, the increased α-spin from the metal delocalised onto oxygen, and the decrease in importance of $d \rightarrow \pi_4$ as a mechanism all point to a steady fall in α-spin on the β-carbons and β-spin on the γ-carbons. However at $Mn(acac)_3$, the net spin delocalised onto the oxygen is known to be positive from ^{17}O nmr data,[35] indicating how very much more this e_g^* electron is delocalised. However the pmr results for $Mn(acac)_3$ are, as a result of this work, rather more difficult to understand. For $Fe(acac)_3$, the spin is α-type on all three carbons, implying that both π_3 and σ-polarisation are important. It may be, though the smooth trends observed in Eaton's work do not suggest this, that pseudo-contact terms are more important in d^4 systems, which would certainly be expected to be more anisotropic. However,

there is little epr data on d^4 systems and very little magnetic anisotropy work. Thus, there is not as good a correlation between the ESCA and nmr data as might have been hoped, and a more rigorous treatment must await a ^{13}C nmr study. Eaton's results, relative to $Co(acac)_3$, are plotted in fig. 6.1. It can be seen that there is an inverse correlation between these figures and those derived from the PES data, in that there are large changes between titanium and vanadium and between chromium and manganese. Whilst this latter jump can be understood in terms of the above discussion, the large jump between titanium and vanadium is very strange, and may be connected with the anomalous ground state of $V(acac)_3$, $(e_a^2;\ ^3A_2)$, to which the nmr method will be much more sensitive than ESCA. Thus, there may be more back donation of α-spin from the metal e_a orbitals to the ligand both into π_4 and σ because e_a is partly σ^* in character. Since the a_1 orbital cannot delocalise by the second of these methods, this would certainly fit very neatly with the ESCA data, which as we saw, suggested that $V(hfa)_3$ was surprisingly ionic. Although this is certainly speculative, it is worth re-emphasising that since the nmr method is not measuring electron densities but spin densities, there will be no easily quantifiable relationship between nmr and ESCA shifts.

To summarise, the nmr data may be explained in terms of

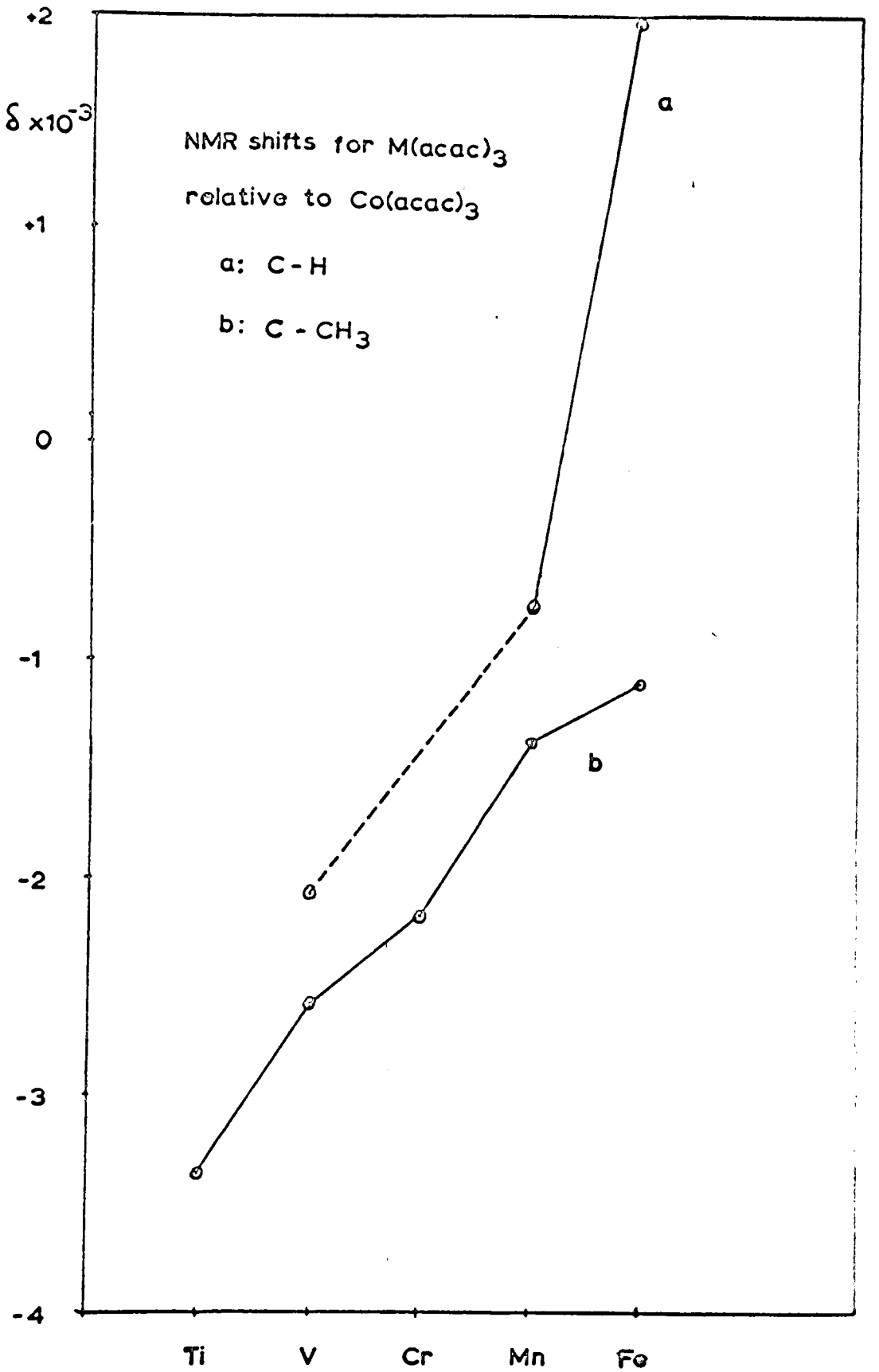
+2
δ x10⁻³
+1
0
-1
-2
-3
-4
NMR shifts for M(acac)3
relative to Co(acac)3
a: C - H
b: C - CH3
a
b
Ti
V
Cr
Mn
Fe

FIGURE 6.1

a steadily increasing σ-interaction and π polarisation between titanium and chromium, the trends indicating that the latter is the more important contribution to ring-spin density; the jump at manganese is a measure of the increasing importance of metal $\rightarrow$ ligand spin transfer through the σ-system, and the figures for $Fe(acac)_3$ are best explained by very considerable σ-interaction, even involving the β-carbons.

Infra-red data

Difficulties of assignment bedevil any real investigation of the infra-red spectra of the tris-acetylacetonates, since all the modes in such a cyclic system are strongly coupled, and in particular, the C=O and C=C stretching frequencies lie very close together. The two regions of interest in the IR spectrum are that between 1600 and 1500 cm^{-1}, where the main skeletal ring vibrations occur, and 400 to 500 cm^{-1}, where the first metal-oxygen stretching mode is seen. Assignment in the lower frequency region has been greatly facilitated by the work of Nakamoto et al.[43] who used the effective, if expensive, technique of metal isotope substitution to pinpoint the metal vibrations. In essence, this confirmed the work of Mikami et al.[44] who had provided a normal coordinate analysis for the tris-chelate systems based on a Urey-Bradley force field. The substitutional work of Nakamoto showed that, in $Fe(acac)_3$, there were two main band shifts; the band at 433 cm^{-1} was found to shift by 1.5 cm^{-1} and that at 298 cm^{-1} by 5 cm^{-1}. These shifts are in qualitative agreement with the normal coordinate analysis, which showed that the former band was 48% M-O stretch and the latter 70% M-O stretch. Unfortunately, although the lower band would be a better index of bond strength than the former, its energy is only known in the two cases of $Cr(acac)_3$ and $Fe(acac)_3$. For this reason,

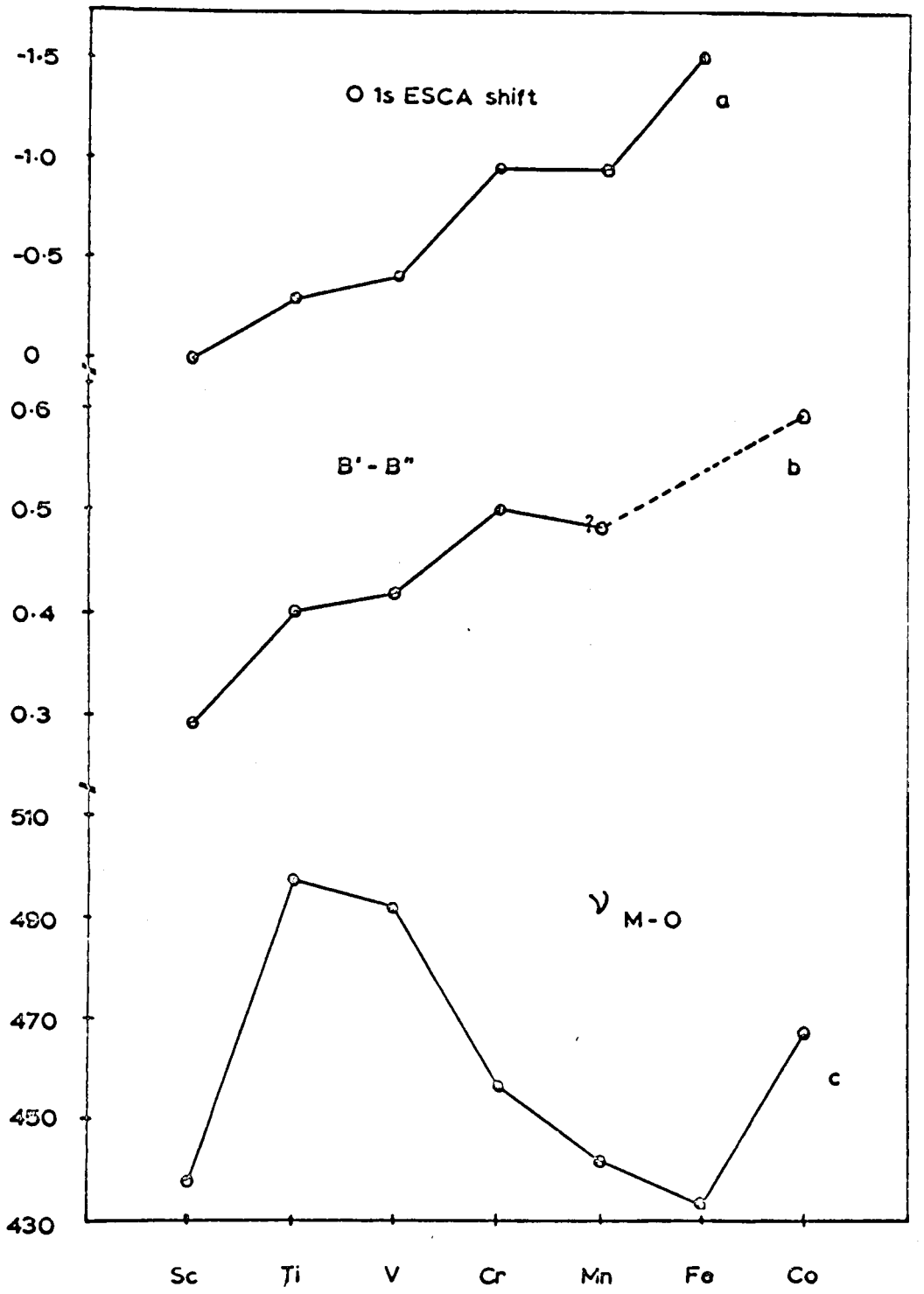

FIGURE 6.2a

a: O 1s ESCA shifts relative to $Sc(hfa)_3$

b: Separation of bands B' and B" in the UV-PE spectra of $M(hfa)_3$

c: Stretching frequency ν_{M-O}

fig. 6.2 shows the variation of the upper level across the first series. The values for $Sc(acac)_3$, $Ti(acac)_3$ and $V(acac)_3$ were obtained from the work of Hancock and Thornton, though since these latter authors reproduced no spectra, and gave no indications as to the reasons for their assignments, the values are somewhat doubtful. In fig. 6.2a are also plotted the splitting between bands B' and B" in the UV-PE spectra of the tris-hexafluoroacetylacetonato complexes, and the shift observed in the O 1s level in the ESCA spectra, both as a measure of σ-covalency and charge shift patterns. It can be seen that there is an inverse correlation for titanium, vanadium and chromium suggesting that the more ionic the bond, the larger the stretching frequency and, neglecting the variation in mass, the larger the force constant. As might have been expected, scandium does not fit this trend, presumably because although the bond is certainly the most ionic, there is a substantial expansion in the bond length on going from $Ti(acac)_3$ to $Sc(acac)_3$ giving rise to a concomitant drop in the force constant. The sequence is broken at manganese since, although the net covalence of the tris-chelate is lower than expected, the fact that we are populating an M-O antibonding σ orbital will presumably act in the opposite direction, weakening the bond as compared to $Cr(acac)_3$. Similar considerations obtain for $Fe(acac)_3$ though the last member of

the series $Co(acac)_3$, has a much stronger force constant than the above analysis might suggest and the most likely explanation is that the greatly increased π bonding in this molecule has strengthened the Co-O bond.

The vibrations observed between 1600 and 1500 cm^{-1} have been assigned by Pinchas et al.[91] on the basis of an ^{18}O isotopic substitution, the upper level being found to be mainly the C=O stretching mode and the lower, by inference, mainly the C=C stretch. This assignment is at variance with Mikami's calculations which indicated that in $Fe(acac)_3$ the band at 1570 cm^{-1} was 70% C=C stretch and that at 1525 cm^{-1} 45% C=O stretch, though their qualitative conclusion, that there is very substantial coupling between the two modes must be correct. For that reason, the two frequencies and their mean are plotted in fig. 6.2b. It can be seen that the mean vibrational energy varies very little across the series, which is very surprising, and must indicate that the major contribution to the bonding to the metal arises from orbitals which, in the ligand anion, are non-bonding. These are precisely those orbitals $n_{\pm}$ and π_3 which we have considered to be the prime bonding orbitals in interpreting the UV-PE spectrum, and it can be seen that the IR spectrum provides a justification for this. On this simple theory, the coupling between the modes is represented by the energy separation between the two bands and in the upper

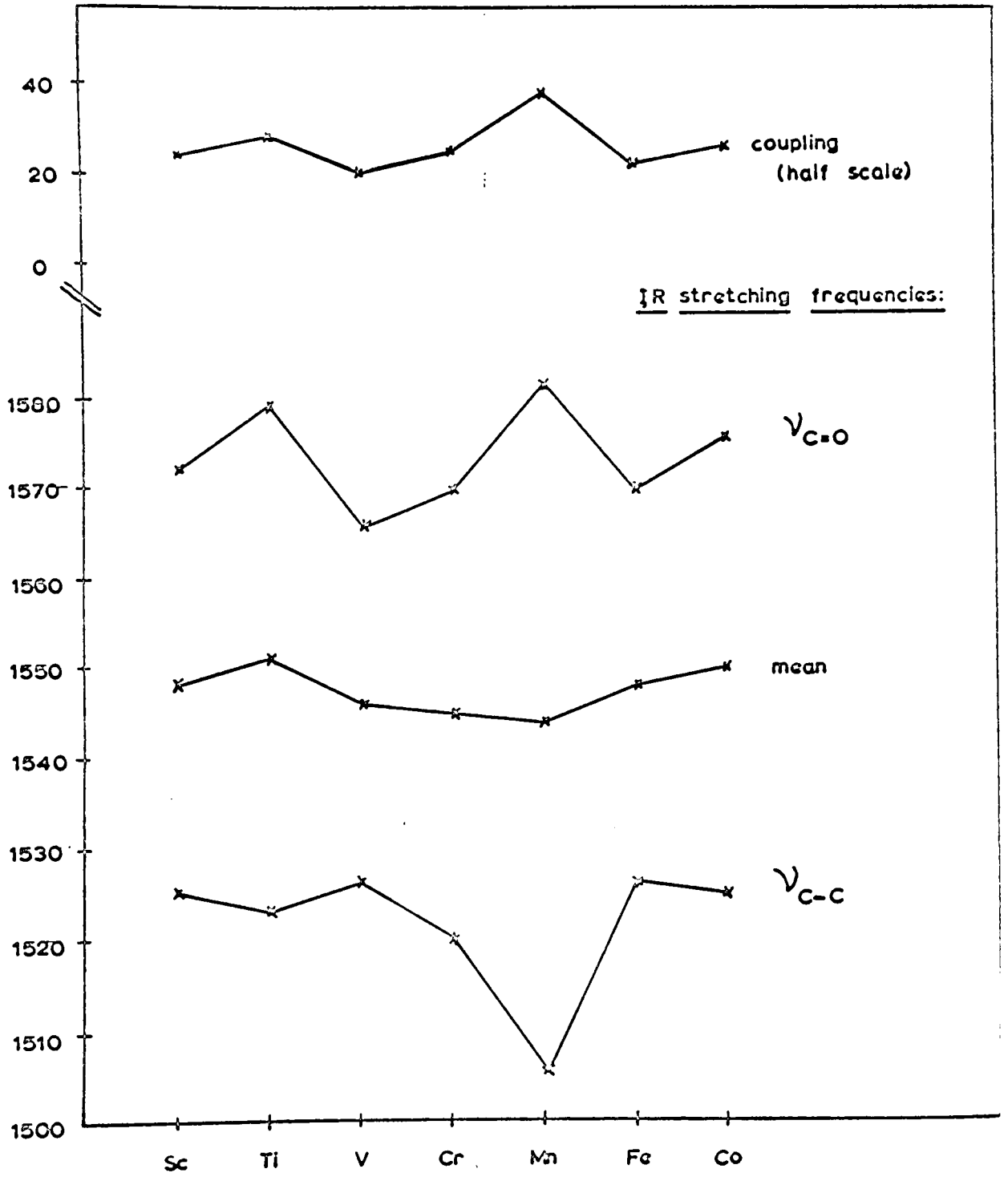
40
20
0
coupling
(half scale)
IR stretching frequencies:
1580
1570
1560
1550
1540
1530
1520
1510
1500
$\nu_{C=O}$
mean
ν_{C-C}
Sc
Ti
V
Cr
Mn
Fe
Co

FIGURE 6.2b

part of fig. 6.3 is plotted one half of this coupling. It is evident that the main coupling is found in $Mn(acac)_3$, presumably because of vibronic effects expected for the d^4 system, which, whilst lower than for many Mn(III) compounds, are rather higher than its neighbours. The variation in the extent of coupling is otherwise difficult to understand on simple electronic grounds and presumably represents the interaction of factors not normally considered in electronic analysis.

Thermodynamic data

The thermodynamic stability of any molecule is dependent on two factors, the entropy and enthalpy of formation, the former of which we have no means of determining or correlating using the PES data which has been presented here. To reduce its importance to a minimum in any comparison across the first row, we will consider the energetics of such processes as

$$M^{3+} + 3L^{-}(g) \rightleftharpoons ML_3(g)$$

which, hopefully, have the same entropy change for each metal. Now, the total energy of a molecule M is given by

$$E_M = \sum (h_i + \varepsilon_i) + N$$

where h_i is the one-electron part and ε_i the orbital energy of a particular MO, and N the total nuclear repulsion energy, which will vary from complex to complex. This energy expression only holds for closed-shell molecules; for open-shell species, various correction factors have to be included. It follows that the movements of individual molecular orbitals are not related in any simple manner to enthalpies of formation. Some simplifications can however be made. We will first partition the electronic energy into core and valence parts, such that

$$E = E_{core} + E_{val}$$

Consider the core orbitals. We saw that the orbital energy inferred from Koopmans' theorem was given by an expression of

the form

$$\varepsilon_i^A = k_i^A q_A + \sum_B q^B/r_{AB} + l_i^A$$

where, for the i^{th} core orbital on centre A, l_i^A is the zero-point referred to a standard charge distribution, which may be taken as neutral. We consider the molecule as a centre Z surrounded by ligands A, such that

$$\varepsilon_j^Z = k_j^Z q_Z + \sum_A q^A/r_{AZ} + l_j^Z$$

$$= -\sum_A q_A k_j^Z + \sum_A q^A/r_{AZ} + l_j^Z$$

where $q_Z = -\sum_A q_A$ and we have assumed electroneutrality. The core energy is given by

$$E_{core} = \sum_A \sum_i \varepsilon_i^A + \sum_j \varepsilon_j^Z + \sum_A \sum_i k_i^A + \sum_j k_j^Z$$

and if we make the assumption that $h_i^B = k_i^B + l_i^B$

$$E_{core} = \sum_A \sum_i (k_i^A + k_i'^A) q_A + \sum_{i,A,B} q_i^B/r_{AB} + \sum_{A,i} q_i^Z/r_{AZ} +$$

$$\sum_{A,i} (l_i^A + l_i'^A) + \sum_j k_j^Z q_Z + \sum_{j,A} q^A/r_{AZ} +$$

$$\sum_j k_j'^Z q_Z + \sum_j (l_j^Z + l_j'^Z)$$

$$\frac{\partial E_{core}}{\partial q_A} = \sum_i (k_i^A + k_i'^A) + \sum_{i,B} 1/r_{AB} - \sum_{i,B} 1/r_{BZ} - \sum_j k_j^Z$$

$$+ \sum_j 1/r_{AZ} - \sum_j k_j'^Z$$

Now

$$E = E_{core} + E_{val} \quad ; \quad \frac{\partial E}{\partial q_A} = \frac{\partial E_{core}}{\partial q_A} + \frac{\partial E_{val}}{\partial q_A}$$

but, since the system is in charge equilibrium

$$\partial E / \partial q_A = 0. \quad \text{for all } q_A$$

hence

$$\sum_A q_A \frac{\partial E}{\partial q_A} = 0 = \sum_A \frac{\partial E_{val}}{\partial q_A} q_A + \sum_A \frac{\partial E_{core}}{\partial q_A} q_A$$

$$= \sum_A q_A \frac{\partial E_{val}}{\partial q_A} + E - E_{val} - \sum_{A,Z,i} (\ell_i^A + \ell_i'^A)$$

and, finally

$$E = E_{val} + \sum_{A,Z,i} (\ell_i^A + \ell_i'^A) - \sum_A q_A \frac{\partial E_{val}}{\partial q_A}$$

Consider now the heat of formation of a given molecule from neutral Z and neutral ligands A. The electronic energy of the reactants is

$$E_r = \sum_{A,Z,i} (\ell_i^A + \ell_i'^A) + E_{val}^A + E_{val}^Z$$

and, the electronic heat of formation is thus

$$E - E_r = \Delta E_{val} - \sum_A \frac{\partial E_{val}}{\partial q_A} \cdot q_A$$

That is, the heat of formation does not depend explicitly on the core orbital energies. ΔE_{val} is the valence energy difference of neutral reagents and the molecule in which the charge separation has been adjusted to the equilibrium value. The term $\sum_A q_A \frac{\partial E_{val}}{\partial q_A}$ is thus the correction term to bring the valence energy back to neutralisation. The nuclear repulsion term is more difficult to deal with rigorously, but we will treat it simply as the net change from neutrality, so

$$R = \sum'_{A,B,Z} \frac{q_A q_B}{r_{AB}}$$

where the primes indicate that we sum over each pair of atoms once only. The overall heat of formation is thus

$$\Delta H = \Delta E_{val} - \sum_A q_A \frac{\partial E_{val}}{\partial q_A} + R$$

For a closed-shell molecule we can write

$$E_{val} = \sum_i \varepsilon_i + h_i$$

assuming that $h_i = k_i \varepsilon_i$

$$E_{val} = \sum_i \varepsilon_i (1 + k_i)$$

and for the neutral species

$$E_r = \sum_j \varepsilon'_j (1 + k'_j)$$

and so

$$\Delta H = \sum_i \varepsilon_i (1 + k_i) - \sum_j \varepsilon'_j (1 + k'_j) - \sum_A q_A \frac{\partial E_{val}}{\partial q_A} + R$$

This may be simplified as follows:

(i) If the system is near electroneutrality, we have

$$R = 0, \quad \sum_A q_A \frac{\partial E_{total}}{\partial q_A} = 0 ,$$

$$\Delta H = \sum_i \varepsilon_i (1 + \delta_i) - \sum_j \varepsilon_j (1 + \delta_j)$$

Thus, for molecules such as the hydrides, the bond dissociation energy will clearly be related to the orbital energies of those orbitals primarily involved in bonding to the hydrogen atoms, and to the ionisation potential of the neutral atom (though the relationship will not be very simple owing to open shell effects).

(ii) For the diatomic hydrides more information is available. Price et al. showed that there was a correlation between the dissociation energy of $H_{n+1}X^+$, and the ionisation energy of H_nX, and between the dissociation energy of $H_{n+1}X^+$ and that of H_nY, where Y is the element prior to X in the peridic table. These correlations are not perfect but do extend, for the diatomic hydrides, over a considerable area of the peridic table. For later rows of the table, the best correlation seems to be between the dissociation energy of HX and the ionisation potential of Z, the element following X in the table. This is rather surprising since for the IA hydrides, the only valence

orbital is the main bonding orbital, but for the others, the highest occupied orbital is one of the p_π lone-pair orbitals, or, for earlier members, an antibonding s orbital strongly mixed with p character. This correlation is probably explicable on the basis of a united-atom approach, though it is not immediately obvious how the formalism developed above can help. In fig. 6.3 the dissociation energy of HX is plotted with the ionisation potential of HX and there can be seen to be only a poor correlation between the two results, but fig. 6.4. shows that there is a much better correlation between the IE of the hydrides and the sum of the ionisation potentials of elements X and Z, especially in the later part of the series where we are ionising non-bonding p_π electrons. This would imply that

$$\varepsilon_i^{XH} \propto \varepsilon_X + \varepsilon_{X+1}$$

so that

$$\varepsilon_i^{XH} - k\varepsilon_X \propto \varepsilon_{X+1}$$

where k is some constant. This is similar to our expression for the enthalpy derived above, so the correlation between dissociation energy and ionisation potential, can be reduced to a correlation between IE's. This is, of course, by no means an explanation of this curious and interesting observation, though it is perhaps

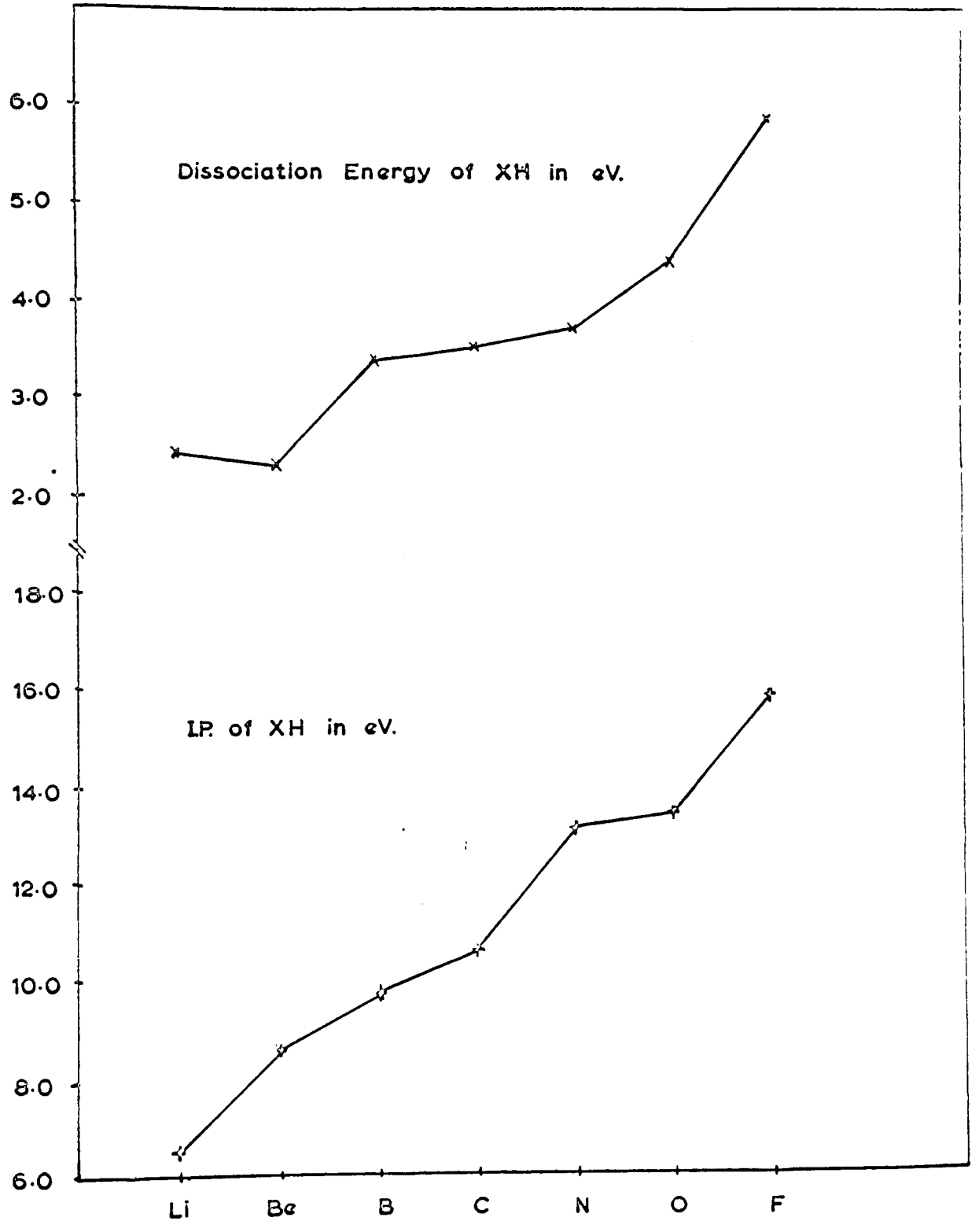
Dissociation Energy of XH in eV.
I.P. of XH in eV.
6·0
5·0
4·0
3·0
2·0
18·0
16·0
14·0
12·0
10·0
8·0
6·0
Li
Be
B
C
N
O
F

FIGURE 6.3

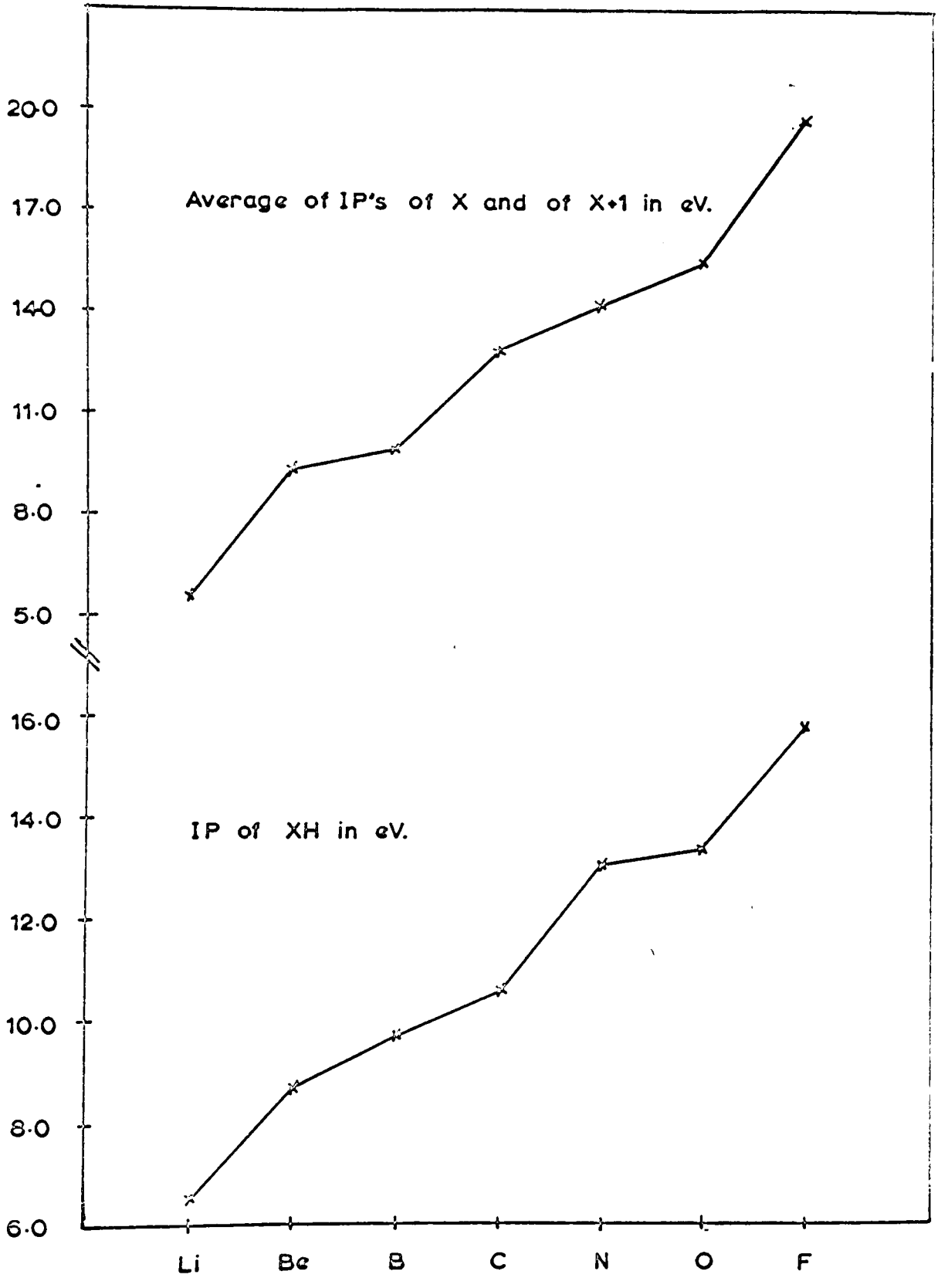
20·0
17·0
14·0
11·0
8·0
5·0
Average of IP's of X and of X+1 in eV.
16·0
14·0
12·0
10·0
8·0
6·0
IP of XH in eV.
Li
Be
B
C
N
O
F

FIGURE 6.4

not wholly surprising that the properties of the non-bonding orbital of XH should be intermediate in behaviour between those of atoms X and X+1, especially as the dipole moments for BH - FH are all fairly large (1.3 - 1.8 deb.). Since the dipole moment is zero for BeH we have correlated this with the neutral Be IP in fig. 6.4.

The difficulties experienced above in trying to interpret the trends in the simple hydrides does indicate that only the most general comments can be made concerning the heats of formation of the tris-chelate complexes of the transition elements. The large number of bonding orbitals and the open-shell nature of the complexes themselves make the use of simple formulae very dangerous.

A plot of the heterolytic bond strength, defined as $\Delta H^\circ/6$, where ΔH° is the heat of the reaction

$$M^{3+} + 3(acac)^- = M(acac)_3$$

is shown in the lower part of fig. 6.5.[105] The value for $Ti(acac)_3$ is that estimated by Jones and Wood.[103] It can be seen that the values of 10Dq calculated using the methods of George and McClure[102] compare rather poorly with the spectroscopic values given in table 6.2.

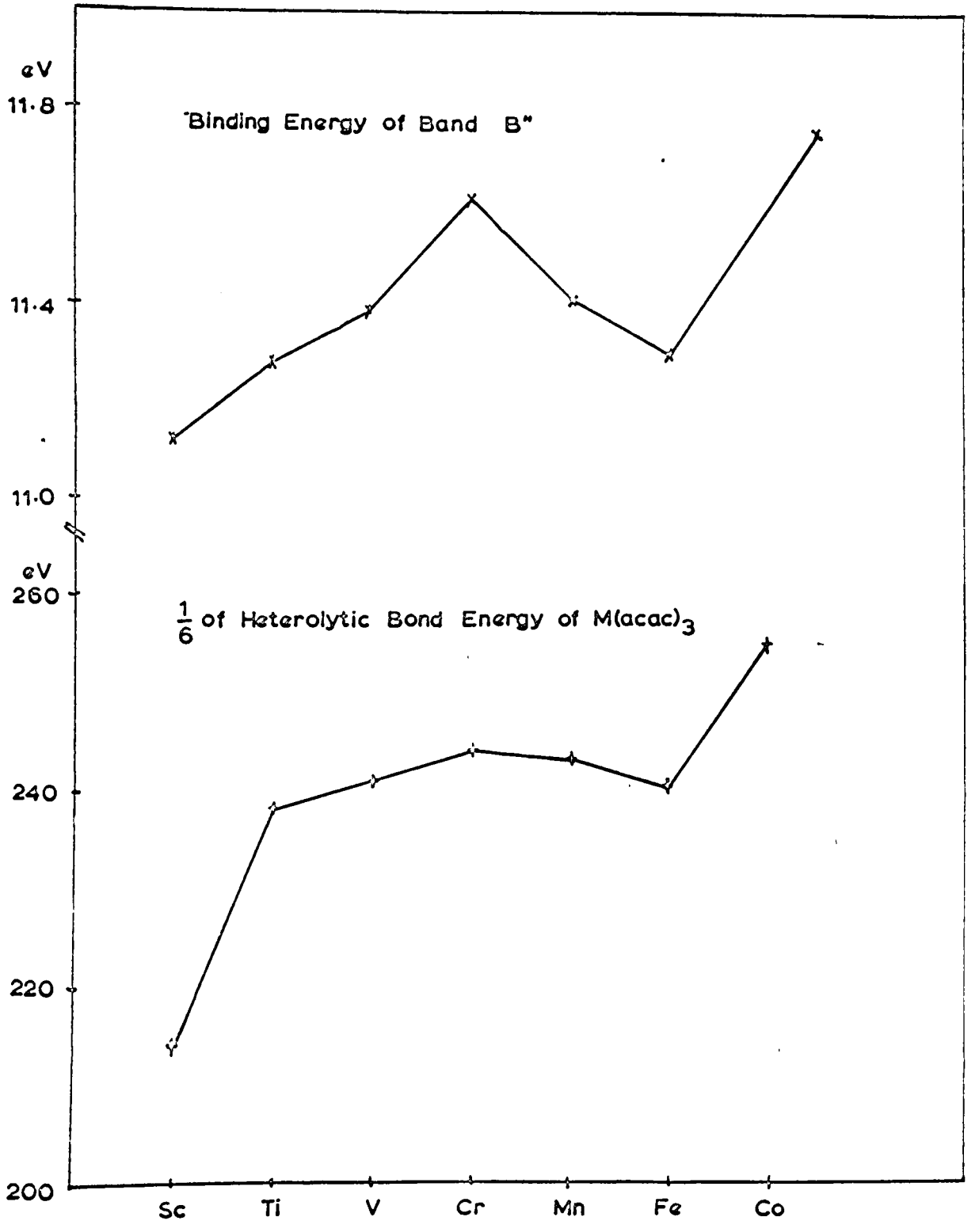
eV
11·8
11·4
11·0
Binding Energy of Band B"
eV
260
240
220
200
1/6 of Heterolytic Bond Energy of M(acac)3
Sc
Ti
V
Cr
Mn
Fe
Co

FIGURE 6.5

TABLE 6.2

Cmpd.	10 Dq (k.m^{-1})	
	Thermal	spectral
$Ti(acac)_3$	(270)	40
$V(acac)_3$	100	51.5
$Cr(acac)_3$	52.1	51.8
$Mn(acac)_3$	25.8	48.6

Especially for the earlier members of the series agreement can be seen to be particularly bad. George and McClure have already noted this effect in the heats of formation of the trivalent halides and ascribed it at that time to an erroneous value for Sc^{3+}. It is however explicable, as is the remaining data for scandium, on the basis of a considerable contraction between Sc^{3+} and Ti^{3+}, which has the effect of rendering Sc^{3+} salts less stable than might have been expected. The reasons for this contraction are rather difficult to understand. It may be, as was suggested in the discussion of the UV-PE spectrum of $Sc(hfa)_3$, that 4s and 4p orbitals make a substantial contribution to the bonding in Sc^{3+} compounds, and, since the spatial extension of these orbitals is substantially greater than that of the 3d orbitals, optimal overlap with the ligand orbitals may only be attained at anomalously high metal-ligand bond-lengths. On a more quantitative level little further information can be gained at the moment, though a plot of the

energy of the main ligand bonding orbital B″ across the series shows a remarkable correlation with the heterolytic bond energy, as is apparent from fig. 6.5. This is a rather interesting observation, though certainly fortuitous, in that it suggests that the effect of increasing IE on the central metal, which makes the major contribution to the observed bond energy, can be reflected by an indirect barometer, whose interaction with the d-orbitals is well represented by a Brillouin-Wigner formula of the type discussed above.

The charge on the metal

If we plot the observed IE's of the various transition elements from Sc to Co for the first three oxidation states, a family of curves, shown in fig. 6.6, is obtained.[116] We now construct the line AB, which represents the destabilisation of the central metal d-orbitals due solely to the potential generated by the (negative) ligands. Thus the first point on AB, at 7.2 eV, represents the potential of six charges, of magnitude 1/6 e, each placed 2Å from the central metal. This potential must be added to the metal ionisation energy to obtain the ionisation energy which the metal would have in the absence of the ligands. (We should, of course, subtract 4Dq, but the figures quoted above indicate that 10Dq is approximately constant across the series, and 4Dq is comparatively small so that a small but constant correction will be needed). This is clearly a problem best solved by graphical construction, and so horizontal lines, whose lengths are the observed IE's of the d-orbitals in the complexes, are drawn so that they just join the potential line and the free metal IE curves. The corresponding charge is then that of the metal in the complex. For the three metals Ti, V and Cr, it is observed that the free ion IE has the same value; that is, the charge distribution within the tris-chelates appears to adjust itself in such a way as to render it equally difficult to transfer

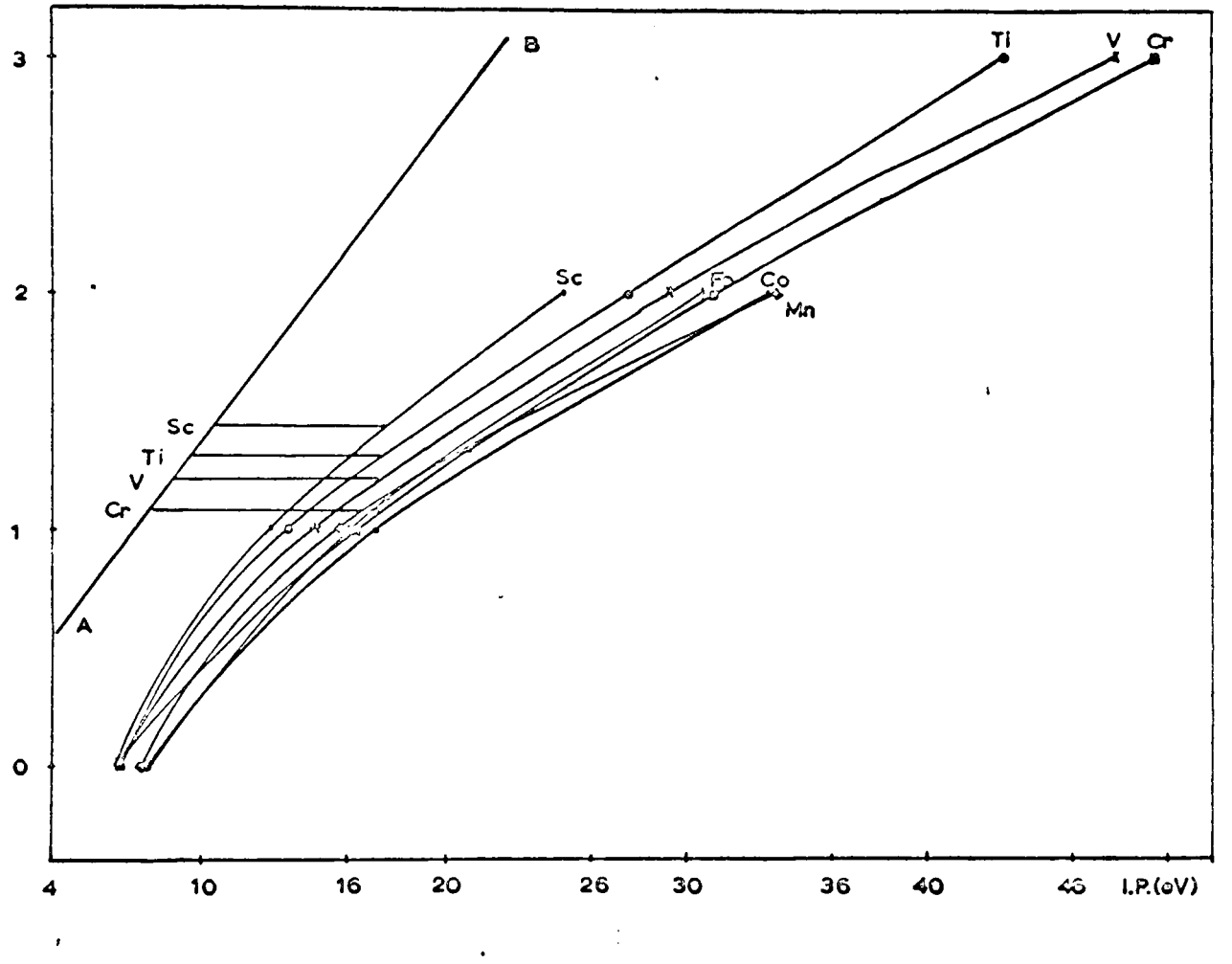

FIGURE 6.6

electrons from the metal. This is clearly related to Sanderson's electronegativity principle, the ligands in effect acting as an electron sponge over a small charge range, so that the distribution of charge is solely dependent on the metal electronegativity, itself a function of the ionisation energy, which adjusts itself to equality in each case. The line for scandium has been drawn in assuming that the same principle holds, and the resultant charges are Sc, +1.43; Ti, +1.30; V, +1.21; and Cr, +1.07 electron units. These charges are plotted against the O 1s shift and the position of band B" in fig. 6.7, and the suggestion that vanadium was slightly more ionic than might have been expected can be seen to be strongly reinforced.

The technique unfortunately will not work for Mn(III) and Fe(III) since spin pairing in the atoms leads to some rather complex behaviour, nor will it work for lower charged species such as the acetylacetonates, since the first IP of the earlier members of the series refers to the 4s rather than 3d orbital. The correction for the second IP, in those cases where the 4s orbital is still occupied in M^+ can be shown, by an examination of Moore's tables to be negligible. To obtain reasonable charges for the acetylacetonates the d-orbital energy must be calculated for the neutral metals from Moore, but figures have not been included here since there is

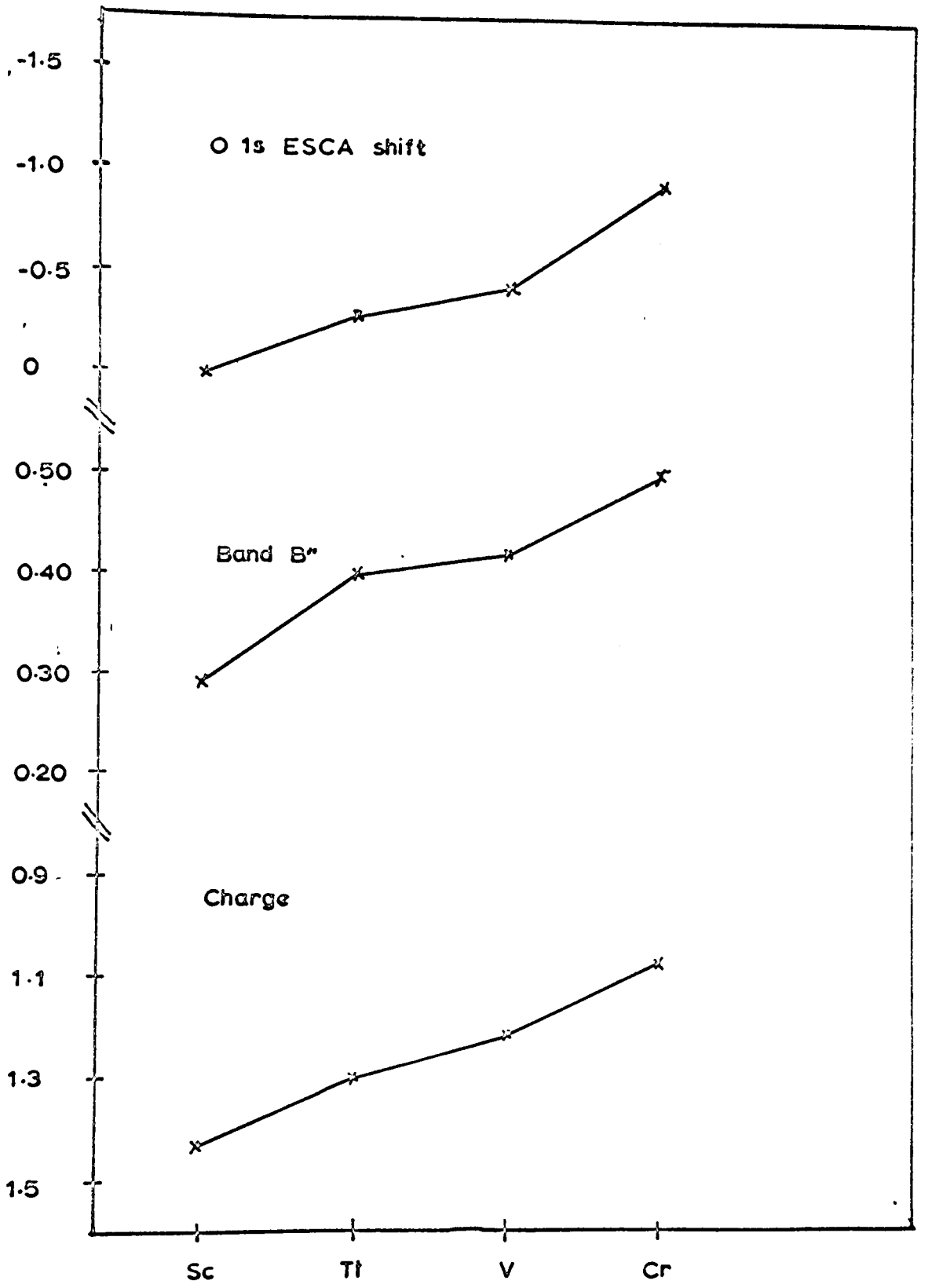
-1·5
-1·0
-0·5
0
0·50
0·40
0·30
0·20
0·9
1·1
1·3
1·5
O 1s ESCA shift
Band B"
Charge
Sc
Ti
V
Cr

FIGURE 6.7

insufficient experimental data from PES work.

A fundamental difficulty with this technique is that the IE's measured for the free ions will require various amounts of spin-randomised correction. Thus, in considering the behaviour of vanadium, the first metal d-ionisation is $d^5 \rightarrow d^4$ at 4.27 eV corresponding to the process $^6S \rightarrow {}^5D$. However, the spin of $V(acac)_3$ is unity; moreover some of the spin will be delocalised onto the ring in such a way as to increase the multiplicity of the central metal and hence the spin-randomised correction, but also introducing a negative correction from the β-spin on the oxygens. It is not possible in any simple way to calculate all these terms and therefore the values given for the charges above should only be taken as indicative.

Energy levels across the first transition series

Finally, in this chapter, we will examine the variation in orbital energy of all the UV-PE bands across the transition series. Without the preceding exposition it would have been very difficult to make even qualitative remarks about the variation of the ligand bands, but many of the trends are now self-evident. Consider first the trends shown by the band we have assigned to $e_2(n_+)$. This bonds quite strongly to both metal e_a and e_b orbitals and can be seen to stabilise steadily from scandium to chromium, with a break at vanadium. At manganese, a discontinuity is observed, traceable presumably to initial occupation of the e_g^* orbital, delocalising negative charge over the ring and thus causing a general destabilisation of all the orbitals. This is also the case for iron, where increasing bonding and increased delocalisation can be seen to have partially cancelled. The rapid stabilisation at cobalt is of course explicable as a result of the complex becoming low-spin $a_1^2 e_a^4$, and the d-electrons no longer being extensively delocalised onto the ring.

The zig-zag behaviour of the less important bonding orbitals is seen most clearly in the trend shown by π_3. It is clear that this orbital is extremely sensitive to ligand charge in general. Thus, it is much less stable in $V(hfa)_3$ than might have been expected on covalency grounds, presumably

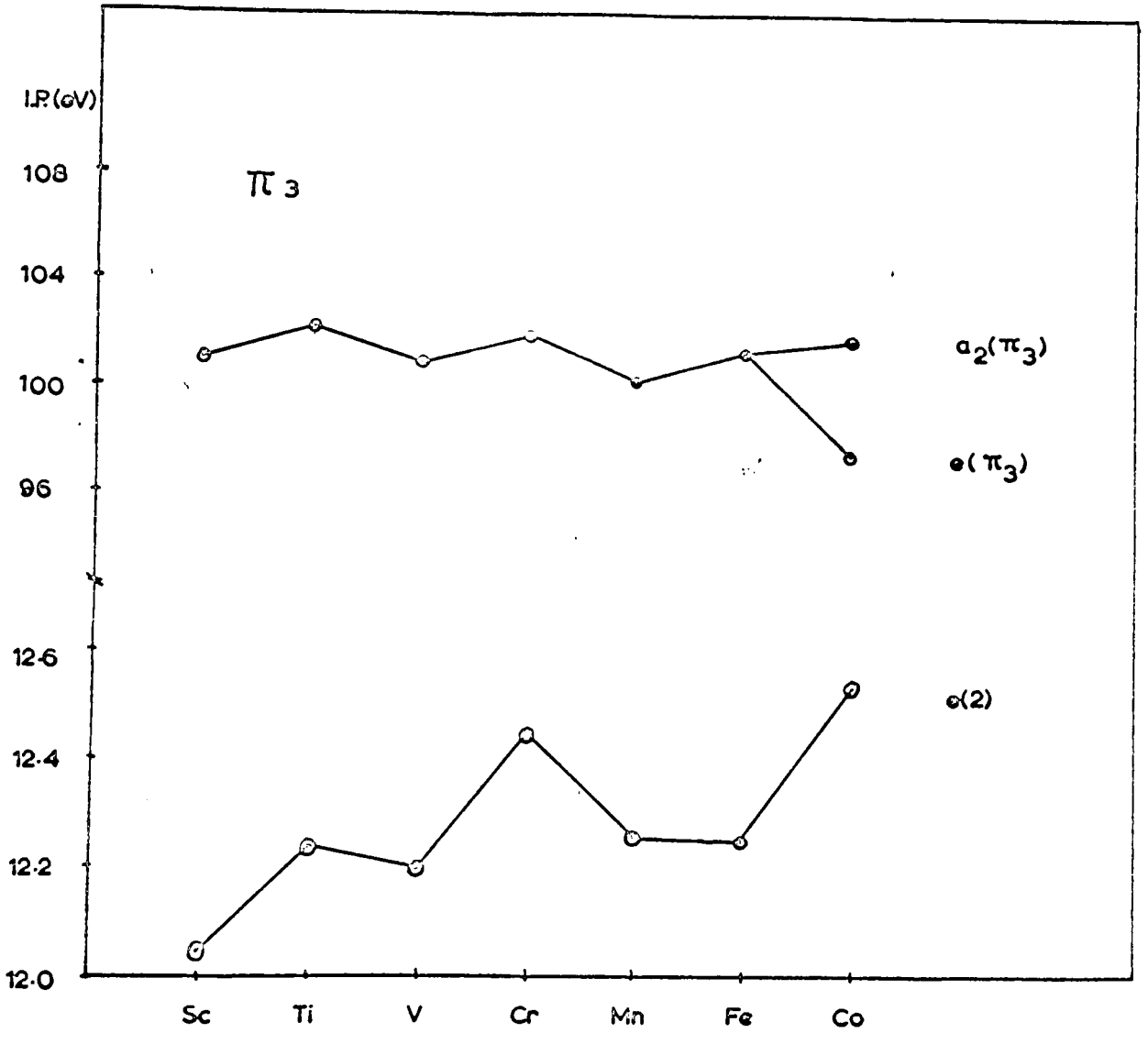
I.P.(eV)
108
104
100
96
12·6
12·4
12·2
12·0
π_3
$a_2(\pi_3)$
$e(\pi_3)$
e(2)
Sc
Ti
V
Cr
Mn
Fe
Co

FIGURE 6.8a

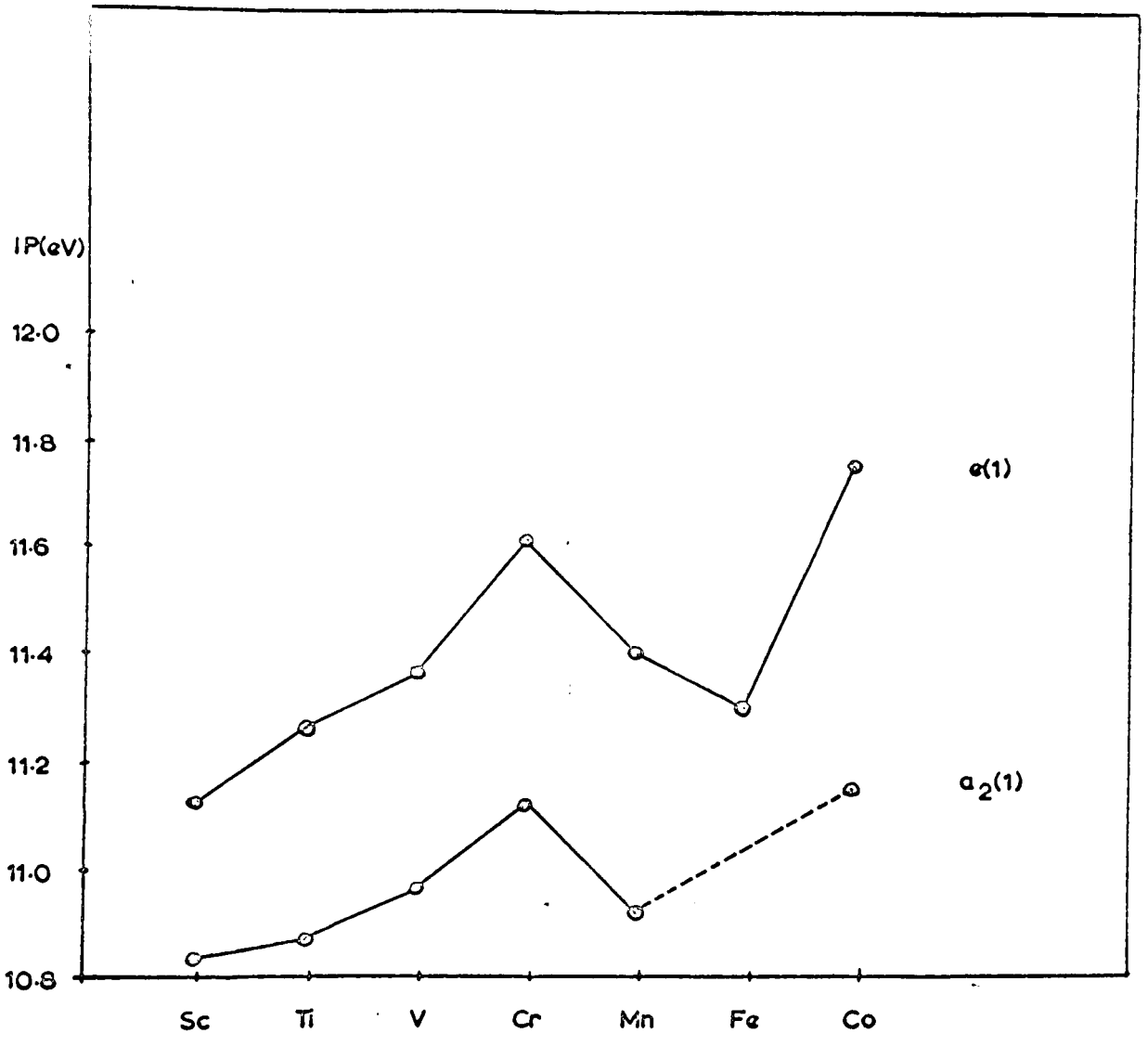

FIGURE 6.8b

since the small delocalisation of the $e_a(\pi)$ orbital onto the ring is found to be largest in $V(hfa)_3$. To see how this might be so we must consider the two effects at work, firstly an electron repulsion effect favouring π delocalisation and the metal electronegativity effect favouring π-donation from ligand to metal. The latter effect appears to dominate in $Cr(hfa)_3$ and in $Ti(hfa)_3$ the former effect is not present in first order; only in the case of $V(hfa)_3$ is the electron repulsion sufficiently dominant to allow the complex to exhibit what is, apparently, anomalous ionicity. The destabilisation of the π_3 level at manganese is understood as above, but, unlike the other orbitals, the π_3 level destabilises at cobalt, an effect which can easily be traced to interaction with the more stable d-orbitals on the central metal.

The orbital energies found for the scandium complex are rather more stable than would have been predicted in comparison to the later members of the series. In particular, the energy of the π_3 orbital is comparable to that in $V(hfa)_3$, and the reason is probably that polarisation of this orbital in passing from $Sc(hfa)_3$ to $Ti(hfa)_3$ causes the electron repulsion and kinetic energy to increase, destabilising the π_3 orbital to some extent as compared to the additional stability gained from the potential term. In other words, there is a fairly substantial change in the <u>orbital</u> π_3 between $Sc(hfa)_3$ and

the remaining members of the series. The same remarks probably apply to the main bonding orbital e(1) which may be destabilised in the later members of the series by increased repulsion with π_3.

In fig. 6.9 are plotted the three main valence bands u, v, and k of the ESCA spectra of the tris-chelates. Comparison with the UV-PE spectra indicates that all three vary in a manner closely similar to π_3. We have assigned these bands primarily to F 2p, and the parallel with π_3 strongly suggests that the π-interaction extends, in the ligands, right over the F 2p orbitals as was postulated in the discussion of the UV-PE spectrum of the free ligand, to account for the anomalously high intensity of the π_3 orbital as compared to acetylacetone. It might be argued then that such an interaction invalidates the use of F 1s as a marker, but, since the effect on the $\underline{C}F_3$ C 1s will be at most second order, and the F 1s and F 2s do not shift sensibly relative to the $\underline{C}F_3$ carbon from complex to complex, it appears that the variations in F 2p are only transmitted to a very small extent to the s orbitals.

Also plotted in fig. 6.9 are the O 2s levels (t) which do not follow any obvious pattern, possibly since they are intermediate in behaviour between core and valence orbitals.

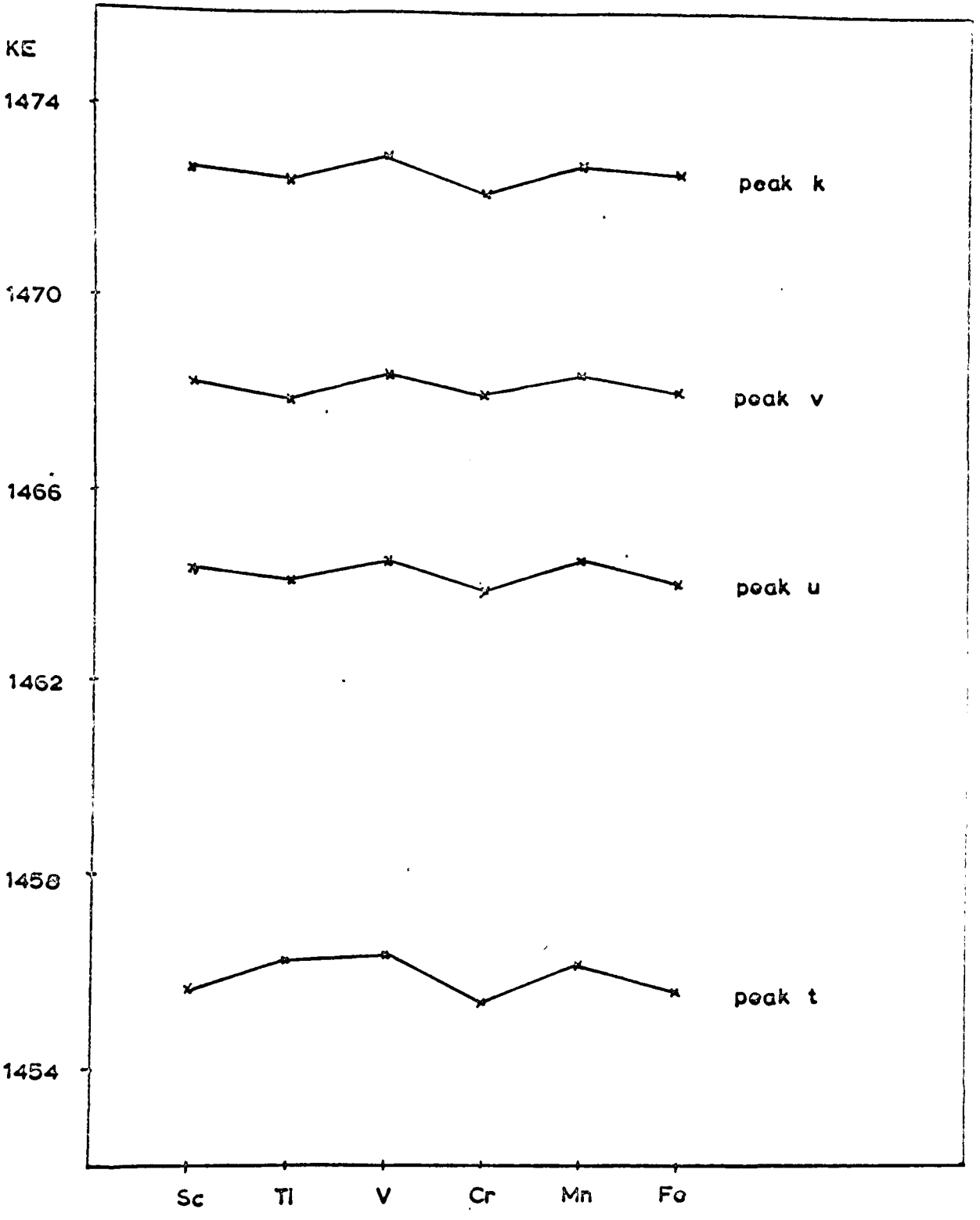
KE
1474
1470
1466
1462
1458
1454
peak k
peak v
peak u
peak t
Sc
Ti
V
Cr
Mn
Fe

FIGURE 6.9a

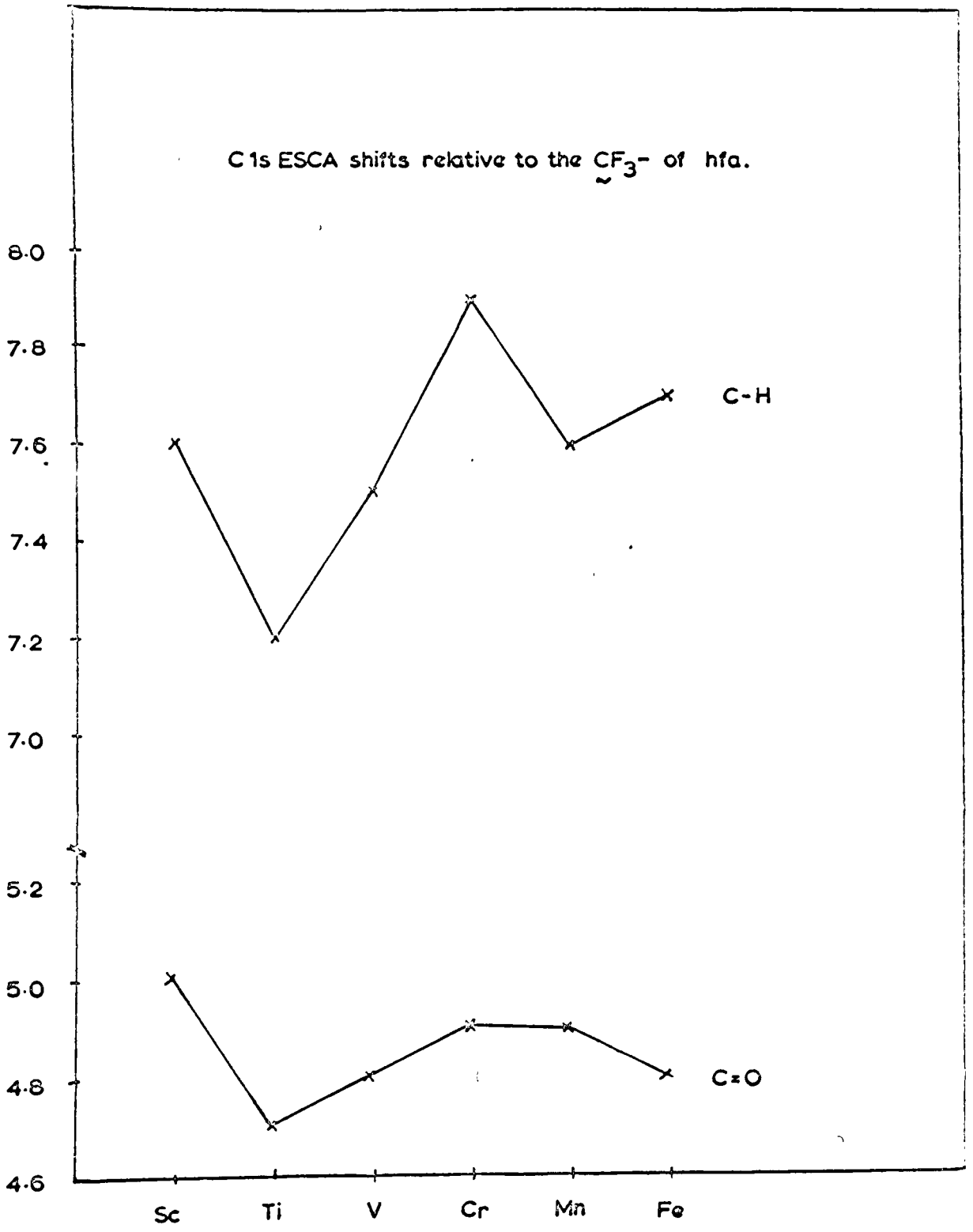
C 1s ESCA shifts relative to the CF_3- of hfa.
8.0
7.8
7.6
7.4
7.2
7.0
5.2
5.0
4.8
4.6
C-H
C=O
Sc
Ti
V
Cr
Mn
Fe

FIGURE 6.9b

SUPPLEMENTUM

Vether it's worth goin' through so much to learn so little, as the charity boy said ven he got to the end of the alphabet, is a matter o' taste.

Charles Dickens
Pickwick Papers

SUPPLEMENTUM

In this last section of the thesis, a simple theory of photoionisation cross-sections will be developed, whose results have been used throughout the interpretative sections. The analysis is based in part on the studies of a number of earlier workers, especially Cooper and Zare, but is extended to cover the cases where variation of fractional intensities with angle is required.

Consider the expression for the photoionisation cross-section:

$$\sigma_{AB} = \frac{8\pi^3\nu}{3c} \cdot \frac{1}{\omega_A} \sum_{A,B} |\langle A|\underset{\sim}{P}|B\rangle|^2$$

where A is the initial state, of degeneracy , and B the final state comprising ion and continuum electron. P is the electric dipole operator

$$-e \sum_i^N \underset{\sim}{r}_i$$

and N the number of electrons. A fairly good approximation is to expand A and B in terms of Slater determinants of individual atomic or molecular orbitals, and, to do this, we define for A a grand-fractional parentage coefficient (G.F.P.), such that, if A can be written as:

$$|A\rangle = \Pi_i a_i^{n_i}$$

we have, for ionisation from the $j^{\underline{th}}$ MO or AO

$$|A\rangle = \sum_{S_1 T_1} \left(a_1^{n_1} \ldots a_j^{n_j - 1} \ldots a_x^{n_x}(S_1 T_1) \cdot a_j(S_A T_A)\right) \left\{\Pi_i a_i^{n_i}(S_A T_A)\right\} \left|a_1^{n_1} \ldots a_j^{n_j - 1} \ldots a_x^{n_x}(S_1 T_1) \cdot a_j\right\rangle$$

$$= \sum_{S_1 T_1} (g.f.p.) \left|a_1^{n_1} \ldots a_j^{n_j - 1} \ldots a_x^{n_x}(S_1 T_1) \cdot a_j(S_A T_A)\right\rangle$$

where standard symbols have been used, and the full-stop in the wavefunction implies that there is no antisymmetrisation between the two parts. In order to proceed we must integrate out the spin part of the wave function:

$$\left|a_1^{n_1} \ldots a_j^{n_j - 1} \ldots a_x^{n_x}(S_1 T_1) \cdot a_j(S_A T_A)\right\rangle = \sum_{M_{S_1} m_{S_j}} \left|a_1^{n_1} \ldots a_j^{n_j - 1} \ldots a_x^{n_x}(T_1) \cdot a_j(T_A)\right\rangle \left\langle S_1 \tfrac{1}{2} M_{S_1} m_{S_j} \middle| S_1 \tfrac{1}{2} S_A M_{S_A}\right\rangle$$

In a similar way, we may consider B as the coupled part of a core function $S_2 T_2$, and a continuum orbital $\chi_c(\underset{\sim}{r}, m_{S_c}, T_c, \mu_{T_c})$ and we couple over the spins here to obtain

$$|B\rangle = \left|T_2 \cdot \chi(\delta)\right\rangle \sum_{M_{S_2}, m_{S_c}} \left\langle S_2 \tfrac{1}{2} M_{S_2} m_{S_c} \middle| S_2 \tfrac{1}{2} S_B M_{S_B}\right\rangle$$

where $|\Gamma_2 \cdot \gamma(\delta)\rangle$ is an abbreviation for the orbital coupled part of the state.

It follows that the cross-section for photoionisation is given by:

$$\sigma = \sum_{\substack{M_{S_A} M_{\Gamma_A} \\ M_{\Gamma_B}}} |\langle (\Gamma_1) \cdot a_j(\delta_j) | \underline{P} | (\Gamma_2) \cdot \gamma_c(\delta) \rangle|^2 \frac{8\pi^3 \nu}{\omega_{ac}} \sum_{S_1 \Gamma_1} (\varrho_{FP})^2_{S_1 \Gamma_1}$$

since spin selection rules demand that $M_{S_A} = M_{S_B}$, $S_A = S_B$. This expression may be simplified down using the Wigner-Eckart theorem to give finally (see appendix one) an averaged photoionisation cross-section:

$$\bar{\sigma} = \frac{8\pi^3 \nu}{3c} (\varrho_{FP})^2_{S_2 \Gamma_2} |\langle \gamma_{a_j} \| P \| \gamma_c \rangle|^2$$

where the major slsection rule is simply that; for an ion state to be formed on photoionsation of the molecule or atom ground state $S_A \Gamma_A$, the coefficient of fractional parentage containing the state $(S_2 \Gamma_2)$ in the expansion of $|A\rangle$ must be non-zero. The relationship between this formula and that derived by Cox et al. is discussed in appendix one. In both cases the definition of fractional parentage used should be renormalised to take into account the number of electron so that ionisation from the $a_j^{n_j}$ subshell will have a relative cross-section:

$$\bar{\sigma} = \frac{8\pi^3 \nu}{3c} n_j (\varrho_{FP})^2_{S_2 \Gamma_2} |\langle \gamma_{a_j} \| \underline{P} \| \gamma_c \rangle|^2$$

where $\underline{P}$ is the reduced tensor of rank unity corresponding to the dipole operator.

Now, in many cases the grand fractional parentage coefficient takes on a particularly simple form and, in the introduction, some cases of importance were discussed. In all such applications it is implicitly assumed that the reduced matrix elements $\langle \gamma_{a_j} \| P \| \gamma_c \rangle$ are at best only weakly dependent on the functional form of both orbitals. A great deal of evidence from He(I) PES and especially from ESCA suggests that this is very far from being the case. There has been some work, chiefly of astrophysical interest, on atomic ionisation cross -sections, in which the continuum orbitals have been specified in greater detail but this approach is difficult to extend to molecules since, as we shall see below, it is best to expand the continuum

orbital about one centre in the molecule which means that the Hartree-Fock solutions must also be transformed to an expansion about this centre to perform the necessary integrations. Even in the few cases where this has been done, quantitative agreement is disappointingly poor, since the neglect of CI in the molecular wave-function, whilst relatively unimportant as regards the total energy, has a drastic effect on the precise form of the wave-function, as does the implicit neglect of orbital rescaling in the moleculr ion.

However, the above theory is incomplete even within the framework of the single electron approximation used. We saw (appendix one) that it was necessary to sum over the J_B values to obtain a formula for $\bar{\sigma}$, since these J_B values were inherently unobservable within the PE technique, essentially because the j_C values are unobservable. Let us consider the precise form of these orbitals more closely. A simple plane wave representation of the continuum orbital will have the form $\exp(i\underline{k}.\underline{r})$ where $\underline{k}$ is the wave vector of the continuum orbital and $\underline{r}$ its radial coordinate. Let us suppose that we are using polarised light to ionise an atom. Then we have two laboratory-defined axes; that of the direction of polarisation of the light, and that of observation of the emitted photoelectrons, and $\underline{r}$ will be measured relative to the former, $\underline{k}$ relative to the latter. Under these conditions, the plane wave may be expanded to give:

$$\exp(i\underline{k}.\underline{r}) = \sum_{l,m} 4\pi i^l j_l(kr) Y_{lm}(\theta,\phi) Y_{lm}^*(\beta,\alpha)$$

where θ,ϕ are the orientation angles of $\underline{r}$ and β,α those of $\underline{k}$ relative to the <u>same</u> space-fixed axes (those of the polarisation vector). The functions $j_l(kr)$ are modified Bessel functions of half-integral order,

$$j_l(kr) = \left(\frac{\pi}{2kr}\right)^{\frac{1}{2}} I_{l+\frac{1}{2}}(kr)$$

A more realistic orbital representation of the continuum may be obtained by modifying the radial part to allow for coulombic interaction. This gives a rather complicated function which we simply write as $G_l(kr$ so that we have, as the continuum orbital:

$$\chi_C = \sum_{l,m} a(l,m)\, \varphi_{l,m}(\theta,\phi).$$

where

$$a(l,m) = Y^*_{lm}(\beta,\alpha)\ ,\quad \varphi_{lm} = Y_{lm}(\theta,\phi)\,\varphi_l(kr)$$

Our final state Ψ_f may be written:

$$\Psi_f = \mathcal{A}\sum_{l,m} a(l,m)\,\Psi_{L_F M_{L_F}}\,\varphi_{lm}$$

where $\mathcal{A}$ is a suitable antisymmetrising operator whose form need not concern us. If A is the initial molecular state, and $S_F L_F$ the final state obtained by ionisation, then after some algebraic manipulation (appendix two) we may write

$$\bar{\sigma} = \frac{8\pi^3\nu}{3c}\sum_{l_1,l_2,m} a(l_1 m)\,a^*(l_2,m)\,(G^{FP})^2_{S_F L_F}\,|\langle l\|\underline{P}\|l'\rangle|^2 \begin{pmatrix} l_1 & 1 & l' \\ -m & 0 & m \end{pmatrix}\begin{pmatrix} l_2 & 1 & l' \\ -m & 0 & m \end{pmatrix}$$

where l is the angular momentum of the continuum orbital and l' that of the orbital from which ionisation has occurred and we have assumed that the reduced matrix element is independent of l. (Actually this assumption is not necessary, as Cooper and Zare point out, but it does help to simplify the algebra). If now a(l,m) is replaced by the spherical harmonic $Y_{lm}(\beta\alpha)$, and the resultant product expanded using the spherical harmonic addition theorem, it is not difficult to see that

$$\bar{\sigma} = \bar{\sigma}_t\,(1 + \gamma P_2(\cos\beta))$$

where $P_2(\cos\beta) = (3\cos^2\beta - 1)/2$, and

$$\bar{\sigma}_t = \frac{8\pi^3\nu}{3c}\,(G^{FP})^2_{S_F L_F}\,n_j\,|\langle l\|\underline{P}\|l'\rangle|^2$$

$$\gamma = \frac{5\sum_{l_1 l_2}(2l_1+1)^{\frac{1}{2}}(2l_2+1)^{\frac{1}{2}}\sqrt{\frac{2}{15}}\begin{pmatrix} l_1 & l_2 & 2 \\ 0 & 0 & 0 \end{pmatrix}\begin{Bmatrix} 1 & 1 & L \\ l_2 & l_1 & l' \end{Bmatrix}}{\sum_{\substack{l_1 l_2 \\ l_1 = l_2}}\begin{pmatrix} l_1 & l_2 & 0 \\ 0 & 0 & 0 \end{pmatrix}\begin{pmatrix} 1 & 1 & 0 \\ 0 & 0 & 0 \end{pmatrix}\frac{(2l_1+1)^{\frac{1}{2}}}{\sqrt{3}}}$$

The constant γ is called the asymmetry parameter, and measures the extent to which $\bar{\sigma}$ will vary with β, the angle of observation of the photoelectron to that of the polarisation vector of the exciting radiation. Even if the light is not polarised, the Poynting vector will provide an axis (normally not well-defined) and under these circumstances, if β' is the angle between the direction of $\underline{k}$ and that of the

incident radiation:

$$\bar{\sigma} = \bar{\sigma}_t \left(1 - \frac{\gamma}{2} P_2(\cos\beta')\right)$$

where $\bar{\sigma}_t$ and γ retain their values above. A few facts should be noted about the expressions above. Firstly they predict that γ will be independent of the precise form of the continuum orbital. This is a direct consequence of the assumption that the reduced matrix element is independent of the angular momentum value l. Secondly, experimental data is available for the atoms He and Ar. Consider the former; then $l' = 0$ and l is restricted to the value one. Under these conditions

$$\gamma = \frac{5.3.\left(\sqrt{\frac{2}{15}}\right)^2 \cdot \frac{1}{3}}{\frac{1}{3}} = 2$$

which agrees with the value quoted by Sampson. Sampson also obtained a value of ca. 0·3 for γ in the case of argon, where l' is unity and l may take the values 0 or 2. This agrees remarkably well with our theoretical value of 0·2, and undoubtedly the major source of error lies in the assumptions made in considering the reduced matrix element. Thirdly, the expression predicts that for open shell species, all states $S_F L_F$ obtained by ionisation from the orbital l' will have the same angular distribution pattern. An experimental test of this will undoubtedly indicate this simple form of reasoning based wholly on symmetry arguments has any quantitative validity.

Any theory of angular distribution in molecules is complicated by the presence of a molecular axis of symmetry and quantisation. The question has been carefully considered by Buckingham et al. for diatomic molecules and, essentially their conclusions are, that if rotational fine structure is not resolved, fromulae may be derived for such a molecule which are closely related to those derived above for atoms. Further developement of these formulae to obtain analogous equations for angular distribution will depend on the use of single centre expansions of the form

$$|\Gamma_i \epsilon\rangle = \sum_{l',m} C^{\Gamma_i}_{nl'} R_{nl,\epsilon} Y_{l'm}(\theta,\phi)$$

whence, the photoionisation cross-section is given by

$$\bar{\sigma}_t = \frac{8\pi^3\nu}{3c} n_i (g_{FP})^2_{S_i\Gamma_i} \left| \sum_{l'} \langle l \| \underline{P} \| l' \rangle C^{\Gamma_i}_{nl'} \right|^2$$

with a similar formula for the asymmetry parameter γ. It follows that the simple intensity pattern derived above for molecules depends on the constancy of such terms as $\langle l \| P \| l' \rangle$ in the expansion of $|\langle \gamma \| P \| l \rangle|^2$. Notice that the precise value of the total reduced matrix element $|\langle \gamma \| P \| l \rangle|$ depends critically on the relative phases of the components of the expansion and will be equal to the sum of the squares only fortuitously. The constancy of this expansion for different values of l will be most likely if the orbitals concerned are closely similar (such as those derived from non-bonding p-orbitals on the halogen atoms in MX_4 species) and where CI is unimportant.

As a final point, the argument is sometimes used that the intensity of a band, whilst not given accurately by the above formulae, might be used to give information about the MO composition of the orbital concerned. This presupposes two conditions:

(i) the photoionisation cross-section can be broken down into atomic or symmetry orbital contributions which remain effectively constant for different MO's,

(ii) all MO's are given by expansions of the form $\varphi + c_i\mu$ where φ and μ are AO's or SO's and the c_i real positive constants.

Unless these two provisos are fulfilled, no simple deductions about MO composition may be made.

Appendix 1

Consider the expression

$$\sigma = \sum_{M_{S_A} M_{\Gamma_A} M_{\Gamma_B}} |\langle (\Gamma_1) . a_j(\gamma_{a_j}) | \underline{P} | (\Gamma_2) . \chi_c(\gamma) \rangle|^2 \; k/\omega_A \sum_{S_1 \Gamma_1} (e_q F P)^2_{S_1 \Gamma_1}$$

P transforms as an irreducible tensor of rank unity. Let q label its components. Then the intensity reduces to a sum over q. We write $k = 8\pi^3 \nu / c$

$$\sigma = \sum_{\substack{M_{S_1}, q \\ M_{\Gamma_A} M_{\Gamma_B}}} |\langle (\Gamma_1) . a_j(\gamma_{a_j}) \| T^{(1)} \| (\Gamma_2) . \chi_c(\gamma) \rangle|^2 \; k/\omega_A \; \langle \Gamma_B \; 1 \; \Gamma_A M_{\Gamma_A} | \Gamma_B \; 1 \; M_{\Gamma_B} \; q \neq \rangle|^2 \sum_{S_1 \Gamma_1} (e_q F P)^2_{S_1 \Gamma_1}$$

which readily simplifies down to

$$\sigma = |\langle (\Gamma_1) . a_j(\gamma_{a_j}) \| T^{(1)} \| (\Gamma_2) . \chi_c(\gamma) \rangle|^2 \; k \sum_{S_1 \Gamma_1} (e_q F P)^2_{S_1 \Gamma_1}$$

We now invoke Koopmans' theorem, namely that a_j and χ_c are orthogonal so that $T^{(1)}$ only acts on the functions following the full stop, and, within this approximation, we have the fundamental selection rule; the final state of the ion, Γ_2, can only arise by photoionisation if the expansion of Γ_A as a fractional parentage sum contains Γ_2. Assuming this to be the case, we have for an ion state Γ_2 :

$$\sigma = k (e_q F P)^2_{S_2 \Gamma_2} \; |\langle (\Gamma_2) . a_j(\gamma_{a_j}) \| T^{(1)} \| (\Gamma_2) . \chi_c(\gamma) \rangle|^2$$

In order to simplify this further, it is advantageous to consider a special case, namely that of atoms. Under these circumstances, replacing Γ_2, γ_{a_j} and γ by J_2, j_1 and j_2, we have:

$$|\langle J_2 \; j_1 \| T^{(1)} \| J_2 \; j_2 \rangle|^2 = (2J_B + 1)(2j_1 + 1) \; W^2(j_1 j_2 J_A J_B ; 1 J_2) \; |\langle j_1 \| T \| j_2 \rangle|^2$$

where W is a Wigner coefficient, closely related to the 6-j coefficients (see below, appendix two).

Finally, for atoms. we obtain the equation

$$\sigma = k (e_q F P)^2_{S_2 \Gamma_2} \; (2J_B + 1)(2j_1 + 1) \; W^2(j_1 j_2 J_A J_B ; 1 J_2) \; |\langle j_1 \| T \| j_2 \rangle|^2$$

Since the J_B are inherently unobservable, we sum over them to obtain a closed formula

$$\bar{\sigma} = \frac{3\pi^3\gamma}{3c} (\varrho_{FP})^2_{j_1 j_2} |\langle j_1 \| T \| j_2 \rangle|^2$$

The derivation may be extended to molecules either using Griffith's irreducible tensor method or by simply expanding the Wigner coefficient and summing over the variables, finally obtaining the text formula.

The connection between this approach and that of Cox et al. can be demonstrated by the following argument. Let there be two open shells, $a_1^{n_1}$ and $a_2^{n_2}$ and suppose we consider shell a_2. The grand fractional parentage equation is derived from the expression:

$$|a_1^{n_1} a_2^{n_2} S M_S L M_L\rangle = \sum_{S_F L_F} (\varrho_{FP})_{S_F L_F} |a_1^{n_1} a_2^{n_2-1} (S_F L_F) \cdot a_2 (j_2)\rangle$$

$$= \sum_{\substack{S_F L_F \\ M_{S_F} M_{L_F}}} (\varrho_{FP})_{S_F L_F} |a_1^{n_1} a_2^{n_2-1}, S_F L_F M_{S_F} M_{L_F}\rangle |a_2, \tfrac{1}{2} j_2, M_S - M_{S_F}, M_L - M_{L_F}\rangle \times$$

$$\times \langle S_F \tfrac{1}{2} M_{S_F} M_S - M_{S_F} | S M_S\rangle \langle L_F j_2 M_{L_F} M_L - M_{L_F} | L M_L\rangle$$

and the fractional parentage coefficients of Cox et al. are derived from an expression of the form:

$$|a_1^{n_1} a_2^{n_2} S M_S L M_L\rangle = \sum_{M_{S_1} M_{L_1}} |a_1^{n_1} S_1 L_1 M_{S_1} M_{L_1}\rangle |a_2^{n_2} S_2 L_2 M_S - M_{S_1}, M_L - M_{L_1}\rangle \times$$

$$\times \langle S_1 S_2 M_{S_1} M_S - M_{S_1} | S M_S\rangle \langle L_1 L_2 M_{L_1} M_L - M_{L_1} | L M_L\rangle$$

where $a_2^{n_2}$ is expanded using the fractional parentage coefficients relative to the a_2 shell only, and the resultant states of $a_2^{n_2-1}$ $(S_3 L_3 M_{S_3} M_{L_3})$ recoupled with $a_1^{n_1}$ $(S_1 L_1 M_{S_1} M_{L_1})$ to yield states $|a_1^{n_1} a_2^{n_2-1} S_F L_F M_{S_F} M_{L_F}\rangle$ to obtain an expression

$$|a_1^{n_1} a_2^{n_2} SLM_SM_L\rangle = \sum_{S_3L_3} \sum_{M_{S_1}M_{L_1}} \sum_{\substack{L_FM_{L_F}\\ S_FM_{S_F}}} \langle S_1S_2M_{S_1}M_S-M_{S_1}|S_1S_2SM_S\rangle \times$$

$$\times \langle L_1L_2M_{L_1}M_L-M_{L_1}|L_1L_2LM_L\rangle \times$$

$$\times \langle L_1L_3L_FM_{L_F}|L_1L_3M_{L_1}M_{L_F}-M_{L_1}\rangle\langle S_1S_3S_FM_{S_F}|S_1S_3M_{S_1}M_{S_F}-M_{S_1}\rangle$$

$$\times \langle S_3\tfrac{1}{2}M_{S_F}-M_{S_1},M_{S_2}-M_{S_F}+M_{S_1}|S_3\tfrac{1}{2}S_2M_{S_2}\rangle (f.p.c.)_{S_3L_3} \times$$

$$\times \langle L_3j_kM_{L_F}-M_{L_1},M_{L_2}-M_{L_F}+M_{L_1}|L_3j_kL_2M_{L_2}\rangle|a_1^{n_1}a_2^{n_2-1}(S_FL_FM_{S_F}M_{L_F})\rangle$$

and we obtain to within a phase factor by contraction

$$(GFP)_{S_FL_F} = (a_1^{n_1}a_2^{n_2-1}(S_FL_F).\,a_2(SL)|\}a_1^{n_1}a_2^{n_2}(SL))$$

$$= W(\tfrac{1}{2},S_3,S,S_1;S_2S_F)W(j_kL_3LL_1;L_2L_F)(2S_2+1)^{\frac{1}{2}}(2L_2+1)^{\frac{1}{2}}\times$$

$$\times(2S_F+1)^{\frac{1}{2}}(2L_F+1)^{\frac{1}{2}}\,(a_2^{n_2-1}(S_3L_3).\,a_2(S_2L_2)|\}a_2^{n_2}(S_2L_2))$$

which gives, on substitution in the cross-section formula

$$\sigma = \frac{8\pi^3\nu}{3c}|\langle j_1\|T\|j_2\rangle|^2|(a_2^{n_2-1}(S_3L_3)a_2(S_2L_2)|\}a_2^{n_2}(S_2L_2))|^2\omega_{S_2L_2}\omega_{S_FL_F}\times$$

$$\times W^2(\tfrac{1}{2}S_3SS_1;S_2S_F)W^2(j_kL_3LL_1;L_2L_F)$$

identical to that derived by Cox et al.

Appendix 2

Consider the coupled final state

$$\underset{\sim}{\Psi}_f = \mathcal{A} \sum_{l,m} \sum_{L_B, M_{L_B}} a(l,m)(2L_B+1)^{\frac{1}{2}} (-)^{l-L_F-M_{L_B}} \begin{pmatrix} L_F & 1 & L_B \\ M_{L_F} & m & -M_{L_B} \end{pmatrix} |\beta\rangle$$

where $|\beta\rangle$ is the electronic state considered above, and can clearly be seen to incorporate the summation which we had to introduce at a later stage in appendix 1. The required transition moment is

$$\langle A|\underset{\sim}{P}|\underset{\sim}{\Psi}_f\rangle = \pm \sum_{l,m} \sum_{L_B, M_{L_B}} a(l,m)(2L_B+1)^{\frac{1}{2}} \begin{pmatrix} L_F & l & L_B \\ M_{L_F} & m & -M_{L_B} \end{pmatrix} \begin{pmatrix} L_A & 1 & L_B \\ M_{L_A} & 0 & -M_{L_B} \end{pmatrix} (2L_A+1)^{\frac{1}{2}} \langle L_A \| P \| L_B \rangle (-)^{\gamma}$$

$$= \pm \sum_{l,m} \sum_{L_B, M_{L_B}} a(l,m)(2L_B+1)(2l+1)^{\frac{1}{2}}(2L_A+1)^{\frac{1}{2}} (\mathrm{GFP})_{S=L_F} (-)^{l'-L_F-M_{L_F}-M_{L_A}} \times$$

$$\times \begin{pmatrix} L_A & 1 & L_B \\ M_{L_A} & 0 & -M_{L_B} \end{pmatrix} \begin{pmatrix} L_F & l & L_B \\ M_{L_F} & m & -M_{L_B} \end{pmatrix} \begin{Bmatrix} L_A & 1 & L_B \\ l & L_F & l' \end{Bmatrix} \langle l' \| P \| 1 \rangle$$

where the function in braces is a 6-j coefficient, related to the Wigner coefficient by a phase change, (GFP) is the relevant grand fractional parentage coefficient discussed in appendix 1, and l' the angular momentum of the orbital whence the electron is ionised. Noting that:

$$\begin{pmatrix} L_A & 1 & L_B \\ M_{L_A} & 0 & -M_{L_B} \end{pmatrix} \begin{Bmatrix} L_A & 1 & L_B \\ l & L_F & l' \end{Bmatrix} = \sum_{\alpha,\beta,\gamma} (-)^{l+L_F+l'+\alpha-\beta+\gamma} \begin{pmatrix} l & L_F & L_B \\ \alpha & -\beta & -M_{L_B} \end{pmatrix} \begin{pmatrix} L_F & l' & L_A \\ \beta & -\gamma & M_{L_A} \end{pmatrix} \begin{pmatrix} l' & 1 & l \\ \gamma & -\alpha & 0 \end{pmatrix}$$

we find that

$$\langle A|\underset{\sim}{P}|\underset{\sim}{\Psi}_f\rangle = \pm \sum_{l,m} \sum_{L_B M_{L_B}} \sum_{\alpha,\beta,\gamma} a(l,m)(2L_B+1)(2l'+1)^{\frac{1}{2}}(2L_A+1)^{\frac{1}{2}} \langle l \| \underline{P} \| l' \rangle \times (-)^{l'-M_{L_F}-M_{L_A}+l'+\alpha+\beta-\gamma}$$

$$\times \begin{pmatrix} l & L_F & L_B \\ \alpha & -\beta & -M_{L_B} \end{pmatrix} \begin{pmatrix} L_F & l' & L_A \\ \beta & -\gamma & M_{L_A} \end{pmatrix} \begin{pmatrix} l' & l & 1 \\ \gamma & -\alpha & 0 \end{pmatrix} \begin{pmatrix} L_F & l & L_B \\ M_{L_F} & m & -M_{L_B} \end{pmatrix} (\mathrm{GFP})$$

$$= \pm \sum_{l,m,\gamma} a(l,m)(2l'+1)^{\frac{1}{2}}(2L_A+1)^{\frac{1}{2}}(-)^{\mu} \begin{pmatrix} L_F & l' & L_A \\ M_{L_F} & \gamma & M_{L_A} \end{pmatrix} \begin{pmatrix} l' & l & 1 \\ \gamma & m & 0 \end{pmatrix} \langle l \| P \| l' \rangle (\mathrm{GFP})$$

on closing over L_B, M_{L_B} and writing μ as the resultant parity.

The cross-section for ionisation is

$$\sigma = \frac{8\pi^3\nu}{3c}\cdot\frac{1}{(2L_A+1)}\sum_{M_{L_A}M_{L_F}}|\langle A|\underset{\sim}{P}|\psi_f^-\rangle|^2$$

$$= \frac{8\pi^3\nu}{3c}\frac{1}{(2L_A+1)}\sum_{M_{L_A},M_{L_F}}\sum_{l_1m_1\gamma}\sum_{l_2m_2\gamma'} a(l_1m_1)\,a^*(l_2m_2)(2L_A+1)(2l'+1)(e_{LFP})^2\langle l_1\|P\|l'\rangle\times$$

$$\times\langle l'\|P\|l_2\rangle\begin{pmatrix}L_A & L_F & l'\\ -M_{L_A} & M_{L_F} & -\gamma\end{pmatrix}\begin{pmatrix}L_A & L_F & l'\\ -M_{L_A} & M_{L_F} & -\gamma'\end{pmatrix}\begin{pmatrix}l_1 & 1 & l'\\ m_1 & 0 & \gamma\end{pmatrix}\begin{pmatrix}l_2 & 1 & l'\\ m_2 & 0 & \gamma'\end{pmatrix}.$$

If we assume that $\langle l\|P\|l'\rangle$ is independent of l, and close over M_{L_A}, M_{L_F} we obtain

$$\sigma = \frac{8\pi^3\nu}{3c}\sum_{l_1l_2m}a(l_1m)\,a^*(l_2m)(e_{LFP})^2|\langle l\|P\|l'\rangle|^2\begin{pmatrix}l_1 & 1 & l'\\ -m & 0 & m\end{pmatrix}\begin{pmatrix}l_2 & 1 & l'\\ -m & 0 & m\end{pmatrix}$$

which is the formula given in the text. It can be seen to contain the product of two spherical harmonics since $a(l,m) = Y^*_{lm}(\beta\alpha)$. Writing this product as a sum, we have

$$\sigma = \frac{8\pi^3\nu}{3c}\sum_L(2L+1)P_L(\cos\beta)\sum_{l_1l_2}(2l_1+1)^{\frac12}(2l_2+1)^{\frac12}\begin{pmatrix}l_1 & l_2 & L\\ 0 & 0 & 0\end{pmatrix}\sum_m(-)^m\begin{pmatrix}l_1 & l_2 & L\\ -m & m & 0\end{pmatrix}\times$$

$$\times(-)^{l_2+l_2}\begin{pmatrix}l_1 & 1 & l'\\ -m & 0 & m\end{pmatrix}\begin{pmatrix}l_2 & 1 & l'\\ -m & 0 & m\end{pmatrix}(2l_1+1)^{\frac12}(2l_2+1)^{\frac12}(e_{LFP})^2|\langle l\|P\|l'\rangle|^2$$

$$= \frac{8\pi^3\nu}{3c}\sum_L(2L+1)P_L(\cos\beta)\sum_{l_1,l_2}(2l_1+1)^{\frac12}(2l_2+1)^{\frac12}\begin{pmatrix}l_1 & l_2 & L\\ 0 & 0 & 0\end{pmatrix}\begin{pmatrix}1 & 1 & L\\ 0 & 0 & 0\end{pmatrix}\times$$

$$\times\begin{Bmatrix}1 & l_1 & l'\\ l_2 & 1 & L\end{Bmatrix}(e_{LFP})^2|\langle n\|P\|l'\rangle|^2$$

where the sum only includes values of $l_1, l_2 = l \pm 1$. Since the 3-j symbol $\begin{pmatrix}1 & 1 & L\\ 0 & 0 & 0\end{pmatrix}$ is non-zero ONLY FOR L = 0,2 we automatically obtain an angular distribution of the form

$$\sigma = \sigma_t\left(1+\gamma P_2(\cos\beta)\right)$$

Appendix Three

Vector Coupling Coefficients for the fivefold rotation groups.
The d orbitals will be represented by the notation

$$a_{1g} \quad \theta = |2,0\rangle$$

$$e_{2g} \quad \varepsilon = (|2,2\rangle + |2,-2\rangle)/\sqrt{2}$$

$$\phi = -i(|2,2\rangle - |2,-2\rangle)/\sqrt{2}$$

$$e_{1g} \quad \eta = -(|2,1\rangle - |2,-1\rangle)/\sqrt{2}$$

$$\xi = +i(|2,1\rangle + |2,-1\rangle)/\sqrt{2}$$

and if we define p, q, r, and s as $\cos 2\pi/5$, $\sin 2\pi/5$, $\cos \pi/5$ and $\sin \pi/5$ respectively, then

$$C_5\theta = C_5^{-1}\theta = C_5^2\theta = C_5^{-2}\theta = \theta$$

$$C_5\varepsilon = (p^2-q^2)\varepsilon - 2pq\phi \qquad C_5\phi = 2pq\varepsilon + (p^2-q^2)\phi$$

$$C_5^{-1}\varepsilon = (p^2-q^2)\varepsilon + 2pq\phi \qquad C_5^{-1}\phi = -2pq\varepsilon + (p^2-q^2)\phi$$

$$C_5^2\varepsilon = (r^2-s^2)\varepsilon + 2rs\phi \qquad C_5^2\phi = -2rs\varepsilon + (r^2-s^2)\phi$$

$$C_5^{-2}\varepsilon = (r^2-s^2)\varepsilon - 2rs\phi \qquad C_5^{-2}\phi = 2sr\varepsilon + (r^2-s^2)\phi$$

$$C_5\eta = p\eta - q\xi \qquad C_5\xi = q\eta + p\xi$$

$$C_5^{-1}\eta = p\eta + q\xi \qquad C_5^{-1}\xi = -q\eta + p\xi$$

$$C_5^2\eta = -r\eta - s\xi \qquad C_5^2\xi = s\eta - r\xi$$

$$C_5^{-2}\eta = -r\eta + s\xi \qquad C_5^{-2}\xi = -s\eta - r\xi$$

1. $e_1 \oplus e_1 = a_1 + a_2 + e_2$

e_1	e_1	a_1	a_2	e_2	
				ε	ϕ
η	η	$1/\sqrt{2}$		$1/\sqrt{2}$	
ξ	ξ	$1/\sqrt{2}$		$-1/\sqrt{2}$	
η	ξ		$1/\sqrt{2}$		$1/\sqrt{2}$
ξ	η		$-1/\sqrt{2}$		$1/\sqrt{2}$

2. $e_1 \oplus e_2 = e_1 + e_2$

e_2	e_1	e_1		e_2	
		η	ξ	ϵ	γ
ϵ	η	$-1/\sqrt{2}$		$-1/\sqrt{2}$	
ϵ	ξ		$1/\sqrt{2}$		$-1/\sqrt{2}$
γ	η		$-1/\sqrt{2}$		$-1/\sqrt{2}$
γ	ξ	$-1/\sqrt{2}$		$1/\sqrt{2}$	

3. $e_2 \oplus e_2 = a_1 + a_2 + e_1$

e_2	e_2	a_1	a_2	e_1	
				ξ	η
ϵ	ϵ	$1/\sqrt{2}$			$1/\sqrt{2}$
ϵ	γ		$1/\sqrt{2}$	$-1/\sqrt{2}$	
γ	ϵ		$-1/\sqrt{2}$	$-1/\sqrt{2}$	
γ	γ	$1/\sqrt{2}$			$-1/\sqrt{2}$

4. $a_2 \oplus e_1 = e_1$

a_2	e_1	e_1	
		ξ	η
a_2	ξ		-1
a_2	η	$+1$	

5. $a_2 \oplus e_2 = e_2$

a_2	e_2	e_2	
		ϵ	γ
a_2	ϵ		γ
a_2	γ	-1	

REFERENCES

1. D.W. Turner, C. Baker, A.D. Baker and C.R. Brundle
Molecular Photoelectron Spectroscopy (J.Wiley 1972, London)
2. A.Einstein
Ann. Phys.(4) 17 132 (1905)
3. K. Siegbahn et al.
ESCA; Atomic, Molecular and Solid State structure studied by means of electron spectrscopy. Uppsala (1967)
4. M.L. Morris and D.A. Aikews
Nature 204 631 (1965)
5. S. Evans
D. Phil. Thesis, Oxford 1971
6. T. Koopmans
Physica 1 104 (1934)
7. B. Bleaney and B.I. Bleaney
Electricity and Magnetism (Oxford, 1965)
8. K. Siegbahn et al.
ESCA applied to Free Molecules (North Holland, 1969)
9. T.C. Waddington
Advan. in Inorg. and Radiochemistry vol. 1 158 (1959)
10. J. Cooper and R.N. Zare
Lectures in Theoretical Physics XI^{c} 317 (1969)
11. P.A. Cox
D. Phil. Thesis, Oxford (1973)
12. U. Fano
Phys. Rev. 137 1364A (1965)
13. F.H. Lies
Phys. Rev. 175 164 (1968)
14. A.Hamnett
Part II Thesis, Oxford 1970
15. S. Evans, A.F. Orchard and D.W. Turner
Int. J. Mass Spec. Ion Phys. 7 261 (1971)
16. J. Berkowitz and P.-M. Guyon
Int. J. Mass Spec. Ion Phys. 6 302 (1971)

17. A.L. Smith
Phil. Trans. Roy. Soc. 268 169 (1970)
18. E.I. Asinovskii, V.A. Kirillin and V.V. Markovets
Teplofiz. Viz. Temp. 8 1083 (1970)
19. T.A. Carlson
Electron Spectroscopy p. 53 (ed. D.A. Shirley, North Holland 1972)
20. J.R. Blackburn, R.Nordberg, F. Stevie, R.G. Albridge and M.M. Jones
Inorg. Chem. 9 2374 (1970)
21. M.L. Morris, R.W. Moshier and R.E. Sievers
Inorg. Synth. IX 28 (1968)
22. F.H. Fry and W.R. Watt
J. Inorg. Nucl. Chem. 30 3115 (1968)
23. G.M. Bancroft, A.G. Maddock, W.K. Ong, R.H. Prince and A.J. Stone
J. Chem. Soc. A 1967 1966
24. J. Selbin, G. Maus and D.L. Johnson
J. Inorg. Nucl. Chem. 29 1735 (1967)
25. E.W. Berg, and J.J.C. Acosta
Anal. Chim. Acta 40 101 (1968)
26. H. Veening, W.E. Bachman, and D. Wilkinson
J. Gas Chromatog. 5 248 (1967)
27. T.S. Davis, J.P. Fackler and M.J. Weeks
Inorg. Chem. 7 1994 (1968)
28. R.G. Charles
Inorg. Synth. 7 183 (1963)
29. R.J. York, W.G. Bonds, B.P. Cotsaradis and R.D. Archer
Inorg. Chem. 8 789 (1969)
30. as reference 26.
31. W.C. Fernelius and B.E. Bryant
Inorg. Synth. 5 105 (1957)
32. A. Arch and R.C. Young
Inorg. Synth 2 17 (1946)
33. R.C. Fay and T.S. Piper
J. Amer. Chem. Soc. 85 500 (1963)
34. G.S. Hammond, D.C. Nonhebel and C.-H. Wu
Inorg. Chem. 2 73 (1963)

35. K. Eisentraut and R.E. Sievers
J. Amer. Chem. Soc. 87 5254 (1965)

36. J.C. Green, M.L.H. Green, P.J. Joachim, A.F. Orchard and D.W.Turne
Phil. Trans. Roy. Soc. 268 111 (1970)

37. A.W. Potts, H.J. Lempka, D.G. Streets and W.C. Price
Phil. Trans. Roy. Soc. 268 59 (1970)

38. I.L.Finar
Organic Chemistry (Longmans, London 1967) pp. 242-275 -
see also
Beilsteins Handbuch der Organischen Chemie 4th. Ed. 1 pt.3, 3115
3124

39. R.N. Haszeldine, W.K.R. Musgrave, F. Smith and L.M. Tutton
J. Chem. Soc. 1951 609

40. G.S. Hammond
Steric Effects in Organic Chemistry (ed. M.S. Newman, J.Wiley 1956
p. 425

41. D.W. Barnum
J. Inorg. Nucl. Chem. 22 183 (1961)

42. A. Streitweiser
MO Theory for Organic Chemists (J.Wiley 1961)

43. P. Bischof, R. Gleiter, and E. Heilbronner
Helv. Chim. Acta 53 1425 (1970)

44. M.B. Robin, N.A. Kuebler and C.R. Brundle
Electron Spectroscopy (ed. D.A. Shirley, North Holland 1972)

45. R.E. Banks
Fluorocarbons and their derivatives (2nd. ed. Oldbourne 1970)

46. see for example H. Remy
Treatise on Inorganic Chemistry (Elsevier, 1956)

47. C.S.G. Phillips and R.J.P. Williams
Inorganic Chemistry vol. 1 (Oxford, 1965)

48. C.K. Jørgensen
Disc. Far. Div. Chem. Soc. 54 (1972)

49. C.J. Ballhausen
Introduction to Ligand Field Theory (McGraw-Hill, 1962)

50. W.M. Gladney and J.D. Swalen
J. Chem. Phys. 42 1999 (1965)

51. actually an epr spectrum cannot be obtained for $V(acac)_3$ and the magnetic data was obtained by
B.N. Figgis, J. Lewis and F.E. Mabbs
J. Chem. Soc. 1960 2480
The UV spectrum is given by
T.S. Piper and R.L. Carlin
Inorg. Chem. 2 260 (1963)
N.S. Hush and R.J.M. Hobbs
Prog. Inorg. Chem. 10 259 (1968)

52. B.R. McGarvey
J. Chem. Phys. 40 809 (1964)

53. T.S. Piper and R.L. Carlin
J. Chem. Phys. 36 3330 (1962)

54. S. Evans, B. Jewitt, M.L.H. Green and A.F. Orchard
J. Chem. Soc. Far. Trans. II 1972 1847

55. P.A. Cox, S. Evans, A. Hamnett and A.F. Orchard
Chem. Phys. Lett. 7 414 (1970)

56. (a) M. Courteis and L.S. Foster
J. Mol. Spec. 18 396 (1965)
(b) K. DeArmond and L.S. Foster
Spectrochim. Acta 19 1393 (1963)
(c) M. Ban and J. Csaszar
Acta Chim. Acad. Sci. Hung. 54 133 (1967)

57. J.S. Griffith
The Theory of Transition-Metal Ions (Cambridge, 1964)

58. C.C.J. Roothaan
Rev. Mod. Phys. 32 179 (1960)

59. R.L. Carlin
J. Chem. Phys. 35 1240 (1961)

60. B. Morosin and R. Brathovde
Acta Cryst. 17 705 (1964)

61. T.M. Dunn
Modern Coordination Chemistry (ed, J. Lewis and R.G. Wilkins
Interscience, 1960)

62. (a) J.P. Fackler, T.S. Davis and I.D. Chawla
Inorg. Chem. 4 130 (1965)
(b) R. Dingle
J. Mol. Spec. 9 426 (1962)
(c) V. Zelentzov
Zh. Struct. Khim. 8 651 (1967)
(d) C.K. Jørgensen
Acta Chem. Scand. 16 2406 (1964)
63. B.N. Figgis, J. Lewis, F.E. Mabbs and G.A. Webb
J. Chem. Soc. A 1966 422
64. A.K. Gregson
Ph. D. Thesis, Melbourne 1971
65. S. Evans, J.C. Green, A.F. Orchard, T. Saito and D.W. Turner
Chem. Phys. Lett. 4 361 (1969)
66. C.S.G. Phillips and R.J.P. Williams
Inorganic Chemistry vol. 2 (Oxford, 1966) p. 286
67. A.F. Wells
Structural Inorganic Chemistry (Oxford, 1961)
68. E.C. Lingafelter
Coord. Chem. Rev. 1 151 (1965)
69. F.W. Milton
Part II Thesis, Oxford 1972
70. C.K. Jørgensen
Modern Aspects of Ligand Field Theory (Elsevier, 1971)
71. P.S. Bagus
Phys. Rev. 139 A 619 (1965)
72. M. Barber, J.A. Connor, L.M.R. Derrick, M.B. Hall and I.H. Hillier
J. Chem. Soc. Far. Trans.II 1973
73. A. Hamnett and A.F. Orchard
Electronic Structure and Magnetism of Transition-Metal Compounds
vol. I (ed. P. Day). The Chemical Society, London.
74. A. Hamnett
Disc. Far. Div. Chem. Soc. 54 1972
75. L.C. Snyder
J. Chem. Phys. 54 97 (1971)

76. P.Bagus and H.F. Schaefer
J. Chem. Phys. 56 224
77. T. Åborg
Ann. Acad. Sci. Fenn. A VI (308) 1 (1969)
78. M. Barber, J.A. Connor and I.H. Hillier
Chem. Phys. Lett. 9 570 (1971)
79. N.F. Mott and H.S.W. Massey
The Theory of Atomic Collisions (3rd. ed. Oxford, 1965)
80. see for example R.G. Parr
Quantum Theory of Molecular Electronic Structure (Benjamin, 1964)
81. see for example H.F. Hameka
Advanced Quantum Chemistry (Addison-Wesley, 1965)
82. J.A. Pople
Proc. Phys. Soc. 68 81 (1955)
83. G.E. Coates, M.L.H. Green and K. Wade
Organometallic Compounds (Methuen, 1968)
84. R. Prins
J. Chem. Phys. 50 4804 (1969)
see also Mol. Phys. 19 603 (1970)
85. V.S. Sohn, D.N. Hendrickson, J.H. Smith and H.B. Gray
Chem. Phys. Lett. 6 499 (1970)
86. I. Pavlik, V. Cerny and E. Maxova
Coll. Czech. Chem. Comm. 35 3045 (1970)
87. D. Mayers
Unpublished Results
88. I. Hanazaki, F. Hanazaki and S. Nagakura
J. Chem. Phys. 50 265, 276 (1969)
89. E.O. Fischer and R. Jira
Z. Naturforsch. 8B 217 (1953)
also G. Wilkinson, P.L. Pauson and F.A. Cotton
J. Amer. Chem. Soc. 76 1970 (1954)
90. (a) R. Prins, P. Biloen and J.D.W. van Woorst
J. Chem. Phys. 46 1216 (1967)
(b) R. Prins, and J.D.W. van Woorst
J. Chem. Phys. 49 4665 (1968)

(c) R. Prins, J.D.W. van Woorst and C.J. Schinkel
Chem. Phys. Lett. 1 54 (1967)
(d) M. Nussbaum and J. Voitlander
Z. Naturforsch. A 20 1417 (1965)

91. (a) A.T. Armstrong, F.J. Smith, E. Elder and S.P. Mcglynn
J. Chem. Phys. 46 4321 (1967)
(b) J.J. Smith and B. Meyer
J. Chem. Phys. 48 5436 (1968)

92. M.E. Schwartz, J.D. Switalski and R.E. Stronski
Electron Spectroscopy (ed. D.A. Shirley, North Holland, 1972)

93. R.S. Drago and M.F. Rettig
J. Amer. Chem. Soc. 91 1361 (1969)

94. D.R. Eaton
J. Amer. Chem. Soc. 87 (1965)
see also Adv. Mag. Res. 1 103 (1965)

95. Z. Luz, B.L. Silver and D. Fiat
J. Chem. Phys. 46 469 (1967)

96. (a) R. Röhrscheid, R.E. Ernst and R.H. Holm
Inorg. Chem. 6 1607 (1967)
(b) J.A. Haffe and R.C. Ward
J. Chem. Phys. 38 1211 (1962)
(c) R.J. Fitzgerald and R.S. Drago
J. Amer. Chem. Soc. 89 2879 (1967)
(d) R.W. Kluiber and W.D. Horrocks
Inorg. Chem. 6 430 (1967)
(e) M.E. Rettig and R.S. Drago
J. Amer. Chem. Soc. 91 3432 (1969)
(f) R.E. Cramer and R.S. Drago
J. Amer. Chem. Soc. 92 66 (1970)

97. A.D. McLachlan
Mol. Phys. 3 233 (1960)

98. K. Nakamoto, C. Uldovich and J. Takemoto
J. Amer. Chem. Soc. 92 3973 (1970)

99. M. Mikami, I. Nakegawa and T. Shimamouchi
Spectrochim Acta A 23 1037 (1967)

100. R.D. Hancock, and D.A. Thornton
Inorg. Nucl. Chem. Lett. 3 419 (1967)

101. S. Pinchas, B.L. Silver and I. Laulicht
J. Chem. Phys. 46 1506 (1967)

102. W.C. Price, T.R. Passmore, and D.M. Roessler
Disc. Farad. Soc. 35 201 (1963)
P.E. Cade and W.M. Huo
J. Chem. Phys. 47 614 (1967)

103. J.L. Wood and M.M. Jones
Inorg. Chem. 3 1553 (1964)

104. S.J. Ashcroft and C.T. Mortimer
Thermochemistry of metal chelate complexes (J. Wiley, 1970)

105. P. George and G.S. McClure
Prog. Inorg. Chem. 1 (ed. F.A. Cotton, 1959)

106. C.E. Moore
Tables of Atomic Energy Levels (Nat. Bur. Stand. circular no. 467, vol.1 (1949) vol.2 (1952)).

SUMMARY

The ultra-violet and X-ray photoelectron spectra of the tris-hexafluoroacetylacetonato complexes of some transition metals are reported amd discussed. For many of these complexes there is either little or no literature experimental data available and, where necessary full details have been given in this thesis, both of the preparation and purification of the complexes. The gas-phase ultra-violet photoelectron spectra are discussed first, and it is shown how the spectra lead unambiguously to an energy level ordering similar to that assumed in ligand-field theory. However, in the high-spin complexes of Mn(III) and Fe(III) and in the low-spin Co(III) complex, the metal levels are observed to have ionisation energies which, for the most part, are higher than those of the least stable ligand molecular orbitals. This is in direct contradiction to the predictions of ligand-field theory and, in the case of the Co(III) complex, leads to an inversion of the trigonally split e and a_1 metal d orbitals. The interpretation of the high-spin complex spectra is shown to be very difficult within the one-electron framework used for the other complexes and the ultra-violet spectra are shown to be the best guide to interpretation. The values for the ligand-field parameters so derived are similar to, though slightly larger than, those for the neutral species.

The ESCA spectra of the complexes were measured and are reported in the second part of the thesis. The movements of the core levels so found are related by an expression derived by Siegbahn et al. to the charge shifts in the complexes as the metal is changed. These charge shifts are of three basic types: a polarisation of the π framework of the ligand towards the metal as the metal-oxygen bond length contracts, a transfer of charge from the ligand σ-system to the metal, increasing as the transition series is traversed and a charge shift from the anti-bonding metal d-orbitals back onto the σ-system of the ligand as a natural consequence of its anti-bonding character.

As a parallel study, the ESCA spectra of the metallocenes were also run and are reported at the end of the second part of the thesis. The charge shifts observed in these compounds show a remarkable parallel to those found in the hexafluoroacetylacetonato complexes, when the different metal charges and ligand characteristics are taken into account. These trends were shown to be in accord with other data on the metallocenes.

In the last part of the thesis, the charge and orbital energy shifts deduced in the first two parts of the thesis for the hexafluoroacetylacetonato complexes are correlated with other physical measurements and a consistent picture of the bonding in these complexes shown to emerge. In particular, the shifts in ionisation energies found for many of the main bands in the ultra-violet photoelectron spectra receive a ready explanation once the ESCA data is considered. On this basis a case is made for the complementarity of the two techniques.